STUDIES OF LIPID PRODUCTION FROM MICROALGAE FOR BIODIESEL PRODUCTION IN FLAT PANEL PHOTOBIOREACTOR

Ph.D THESIS

by

SHAILENDRA SINGH KHICHI

DEPARTMENT OF BIOTECHNOLOGY
INDIAN INSTITUTE OF TECHNOLOGY ROORKEE
ROORKEE-247667(INDIA)
OCTOBER, 2018

STUDIES OF LIPID PRODUCTION FROM MICROALGAE FOR BIODIESEL PRODUCTION IN FLAT PANEL PHOTOBIOREACTOR

A THESIS

Submitted in partial fulfilment of the requirements for the award of the degree

of

DOCTOR OF PHILOSOPHY

in

BIOTECHNOLOGY

by

SHAILENDRA SINGH KHICHI

DEPARTMENT OF BIOTECHNOLOGY
INDIAN INSTITUTE OF TECHNOLOGYROORKEE
ROORKEE-247667(INDIA)
OCTOBER, 2018

INDIAN INSTITUTE OF TECHNOLOGY ROORKEE
ROORKEE

CANDIDATE'S DECLARATION

I hereby certify that the work which is being presented in the thesis entitled "**STUDIES OF LIPID PRODUCTION FROM MICROALGAE FOR BIODIESEL PRODUCTION IN FLAT PANEL PHOTOBIOREACTOR**" in partial fulfilment of the requirements for the award of the degree of Doctor of Philosophy and submitted in the Department of Biotechnology of the Indian Institute of Technology Roorkee, Roorkee is an authentic record of my own work carried out during a period from July, 2012 to October, 2018 under the supervision of Dr. Sanjoy Ghosh, Associate Professor, Department of Biotechnology, Indian Institute of Technology Roorkee, Roorkee.

The matter presented in the thesis has not been submitted by me for the award of any other degree of this or any other institution.

(SHAILENDRA SINGH KHICHI)

This is to certify that the above statement made by the candidate is correct to the best of my knowledge.

(Sanjoy Ghosh)
Supervisor

Date: **October, 2018**

ABSTRACT

Global energy demand and its dependence on fossil fuel have prompted the search for alternative fuel. Noteworthy, the photosynthetic microalgae have gained significant interest as one of the most promising alternative feedstock for biolipid production. In addition, the commercial cultivation of microalgae for biolipid production is commonly achieved by photobioreactor systems, nowadays flat panel photobioreactor are extensively used for mass cultivation of different types of microalgae. Microalgae lipid in photobioreactor is affected by several chemical (nitrogen and phosphate) and physical parameters (temperature, irradiance, and pH). In this study various physical and chemical parameters were optimized for higher biomass and lipid productivity for *Botryococcus braunii* in flat panel photobioreactor.

In the key finding, a pH stat process was developed to enhance the biomass and lipid productivity at high CO_2 concentrations The algal strain showed the maximum specific growth rate, biomass productivity and CO_2 consumption rate at 20% CO_2concentration.

A novel consolidate real time model was developed to study the nitrate depletion dynamics in flat panel photobioreactor. This study suggests that optimum nitrate concentration of 1.125 g L^{-1} in the nutrient medium significantly enhance the process productivity of the photobioreactor.

Light availability inside the photobioreactor is often measured by the Lambert – Beer law, and Lambert - Beer law assumptions are not valid at high cell density cultural conditions, because light scattering and differential absorption have significant impact on light transfer in photobioreactor. In this study the Lambert – Beer law was modified by applying differential absorbance in flat panel photobioreactor. Maximum biomass concentration, maximum lipid content and lipid productivity rate were 2.52 g L^{-1}, 19.76% and 114.92 mg L^{-1} d^{-1} at 261 μmol m^{-2} s^{-1} light intensity respectively.

Photoheterotrophic cultivation of microalgae significantly enhances growth, biomass and lipid yield than the autotrophic cultural conditions. The lipid productivity of microalgae is highly influenced by carbon and nitrogen sources present in their nutrient medium. Carbon sufficient and under nitrogen-limited cultural conditions induces high neutral lipids accumulation in microalgae. In heterotrophic cultivation condition the maximum values of biomass productivity, specific growth rate and lipid productivity were 1.11 g $L^{-1}d^{-1}$, 0.073 h^{-1} and 0.39 g $L^{-1}d^{-1}$ obtained respectively.

Single stage two-phase fed batch cultivation for microalgae biomass is a promising strategy to boost lipid accumulation and productivity. A cultivation system in the two-phase fed batch mode

was adapted to maximize lipid productivity of *B. braunii* in flat panel photobioreactor. Importantly, during two-phase fed batch cultivation for *B. braunii* the biomass was increased to 7.9 g L^{-1}, and the lipid productivity was increased from 0.536 g L^{-1} d^{-1} to 1.32 g L^{-1} d^{-1} compared to single stage heterotrophic batch cultivation

Acknowledgements

The present thesis is the result of work done in last few years whereby I have been accompanied and supported by a lot of wonderful people. It would not have seen the light of the day without their tremendous contribution and support.

First and foremost, I am eternally grateful to my supervisor Dr. Sanjoy Ghosh for giving me the amazing opportunity to work and learn in the area of biochemical engineering. I am grateful to him to give me a chance to work on entirely pioneer area in my lab i.e. photobioreactor technology. He provides me the extensive freedom to think and learn the philosophy of the subject. His insight in the subject of biochemical engineering and his keen affection to the mathematics brings a new horizon in front of me as a mathematical modelling of bioprocess. The mathematical mind of my supervisor always raises the bar for me to perform up to the mark. His strong belief in mathematics inspires me a lot to learn the subject from the mathematical point of view. His passion for science, unlimited energy and dedication has always been an inspiration for everyone in our group. I owe him more than I can put into words for all the moral support, freedom and kindness I received from him since I joined his lab. I cannot imagine a better advisor and mentor for my Ph.D.

I would like to thank the members of my Student Research Committee Dr. Vikas Pruthi, Dr. R. Prasad, Dr. S. Chand and Dr. G. S. Randhava for taking out time from their busy schedule and giving me useful ideas and suggestions to improve my thesis work. Their critical assessment of my work and generous support has greatly improved the quality of my work. I was fortunate to have such great committee members.

I greatly acknowledge the help rendered from Dr A.K. Sharma (Current), Dr. Partha Roy (Former) and Dr. Ramasare Prasad (Former) Head, Department of Biotechnology for providing us basic facilities in the department. I gratefully acknowledge the support and cooperation of all the faculty members of the Department of Biotechnology. Their immense interest in science, enthusiasm and valuable advice motivate each one of us to work twice as hard. I would also like to thank the office staff at Biotechnology department of IIT Roorkee who painstakingly listened and acted upon every plea of students like me on a day to day basis in addition to their regular work-load.

I would like to express my gratitude towards my lab members Dr. Sidharth Arora, Ms. Noopur, Ms. Gunjan, Ms. Rukmini, Ms. Arcahna, Mr. Kartik, Ms. Raikamal, Mr. Sharth, Mr. Rohit and Mr. Nikhil, Ms. Preeti, Ms. Rashmi for their support and providing me the enjoyable and ethical work culture during my PhD.

I would like to express a special thank to Mr. Pritam Singh my junior cum younger brother and an exceptional student with whom I discussed a lot about the research and also learn from him. He

was the true source of inspiration throughout my research. I have enjoyed working with him in our lab during my entire PhD.

Words fall short to describe the support which my friends Alok, Atin, Madhu, Mudgal, Snehashish and Tamoghna were throughout these past years. The incorrigible love, respect and mutual admiration we share for each other is inexplicable. Their collective enthusiasm towards science has always motivated me to stay focused on my work. The scientific conversations and creative ideas we shared have helped a great deal in the accomplishment of the work presented in this thesis. Being your friend is something I will treasure forever.

Finally and more importantly, I would like to express my heartfelt gratitude towards my I.Q.(i.e. my father) and my E.Q. (i.e. my mother). Without this wonderful family the life becomes impossible. They are always there for me throughout my entire journey of research. I would express a sincere thank to my father because the first lab scale flat panel airlift photobioreactor was designed by himself only and because of that I was able to start my research journey. He is the true source of inspiration for my entire life. I am forever indebted to my father for his constant love, support and the freedom he always gave me to do what I love. The inheritance of E.Q. which I have received from my mother helps me to develop the moral values and ethics in my life. She is the true moral support whenever I lose hope in my life and because of her I was able to finish my Ph.D. Her unconditional love and the continuous emotional support through the thick and thin of my life has always been the driving force of whatever I have done and will do in my life.

I would like to express a special gratitude to my loving sister (Ruchika) or my true crime partner who witnessed all the up and downs in my life and always cheer me up in the worst of times is something I would never be able to reciprocate. It is having you in my life that makes everything else matter.

I would like to thank Department of Biotechnology, New Delhi for the financial assistantship given during my thesis work as JRF and SRF.

Beyond all this, I thank almighty god for being with me throughout this journey and blessing me to remain strong and calm throughout this journey. I thank god for putting me through some tough tests in life and getting me out of them. You are the one who made it all happen.

Thank you all for everything you have given me.

(Shailendra)

List of Figures

List of Tables

List of Abbreviations

BP = Biomass Productivity

CSTR = Continuous stirrer Tank reactor

FPBR = Flat Panel Photobioreactor

FALPBR= Flat Panel Airlift Photobioreacto

GL = Glucose Limited

NL= Nitrate Limited

LP = Lipid Productivity

PA= Photosynthetic Activity

PE= Photosynthetic Efficiency

PBR = Photobioreactor

PFD = Photon Flux Density

PPFD = Photosynthetic Photon Flux Density

RTE = Radiative Transfer Equation

GL = Glucose Limited

NL= Nitrate Limited

Nomenclatures

$I_{c,\lambda}$ = Incident light energy (µmol m^{-2} s^{-1})

$\beta_{eff,\lambda}$ = Effective extinction coefficient of microalgae (m^{-1})

$K_{eff,\lambda}$ = Effective absorption coefficient of microalgae (m^{-1})

$\sigma_{eff,\lambda}$ = Effective scattering coefficient of microalgae (m^{-1})

$A_{abs,\lambda}$ = Mass absorption cross section of microalgae (m^2 kg^{-1})

$S_{sca,\lambda}$ = Mass scattering cross section of microalgae (m^2 kg^{-1})

$\bar{C}_{ext,\lambda}$ = Average extinction cross section of microalgae cell (m^2 $cell^{-1}$)

$\bar{C}_{abs,\lambda}$ = Average absorption cross section of microalgae cell (m^2 $cell^{-1}$)

$\bar{C}_{sca,\lambda}$ = Average scattering cross section of microalgae cell (m^2 $cell^{-1}$)

$k_{L,\lambda}$ = Absorption coefficient of the medium (m^{-1})

k'_{λ} = Absorption index of water (dimensionless)

ϕ_{λ} = Phase function (dimensionless)

$\hat{r}$ = Position vector (dimensionless)

$\hat{s}$ = Direction (dimensionless)

X = Biomass concentration (g L^{-1})

μ = Specific growth rate (d^{-1})

X_m = Maximum biomass concentration (g L^{-1})

X_0 = Initial biomass concentration (g L^{-1})

K_c = Apparent specific growth rate (d^{-1})

q_S^{max} = Maximum specific substrate consumption rate (g g_b h^{-1})

μ_{max} = Maximum specific growth rate (d^{-1})

P = Lipid concentration (g L^{-1})

α = Growth associated coefficient (g g^{-1})

β = Non growth associated coefficient (g g^{-1})

M_{CO_2} = Molecular weight of CO_2

M_c = Molecular weight of carbon

C_c = Carbon content of the cell

P_{areal} = Areal biomass productivity (g m^{-2} h^{-1})

V = Volume of the photobioreactor (L)

A = Illuminated surface area of photobioreactor (m^2)

$Y_{X,E}$ = Biomass yield on light energy (g mol $photons^{-1}$)

R^2 = Coefficient of determination (-)

Table of Content

CHAPTER 9

Mathematical Modeling of Light Energy Flux Balance in Flat Panel Photobioreactor for *Botryococcus braunii* Growth, CO_2 Biofixation and Lipid Production under Varying Light Regimes 151

Chapter 1

Introduction

1.1. Background

The increasing dependence of global economic developments on fossil fuel based non renewable energy resources (coal, natural oil and gas) have placed compelling insistence on the perpetual supply of fossil fuels in order to accommodate the rising demand (Capellan-Parez et al.,2014). The progressive depletion of fossil fuel is extensively recognized and already continuing process. These non renewable resources are thus physically, stringently and economically limited (Capellan-Parez et al.2014). This rapid reduction of fossil fuel resources and global warming of earth has suggested the immediate requirement of alternative renewable resources (Satyanaryana et al., 2011). Among various renewable resources available, microalgae have been assessed as most promising feedstock for bio-oil and value added metabolites production (Chisti, 2007; Satyanaryana et al., 2011). Microalgae ingest carbon dioxide (CO_2) and emit oxygen via photosynthesis.

Microalgae are unicellular photosynthetic microorganisms that methodically capture CO_2 and store sun light in complex chemical bonds. Microalgae cultivation technology does not compete with the agricultural land as they can easily grow on non-crop land (Teresa et al., 2010). Similarly microalgae don't requires nutrients and freshwater resources either as they can grow on inexpensive wastewater also (Brennan and Owende, 2010). Algae cultivation technology has the potential for biofuel generation, carbon dioxide sequestration and source for animal nutrition simultaneously. The large scale algae farming can be achieved by open pond systems or photobioreactor technology (Kunjapur et al., 2010). The advantage of photobioreactors includes dynamic control of temperature, light, CO_2, O_2, and nutrient availability which improves the biofuel productivity of algae compared with the traditional pond cultivation technology. The optimum cultivation conditions can be controlled inside the PBR; and light intensity, duration, and wavelength are predominant variables for microalgae growth (Carvalho et al., 2011)

In recent years, sustainable and large scale production of microalgae in photobioreactor required an immediate attention to link the scientific findings to the commercial needs (Velarde et al., 2010).

Large scale photo-fermentation can be achieved by using either by conventional CSTR/tubular/flat panel photobioreactor (Kunjapur et al., 2010). The advantage of flat panel photobioreactor over conventional CSTR or tubular is that; it provides the substantial feasible ratio between the illuminated area and working volume to accompanied maximum photosynthetic efficiencies compared to any other photobioreactor. However, the thin panel flat photobioreactors are subjected to the moderate mass transfer rates due to limiting light path which in turn lessen the removal capacity of the dissolved oxygen produced during photosynthesis (Sierra et al., 2008). Noteworthy, the Flat panel airlift PBR with higher light paths adequately use light supply to cover nutritional requirements of photosynthetic microorganisms. In particular, the other advantages of using high light path PBRs are the reduction in construction costs and in energy expenditure during process operation (Velarde et al. 2010). Moreover, the accumulation of dissolved oxygen concentration in flat panel photobioreactor is relatively low compared to horizontal tubular photobioreactors. It has been reported that in flat panel photobioreactors high photosynthetic efficiencies can be achieved (Hu et al., 1996; Richmond, 2001). This allows adequate light penetration and increases photosynthetic efficiency. In addition, the adjoin region near the surface of the illuminated reactor is known as photic zone where light saturation and consequently the photo inhibition of algal growth repeatedly occurs (Hankamer et al., 2007). This photo-inhibition leading to decreased photosynthetic product can adversely affect the lipid production through algae. It is imperative to use the legitimate irradiance to make biodiesel more economical.

Biosequestration of CO_2 by microalgae has been determined as adequate and economical process. The photosynthetic process in microalgae efficiently captured CO_2 and converts it into potential biomass; biofuel feed stocks, and high value biochemicals (Mondal et al., 2017). The carbonic anhydrase (CA) is the possible key enzyme, which facilitate carbon concentration mechanism (CCM) in microalgae. In this mechanism, CO_2 is incorporated into a 5-carbon compound to produce two molecules of PGA (phosphoglyceraldehyde) by Ribulose-1,5-bisphosphate carboxylase/oxygenase (RuBisCo) enzyme, here RuBP work as co-sbustrate for CO_2 (Mondal et al., 2017). Biosequestration efficiency of microalgae is dependent on microalgae species, nutrients ratio, light intensity, temperature, pH, CO_2 concentration, air flow rate, and photo-bioreactor type (González López et al., 2009). Microalgae efficiently grow at alkaline pH and high CO_2 concentration reduces the pH of growth medium which inhibits the microalgae growth. Hence, microalgae growth kinetics is strongly influenced by pH variations and high CO_2 concentration.

The pH stat cultivation of microalgae can increase carbon fixation efficiency, growth and lipid productivities and hence becomes an effective tool for carbon dioxide capture.

Nitrate is the most crucial chemical variable that affects the process productivity of microalgae in photobioreactor. Nitrogen limitation is precisely correlated with lipid accumulation, whilst it has an adverse effect on biomass and lipid productivity because nitrogen containing molecules (i.e. proteins, amino acids etc.) reduced in suboptimal nitrogen medium (Ordog et al., 2012). A complete nitrogen limitation strategy have disadvantage of sub-optimal biomass and lipid productivity (Ordog et al., 2012; Pancha et al., 2014), However, intermediate nitrogen concentrations have increased photobioreactor process productivity more efficiently than total nitrogen limitation strategy (Dean et al., 2010; Ordog et al., 2012). Thus, efficient and economically viable large-scale lipid production in photobioreactor can be achieved under intermediate nitrate concentration (Chen et al., 2011).

In heterotrophic cultivation of microalgae organic substrates is used as sole carbon and energy sources (Perez-Garcia et al., 2011), whilst in mixotrophic culture conditions light energy is responsible for photosynthesis and organic substrate concentration provide the carbon source to the microalgae (Rym et al., 2010). Heterotrophic cultivation of microalgae eliminated the light requirement and significantly enhances growth, biomass and lipid yield than the autotrophic cultural conditions. The lipid productivity of microalgae is highly influenced by carbon and nitrogen sources present in their nutrient medium. Carbon sufficient and under nitrogen-limited cultural conditions induces high neutral lipids accumulation in microalgae. In comparison to autotrophic growth, PPP is mainly metabolized in the darkness, while EMP is the main glycolytic pathway under light. In conclusion, heterotrophic cultural conditions are useful for the production of value added biochemical and metabolite production economically. Heterotrophic cultivation is simple and cheap and generally preferred by fermentation industries for other production applications.

1.2. Research Objectives

To address the sources for alternative renewable energy production, microalgae were explored as a potential option to produce lipid/biodiesel in photobioreactor to conquer the limitations of finite available fossil fuel resources. The main objective of this PhD thesis was to intensify the flat panel photobioreactor process productivity of microalgal CO_2 biosequestration, biomass and lipid

production; and to develop a novel mathematical model for online monitoring of algal dynamics in flat panel photobioreactor.

To accomplish these objectives, the present investigations will examine the primary concern related to flat panel photobioreactor as follows:

(1) Investigate and discuss the effect of CO_2 concentration on *B. braunii* growth and lipid productivity under pH stat cultivation strategy (5.37 L FPALPBR).

(2) Proposing a novel mathematical model is to measure algal dynamics in flat panel photobioreactor under nitrate limiting conditions (5.37 L FPALPBR).

(3) Development of an innovative light evolution kinetic model coupled with the microalgae growth model, to study the effect of light intensity on *B. braunii* biomass growth and lipid productivity (5.37 L FPALPBR).

(4) Examine the effect of various C:N ratio on *B. braunii* growth, lipid production, glucose and nitrate uptake kinetics in carbon-limited and nitrogen-limited photoheterotrophic cultural conditions (Flask cultivation).

(5) Process development for fed-batch cultivation of *B. braunii* using single stage two phase process strategy in flat panel airlift photobioreactor under mixotrophic cultivation conditions (5.37 L FPALPBR).

(6) Photosynthetic characterization of Flat panel Photobioreactor (30 L PBR)

(7). Development of mathematical model for light energy flux balance in flat panel photobioreactor for *B. braunii* growth, CO_2 biofixation and lipid production under varying light regimes (30 L PBR).

1.3. Thesis Structure

This thesis organized into 9 chapters that are connected meticulously in order to accomplish the targeted objectives. The brief discussion about the chapters as follows:

Chapter 1 is the general introduction which delivers a prevalent synopsis of the present research work which encompasses the concise framework of the thesis topic, the decisive parameters key

factors affecting photobioreactor process productivity for efficient CO_2 biosequestration, biomass and lipid production. This chapter also comprises the major objectives of the thesis, its implications, significance and structure.

Chapter 2 included a laconic literature review dedicated to represent the importance of microalgae cultivation in flat panel photobioreactor. A concise discussion on different type of photobioreactor systems, growth limiting factors, various growth kinetic models and their limitations are summarized.

Chapter 3 described the improvement of CO_2 biosequestration efficiency of *B. braunii* in flat panel airlift photobioreactor. In this chapter pH stat cultivation strategies were developed for high CO_2 concentrations to intensify the biomass and lipid productivity of *B. brunii* in modified BG -11 medium.

Chapter 4 explicates the role of nitrate on biomass and lipid production in flat panel airlift photobioreactor. In this chapter, we have introduced light absorption factor (A), as a instantly measured variable to develop a novel mathematical model, for real time estimation of biomass concentration as a function of absorbance factor (A) inside the flat panel airlift photobioreactor.

Chapter 5 describes the effect of varying light regimes on biomass and lipid production of *B. braunii* in flat panel airlift photobioreactor. In this chapter the Lambert – Beer law was modified by applying differential absorbance in flat panel photobioreactor. As light intensity varies with location and age in the photobioreactor, an consolidate model based on Lambert – Beer law including temporal light evolution and microorganism growth is presented in this chapter.

Chapter 6 This chapter evaluates the footprints of the C:N ratio, on kinetics, biomass and lipid productivity of *B. braunii* in glucose limited and nitrate limited photoheterotrophic culture conditions.

Chapter 7 describes the two-phase single stage fed batch cultivation strategies for *B. braunii* in flat panel photobioreactor. Two-phase fed batch cultivation for microalgae biomass is a promising strategy to boost lipid accumulation and productivity of *B. brauniin* in flat panel photobioreactor.

Chapter 8 demonstrates the effect of photosynthetic parameters (i.e. aeration rate, temperature and light wavelength) on the process productivity of microalgae in photobioreactor. This chapter

evaluates the response of these photosynthetic parameters on photosynthetic efficiency and photosynthetic activity of *B. braunii* inside the photobioreactor through oxygen measurements.

Chapter 9 focuses on radiative transfer of light in flat panel photobioreactor. In this chapter mathematical modeling of light energy flux balance was applied in flat panel photobioreactor under varying light regimes.

1.4.References

Brennan L., Owende, P., 2010. Biofuels from microalgae—A review of technologies for production, processing, and extractions of biofuels and co-products. Renew. Sustain. Energy Rev. 14(2), 557-577.

Capellán-Pérez I., Mediavilla M., de Castro C., Carpintero Ó., Miguel L.J., 2014. Fossil fuel depletion and socio-economic scenarios: an integrated approach. Energy. 77, 641-666.

Carvalho A.P., Luı´s A.M., Malcata F.X., 2006. Microalgal reactors: a review of enclosed systems design and performances. Biotechnol. Prog. 22, 1490–1506.

Chen M., Tang H., Ma H., Holland T.C., Ng K.Y., Salley S.O., 2011. Effect of nutrients on growth and lipid accumulation in the green algae *Dunaliella tertiolecta*. Bioresour. Technol. 102, 1649-1655.

Chisti Y., 2007. Biodiesel from microalgae, Biotechnol. Adv. 25, 294-306.

Dean A.P, Sigee D.C., Estrada B., Pittman J.K., 2010. Using FTIR spectroscopy for rapid determination of lipid accumulation in response to nitrogen limitation in freshwater microalgae. Bioresour. Technol., 101, 4499-4507.

Gonzalez-Lopez C.V., Acién-Fernández F.G., Fernández-Sevilla J.M., Sánchez-Fernández J.F., Molina G. E., 2012. Development of a process for efficient use of co_2 from flue gases in the production of photosynthestic microorganism. Biotechnol. Bioeng. 109, 1637-1650.

Hankamer B., Lehr F., Rupprecht J., Mussgnug J.H., Posten C., Kruse O., 2007. Photosynthetic biomass and H_2 production by green algae: from bioengineering to bioreactor scale-up. Physiol. Plan. 131, 10-21.

Hu Q., Guterman H., Richmond A., 1996a. A flat inclined modular photobioreactor for outdoor mass cultivation of photoautotrophs. Biotechnol. Bioeng. 51, 51–60.

Kunjapur A.M., Eldridge R.B., 2010. Photobioreactor design for commercial biofuel production from microalgae. Ind. Eng. Chem. Res. 49, 3516–3526.

Mondal M., Goswami S., Ghosh A., Oinam G., Tiwari O.N., Das P., Gayen K., Mandal M.K., Halder G.N., 2017. Production of biodiesel from microalgae through biological carbon capture: a review. 3 Biotech. 7(2), 99.

Ördög V., Stirk W.A., Bálint P., Staden J., Lovász C., 2012. Changes in lipid, protein and pigment concentrations in nitrogen-stressed *Chlorella minutissima* cultures. J. Appl. Phycol. 24,907-914.

Pancha I., Chokshi K.,Georgea B.,Ghosh T.,Paliwal C.,Maurya R.K.,Mishra S., 2014. Nitrogen stress triggered biochemical and morphological changes in the microalgae *Scenedesmus* sp. CCNM 1077. Bioresour.Technol. 156,146-154.

Perez-Garcia O., Escalante F.M., de-Bashan L.E., Bashan Y., 2011. Heterotrophic cultures of microalgae: metabolism and potential products. Water Res. 45(1), 11-36.

Richmond A., Cheng-Wu Z., 2001. Optimization of a flat plate glass reactor for mass production of *Nannochloropsis* sp. outdoors. J Biotechnol. 85, 259–269.

Rym B.D., Nejeh G., Lamia T., Ali Y., Rafika C., Khemissa G., Jihene A., Hela O., Hatem B.O., 2010. Modeling growth and photosynthetic response in *Arthrospira platensis* as function of light intensity and glucose concentration using factorial design. J. Appl.Phycol. 22(6), 745-752.

Satyanarayana K.G., Mariano A. B., Vargas J. V. C., 2011. A review on microalgae, a versatile source for sustainable energy and materials. Int. J. Energy Res. 35, 291-311.

Sierra E., Acién F.G., Fernández J.M., García J.L., González C., Molina E., 2008. Characterization of a flat plate photobioreactor for the production of microalgae. Chem. Eng. J. 138(1-3), 136-147.

Teresa M.M., Antonio A.M., Nidia S.C., 2010. Microalgae for biodiesel production and other applications: A review. Renew. Sustain. Energy Rev. 14, 217–23.

Velarde R.R., Urbina E.C., Melchor D.J.H., Thalasso F., Villanueva R.O.C., 2010. Hydrodynamic and mass transfer characterization of a flat-panel airlift photobioreactor with high light path. Chem. Eng. Process. 49, 97–103.

Chapter 2

Review of Literature

2.1. Energy consumption and alternative renewable resources

The global energy consumption has reached approximately 11791 MTOE in 2017, in the form of oil, natural gas and coal. Global substantiate reserves (i.e. oil, gas and coal) are 1696.6 billion barrels (Bb), 193.5 trillion cubic meter (TCM) and 1.035 trillion tons (Tt) respectively. The global consumption of oil, gas and coal is increasing annually at the rate of 1.7%, 3% and 1% MTOE (million tons of oil equivalent) respectively (BP statistical review 2017). Worldwide annual energy requirement of over 12 billion tons of oil equivalent (BTOE) produces around 39.5 Giga tons (Gt) of CO_2 annually. In near future, the global energy demand of 24-25 BTOE will estimate to produce 75 Gt-CO_2 annually (Abas et al., 2015).

Over 85% of the primary energy consumption has been shared by fossil fuels with maximum utilization in the form of oil up to 33% followed by coal 30% and natural gas 24% while remaining is shared by hydroelectricity, nuclear energy and renewable energy (Fig. 2.1). This means around 98.186 million barrels of oil are being utilized per day by the world population, while India alone consumes 4.2% of the total petroleum resources per day (BP statistical review 2017). At current consumption levels, worldwide reserves of oil are expected to exhaust in the next 50 years.

Use of these non renewable resources has also been causing massive damage to the earth in terms of global warming with increasing anthropogenic greenhouse gas emissions (GHG). The world's CO_2 emissions in to the atmosphere are increasing day by day with an increase of 40% was reported in the year 2013 compared to the year 2000. India is the 3rd largest CO_2 emitter country in the earth with 5.5% of total CO_2 released by the world nations (BP statistical review, 2017).

Worldwide oil expenditure proliferates at the average rate of 1.6 million barrels per day (Mb/d), or 1.6%, above its 10-year average (1.2%) for the second successive year. China (400,000 b/d) and India (330,000 b/d) rendered the massive hike during this period (BP statistical review, 2017).

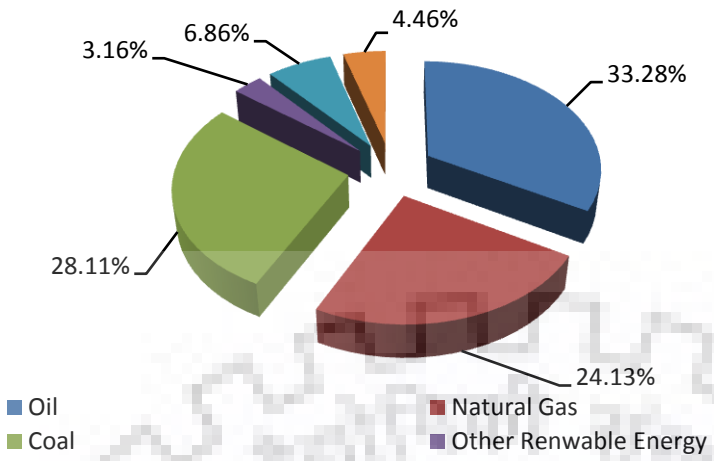

Fig. 2.1. Percentage distribution of world's primary energy consumption (Source BP stasttical Review 2018).

This increasing demand in conventional non renewable energy resources and associated environmental concerns have compelled to look for alternate energy sources which can effectively fulfill the energy fuel demands in a sustainable manner with reduced greenhouse gas emissions (Brennan and Owende, 2010).

2.2. Microalgae as alternative renewable resource

Microalgae are recognized as the most providential species for biodiesel production since they have ability to accumulate high amount of lipid contents within their cells. Photosynthesis process in microalgae converts sun energy into chemical energy (Teresa et al., 2010). Microalgae are classified as unicellular or simple multicellular photosynthetic microorganisms that have ability to sequester CO_2 orderly from multiple provenances such as industrial waste gases, and soluble carbonate salts (Teresa et al., 2010).

Microalgal biomass can be an affluent carbon source that can be employed in biofuels, pharmaceuticals, and cosmetic industries (Khan et al., 2018). They also have capacity to utilize CO_2 and waste water simultaneously, and out-turn different value added products such as polysaccharides, pigments, lipids, proteins, vitamins, bioactive compounds, and antioxidants. Microalgae based biofuels are now expanding as a replacement to the fossil fuels. The lucrative characteristic of microalgal biofuels are renewability and ecofriendliness. Microalgae have the ability to produce algal oil up to 58,700 L/hac (Khan et al., 2018). The low or no sulphur content in microalgal fuel has advantage of zero sulphur emission compared to the petroleum fuels. Most

of the microalgae species are expected to produce high level of biodiesel because of their higher lipid contents (i.e. 50-70%) and may reach to 80% for eg. the microlaga *B. braunii* can accumulate up to 80% of oil in it biomass (Chisti, 2007; Mata et al., 2010).

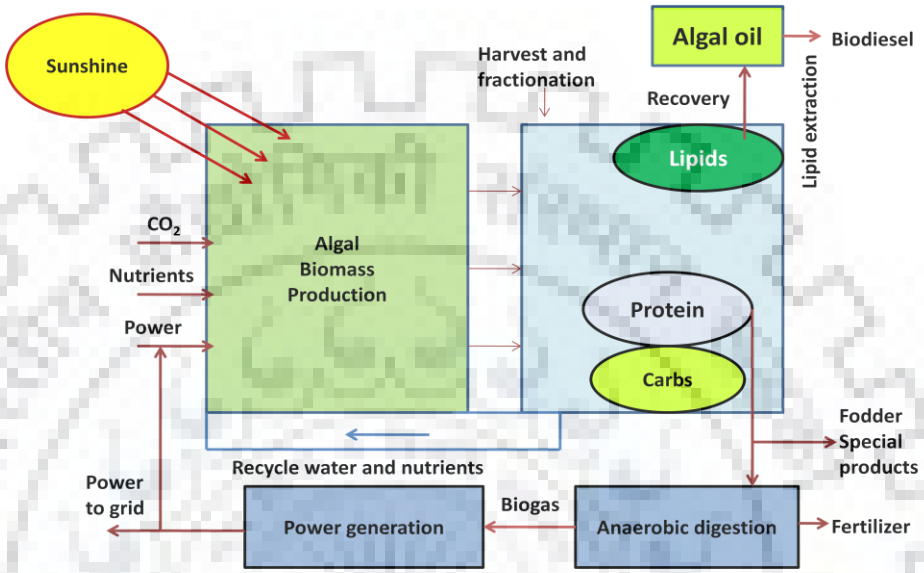

Fig 2.2. A consolidate microalgae bioprocess for the production of alternative renewable energy resource

2.3. Biochemistry of microalgae

2.3.1. Photosynthesis in microalgae

Photosynthesis is an exclusive process that transforms light energy into chemical energy in which photosynthetic apparatus methodically capture CO_2 into organic compounds. The photosynthesis process occurs in two steps light reaction and dark reaction.

2.3.2. Light reaction in photosynthesis

The thylakoid membrane present in chloroplast is the site for the light dependent reaction of photosynthesis. A stack of thylakoids is called a granum which is connected by stromal lamellae. The thylakoid membranes incorporate five crucial complexes: LHC, PS II, PS I, cytochrome b6/f, and ATP synthase, which prolong photosynthetic electron transport and photophosphorylation (Masojidek et al., 2004). The light energy captured primarily by LHC present in PS II and photon induced charge separation reaction released an electron. The movement of electrons in

photosystems PS I and PS II are called as "Z" scheme. In this scheme electron transport reactions progressed energetically downhill (i.e., from a lower (more negative) to a higher (more positive)) according to their redox potential (Masojidek et al., 2004). Two electrons released from water (O_2 evolved) move across the series of electron carriers to produce one molecule of $NADPH_2$. In addition, this creates a pH gradient across the thylakoid membrane to produce ATP in the presence of ATP synthase. This reaction is called photophosphorylation.

2.3.2. Dark reaction in photosynthesis

In the Dark reactions, fixation of CO_2 into carbohydrates occurs in the presence of the RuBisCO enzyme. This process is also called as Calvin-Benson cycle, and it uses $NADPH_2$ and ATP (i.e. produced during photosynthetic light reaction) to carry out the CO_2 fixation (Masojidek et al., 2004). The reaction can be expressed as

$$CO_2 + 4\,H^+ + 4\,e^- \xrightarrow[\text{enzymes}]{2\ NADPH_2, 3\ ATP} \underset{\text{carbohydrates}}{(CH_2O)} + H_2O$$

In this process CO_2 combines with a ribulose 1,5-bisphosphate (i.e. 5-C sugar), and produced two molecules of a glycerate 3-phosphate (i.e. 3-C compound), which further reduced into glyceraldehyde 3-phosphate in the presence of ATP and NADPH that produced during the light-dependent reactions (Masojídek et al., 2004). The sugars produced by this reaction generate carbon skeletons for the production of other metabolites i.e. amino acids and lipids.

2.3.3. Nitrogen metabolism

Nitrogen is considered as most compelling parameter that affects the growth of the microalgae. Nitrogen is required for the generation of the pyrol ring in photosynthetic pigment. The C and N metabolism are interlinked in microalgae (Goncalves et al., 2016). Assimilation of ammonium nitrogen is less energy intensive compared to the assimilation of nitrate nitrogen. Nitrogen metabolism in microalgae is catalyzed by glutamine synthase. This enzyme has higher affinity for ammonia and can readily assimilate it into the cells (Enamala et al., 2018). The freely available ammonium (NH4 +) coupled with the inorganic form to synthesize the amino acids. Furthermore, a carbon skeleton is required to form a keto acid and the energy is released as ATP, which is

required to produce different amino acids like glutamate, aspartate, glutamine (Goncalves et al., 2016; Enamala et al., 2018).

2.3.4. Biosynthesis of Fatty Acids

Plastid is the elementary cite for biosynthesis of lipid in microalgae. In fatty acid biosynthetic pathway, the production of malonyl-CoA from acetyl-CoA in the presence of acetyl-CoA carboxylase (ACCase) enzyme is considered as the first step of this pathway. In addition, this step is considered as the rate limiting step of the fatty acid biosynthetic pathway. Furthermore, the multi-enzymatic complex subunit of fatty acid synthase (FAS) is malonyl-CoA ACP transacylase, which transferred malonyl-CoA to an acyl-carrier protein (ACP) and formed a malonyl-acyl-carrier protein (molonyl-ACP). The malony-ACP enters a cycle of condensation, reduction, dehydration, and again reduction reactions to form 16- or 18-carbon fatty acid. Moreover, this fatty acid converted into glcerolipid in the presence of either acyl-ACP thioesterase or plastidic acyltansferase (Joyard et al., 2010). In the plastid, the available free fatty acid is thereafter converted to the acyl-CoA molecule by long-chain acyl-CoA synthetases. The evolved acyl-CoA molecules during this reaction further transferred to the endoplasmic reticulum (ER) by the aid of cytosolic acyl-CoA binding proteins (ACBPs) (Hao et al., 2017).

2.3.5. Biosynthesis of TAGs

ER or the chloroplast is the major cite for the glycerolipid biosynthesis pathway. Microalgae store lipid in the TAG form via the Kennedy pathway. TAG biosynthesis pathway commences with two successive transfer of acyl group from acyl-CoA to glycerol-3-phosphate at positions 1 and 2, to produce lysophosphatidic acid and phosphatidic acid (PA) (Hao et al., 2017).

Glycerol-3-phosphate acyltransferase (GPAT, EC 2.3.1.15) and lysophosphatidic acid acyltransferase (LPAAT, EC 2.3.1.51) enzymes catalyzed these reactions in ER while in the chloroplast membranes these reactions are catalyzed by ATS1 and ATS2 (Hao et al., 2017). The chloroplastal phosphatidylglycerol phosphate synthase enzyme converted phosphatidic acid into phosphatidylglycerol (PG) whereas phosphatidate phosphatase dephosphorylated the phosphatidic acid to generate 1,2-diacylglycerol (DAG). The other enzymes present in the chloroplastal membrane are monogalactosyldiacylglycerol synthase digalactosyldiacylglycerol synthase and sulfoquinovosyl transferase.

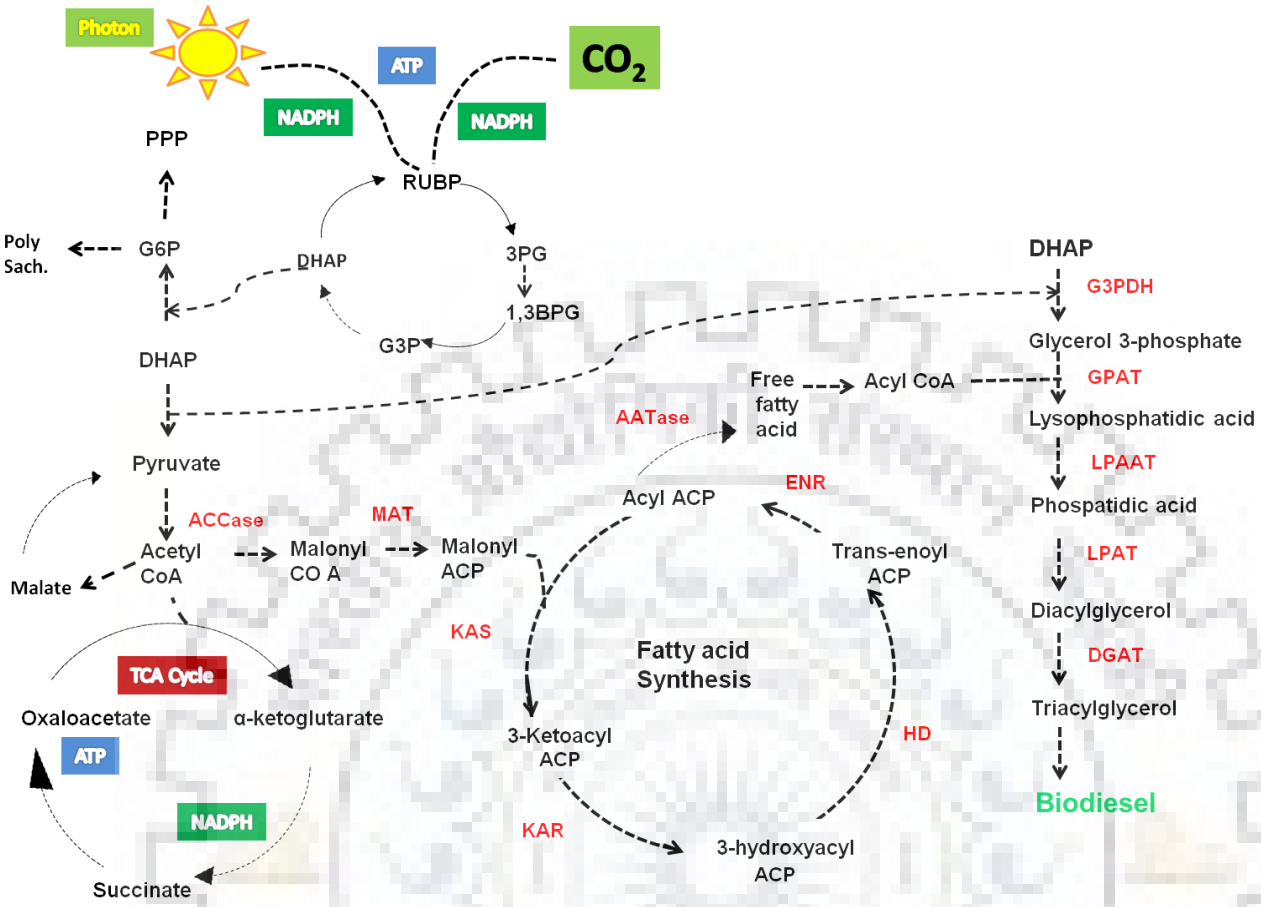

Fig. 2.3. Central metabolic pathways in the microalgae showing the fatty acid and triacyl glycerol biosynthesis along with photosynthetic carbon fixation and tri carboxylic acid cycle. ACCase acetyl co-A carboxylase; ACP acyl carrier protein; CoA coenzyme A; DGAT diacylglycerolacyltransferase; DHAP dihydroxyacetone phosphate; ENR enoyl ACP reductase; AATase Acyl-ACP thioesterase; G3PDH glycerol-3-phosphate dehydrogenase; GPAT glycerol-3-phosphate acyltransferase; HD 3-hydroxyacyl-ACP dehydratase; KAR 3-ketoacyl-ACP reductase; KAS 3-ketoacyl-ACP synthase; LPAAT lyso-phosphatidic acid acyltransferase; LPAT lyso-phosphatidyl choline acyltransferase; MAT malonyl-Co A:ACP transacylase; RuBPRibulosebis-phosphate; 3PG 3-phosphoglycerate; 1,3BPG 1,3-bis-phosphoglycerate; G3P glyceraldehyde-3-phosphate; G6P glucose-6-phosphate.

Furthermore, these enzymes subsequently catalyze DAG into monogalactosyldiacylglycerol (MGDG), digalactosyldiacylglycerol (DGDG), and sulfoquinovosyldiacylglycerol (SQDG) respectively (Hao et al., 2017). DAG is further converted into to TAG by the DAG acyltransferase following the canonical Kennedy pathway.

2.4. Mode of nutrition

2.4.1. Phototrophic cultivation

In phototrophic mode of nutrition microalgal cell employ light energy as their energy source whilst carbon source was derived from inorganic CO_2 to synthesize the organic compounds via photosynthesis (Huang et al., 2010). Industrial scale cultivation of microalgae in photobioreactor systems extensively use phototrophic mode of nutrition since there is less possibility of being contaminated by external pathogens or organisms (Chen et al., 2011).This is most prevalent mode of nutrition for microalgae growth (Yoo et al., 2010). The considerable advantage of employing phototrophic mode of nutrition is the utilization of CO_2 as a carbon source for biomass growth and lipid production.

2.4.2. Heterotrophic cultivation

A heterotrophic cultivation is defined as cultivation of microalgae in the organic substrate medium under dark conditions. Here, organic substrate is exclusive source of both the energy and carbon source for microalgae growth (Chojnacka and Marquez-Rocha, 2004). Heterotrophic cultivation of microalgae generally achieved higher biomass and lipid productivity compared to the phototrophic cultivation conditions. The lipid content of certain microalgae is highly affected by the mode of nutrition, and a 40% upsurge in the lipid content was observed in *Chlorella protothecoides* under heterotrophic culture conditions in comparison to the phototrophic cultural conditions (Xu et al., 2006). The other advantage of heterotrophic cultivation includes elimination of bioreactor design modification for their growth. Heterotrophic culture conditions can easily achieved in existing bioreactor system (i.e CSTR). Microalgae can utilize various organic substrates (such as glucose, glycerol, acetate, galactose etc) for growth (Liang et al., 2009). Heterotrophic cultivation systems attained much higher biomass and lipid productivity compared to the phototrophic cultivation systems. However, the organic substrate based heterotrophic systems usually encounter frequent contamination problems (Chen et al., 2011).

2.4.3 Photoheterotrophic cultivation

Photoheterotrophic cultivation of microalgae requires light and organic substrate for their growth. Notably, light is act as energy source for photoheterotrophic cultivation whilst the carbon source is provided by the organic substrate in these systems. Utilization of light as the energy source in the

presence of organic substrate is the only difference between heterotrophic and photoheterotrophic cultivation of microalgae (Chojnacka and Marquez-Rocha, 2004). The photoheterotrophic cultivation system is generally associated with the production of certain light – regulated metabolites along with the biomass and lipid production.

2.4.4 Mixotrophic cultivation

In mixotrophic cultivation microalgae utilizes light, organic substrate and inorganic carbon (i.e. CO_2) simultaneously for their growth. In mixotrophic cultivation system organic substrate and inorganic carbon (i.e. CO_2) both provides the carbon source for microalgae growth whilst light is required for energy source to carry out photosynthesis. Notably, the photosynthetic process and oxidative metabolism occurs simultaneously under mixotrophic cultivation conditions (Liu et al., 2009). The specific growth rate obtained in mixotrophic culture is greater than the sum of specific growth rates in photoautotrophic and heterotrophic cultures (Chojnacka and Noworyta, 2004; Liu et al., 2009). Light limitation is no longer issue in mixotrophic conditions since microalgae growth in these conditions generally requires low irradiance and the consumption of organic substrate is more dominant (Ogbonna and Tanaka, 2000). Therefore, some microalgae in mixotrophy grow faster than in either heterotrophy or phototrophy. Moreover, the biomass and lipid productivity in mixotrophic conditions are higher than other cultivation systems (Kim et al., 2012; Liang et al., 2009; Zhang et al., 2011). Due to rising demand in mass cultivation of algae, mixotrophic cultivation could be a prospective technology for algal production.

2.5. Microalgae cultivation systems

2.5.1. Open ponds

Open pond cultivation systems (raceway ponds, circular ponds and unstirred ponds) are extensive and cost competent systems used for mass cultivation of microalgae (Ho et al., 2011). Raceway pond systems are recognized as most prevailing artificial system for the large scale cultivation of microalagae. A raceway pond is a shallow and elongated close loop with a recirculating flow channels. They are typically constructed with a rotating paddlewheel which allows proper mixing and slow recirculation of nutrient media in order to sustain better algal growth and productivity. Operating a raceway pond system is comparatively easy and economical with respect to the closed photobioreactor systems. These systems entail small power inputs and are simple to clean and

maintain (Ugwu et al., 2008). However, the considerable restrain include indigent light usage by microalgal cells, evaporative water loss, low mass transfer, CO_2 diffusion into the environment and extensive space prerequisite. Moreover, contaminations from other microorganism may repercussion of non axenic culture growth, and confine the mass cultivation of algae in open pond system. In addition, inept stirring consequently leads to low mass transfer rate and subsequently reduced the biomass productivity. The contemporary advancement in raceway open system technology comprises effective mixing system to avert the settling of algal biomass and to increase effective light penetration efficiency.

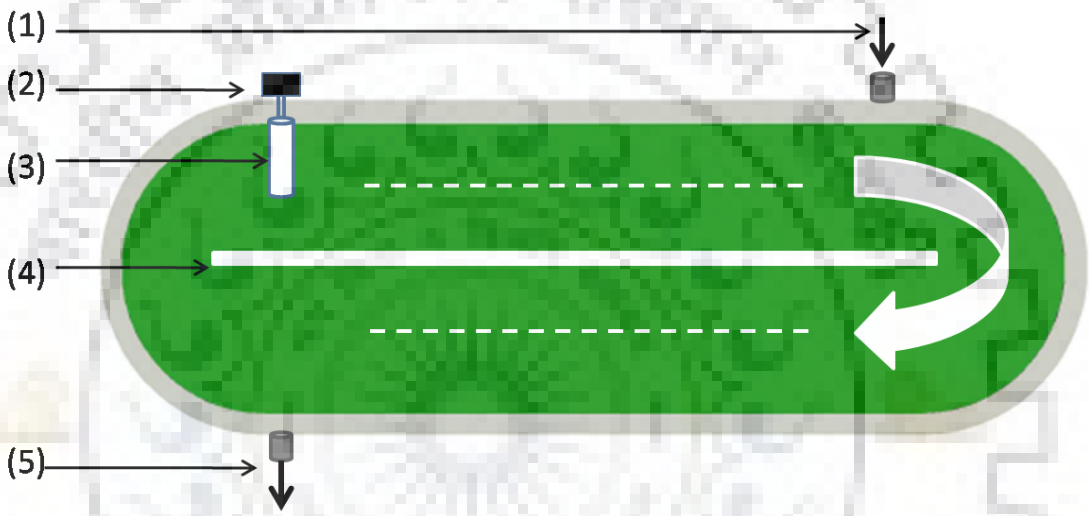

Fig.2.4. Schematic representation of open raceway pond and the nomenclature as follows (1) Inlet, (2) Motor, (3) Paddle, (4) Divider, (5) Outlet.

2.5.2. Closed systems

Closed systems are devised to conquer the issues (i.e. low mass transfer, indigent light utilization, CO_2 diffusion to the environment etc.) related to the open pond cultivation technology. A photobioreactor is a close vessel for photosynthetic cultivation of algae in a well controlled environment under the influence of artificial lighting system (Andersen, 2005). Notably, PBR systems have other benefits of uniform light distribution, homogenous mixing, efficient mass transfer, lower contamination exposure, and considerable large surface area in contrast to the conventional open pond systems (Grima et al., 1999, Sierra et al., 2008). However, the scaling up of PBRs features reasonable constraints regarding effective light penetration, mass transfer, growth control variables, and biomass dispersion systems (Grima et al., 1999).

Generally close system PBR can be categorized into different type of reactors based on their mode of operation. Such as surface irradiant, PBR are classified as flat plate (Sierra et al., 2008; Slegers et al., 2011), tubular (Molina et al., 2001), and column (Eriksen, 2008) while based on liquid flow mode, PBRs can be sorted into stirred type, bubble column and airlift reactor (Gupta et al., 2015). In addition, the following section describes different types of PBRs systems.

2.5.2.1. Stirred tank PBRs

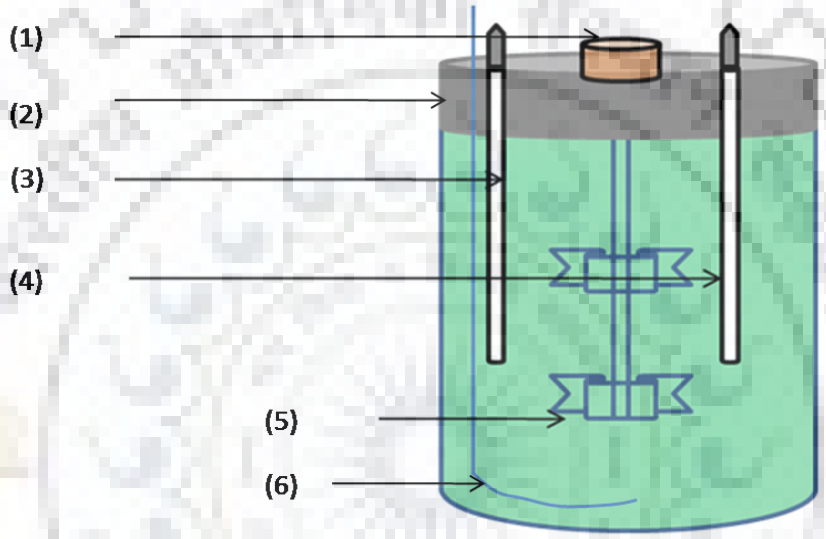

Fig. 2.5. Schematic representation of CSTR and the nomenclature as follows (1) Motor, (2) Head Plate, (3) pH probe, (4) Temperature probe, (5) Impeller, (6) Sparger.

Stirred tank PBRs are the typical CSTR surrounding with the well controlled illumination chamber. The stirred tank PBRs consists of a transparent reactor wall, a central shaft, impellers and baffles. The various functions of the different parts of stirred tank PBR includes: 1) the transparent reactor wall provide effective light penetration to the microalgae culture. 2) A central shaft is required to grip the impellers for mechanical agitation. 3) Impellers administer effective aeration, mixing, heat and mass transfer in reactor. 4) Baffles are used to reduce the vortex formation in the stirred tank reactor (Doran, 2013). The main advantage of stirred tanks PBRs is the adequate agitation mechanism which reduces extent of dark zones in the reactor and enhances the mass transfer rates and light diffusion for microalgal growth (Gupta et al., 2015). However, the drawback of this system is small SA/V ratio, which subsequently reduces the light harvesting efficiency (Franco-Lara et al., 2006).Moreover, in these systems, the heat generation rate due to

mechanical agitation is higher than the air sparging based PBR systems; hence scaling up of stirred tank PBRs are not economically and commercially viable.

2.5.2.2. Vertical column photobioreactors

Vertical column photobioreactors are contemplated as most convenient system for mass microalgae cultivation because of their low shear stress and high surface area. These photobioreactors are constructed of transparent tubes that enable effective light infiltration. Mixing in the vertical column reactors are provided by the compressed air only because mechanical agitation is absent in these reactors. Vertical column PBRs can be grouped into bubble column and airlift reactors, based on their liquid flow mode.

2.5.2.2.1. Bubble column photobioreactor

Bubble column photobioreactors are simple vertical column reactor, in which air sparging based gas dispersion system provides the effective mixing for the mass cultivation of microalgae. The design of bubble column PBR system is quite simple, with height to diameter ratio is 2:1. The sparger is the only component presents inside the bubble column and no other internal structure is required to design the bubble column PBRs. In bubble column reactor perforated horizontal plate are used above the sparger to disintegrate and reshuffle the coalesced bubbles. Bubbles discharged from the sparger determined the mass transfer and hydrodynamics features of the reactor. At lower air flow rates, bubbles are uniformly disbursed across the column cross section and the back mixing is vanished.

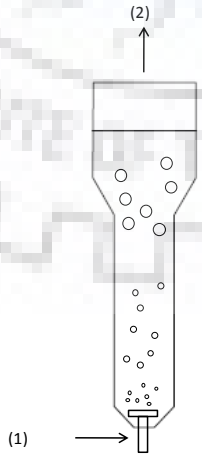

Fig. 2.6. Bubble Column PBR and the nomenclature as follows (1) Gas Input, (2) Gas Output for respectively (adapted from Singh et al. 2012).

Hence, the low air flow rates provide the homogenous flow in these reactors. While at high flow rates, bubbles and liquid upswing up the column center, and a corresponding downward movement of liquid appears adjacent to the reactor walls. This continuous dispersal of liquid entrains bubbles, and creates some back mixing which leads to heterogeneous flow in the reactor at high flow rates (Doran, 2013).

Bubble column PBR typically used either internal or external illumination system for algal growth. At higher gas flow rates effective liquid circulation creates a central dark zone and external photic zones inside the reactor. This continuous movement of microalgae into the light and dark zone is known as flashing light effect. The photosynthetic efficiency of bubble column PBR is depends on these light and dark cycles at a high air flow rate (Barbosa et al., 2003). The advantages of bubble column PBRs includes low cost, high SA/V ratio, effective heat and mass transfer, comparative congruent culture environment, and the adequate removal of oxygen and superfluous gas mixtures (Gupta et al., 2015).

2.5.2.2.3. Airlift PBRs

Airlift PBRs are modified form of the bubble column PBRs by introducing a central draft tube and physically separates the liquid circulation in two pertinent region the riser (up comer) and the down comer regions (Fig. 2.6). Air is introduced via the riser zone, and the emerging gas holdup reduce the density of the liquid. Then, eventually the less dense fluid in the riser zone proceed upwards and gas bubbles extricate from the liquid surface, resulting in recirculation of heavier bubble-free liquid across the down comer zone. In particular, this bubble distribution scheme in airlift reactors continuously creates light and dark phases providing a flashing light effect to microalgal cells (Barbosa et al., 2003). The airlift PBRs are of 3 types:

1) Internal loop vessels: In these types of reactors a baffle is introduced in the center of the reactor to separate the riser and down comer zone.

2) Internal loop concentric reactor: A concentric draft tube is inserted in the center of reactor, through which the gas is sparged. This result in liquid circulation from riser area (dark section) to the down comer (irradiate section), thereby administer algal cells to face alternate light and dark cycles (i.e. flashing effect).

3) External loop reactors: vertical tubes are associated with an external loop (as a ‘C’ section). Since the up comer and down comer zones are distantly related, gas departure is highly efficient.

Accordingly, mixing in this reactor is comparatively better than the internal loop reactors (Doran 2013).

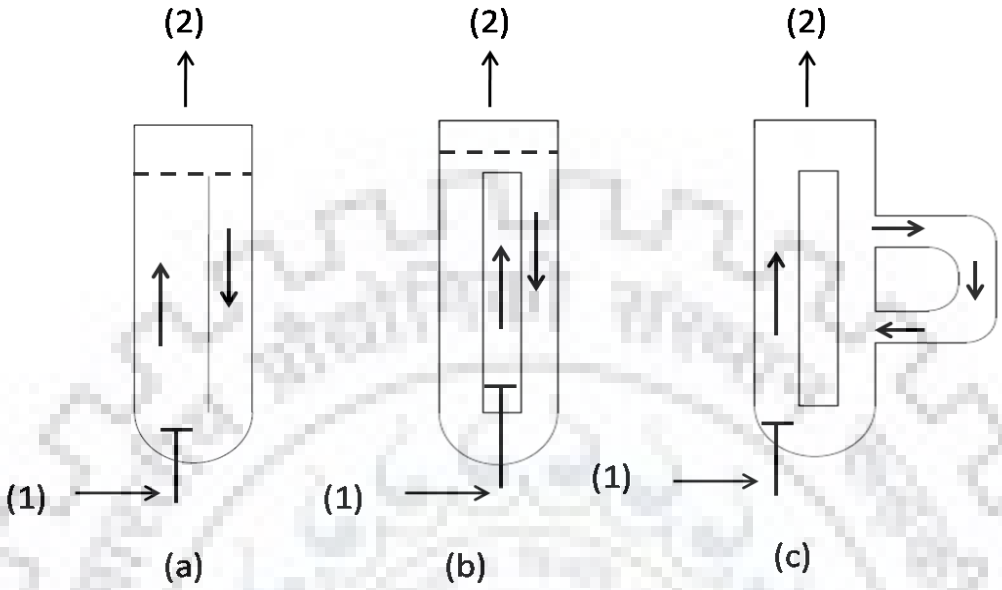

Fig. 2.7. Schematic representation of Airlift PBR and the nomenclature as follows (1) Gas Input, (2) Gas Output for (a) Internal loop vessels, (b) Internal loop concentric reactor and (c) External loop reactors respectively (adapted from Singh et al. 2012).

2.5.2.3. Tubular PBRs

2.5.2.3.1. Horizontal tubular

Horizontal tubular PBRs are slightly different from bubble column in many ways, such as higher A/V ratio and gas dispersion. The homogeneous fluid movement, internal irradiance levels and the effective gas–liquid mass transfer in tubular reactor have advantage of better mixing compared to the bubble column reactors (Sánchez Mirón et al., 1999). Tubular photobioreactor features substantial illumination area for adequate biomass and lipid production in cost effective manner comparative to the other systems. The limitations of tubular PBRs includes: non-uniform mass transfer in radial directions resulting in inconsistent temperature and CO_2 distributions eventually lead to dissolved oxygen accumulation (Gupta et al., 2015). The scale up of tubular PBRs is not commercially feasible due to its large space requirement. Moreover, the cooling of these reactors is also problematic as they have high SA/V ratio. Furthermore, the photo inhibition which is caused by surface biological deposition will lead to difficulty in cleaning the tubes.

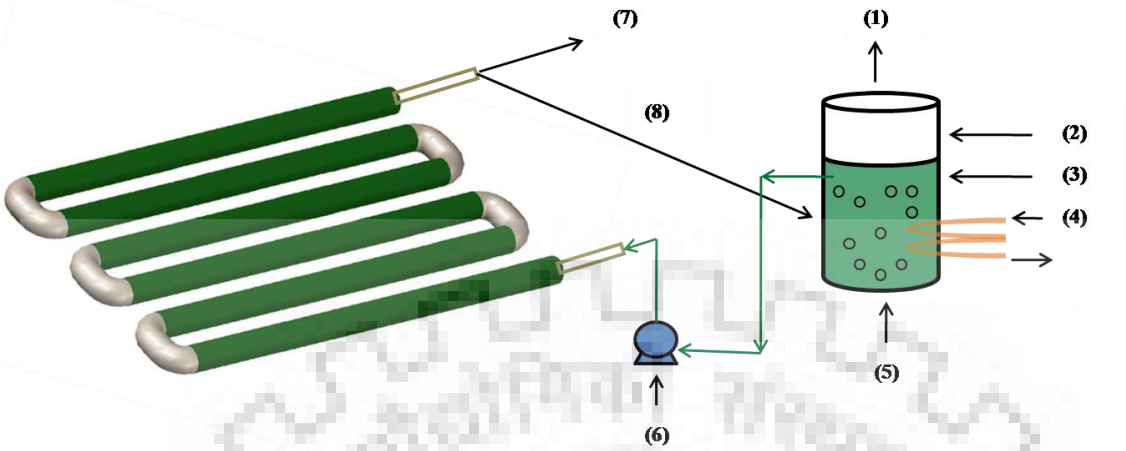

Fig. 2.8. Working of a horizontal tubular photobioreactor nomenclature as follows: (1) Exhaust, (2) Degassing column, (3) Fresh medium, (4) Cooling water, (5) Air, (6) Pump, (7) Harvest, (8) Recycle

2.5.2.3.2. Vertical tubular photobioreactor

Vertical tubular photobioreactor implements higher association of the irradiance and microalgae culture. The effective gas residence time increase the nutrient utilization efficiency in the vertical tubular photobioreactors (Henrard et al., 2011). Vertical tubular photobioreactors are fabricated as transparent tubes in which the culture is disseminated at 0.5 m s^{-1} liquid velocities (Norsker et al., 2011).

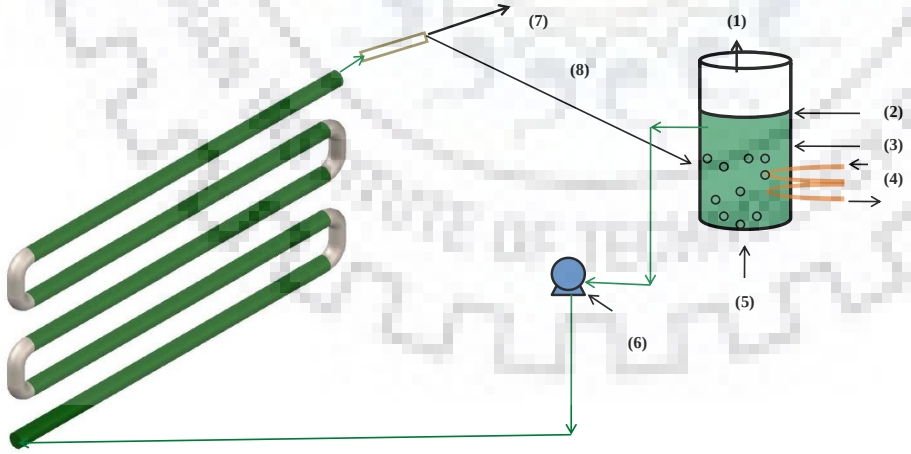

Fig. 2.9. Working of a vertical tubular photobioreactor nomenclature as follows: (1) Exhaust, (2) Degassing column, (3) Fresh medium, (4) Cooling water, (5) Air, (6) Pump, (7) Harvest, (8) Recycle.

In addition, a degasser is connected to prevent high O_2 accumulation in the reactor. The disadvantage of vertical tubular photobioreactors is higher construction cost compared to the open raceway ponds which limits its application for mass cultivation.

2.5.2.4. Flat panel PBRs

Flat panel PBRs are constructed of transparent flat plates arranged in a rectangular manner to maximize the light utilization efficiency for algal growth. Liquid circulation in flat panel PBRs is achieved by sparged gas produced from the bottom attached sparger in the reactor. The distinctive features of flat panel PBRs are high SA/V ratio, low shear stress due to absence of any mechanical device, and effective light penetration. Flat Panel Photobioreactor is generally consists of rectangular plates with small interval between them to use optimal light energy for mass cultures of algae (Carvalho et al., 2006).

A Flat Panel photobioreactor can be divided into 3 zones. (i)The region instantly near to the irradiate reactor facet is a known as photic zone where light saturation and consequent photo inhibition of algal growth frequently occurs. This photo-inhibition diminishes photosynthetic productivity that can adversely affect the lipid production through algae. (ii) In light limited region cell absorption at a specific point reached a balance state with the input light intensity. (iii) stagnant region is the lowest light intensity zone which is insufficient to sustain the microalgae growth (Wang et al., 2014).

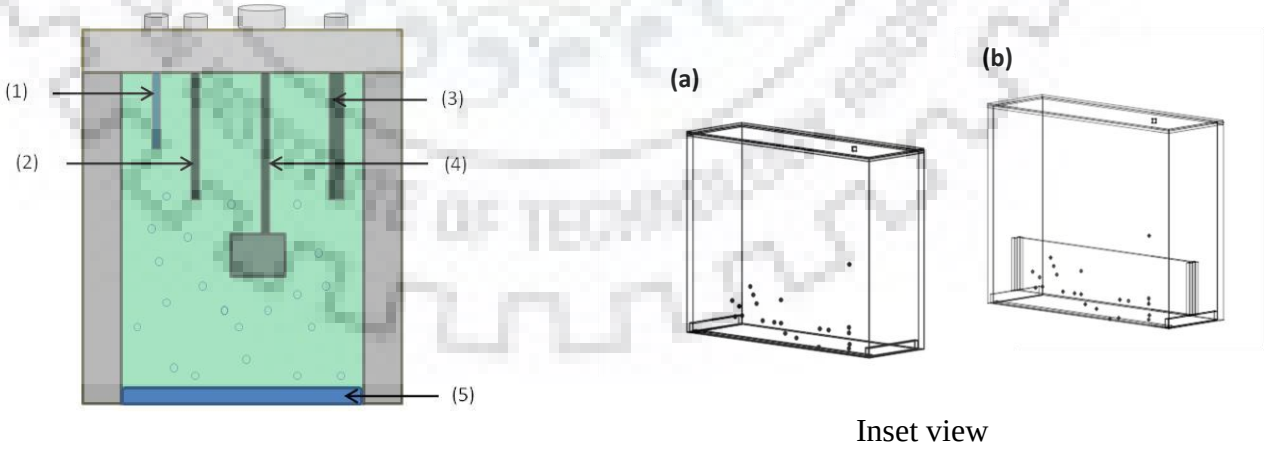

Fig. 2.10. Schematic diagram of flat panel photobioreactor and the nomenclature as follows (1) pH probe, (2) Temperature probe, (3) Heating or cooling coil, (4) Online biomass monitor, (5) Porous type sparger. Inset view: (a) Flat panel bubble column, (b) Flat panel airlift Photobioreactor.

In Flat panel airlift PBR low values of light path has to be maintained which results in large SA/V and height/light path ratios. Flat panel airlift PBR with higher light paths adequately use light supply to cover nutritional requirements of photosynthetic microorganisms. The utility of high path length flat panel PBRs are the reduction of manufacturing costs and less energy dissipation during operation (Velarde et al., 2010). As self shading of microalgae in photobioreactor reduces light utilization efficiency of the organism (Gupta et al 2015). Light distribution in flat panel photobioreactor is a critical factor affecting process productivity of photosynthetic organism.

Photobioreactor design criteria depend upon the effective mixing and evenly distributed light profile inside the photobioreactor. Therefore, new designs of high light path photobioreactors are required for efficient light utilization, with low energy expenditure, and have sufficient mass transfer rates for higher biomass production. Therefore, enhancing the irradiance by altering the reactor dimensions was considered as a compelling approach to boost the biomass productivity (Gupta et al 2015). Furthermore, optimization of the light path length for higher reactor productivity paved the path to establish ultrahigh cell density cultures.

2.6. Factors affecting microalgae growth

2.6.1. Light

Light can be simultaneously behaved as particle or wave in nature. The electromagnetic spectrum of radiation (Fig) varied with different wavelength regions and corresponding energy content stored in their individual quanta. The high energy content in ≥380 nm wavelength brings ionizing effects after its absorption, whilst the low energy content in radiation of ≤750 nm is insufficient to produce chemical transformations and brings the thermal effects after its absorption. The region between 380 and 750 nm, the energy content is sufficient to mediate photochemical changes in microalgae to produce organic compounds. Therefore, visible light region is the major energy for photosynthesis in microalgae (Carvalho et al., 2010).

Light intensity is considered as one of the most significant variable for microalgae growth in photobioreactor. Optimization of light availability to the microorganism in PBR is a compelling facet for biomass and process productivity (Kandilian et al., 2014). The microalgal growth is highly influenced by light intensity, its duration, and the type of wavelength inside the PBR (Carvalho et al., 2010). Inadequate light penetration and transfer are the key factors affecting the

photobioreactor performance. Light intensity distribution inside the PBR is an imperative characteristic for photobioreactor design.

Photobioreactor process productivities are affected by suboptimal light supply, effective light penetration and limiting biological efficiency. Suboptimal light availability reduced the photobioreactor process productivity and excessive light intensity cause photo-oxidative damage to PSII unit of microalgae (Kandilian et al., 2014). Light penetration and supply inside the photobioreactor is most challenging task (Kandilian et al., 2014). Low Light energy conversion efficiency is the main bottleneck in scale up photobioreactor. Light diffusion across the photobioreactor highly depends upon the absorption and scattering phenomena of microalgae cell concentration. An accurate prediction of radiative transfer model requires absorption, scattering coefficient and scattering phase function of microalgae in photobioreactor (Lee et al., 2014).

2.6.2. CO_2

CO_2 fixation ability of microalgae is recognized as an additional advantage of mass cultivation of microalgae to produce bio-oil and other value added products (Yoo et al., 2010). Microalgae have ability to capture CO_2 in their exponential growth phase and can be instantly consolidate into engineered photobioreactors systems for their rapid growth (Carvalho et al., 2006). CO_2 biosequestration efficiency of microalgae is reliant on light intensity, temperature, CO_2 concentration, pH, nutrients ratio, gas flow rate, and photo-bioreactor type. As microalgae grow efficiently at neutral or alkaline cytosolic pH, and many pH dependent enzymes turns into inactive state under acidic pH. CO_2 mass transfer in photobioreactor increased at high CO_2 concentration but diminish the microalgae growth due to reduction in pH at high CO_2 concentration.

2.6.3. Temperature

Temperature is advised as compelling parameters but also considered as intricate factor to optimize in large scale cultivation of algae in photobioreactor or open pond cultivation system. The temperature usually regulates various physiological, morphological, cellular and biochemical responses of microalgae cultures (Kalita et al., 2011) including CO_2 biosequestration (Mohan et al., 2015). Daily temperature variations can reduce the cell volume and lipid production efficiency of microalgae. The optimum temperature for algal growth may vary in between 20ºC to 30ºC

(Venkata et al., 2014). Temperature tolerance of various algal species up to 15ºC lesser than their optimum, with decreased growth rate, whilst a few degree higher temperatures can be detrimental to algal cells due to inhibition of the respiration metabolism. However, low evening and low seasonal temperatures naturally decrease the biomass productivity (Griffiths et al., 2011). In addition, the favorable temperature and light intensity for the strain of *B. braunii* is in the rage of 20ºC-30ºC and 33–400 µmol m^{-2} s^{-1} respectively (Singh and Singh, 2015; Lee et al., 2011).

2.6.4. pH

The pH of the nutrient medium has a crucial asopect in the algal growth. The pH is essential for the ion uptake within the microalgae for their optimum growth. In addition, the pH regulates phosphorus availability, metabolic enzymatic activity, inorganic carbon availability and ammonia toxicity of the photosynthetic microalgae (Khalil et al., 2010; Ho et al., 2014; Cornet et al., 1995; Havlik et al., 2016). Moreover, alkaline conditions favor more CO_2 sequestration from the environment and yield increased biomass (Li et al., 2011). The pH progressively upturns to basic as the algal growth prevails in the growth medium, a rapid enhancement in photosynthetic process and OH- ions aggregation occurs during this process (Mahapatra et al., 2012). pH evolution during photosynthesis effect the carbon dioxide species distribution, carbonic anhydrase enzyme activity and carbon capture mechanism(Concas et al., 2012). In neutral pH condition hydrogen ion is non-competitive inhibitor whereas at very high or very low pH conditions it can limit photosynthetic growth or substrate utilization. Several studies suggested that at low pH level the microalgae growth is limited. But, at high pH stress inhibition of cell cycle prevails that triggers the lipid biosynthetic pathways, which further augments the lipid quality of the microalgae (Breuer et al., 2013; Santos et al., 2012; Gardner et al., 2011).

2.6.5. Nitrogen

Nitrogen is an essential factor to determine the microalgae growth. The key role of nitrogen in metabolic pathways includes biosynthesis of chlorophyll, proteins and nucleic acids. The medium nitrogen concentration affects the microalgae growth rate and their biochemical compositions (Wang et al., 2013). Several studies suggest that nitrogen limited nutrient conditions slows down microalgae growth rate and reduce protein synthesis whilst enhance their lipid or carbohydrate content (Ho et al., 2014). Most of the microalgae are adept to use different forms of nitrogen (i.e. NO_3^-, NO_2^-, NH_4^+ and urea) for their growth (Becker, 1994). Each nitrogen source primarily

transformed into the ammonium ion and incorporated it into amino acids via different metabolic pathways (Cai et al., 2013). Generally, ammonium is recognized as most desirable nitrogen source by most the microalgae, as it require less energy to assimilate ammonium into amino acid, but certain microalgal species such as *B. braunii* and *D. tertiolecta* grow effectively in nitrate containing growth medium compared to the ammonium rich nutrient medium (Chen et al., 2011, Ruangsomboon, 2015).

2.6.6. Salinity

Salinity of the nutrient medium is recognized as another salient parameter that affects microalgae growth. High saline growth medium induce osmotic shock within microalgae cell and release several osmo-protective solutes in the growth medium (Vuppaladadiyam et al., 2018). These osmotic stresses are not beneficial for microalgae growth and alter the cellular metabolism within algal cell. In some high salinity tolerant microalgae species such as *Dunaliella* sp, the carbon fluxes of their metabolic pathway regulate between cytoplasm and chloroplast for glycerol synthesis and starch production respectively. The salinity tolerance is a crucial facet to scale down fresh water requirements (Vuppaladadiyam et al., 2018).

2.7. Harvesting of algal biomass

Harvesting is defined as the separation of algae from the suspended nutrient growth medium. Selection of the effective harvesting process is both density and product dependent. The microscopic cell structure (3–30 μm) of algae makes the harvesting process quite difficult. The different methods of algal harvesting describe as follows:

2.7.1. Filtration

Filtration is a described as a separation of liquid and solid phases from the heterogeneous mixtures different phases. Membrane filtration is most commonly considered as clean (i.e. without chemicals) filtration process in which water can be recycled in the absence of coagulant (Enamala et al., 2018). Filtration efficiency of these systems can be enhanced by vacuum pressure (Greenwell et al., 2010). But membrane filtration is a lavish operation due to essential membrane restitution process. Membrane filtration is inconvenient for large scale objectives because membrane fouling and clogging significantly increase the process cost (Enamala et al., 2018)

2.7.2. Flocculation

Flocculation is determined as aggregation of algal cells into large particles. A negatively charged microalgal cell usually avoids cell aggregation, so a flocculent (i.e. multivalent cations or cationic polymer) is required to neutralize the negative charge present on the microalgal cells surface to facilitate flocculation (Enamala et al., 2018). Flocculation is categorized in two different types: auto flocculation and chemical flocculation. In auto flocculation or bioflocculation microalgal cells immediately aggregates and settle down in the pond extremity (Pittman et al., 2011). Chemical flocculation incorporates additional chemicals or ions to activate the flocculation process (Chen et al., 2011).

2.7.3. Centrifugation

Centrifugation process implicates the centrifugal forces to separate solid particle (i.e algal biomass) from the suspended heterogeneous mixtures. Microalgal cell sedimentation will enhance under high gravitational field (Pittman et al., 2011). This technique is more useful due to its readiness, quick, non-disruptive and universal nature (Chen et al., 2011). In large scale recovery process centrifugation technique require more energy consumption which makes this method economically unviable.

2.7.4. Flotation

Flotation process is defined as an inverted sedimentation process in which gas bubbles pass across a liquid-solid suspension. Therefore, microalgal cells adhere to the gaseous bubbles and subsequently float to the medium surface (Sharma et al., 2017). This process also removes volatile organic compounds from solution. In flotation method, particle size determined the efficiency of the process, smaller particle size easily rise to the surface of the medium by the gaseous bubbles. This technique can be applied with particle sizes of less than 500 μm.

2.7.5. Gravity sedimentation

Gravity sedimentation characterized as settling of microalgal cell under gravity, and is based on stokes law. This is primitive and energy efficient process which is advisable for comparatively larger species. The disadvantages of this method are such as cumbersome, time intensive, and possibility of product degradation (Bosma et al., 2003).

2.7.6. Electrophoresis

Electrophoresis harvesting method implied electric field to separate negatively charged algal species. In this method algal cells are concentrated by moving towards positive electrodes under the influence of electric field. These aggregated algal cells on electrode surface can be easily separate out. Thus, electrophoresis harvesting method is chemically free harvesting method in which biomass is recovered efficiently from heterogeneous solution mixture (Sharma et al., 2017).

2.8. Algal oil Extraction Processes

2.8.1. Mechanical Approach

Mechanical methods perceived as an adequate approach because it is independent of processed algal species and least expected to produce contaminated lipid extracts and other bioproducts. However, these methods contemplate as energy intensive process compared to the other extraction methods. Moreover, mechanical disruptions generate heat that can be harmful for the end products. Therefore temperature controller system is required for the extraction of heat-sensitive products. The high input energy and requirement of temperature controller system eventually increase the operational cost (Lee et al., 2012).

2.8.1.1. Expeller Press

Expeller press or oil press is an efficient mechanical crushing method which is used for used for extracting oil from algal biomass (Demirbas, 2009). In this method the high mechanical pressure is applied to crush and break the algal cells, and eventually extract the oil form the algal biomass. The optimum pressure range revamps the extraction adaptability of the process. Whilst extreme pressure consequently results in curtailed lipid yield and increase the heat production during the process (Ramesh, 2013). The major drawbacks of the press methods are cost intensive, prolonged processing times, prerequisite of proficient labor, and less efficient in contrast to the other extraction methods (Ramesh, 2013).

2.8.1.2. Bead Beating

In bead beating process spinning of the fine beads along with the biomass slurry under the influence of high speed is required for direct cell disruption (Lee et al., 1998; Geciova et al., 2002). Therefore, the cell disruption occurs due to collision of these grinding beads with the algal cells. In

addition, these consolidate events of collision, agitation and bead grinding creates an efficient cell disruption process (Lee et al., 2012). Noteworthy, this process does not require removal of water from the algal slurry which subsequently reduces the process cost.

2.8.2. Osmotic Shock Method

Osmotic shock method perturbs the algal cell wall by fluctuating the salt concentrations of the aqueous media; this can disturb the osmotic pressure between the exterior and interior of the algal cells. This method is considered as most elementary, accessible and adequate oil extraction method from microalgae (Yoo et al., 2012; Kim and Yoo, 2013).

Osmotic stresses can damage the algal cell in two different ways

1) Hyper-osmotic: It occurs at higher exterior salt concentration in which water content inside the cell diffuse outwards. Hyper-osmotic stresses causes damage to the cell envelope which eventually results in cell shrinkage

2) Hypo-osmotic stress occurs at lower exterior salt concentration in which water content flows into the cell and cell become swell or burst. This is the most prevalent method to produce intracellular products from microorganisms.

2.8.3. Isotonic Extraction Method

Isotonic extraction method uses ionic liquid instead of toxic organic solvents to separate oil from the algae. Ionic liquids are mixtures of a large asymmetric organic cation and an inorganic or organic anion in non-aqueous salt solution. Solvent specificity (i.e. polarity, hydrophobicity, conductivity, and solubility) of the ionic liquid can be modified by using specific combination of the cation and anion according to the desirable extraction requirements (Cooney et al., 2009). This technology considered as an eco-friendly and cost effective technology for algal oil separation

2.8.4. Microwave assisted oil extraction

Microwave assisted oil extraction technology recognized as rapid, safe, and economical methods in which water removal from the algal biomass is not required (Pare et al., 1997). Microwave radiations produced an oscillating electric field around the dielectric or polar material. This oscillating electric field induces inter- and intra-molecular movements in dielectric or polar material. The frictional forces originating from these molecular movements will generate

intracellular heat which consequently produces water vapors within the cell. This in turn disrupts the cell and conducted an electroprorating event which eventually dissolve the cell membrane, subsequently enhance the production of intracellular metabolites (Rosenberg and Bogl, 1987). Microwave-assisted process is envisaged as an efficient extraction process due to small reaction time and low running cost. However, the disadvantage of this technology is the requirement of maintenance cost on a large scale.

2.8.5. Electroporation

Electroporation is defined as membrane phenomena within the cell developed by externally applied electrical field. The characteristic feature of this phenomenon includes notable increase in permeability and electrical conductivity of microalgal cell wall and cytoplasmic membrane. Furthermore, this process enhances the lipid recovery yield, decrease the process time and reduces the solvent utilization. In addition, the elctroporation process does not affect the nature and composition of the extracted lipid product.

2.8.6. Enzyme-Assisted Extraction

Enzyme-assisted extraction includes sequential utilization of different enzymes such as laccase, and cellulase to facilitate the cell disruption. These enzymes degrade rigid polymers present on the cell surface structures and concede intracellular extraction of lipid from the cell easily (Taher et al., 2014). This method is extremely precise and expeditious in nature, but it is considered as cost intensive process.

2.8.7. Ultrasonic assisted extraction

Ultrasonication extraction methods involve sound waves to agitate the particles which results into cell disruption. Ultrasound can damage the algal cell by two mechanisms namely, cavitation and acoustic streaming. After applying ultrasound waves, the acoustic streaming enables mixing of microalgal culture (Khanal et al., 2007) whist cavitation (i.e. microbubble formation) can generate pressure for the cell disintegration (Suslick and Flannigan, 2008). The rapid compression/decompression of ultrasonic waves generates transient and stable cavitation. Unsteady oscillations consequently produce transient cavitation, which eventually implode. A cavitation implosion generates particular localized heat shock waves, which disrupt the algal cells (Brujan et al., 2001).This process handle small volume of algal biomass at a particular time.

Therefore, the process is not advisable at pilot scale level. As compared with other methods, ultrasonication method can be operated at low temperature to carry out extraction process.

2.9. Growth kinetic models

2.9.1. Group (I) growth kinetic models based on single limiting substrate factor

Microalgae growth kinetics is described by the external substrates (i.e. nitrogen, phosphorous, and carbon) available in nutrient medium, under light saturating conditions (Lee et al., 2015). Most kinetic growth models are expressed as a function of single substrate concentration. These growth models are classified into two groups as follows:

2.9.1.1 Group I (a) models: based on external substrate concentration

Group I (a) models assumed that the growth rate of microalgae is governed by an external substrate concentration in culture solution. The kinetic models in this group are extensively tested for various microalgal species because measurement of an external substrate concentration is much easier in culture solution (Lee et al., 2015). The Monod model is recognized as an exemplary model in this group which considers only substrate limitation conditions.

The Monod model is reasonable to define microalgae growth kinetics in low and balanced substrate concentrations (Lee et al., 2015). The limitation of this model is that it cannot describe growth inhibition kinetics under high substrate concentrations.

To conquer such a limitation, the Monod model was modified by introducing Haldane type of inhibition kinetic models (i.e. use for enzyme inhibition). In the case of microbial growth, it is assigned as the Andrews model (Andrews, 1968) which incorporates a S^2/K_i term in the denominator to explain the substrate inhibition effects on the growth rate at high substrate concentration.

The microalgal growth kinetics cannot be described by the Monod model in the absence of substrate in culture solution. Additionally, when a substrate is absent from the culture solution, algal growth still occurs due to nutrient storage in the cell. For eg., when external phosphorus is absent from growth medium, algal growth is assisted by the internally stocked phosphorus reserves (Yao et al., 2013). In order to describe this phenomenon, Monod model has been modified by incorporating an additional term (i.e. maximum specific growth rate (μ_{m2})) in the nonappearanceof the another extracellular substrate in the growth medium (Martínez et al., 1997) (Eq. 3, Table 2.1).

Table 2.1 Group I (a) model: based on external substrate concentration

Growth Model	Equation No.	Reference
$\mu = \mu_m \frac{S}{K_S+S}$	(E2.1)	Monod, 1949
$\mu = \mu_m \frac{S}{K_S+S+\frac{S^2}{K_i}}$	(E2.2)	Andrews, 1968
$\mu = \frac{\mu_{m1}S+\mu_{m2}K_S}{K_S+S}$	(E2.3)	Martinez et al., 1997
$\mu = \frac{\mu_{m1}S+\mu_{m2}K_S+\mu_{m3}S^2/K_i}{K_S+S+S^2/K_i}$	(E2.4)	Martinez et al., 1999

Thus, in the absence of the other substrate in the growth medium (S = 0), the specific growth rate μ is equivalent to μm2 not to zero. In addition other improved model by Martínez (1999) integrates all 3 conditions i.e. (i) no substrate concentration, (ii) low substrate concentration, and (iii) high substrate concentration by introducing the inhibition constant (Ki) and two maximum specific growth rates (μ_{m2} and μ_{m3}). At (S=0) the value of $\mu = \mu_{m2}$. At ($S > K_i$), the specific growth rate of μ reduces with the increment is substrate concentration because μ_{m3} is less than 1. Although, the limitations of Monod model can be subjugate by the modified Martínez model, however the application these models are rarely used because determination of additional parameters (i.e. K_i, μ_{m2} and μ_{m3}) are cumbersome and time consuming.

2.9.1.2. Group I (b) models based on internal substrate concentration

Group I (b) models described the growth rate (μ) based on their internal nutrient quota of the limiting substrate concentration. These types of models explain the microalgal growth rate more rationally, since it describes algal growth in the absence of extracellular substrate due to acquired nutrients in the algal cell. Droop model is considered as the representative model for this group. Several studies suggest that under N limiting conditions algal growth behavior in culture solution is best described by the Droop model instead of Monod model (Sommer,1991).

The limitation with the mathematical formula of Droop model is the term Q_{min}/Q, when the growth rate (μ) reach to the μ'_{max}, quota (Q) would reach to the infinity which is not possible in realistic conditions. To conquer the limitation of Droop model, Caperon and Meyer (1972), introduced Monod type half saturation constant (K_C) into the Eq. (E2. 5).

Table 2.2 Group I (b) models based on internal substrate concentration

Growth Model	Equation No.	Reference
$\mu = \mu'_{max}\left(1 - \frac{Q_{min}}{Q}\right)$	(E2.5)	Droop, 1968
$\mu = \mu^{*}_{max}\frac{Q-Q_{min}}{Q-Q_{min}+K_C}$	(E2.6)	Caperon and Meyer, 1972
$\mu = \mu'_{max}\frac{(1+K_q)(Q-Q_{min})}{(Q-Q_{min})+K_q(Q-Q_{min})}$	(E2.7)	Flynn, 2002

This model describes the algal growth in better way than the Droop model. The limitation of this model is the determination of an additional parameter (K_C) which restrains the applicability of this model.

2.9.2. Group II growth kinetic models based on limiting light conditions

Growth kinetics of microalgae in this category is characterized by the light intensity in saturated substrate concentrations. Light is a considered as essential parameter to determine the photosynthetic activity of microalgae that is associated with the energy metabolism, because suboptimal light availability restrain algal growth whilst higher than saturated light level algal growth is halted due to photoinhibition (Hannon et al., 2010). Therefore, the light limited growth kinetic models are crucial for the designing of the open pond and photobioreactor system, and for the performance optimization.

2.9.2.1. Group II (a) models consider light-limitation conditions under substrate saturation conditions.

The Tamiya model is the representative group in this group which is equivalent to the Monod –like assertion and determines light intensity effects on the algal growth.

In this model, the light limited growth rate is associated to the μ_{max} and K_I. When (I) < K_I, the growth kinetic model follow the first order kinetics. When I > K_I, the growth becomes light independent and $\mu = \mu_{max}$. In addition to the Tamiya model, van Oorschot et al. (1955) used a Poisson function ($1 - e^{-I/K_I}$) (Eq. 8, Table 2.3) to determine the limited algal growth kinetics. Bannister model (Bannister, 1979) is similar to the theoretical model, and based on the microalgae species introduces a shape parameter (m) to determine the growth kinetics.

Table 2.3 Group II (a) models consider light-limitation conditions under substrate saturation conditions

Growth Model	Equation No.	Reference
$\mu = \mu_m \frac{I}{K_I + I}$	(E2.8)	Tamiya et al., 1953
$\mu = \mu_{max} (1 - e^{-I/K_I})$	(E2.9)	Von Oorschot, 1955
$\mu = \mu_{max} \frac{I}{(K_I^m + I^m)^{1/m}}$	(E2.10)	Bannister, 1979

These models are applicable for low and moderate substrate concentration in nutrient medium. The drawback of these models is that it does not consider light attenuation which is most frequently noticed phenomena in microalgae cultivation systems.

2.9.2.2. Group II (b) models consider light attenuation phenomena under light limited and substrate saturation conditions

The Grima model is the most applied model under this group which examines the light attenuation in the culture solution. This model is a modified Tamiya model in which an average light intensity with an exponent (n) is introduced into the equation. This model is mostly used in the photobioreactor optimization for both outdoor and indoor culture (Lee et al., 2015).

The limitation of this model is the use of average irradiance which might not be the relevant parameter to describe the light heterogeneity obtained by singular cells in the culture solution and its effect on microalgal growth.

Table 2.4 Group II (b) model considering light-limitation associated with light attenuation by cells

Growth Model	Equation No.	Reference
$\mu = \mu_m \frac{I_{av}^n}{K_I^n + I_{av}^n}$	(E2.11)	Grima et al., 1994
$I_{av} = \frac{I}{K_a p X}[1 - e^{-K_a p X}]$		
$\mu = K \left\{ \frac{I_{abs}}{X V} - I_{max}(1 - V_F) \right\}$	(E2.12)	Ogbonna et al., 1995

In addition of Grima model Ogbonna et al. (1995) defines a linear equation which incorporates a cell concentration (X), reactor volume (V) and the non-illuminated volume fraction ($1 - V_F$). Here, cell concentration(X) and non-illuminated volume fraction ($1 - V_F$) incorporates the effect of light attenuation and dark zone on algal growth respectively.

2.9.3. Group (III) growth kinetic models considering multiple factors

In this category, the microalgae growth models includes multiple factors in their equation to describe the algal growth behavior in culture solution. These models are based on the notion of the co-limitation of nutrients and light which is frequently exist in natural environments. These models can be classified into two groups.

2.9.3.1 Group III (a) models (Threshold models)

This group model is also known as threshold models which is based on the concept of minimum law, and suggest that the microalgae growth rate in the nutrient medium is influenced by the most limiting substrate concentration present in the culture solution.

Table 2.5 Threshold models

Growth Model	Equation No.	Reference
$\mu = \mu'_{max,min}\left(1 - \frac{Q_{min,N}}{Q_N}, 1 - \frac{Q_{min,P}}{Q_P}\right)$	(E2.13)	Klausmeir et al., 2004
$\mu = \mu'_{max,min}\left(\frac{1 - \frac{Q_{min,N}}{Q_N}}{1 - \frac{Q_{min,N}}{Q_{max,N}}}, \frac{1 - \frac{Q_{min,P}}{Q_P}}{1 - \frac{Q_{min,P}}{Q_{max,P}}}\right)$	(E2.14)	Bougaran et al., 2010

The substructure of the threshold models is:

$\mu = \mu max , min(f(x1), f(x2), f(x3) \cdots f(xi)$

where $\mu max , min$ is a maximum growth rate with respect to the most limiting substrate concentration and f(xi) is a function of different limiting substrates such as N, P, CO_2 and irradiance.

2.9.3.2 Group III (b) (Multiplicative models)

The multiplicative model considers that the different substrates (i.e. major) present in the culture solution fairly contribute to microalgae growth. This means all the major substrates available in the culture solution which can concurrently affect the algal growth in the cultivation systems.

$\mu = \mu_{\max} f(x_1) \cdot f(x_2) \cdot f(x_3) \cdots f(x_i)$

where $\mu_{\max}$ is the global maximum specific growth rate.

Table 2.6 Multiplicative models

Growth Model	Equation No.	Reference
$\mu = [\mu_{c,max} \cdot \left\{f\left(\frac{C_p}{C_n}\right)\right\}^a - \left(\frac{1}{y_c} - 1\right) \cdot \mu_{f,max} \left\{f\left(\frac{C_p}{C_n}\right)\right\}^b \cdot \left(\frac{S_N}{K_{S,N} + S_N}\right) - k_d] \cdot \left(\frac{C_n}{C_{n,max}}\right)$	(15)	KuniKane and Kaneko, 1984
$\mu = \mu_{max} \left(\frac{S_{OC}}{K_{s,OC} + S_{OC} + \frac{S_{OC}^2}{K_{i,OC}}}\right)\left(\frac{I}{K_I + I}\right)\left(1 - \frac{C_x}{C_{x,m}}\right)\left(1 - \frac{C_{pro}}{C_{pro,m}}\right)$	(16)	Zhang et al., 1999
$\mu = \mu_{max} \cdot 1.066^{T-20} \left(\frac{I_{av}^m}{K_I^m + I_{av}^m}\right)\left(\frac{S_{OC}}{K_{s,OC} + S_{OC} + \frac{S_{OC}^2}{K_{i,OC}}}\right)$	(17)	Pegallapati and Nirmalakhandn, 2012

Most of the kinetic rate equations considering different factors were based on either external substrate concentrations (i.e. Monod model) or internal nutrient quota (i.e. Droop model). However, the kinetic rate equation established by Kunikane and Kaneko (1984) combined the external nitrogen, internal phosphorous and internal nitrogen for the growth of *Scenedesmus dimorphus* and describe a full scale multiplicative model. But, it is arduous to use multiplicative model because of their complex nature and cumbersome parameter estimation procedures.

2.10. References

Abas N., Kalair A., Khan N., 2015. Review of fossil fuels and future energy technologies. Futures 69, 31–49.

Andersen R.A., 2005.Algal culturing techniques, vol 13. Academic Press, New York, p 189.

Andrews J.F., 1968. A mathematical model for the continuous culture of microorganisms utilizing inhibitory substrates. Biotechnol. Bioeng. 10, 707–723.

Bannister T., 1979. Quantitative description of steady state, nutrient-saturated algalgrowth, including adaptation, Limnol. Oceanogr. 24, 76–96.

Barbosa M.J., Janssen M., Ham N., 2003. Microalgae cultivation in air-lift reactors: modeling biomass yield and growth rate as a function of mixing frequency. Biotechnol Bioeng 82, 170–179.

Becker E. W., 1994. Microalgae biotechnology and microbiology. Cambridge University Press, New York, 18 pp.

Bosma R., van Spronsen W.A., Tramper J.,Wijffels R.H., 2003. Ultrasound, a new separation technique to harvest microalgae. J Appl Phycol. 15, 143–53.

BougaranG., Bernard O., Sciandra A., 2010. Modeling continuous cultures of microalgae colimited by nitrogen and phosphorus. J. Theor. Biol. 265, 443–45.

Breuer G., Lamers P.P., Martens D.E., Draaisma R.B., Wijffels R.H., 2013. Effect of light intensity, pH, and temperature on triacylglycerol (TAG) accumulation induced by nitrogen starvation in *Scenedesmus obliquus*. Bioresour Technol. 143, 1–9.

Brujan E. A., Nahen K., Schmidt P., Vogel A., 2001. Dynamics of laser induced cavitation bubbles near an elastic boundary. J. Fluid Mech. 433, 251–281.

Carvalho A.P., Silva S.O., Baptista J.M., Malcata F.X., 2010. Light requirements in microalgal photobioreactors: an overview of biophotonic aspects. Appl. Microbiol. Biotechnol. 89, 1275-1288.

Cai T., Park S.Y., Li Y., 2013. Nutrient recovery from wastewater streams by microalgae: status and prospects. Renew.Sustain. Energy Rev. 19, 360-369.

Caperon J., Meyer J., 1972. Nitrogen-limited growth ofmarine phytoplankton—I. Changesin population characteristics with steady-state growth rate, Deep Sea Res.Oceanogr. Abstr. 19, 601–618.

Chen C.Y., Yeh K.L., Aisyah R., Lee D.J., Chang J.S., 2011. Cultivation, photobioreactor design and harvesting of microalgae for biodiesel production: a critical review. Bioresour Technol. 102,71–81.

Chen M., Tang H., Ma H., Holland T.C., Ng K.Y., Salley S.O., 2011. Effect of nutrients on growth and lipid accumulation in the green algae *Dunaliella tertiolecta*. Bioresour. Technol. 102, 1649-1655.

Chisti Y., 2007. Biodiesel from microalgae. Biotechnol Adv. 25, 294–306.

Chojnacka K., Noworyta A., 2004. Evaluation of *Spirulina* sp. growth in photoautotrophic, heterotrophic and mixotrophic cultures. Enzyme MicrobTechnol. 34, 461-465.

Cooney M., Young G., Nagle N., 2009. Extraction of bio-oils from microalgae. Sep. Purif. Rev. 38, 291–325.

Cornet J.F., Dussap C., Gros J.B., Binois C., Lasseur C., 1995. A simplifi ed monodimensional approach for modeling coupling between radiant light transfer and growth kinetics in photobioreactors. Chem Eng Sci. 50, 1489–1500.

Demirbas A., 2009. Production of biodiesel from algae oils. Energ. Source. 31, 163–168.

Doran P.M., 2013. Bioprocess engineering principles. Academic Press, New York. 14, 751–852.

Droop M., 1968. Vitamin B12 and marine ecology. IV. The kinetics of uptake, growth andinhibition in Monochrysis lutheri. J. Mar. Biol. Assoc. UK 48, 689–733.

Enamala M. K., Enamala S., Chavali M., Donepudi J., Yadavalli R., Kolapalli B., Aradhyula T.V., Velpuri J., Kuppam C., 2018. Production of biofuels from microalgae - A review on cultivation, harvesting, lipid extraction, and numerous applications of microalgae. Renew Sustain Energy Rev. 94, 49–68.

Eriksen N.T., 2008. The technology of microalgal culturing. Biotechnol Lett. 30, 1525–1536.

Flynn K.J., 2002. How critical is the critical n: P ratio?. J. Phycol. 38, 961–970.

Franco L.E., Havel J., Peterat F., Weuster B.D., 2006. Model supported optimization of phototrophic growth in a stirred-tank photobioreactor. Biotechnol Bioeng. 95,1177–1187.

Gardner R., Peters P., Peyton B., Cooksey K.E., 2011. Medium pH and nitrate concentration effects on accumulation of triacylglycerol in two members of the chlorophyta. J Appl Phycol. 23,1005-1016.

Greenwell H.C., Laurens L.M.L., Shields R.J., Lovitt R.W., Flynn K.J., 2010. Placing microalgae on the biofuels priority list: a review of the technological challenges. J Am Oil Chem Soc. 7, 703–26.

Griffiths M.J., Dicks R.G., Richardson C., Harrison S.T.L., 2011. Advantages and challenges of microalgae as a source of oil for biodiesel. Biodiesel - Feed Process Technol. 178–200.

Grima E.M., Camacho F.G., Pérez J., Sevilla J., Fernandez F., GomezA.C., 1994. A mathematical model of microalgal growth in light-limited chemostat culture, J. Chem.Technol. Biotechnol. 61, 167–173.

Grima E.M., Fernandez F.G.A., Camacho F.G., Chisti Y., 1999. Photobioreactors: light regime, mass transfer, and scaleup. Journal of Biotechnolog., 70**,** 231-247.

Goncalves E.C., Wilkie A.C., Kirst M., Rathinasabapathi B., 2016. Metabolic regulation of triacylglycerol accumulation in the green algae: identification of potential targets for engineering to improve oil yield. Plant Biotechnol J. 14, 1649–60.

Gupta P.L., Lee S.M., Choi H.J., 2015. A mini review: photobioreactors for large scale algal cultivation. World Journal of Microbiology and Biotechnology.**31**(9), 1409-1417.

Hannon M., Gimpel J., Tran M., Rasala B., Mayfield S., 2010. Biofuels from algae: challenges and potential. Biofuels. 1, 763–784.

Hao H.C., Jian G.J., 2017. Lipid accumulation mechanisms in auto- and heterotrophic microalgae. J. Agric. Food Chem. 65, 8099−8110.

Havlik I., Scheper T.,Reardon K.F., 2016. Monitoring of microalgal processes, in microalgae biotechnology ed. by Posten C and Feng Chen S. Springer International Publishing, Cham. 89–142.

Henrard A.A., Morais De M.G., Costa J.A.V., 2011.Vertical tubular photobioreactor for semicontinuous culture of *Cyanobium* sp. Bioresour Technol, 102, 4897-4900.

Ho S.H., Chen C.Y., Lee D.J., Chang J.S., 2011. Perspectives on microalgal CO_2 emission mitigation systems-a review. Biotechnol Adv.29**,**189-98.

Ho S.H., Ye X., Hasunuma T., Chang J.S., Kondo A., 2014. Perspectives on engineering strategies for improving biofuel production from microalgae – a critical review. Biotechnol Adv. 32, 1448–1459.

Huang G.H., Chen F., Wei D., Zhang X.W., Chen G., 2010. Biodiesel production by microalgal biotechnology. Appl. Energ. 87, 38–46.

Joyard J., Ferro M., Masselon C., Seigneurin-Berny D., Salvi D.,Garin J., Rolland N., 2010. Chloroplast proteomics highlights the subcellular compartmentation of lipid metabolism. Prog. Lipid Res. 49, 128−158.

Kalita N., Baruah G., Dev G.R., Talukdar J., Kalita M., 2011. *Ankistrodesmus falcatus*: A promising candidate for lipid production, its biochemical analysis and strategies to enhance lipid productivity. J Microbiol Biotechnol Res 1, 148–157.

Kandilian R., Tsao T.C., Pilon L., 2014. Control of incident irradiance on a batch operated flat-plate photobioreactor. Chem. Eng. Sci. 119, 99-108.

Khalil Z.I., Asker M.M.S., El-Sayed S., Kobbia I.A., 2010, Effect of pH on growth and biochemical responses of *Dunaliella bardawil* and *Chlorella ellipsoidea*. World J Microbiol Biotechnol 26, 1225–1231.

Khan M.I., Shin J.H., Kim, J.D.,2018. The promising future of microalgae: currentstatus, challenges, and optimization of a sustainable and renewable industry forbiofuels, feed, and other products. Microb. Cell Fact. 17, 1–21.

Khanal S.K., Grewell D., Sung S., Leeuwen J., 2007. Ultrasound applications in wastewater sludge pretreatment: a review. Crit. Rev. Environ. Sci. Technol. 37, 277–313.

Kim J., Yoo G., 2013. Methods of downstream processing for the production of biodiesel from microalgae. Biotechnol. Adv. 31, 862–876.

Kim W., Park J., Gim G., Jeong S.H., Kang C., Kim D.J., Kim S., 2012. Optimization of culture conditions and comparison of biomass productivity of three green algae. Bioprocess Biosyst Eng. 35, 19-27.

Klausmeier C.A., Litchman E., Levin S.A., 2004. Phytoplankton growth and stoichiometry under multiple nutrient limitation, Limnol. Oceanogr. 49, 1463–1470.

Kunikane S., Kaneko M., 1984. Growth and nutrient uptake of green alga, *Scenedesmus dimorphus*, under a wide range of nitrogen/phosphorus ratio—II. Kinetic model.Water Res. 18, 1313–1326.

Lee A. K., Lewis D.M., Ashman P.J., 2012. Disruption of microalgal cells for the extraction of lipids for biofuels: processes and specific energy requirements. Biomass Bioenergy 46, 89–101.

Lee E., Jalalizadeh M., Zhang Q., 2015. Growth kinetic models for microalgae cultivation: a review. Algal Res. 12, 497–512.

Lee, E., Pruvost, J., He, X., Munipalli, R., Pilon, L. 2014. Design tool and guidelines for outdoor photobioreactors. *Chemical Engineering Science*, 106, 18-29.

Lee S.J., Go S., Jeong G.T., Kim S.K., 2011. Oil production from five marine microalgae for the production of biodiesel. Biotechnol Bioprocess Eng. 16,561–566.

Lee S.J., Yoon B.D.,Oh H.M., 1998. Rapid method for the determination of lipid from the green alga *Botryococcus braunii*. Biotechnol. Tech. 12, 553–556.

Liang Y., Sarkany N., Cui Y., 2009. Biomass and lipid productivities of *Chlorella vulgaris* under autotrophic, heterotrophic and mixotrophic growth conditions. Biotechnol Lett. 31, 1043-1049.

Liu X., Duan S., Li A., Xu N., Cai Z., Hu Z., 2009. Effects of organic carbon sources on growth, photosynthesis, and respiration of *Phaeodactylum tricornutum*. J Appl Phycol. 21, 239-246

Li Y., Chen Y.F., Chen P., Min M., Zhou W., Martinez B., 2011. Characterization of a microalga *Chlorella* sp. well adapted to highly concentrated municipal wastewater for nutrient removal and biodiesel production. Bioresour Technol. 102, 5138–44.

Mahapatra S.S., Sahu M., Patel R.K., Panda B.N., 2012. Prediction of water quality using principal component analysis. Water Qual Expo Heal. 4, 93–104

Martínez M., Jimenez J., El Yousfi F., 1999. Influence of phosphorus concentration and temperature on growth and phosphorus uptake by the microalga *Scenedesmus obliquus*, Bioresour. Technol. 67, 233–240.

Martínez M., Jimenez J., El YousfiF., 1997. Influence of phosphorus concentrationon the growth kinetics and stoichiometry of the microalga *Scenedesmus obliquus*. Process Biochem. 32, 657–664.

Masojídek J., Koblížˇek M., Torzillo G.,2004. Photosynthesis in microalgae. In:Richmond, A. (Ed.), Handbook of Microalgal Culture Biotechnology and AppliedPhycology. Blackwell Publishing, Iowa, p. 34.

Mata T.M., Martins A.A., Caetano N.S., 2010. Microalgae for biodiesel production and other applications: a review. Renew. Sust. Energ. Rev. 14, 217–232.

Mohan S.V., Rohit M., Chiranjeevi P., Chandra R., Navaneeth B., 2015. Heterotrophic microalgae cultivation to synergize biodiesel production with waste remediation: progress and perspectives. Bioresour Technol. 184, 169–178.

Molina E., Fernández J., Acién F.G., Chisti Y., 2001. Tubular photobioreactor design for algal cultures. J Biotechnol. 92, 113–131.

Monod J., 1949. The growth of bacterial cultures. Annu. Rev. Microbiol. 3, 371–394.

Norsker N.H., Barbosa M.J., Vermuë M.H., Wijffels R.H., 2011. Microalgal production – A close look at the economics. Biotechnology Advances 29 (1), 24–27.

Ogbonna J.C., Yada H., Tanaka H., 1995. Kinetic study on light-limited batch cultivation ofphotosynthetic cells. J. Ferment. Bioeng. 80, 259–264.

Ogbonna J.C., Tanaka H., 2000. Light requirement and photosynthetic cell cultivation - Development of processes for efficient light utilization in photobioreactors. J Appl Phycol. 12, 207-218.

Pare J.R.J., Matni G., Bélanger J.M.R., Li K., Rule C., Thibert B., 1997. Use of the microwave-assisted process in extraction of fat from meat, dairy, and egg products under atmospheric pressure conditions. J. AOAC Int. 80, 928–933.

Pegallapati A.K., Nirmalakhandan N., 2012. Modeling algal growth in bubble columnsunder sparging with CO2-enriched air, Bioresour. Technol. 124, 137–145.

Pittman J.K., Dean A.P., Osundeko O., 2011. The potential of sustainable algal biofuel production using wastewater resources. Bioresour Technol. 102, 17–25.

Ramesh D., 2013. Lipid identification and extraction techniques, in biotechnological applications of microalgae: biodiesel and value-added products, ed. F. Bux (Boca Raton, FL: CRC Press), 89–97.

Rosenberg U., Bogl W., 1987. Microwave thawing, drying, and baking in the food industry. Food Technol. 41, 85–91.

Ruangsomboon S., 2015. Effects of different media and nitrogen sources and levels on growth and lipid of green microalga *Botryococcus braunii* KMITL and its biodiesel properties based on fatty acid composition. Bioresour.Technol. 191, 377-384.

Sánchez Mirón A., Contreras Gómez A., Garcıa Camacho F., 1999. Comparative evaluation of compact photobioreactors for large-scale monoculture of microalgae. J Biotechnol 70,249–270.

Santos A.M., Janssen M., Lamers P.P., Evers W.A.C., Wijffels R.H., 2012. Growth of oil accumulating microalga *Neochloris oleoabundans* under alkaline–saline conditions. Bioresour Technol. 104, 593–599.

Sharma Y.C., Singh V., 2017. Microalgal biodiesel: a possible solution for India's energy security. Renewable Sustainable Energy Rev. 67, 72–88.

Sierra E., Acie´n F.G., Fernández J.M., Garcia J.L., Gonzalez C., Molina E., 2008. Characterization of a flat plate photobioreactor for the production of microalgae. Chem Eng J. 138,136–147.

Singh R.N., Sharma S., 2012. Development of suitable photobioreactor for algae production – a review. Renew. Sust. Energy Rev. 16, 2347–2353

Singh S.P., Singh P., 2015. Effect of temperature and light on the growth of algae species: a review. Renew Sustain Energy Rev. 50, 431–44.

Slegers P.M., Wijffels R.H., van Straten G., van Boxtel A.J.B., 2011. Design scenarios for flat panel photobioreactors. Appl Energy. 88, 3342–3353.

Sommer U., 1991. A comparison of the Droop and the Monod models of nutrient limited growth applied to natural populations of phytoplankton. Funct. Ecol. (1991) 535–544.

Suslick K.S., Flannigan D.J., 2008. Inside a collapsing bubble: sonoluminescence and the conditions during cavitation. Annu. Rev. Phys. Chem. 59, 659–683.

Taher H., Al-Zuhair S., Al-Marzouqi A.H., Haik Y., Farid M., 2014. Effective extraction of microalgae lipids from wet biomass for biodiesel production. Biomass Bioenergy 66, 159–167.

Tamiya H., Hase E., Shibata K., Mituya A., Iwamura T., Nihei T., Sasa T., 1953. Kinetics of growth of Chlorella, with special reference to its dependence on quantity ofavailable light and on temperature, Algal culture from laboratory to pilot plant. 204–234.

Teresa M.M., Antonio A.M., Nidia S.C. 2010. Microalgae for biodiesel production and other applications: A review. Renewable and Sustainable Energy Reviews. 14, 217–232.

Ugwu C.U., Aoyagi H., Uchiyama H., 2008. Photobioreactors for mass cultivation of algae. Bioresour Technol. 99, 4021–4028.

van Oorschot J.L.P., 1955.Conversion of Light Energy in Algal Culture, Veenman,Wageningen,

Venkata Subhash G., Rohit M.V., Devi M.P., Swamy Y.V., Venkata Mohan S., 2014. Temperature induced stress influence on biodiesel productivity during mixotrophic microalgae cultivation with wastewater. Bioresour Technol. 169, 789–93.

Vuppaladadiyam A.K., Prinsen P., Raheem A., Luque R., Zhao M., 2018. Microalgae cultivation and metabolites production: a comprehensive review. Biofuels, Bioprod. Bioref. 12, 304–324.

Wang Z., Hou J., Bowden D.,Belovich J.M., 2014. Evaluation of an inclined gravity settler for microalgae harvesting.J ChemTechnolBiotechnol. 89, 714-120.

Wang J., Sommerfeld M.R., Lu C., Hu Q., 2013. Combined effect of initial biomass density and nitrogen concentration on growth and astaxanthin production of *Haematococcus pluvialis* (Chlorophyta) in outdoor cultivation.Algae 28, 193-202.

Xu H., Miao X.L., Wu Q.Y., 2006. High quality biodiesel production from a microalga *Chlorella protothecoides* by heterotrophic growth in fermenters. J.Biotechnol. 126, 499–507.

Yao C., Ai J., Cao X., Xue S., 2013. Characterization of cell growth and starch production in the marine green microalga *Tetraselmis subcordiformis* under extracellular phosphorus-deprived and sequentially phosphorus-replete conditions. Appl. Microbiol. Biotechnol. 97, 6099–6110.

Yoo C., Jun S.Y., Lee J.Y., Ahn C.Y., Oh H.M., 2010. Selection of microalgae for lipid production under high levels carbon dioxide. Bioresource Technol. 101, S71–S74

Yoo G., Park W.K., Kim C.W., Choi Y.E., Yang, J.W., 2012. Direct lipid extraction from wet *Chlamydomonas reinhardtii* biomass using osmotic shock. Bioresour. Technol. 123, 717–722.

Zhang X., Gong X., Chen F., 1999. Kinetic models for astaxanthin production by high cell density mixotrophic culture of the microalga *Haematococcus pluvialis*. J. Ind. Microbiol. Biotechnol. 23, 691–696.

Zhang H., Wang W., Li Y., Yang W., Shen G., 2011. Mixotrophic cultivation of *Botryococcus braunii.* Biomass Bioenergy. 35, 1710-1715

Chapter 3

Biosequestration of CO_2 using *Botryococcus brunii* in Flat Panel Airlift photobioreactor under pH stat cultivation strategies

3.1. Introduction

Currently, the planet earth is on the brink of facing an expeditious climate change by virtue of candid CO_2 emission. The atmospheric CO_2 concentration has passed over figuratively 400 ppm threshold. The upsurge in CO_2 concentration in the atmosphere is anticipated to increase up to 32.73%, from the current 370 $\mu mol \cdot mol^{-1}$ by 2050 and it will further predict to 50.67% rise, by the end of the 21st century (Liu et al., 2017). The global exterior temperature of earth will rise approximately 2°C compared to 1990 by 2050. The comprehensive emission of greenhouse gas increased to 50.70% in the year 2010 compared to 1999, principally due to consumption of fossil fuel by transportation services (USEPA) (Liu et al., 2017). Although, in 2012 the worldwide CO_2 emissions was declined slightly even after 2.4% renewable energy usage, and the global average annual growth rate of 2.4 ppm in atmospheric CO_2 was recorded. Generally, the typical CCS plants are efficient in capturing CO_2 from different thermal and cement manufacturing plants (Pradhan et al., 2015). However, these CCS technologies cannot present perpetual solution due to consequent CO_2 leakage. This disadvantage may be conquered by the implementation of CO_2 bio-sequestration processes using photobioreactor technologies.

Microalgae have obtained colossal attention as auspicious alternative source for biodiesel production by virtue of their higher biomass and lipid yield. Microalgae also have potential to grow on waste-water and do not contest with the agricultural land for their production. Photosynthesis process in microalgae converts sun energy into chemical energy (Teresa et al., 2010). Microalgae have multiple abilities such as higher CO_2 biofixation efficiency, production of bio-oil and other value added products through their biomass (Yoo et al. 2010). CO_2 fixation efficiency by microalgae is dependent on microalgae species (Toledo-Cervantes et al., 2013), nutrients ratio, light intensity, temperature, pH, CO_2 concentration, flow rate, and photo-bioreactor type. In general, the CO2 biofixation efficiency is explicitly corresponding to the microalgae growth rate (Gonzalez-Lopez et al.,2009).

Microalgae efficiently use CO_2 and ability to grow expeditiously when they readily incorporated into photobioreactor normal engineered systems, such as photobioreactors (Chiu et al., 2008 and Carvalho et al., 2006). High CO_2 concentration may increase the CO_2 mass transfer but also reduces the pH that inhibits microalgae growth rate. As microalgae grow efficiently at neutral or alkaline cytosolic pH, and many pH dependent enzymes become inactive in acidic pH (Gimmler, 2001). pH evolution during photosynthesis effect the carbon dioxide species distribution, carbonic anhydrase enzyme activity and carbon capture mechanism (Concas et al.,2012). In neutral pH condition hydrogen ion is non- competitive inhibitor whereas at very low or very high pH levels it can limit photosynthetic growth or substrate utilization.

Microalgae growth kinetics is strongly influenced by pH variations and high CO_2 concentration. Therefore, to optimize and properly control microalgae photobioreactors the quantitative description of pH evolution seems to be a key goal.

The objectives of this study were to evaluate biomass growth, lipid production and to quantify the carbon dioxide assimilation of the *B. braunii* using pH stat cultivation under different CO_2 concentration. The pH stat cultivation of microalgae can increase carbon fixation efficiency, growth and lipid productivities; hence pH stat cultivation becomes effective tool for growth and lipid productivities.

3.2. Material and methods

3.2.1. Microalgae and culture medium

The culture of *Botryococcus braunii* was obtained from Institute of Bioresources and Sustainable Development (IBSD,Takyelpat, Imphal,). The microalgae were grown in modified BG-11medium having composition which includes macronutrients such as $NaNO_3$ (1.5g), $MgSO_4{\cdot}7H_2O$ (0.75 mg), $K_2HPO_4{\cdot}$ (40m g), $CaCl_2{\cdot}H_2O$ (36 mg), Na_2CO_3(20mg), EDTA (1 mg), Citric acid (6mg), Ferric ammonium chloride (6mg) and micronutrients i.e. H_3BO_3 (286 mg), $MNCl_2{\cdot}4H_2O$ (181 mg), $ZnSO_4{\cdot}7H_2O$ (22 mg), $Na_2MoO_4{\cdot}2H_2O$ (39 mg), $CuSO_4{\cdot}5H_2O$ (8 mg) and $CO(NO_3)_2.6H_2O$ per liter. The inoculated medium was incubated at 27 ± 1 °C and 130 rpm in the light incubator shaker and initial pH of the medium was maintained at 8.

3.2.2. The photobioreactor

Airlift Flat Panel photobioreactor was constructed using Borosilicate glass. Height, Length and light path for flat panel photobioreactor were 24.13, 29.21and 7.62 cm respectively. For air flow porous type sparger and was placed at the bottom of the reactor was used. Bubble column was converted into airlift bioreactor by inserting a center glass plate into them (Fig.1). During all the experiments room temperature was maintained at 27±2 °C. The temperature of the culture medium was continuously monitored with the help of temperature probe. Flat panel airlift photobioreactor were constantly illuminated by light intensity of 83.4 μmol m^{-2} s^{-1} by compact florescent lights placed at one side of the reactors. Light intensity was measured by the light meter (Li-COR SA-119) at the surface of the reactor. *B. brunii* cultivation parameters inside the photobioreactor like illuminated surface area, flow rate and down comer to up comer ratio (A_d/A_r) were kept constant throughout the experiments (Table 1).

3.2.3. pH stat Cultivation System

The pH of culture medium was controlled by 4N NaOH solution inside flat panel airlift photobioreactor. The pH-stat systems equipped with pH-electrode (Mettler Toledo, Switzerland) and a peristaltic pump was controlled by the bioreactor (Applikon, Schiedam, the Netherlands). Online pH measurement and control were recorded by the Bioexpert software. The pH of the microalgal culture was controlled at 7.8 when CO_2 used as the carbon sources. A pH-stat cultivation strategy (pH 7.8) at different concentration of CO_2 was applied to improve the growth of *Botrycoccus braunii*.

3.2.4. Determination of biomass concentration

Microalgae Biomass was estimated as a function of optical density of cell. The Optical density (OD) of cells in the circulated liquid was determined using an UV–Visible spectrophotometer (Carry 60Varian) at an absorbance of 680 nm (OD_{680}). Dry cell weight (Dwt) was calculated using following formula generated using OD data and a calibration plot.

C_b (g/l) = 2.155 OD_{680} (R^2 = 0.99)

in which C_b is the dry weight of biomass and OD_{680} is the optical density measured at 680 nm. Therefore, the optical density can be used to precisely determine the dry weight of biomass.

3.2.5. Net specific growth rate

Net specific growth rate was calculated from Eq. (E3.1) (Issarapayup et al., 2009).

$$\mu_{net} = \frac{(\ln N_2 - \ln N_1)}{(t_2 - t_1)} \qquad \text{(E3.1)}$$

where N_2 and N_1were the biomass concentration at days $t_2$and t_1 respectively. Net specific growth rate was taken in exponential phase.

3.2.6. CO_2 fixatation Rate

The CO_2 Fixation rate was determined from the carbon content of algal cells and the growth rate as follows:

$$R_{CO_2} = 2.31 \times \mu_L \qquad \text{(E3.2)} \qquad \text{(Yun et al., 1997)}$$

where RCO_2 and μ_L are the Fixation rate (g $CO_2 m^{-3}$ h^{-1}) and the volumetric growth rate (g dry weight m^{-3} h^{-1}), respectively, in the linear growth phase. MCO_2 and M_C represented the molecular weights of CO_2 and elemental carbon, respectively. The average C_C carbon content was 0.63g carbon per g dry cell weight. The algal growth rate was determined in the linear growth phase because most of the algal growth occurred during this phase.

3.2.7. Lipid extraction and estimation

Extraction of lipid was done by modified Bligh and dyer method with chloroform and methanol as solvents, and water as co-solvent (Bligh and Dyer 1959). The cells were harvested by centrifugation at 10,000 rpm for 10 min at 4°C. After centrifugation the pellet was dried in oven for 2 h at 80°C. The chloroform/methanol (2:1 v/v) solvent system was used to extract the lipid from dried algal cells. The layers were separated by centrifugation for 10 min at 2000 rpm. The lower layer was separated and the procedure was again repeated with the pellet. The lipid content was measured gravimetrically and expressed as a dry weight percentage. The lipid productivity was calculated by the following equation

$$P_{\text{lipid}} = \frac{C_{\text{lipid}} \text{ X DCW}}{Time} \qquad \text{(E.3.3)}$$

Where P_{lipid} is lipid productivity in g l^{-1} d^{-1}, C_{lipid} is lipid content of cells or lipid yield of the cells in g/g, DCW is dry cell weight g/l, and Time is the cultivation period in days.

3.3. Results and discussion

3.1. Effect of CO_2 concentrations on biomass growth and CO_2 biofixation

Effects of six different CO_2 concentrations (v/v) i.e. 5%, 10%, 15%, 20%, 30% and 50% on biomass growth of *B. braunii* were studied in 5.37 L flat panel airlift photobioreactor using pH stat cultivation strategies (Fig 3.1(a) and 3.1(b)). Maximum biomass concentration and maximum biomass productivity of 1.56 g L^{-1} and 222.86 mg L^{-1} d^{-1} were obtained at 20% CO_2 concentration respectively. In addition, at CO_2 concentration of 5%, 10%, 15% and 30% maximum biomass concentration and biomass productivity were rate were 0.69 g L^{-1} and 98.57 mg L^{-1} d^{-1}, 0.91 g L^{-1} and 130 mg L^{-1} d^{-1}, 1.43 g L^{-1} and 204.28 mg L^{-1} d^{-1}, 1.13 g L^{-1} and 161.43 mg L^{-1} d^{-1} respectively under pH stat operational strategies (Table 3.1). Notably, at 50% CO_2 concentration the pH stat cultivation strategy does not work and resulted in growth inhibition. The lowest biomass and specific growth rate of 0.28 g L^{-1} and 40 mg L^{-1} d^{-1} obtained under this condition (i.e. 50% CO_2 concentration in pH stat).

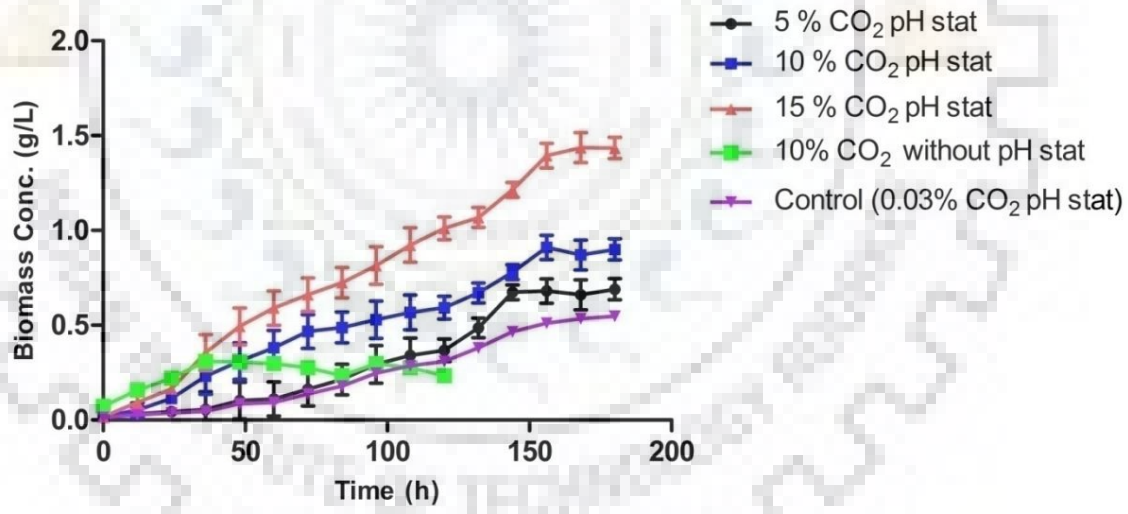

Fig. 3.1 (a). Plot of experimental data showing the effect of CO_2 concentration (v/v) on total biomass density for (Control, 5%, 10%, 15% CO_2 pH stat and 10% CO_2 without pH stat respectively)

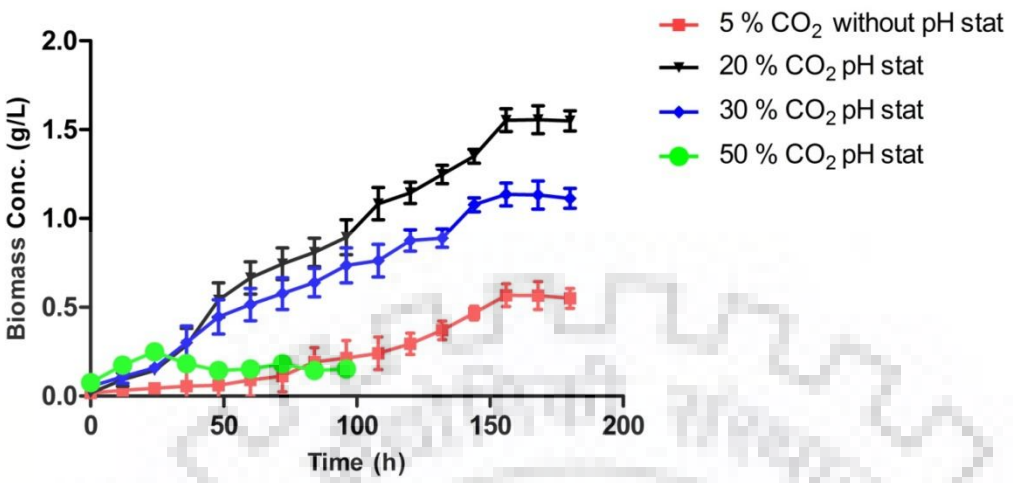

Fig. 3.1 (b). Plot of experimental data showing the effect of CO_2 concentration (v/v) on total biomass density for (20%, 30%,50% CO_2 pH stat and 5% CO_2 without pH stat respectively).

In present study, to analyze the effect of pH on *B. braunii* growth and biomass productivity, one set of control experiment (i.e. 0.03% CO_2 in pH stat) and two sets of different limiting substrate concentrations (i.e. 5% and 10% CO_2) without pH stat were also conducted. Moreover, in control experiment the maximum biomass concentration and biomass productivity of 0.51 g L^{-1} and 72.86 were obtained. Although the biomass growth and productivity of *B. braunii* were significantly decreased (i.e. 0.29 g L^{-1} and 72.5 mg L^{-1} d^{-1}) at higher CO_2 concentration (i.e. 10%) when pH of the experiment was not controlled. Notably, the microalgae growth does not affected much in 5% CO_2 concentration when pH stat control strategy was not applied, but the lag phase of *B. braunii* was slightly increased compared to the pH stat cultivation strategy under similar CO_2 concentration. The results obtained in present studies indicate that 20% CO2 concentration under pH stat methods significantly enhance the biomass productivity of the photobioreactor systems. Whilst previous studies suggest that optimal concentration of CO_2 aeration for *B. braunii* growth was 2% (Chiu et al., 2008; Ranga Rao et al., 2007b) and the biomass productivity of 26.55 mg L^{-1} d^{-1} (Yoo et al., 2010) at 10% CO_2 concentration and 92.4 mg L^{-1} d^{-1} (Yaming et al., 2011) at 20% CO_2 were obtained respectively, but pH of culture medium was not controlled in these studies.

Table 3.1. Effect of different CO_2 concentration on maximum biomass (X_{max}), maximum lipid (P_{max}), lipid content (%), biomass productivity and CO_2 fixation rate ($\boldsymbol{R_{CO_2}}$) for *B. braunii*.

CO_2 conc. (%)	X_{max} (g L^{-1})	P_{max} (mg L^{-1})	Lipid Content (%)	Biomass Productivity (mg L^{-1} d^{-1})	R_{CO_2} (mg L^{-1} d^{-1})
0.03 (pH stat)	0.51	50.64	9.93	72.86	168.3
5 (pH stat)	0.69	73.59	10.66	98.57	227.70
10 (pH stat)	0.91	147.36	16.19	130	300.3
15 (pH stat)	1.43	272.99	19.09	204.28	471.89
20 (pH stat)	1.56	299.83	19.22	222.86	514.81
30 (pH stat)	1.13	213.57	18.90	161.43	372.90
50 (pH stat)	0.28	15.4	5.50	40	92.4
5 (No pH stat)	0.58	67.34	11.61	82.86	191.41
10 (No pH stat)	0.29	25.98	8.96	72.5	167.48

The CO_2 biofixation efficiency of *B. braunii* was quantitatively analyzed to study the effect of various CO_2 concentrations on the performance of carbon dioxide removal under pH stat cultivation methods. The CO_2 fixation rate of *B. braunii* was calculated based on Eq. (E3.3). The rate of CO_2 fixation is proportional to the biomass growth rate. The maximum CO_2 fixation rate of 514.81 mg L^{-1} d^{-1} was observed at 20% CO_2 under pH stat cultivation approach. At CO_2 concentration of 5%, 10%, 15%, 30% and 50% the CO_2 fixation rate were 227.70, 300.3, 471.89, 372.90 and 92.4 mg L^{-1} d^{-1} respectively (Table 1).

As shown in Table 2, this biomass productivity and CO_2 fixation rate is higher that obtained from other Botryococcus sp. such as 92 mg L^{-1} d^{-1} and 212.52 mg L^{-1} d^{-1} (Yaming et al. 2011), 170 mg L^{-1} d^{-1} and 392.7 mg L^{-1} d^{-1} (Pooja et al. 2012), 26.0 mg L^{-1} d^{-1} and 60.06 mg L^{-1} d^{-1} (Yoo et al., 2010), 150 mg L^{-1} d^{-1} and 346.5 mg L^{-1} d^{-1} (Yeesang et al., 2014) respectively. The results obtained in present studies indicate that optimum CO_2 concentration under pH stat cultivation approach in the photobioreactor significantly enhanced the biomass productivity and CO_2 biofixation rate in B. braunii.

3.2. Effect of CO_2 concentrations on lipid productivities

Lipid productivities of *B. braunii* at different CO_2 concentrations are shown in (Table 1). As shown in Fig. 3.2 the maximum lipid content of 19.22 and maximum lipid productivity of 42.83 mg L^{-1} d^{-1} (Table 1) obtained respectively at 20% CO_2 concentration in pH stat cultivation mode. Different CO_2 concentration had different effect on cell growth and lipid productivities. Generally it seems lipid productivity rate is proportional to the cell growth up to the range of 20% CO_2 concentration. Lipid productivities of 10.51, 21.05, 39.0, 30.51 and 2.20 mg L^{-1} d^{-1} were obtained for 5%, 10%, 15%, 30% and 50% CO_2 concentration respectively at pH stat condition. Lipid productivities were also calculated in the absence of pH stat conditions. Furthermore, in case of 5% CO2 without pH control a slight increase in lipid content (11.61%) was observed compared to the pH control 5% aerated CO_2 whilst at 10% CO_2 aerated without pH stat condition the lipid productivities were significantly decreased (8.96) compared to the pH stat cultivation condition under similar condition (Table 3.1).

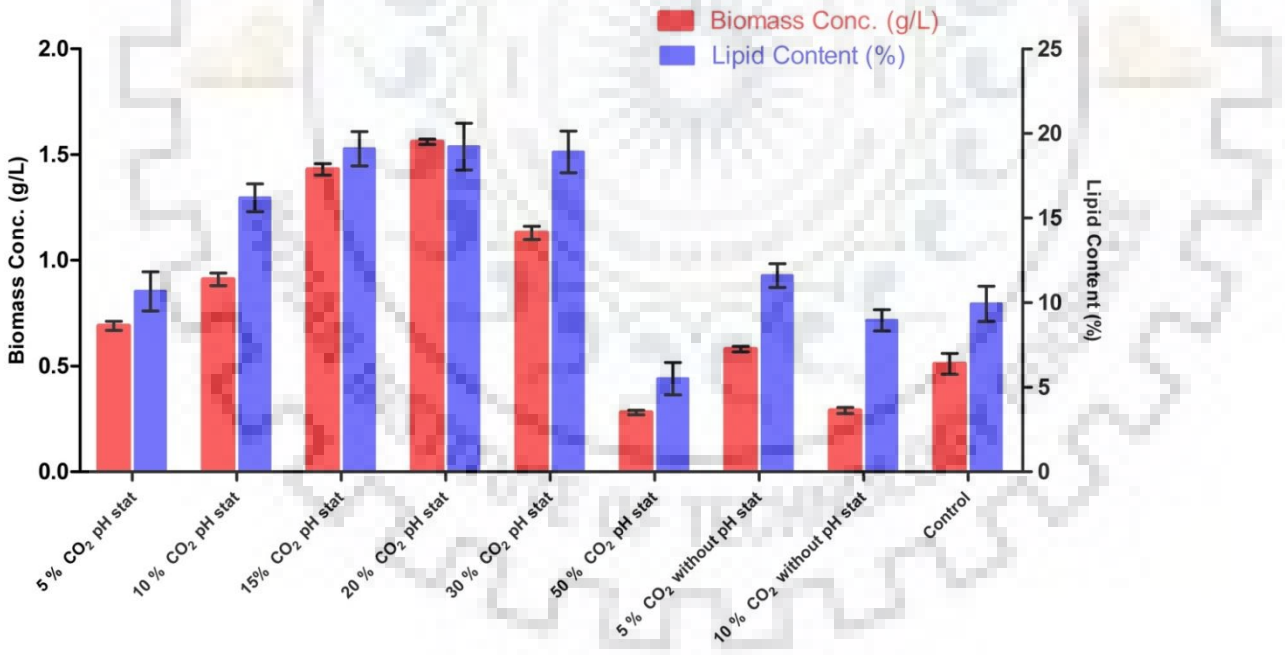

Fig. 3.2. Effect of different CO_2 concentration (v/v) on lipid content of *B. braunii* growing in flat panel airlift photobioreactor.

In present study, the observed lipid productivities of *B. braunii* was in accordance to Yaming et al. (2011), who achieved a lipid content of 12.71% at 20% CO_2 concentration (Table 2). Lipid content of *B. braunii* was also compared to the previously reported data. It was observed that lipid content

(19.22%) measured in the present study was slightly lower than previously reported values such as 15.83% (Pooja et al. 2012), 20.75% (Yoo et al. 2010), 30.3% (Yeesang et al. 2014) and 31.52% (Rao et al. 2007) (Table 2). It must be noted that the results can differ due to use of different lipid extraction methods to determine the lipid content. Moreover, lipid content within the microalgae depends upon the type of microalgal strain and cultivation conditions used, such as nitrogen depletion in the culture solution which substantially enhances the algal lipid content (Zhang et al., 2011). The relative higher lipid content resulted from the much lower nitrogen content of culture medium in previous studies. This might be due to the difference of culture medium. Besides, as BG-11 medium having high nitrogen content than any other growth medium this may decrease the algal lipid content (Hsieh and Wu, 2009).

Table 3.2. Comparison of phototrophic growth and lipid production using *B. braunii* with the literature reported values.

CO_2 concentration	Medium type	X_{max} (g L^{-1})	Biomass Productivity (mg L^{-1} d^{-1})	Lipid Content (%)	Lipid Productivity (mg L^{-1} d^{-1})	Reference
20% CO_2	BG-11	2.31	92	12.71	11.74	Yaming Ge et. al (2011)
6% CO_2	CHU-13	1.20	170	15.83	27.14	Pooja K. et al. (2012)
2% CO_2	CHU-13	1.82	N/A	31.52	N/A	Ranga Rao et. al. (2007)
10% CO_2	CHU-13	0.371	26	20.75	5.50	Yoo et al. (2010)
20% CO_2 pH Stat	BG-11	1.56	222.86	19.22	42.83	Present study
2 % CO_2	Wastewater	2.26	150	30.3	45.65	Yeesang and Cheirsilp. (2014)

3.4. Conclusions

In the present study, pH stat cultivation strategies in flat panel airlift photobioreactor have been used to enhance the CO_2 biofixation, biomass and lipid productivity. The pH stat cultivation strategies determine the effect of different CO_2 concentration on biomass and lipid yield. The pH stat cultivation strategies develop more tolerance to CO_2 up to the range of 30% CO_2 concentration which leads to enhance the biomass and lipid productivity. The adequacy of the methodological

procedure was confirmed by independent experimentation under different CO2 concentration using developed pH stat process, to maximize the CO_2 consumption rate, biomass productivity and lipid productivities in flat panel airlift photobioreactor.

It is concluded that *B. brunii* shows optimum biomass and lipid productivities with improved CO_2 biofixation rate at 20% CO_2 concentration with pH stat cultivation strategies which expedite its application to improve the photobioreactor productivity systems.

3.5. References

Bligh E.G., Dyer W.J. 1959. A rapid method of total lipid extraction and purification Can. J. Biochem. Physiol. 37, 911–917.

Carvalho A.P., Lu´s A.M., Malcata F.X. 2006. Microalgal reactors: a review of enclosed systems design and performances. Biotechnol. Prog. 22, 1490–1506.

Chiu S.Y., Kao C.Y., Chen C.H., Kuan T.C., Ong S.C., Lin C.S. 2008. Reduction of CO_2 by a high-density culture of *Chlorella* sp. in a semi continuous photobioreactor. Bioresour.Technol. 99, 3389–3396.

Concas A., Lutzu G.A., Pisu M., Cao G. 2012. Experimental analysis and novel modeling of semi-batch photobioreactors operated with *Chlorella vulgaris* and fed with 100% (v/v) CO_2. Chemical Engineering Journal. 213, 203–213.

Gimmler H. 2001. Acidiophilic and acidotolerant algae. In: Rai LC, Gaur JP, eds. Algal adaptation to environmental stresses. Physiological, biochemical and molecular mechanisms. Berlin, Germany: Springer, 291–322.

Gonzalez-Lopez C.V., Acién-Fernández F.G., Fernández-Sevilla J.M., Sánchez-Fernández J.F., Molina Grima E. 2012. Development of a process for efficient use of CO_2 from flue gases in the production of photosynthestic microorganism. Biotechnol Bioeng. 109, 1637-1650.

Grima E.M., Camacho F.G., Perez J.A.S., Fernandez F.G.A., Sevilla J.M.F. 1997. Evaluation of photosynthetic efficiency in microalgae cultures using averaged irradiance. Enzyme Microb. Technol. 21, 375-381.

Hsieh C., Wu W., 2009. Cultivation of microalgae for oil production with a cultivation strategy of urea limitation. Bioresour. Technol. 100, 3921–3926.

Issarapayup K., Powtongsook S., Pavasant P. 2009. Flat panel airlift photobioreactors for cultivation of vegetative cells of microalga *Haematococcus pluvialis*. J. Biotechnol. 142, 227–232.

Liu S., Waqas M.A., Wang S-h., Xiong X-y., Wan Y-f., 2017. Effects of increased levels of atmospheric CO_2 and high temperatures on rice growth and quality. PLoS ONE 12, e0187724.

Pradhan L., Bhattacharjee V., Mitra R., Bhattacharya I., Chowdhury R., 2015. Biosequestration of CO_2 using power plant algae (*Rhizoclonium hieroglyphicum* JUCHE2) in a Flat Plate Photobio-Bubble-Reactor – experimental and modeling, Chem. Eng. J. 275, 381–390.

Pooja K., Himabindu V. 2012. CO_2 Removal from industrial flue gas using *Botryococcus braunii* for simultaneous lipid production. International Journal of Science and Research (IJSR) ISSN (Online): 2319-7064.

Rao R., Sarada A.R. and Ravishankar G.A. 2007. Influence of co_2 on growth and hydrocarbon production in *Botryococcus Braunii*. J. Microbiol. Biotechnol, 17, 414–419.

Teresa M.M., Antonio A.M., Nidia S.C. 2010. Microalgae for biodiesel production and other applications: A review. Renewable and Sustainable Energy Reviews. 14, 217–232.

Toledo-Cervantes A., Morales M., Novelo E., Revah S., 2013. Carbon dioxide fixation and lipid storage by *Scenedesmus obtusiusculus*. Bioresource Technol. 130, 652–658.

Yaming G., Junzhi L., Guangming T. 2011. Growth characteristics of *Botryococcus braunii* 765 under high CO_2 concentration in photobioreactor. Bioresource Technology. 130–134.

Yeesang C., Cheirsilp B. 2014. Low-cost production of green microalga *Botryococcus braunii* biomass with high lipid content through mixotrophic and photoautotrophic cultivation Appl Biochem Biotechnol. 174, 116–129.

Yoo C., Jun S.Y., Lee J.Y., Ahn C.Y., Oh H.M. 2010. Selection of microalgae for lipid production under high levels carbon dioxide. Bioresource Technology. 101, S71–S74.

Yun Y.S., Lee S.B., Park J.M, Lee C., Yang J.W. 1997. Carbon Dioxide Fixation by Algal Cultivation Using Wastewater Nutrients J. Chem. Tech. Biotechnol. 69, 451-455.

Zhang H., Wang W., Li Y., Yang W., Shen G., 2011. Mixotrophic cultivation of *Botryococcus braunii*. Biomass Bioenergy. 35, 1710-1715.

Chapter 4

Real Time Monitoring of Algal Dynamics using Explicit Analytical Solution of Monod Kinetics Coupled with the Light Evolution Kinetic Model in Flat Panel Airlift Photobioreactor under Nitrate Limiting Conditions

4.1. Introduction

Microalgae are recognized as most favorable types of algae for the production of biofuel and other value added metabolites. Photosynthesis process in microalgae has ability to fix CO_2 into complex carbohydrate molecules (Teresa et al., 2010). Microalgae cultivation in photobioreactor has advantage of large scale production of biomass and lipid. Microalgae have higher growth rates and small doubling time, use inexpensive nutrients (i.e. wastewater), and do not contest with food crops or forests for agricultural land (Chanona et al., 2017; Sheehan et al., 1998; Schenk et al., 2008; Brennan and Owende, 2010). Therefore, photosynthetic microalgae are considered as ideal feedstock for the bio-oil production. Biolipid production from mass cultivation of microalgae can contribute up to 70 wt% of cell dry weight which can be employed as fossil fuel substitute if readily converted into biodiesel (Chanona et al., 2017). Commercial cultivation of microalgae for lipid production is commonly achieved by photobioreactor systems, nowadays flat panel photobioreactor are extensively used for mass cultivation of microalgae (Kunjapur et al., 2010).

Microalgal lipid in photobioreactor is affected by several chemical (nitrogen and phosphate) and physical parameters (temperature, irradiance, pH, etc.) (Breuer et al., 2013, Bamba et al., 2015, Cabello et al., 2015; Pancha et al., 2014). Among all, nitrate concentration is considered as the most prominent chemical variable to enhance microalgal growth rate and process productivity of microalgae in photobioreactor. Nitrogen limitation is positively correlated with lipid accumulation, whilst it has a negative impact on microalgae cell division, metabolic activity, biomass and lipid productivity (Brennan and Owende, 2010; Converti et al., 2009; Ordog et al., 2012). Nitrogen limitation reduced biomass growth and lipid productivity because availability of nitrogen containing molecules reduced under the influence of sub optimal nitrogen level in the medium, which affected cell growth (Wu et al., 2014). Nitrogen limitation also affects protein synthesis and chlorophyll formation, and suboptimal nitrogen supply leads to chlorosis in microalgae cells (kolber et al., 1988). In particular, different studies recommended that complete nitrogen limitation strategy have disadvantage of sub optimal biomass and lipid productivity (Ordog et al., 2012; Pancha et al., 2014), which subsequently increased the process harvesting cost (Chisti, 2007;

Grima et al., 2003; Ordog et al., 2012). Howbeit, intermediate nitrogen concentrations have increased photobioreactor process productivity more efficiently than total nitrogen limitation strategy (Dean et al., 2010; Ordog et al., 2012). Thus, efficient and economically viable large-scale lipid production in photobioreactor can be obtained under precise nitrogen starvation (Chen et al., 2011).

Microalgae growth kinetics in photobioreactor is generally described by the Monod kinetics under light saturating conditions (Lee et al., 2015). Monod kinetics assumed that the microalgae growth rate (μ) is governed by an external substrate concentration in culture solution under limiting substrate and light saturating conditions. The Monod kinetics includes one chemical and one biological parameter, i.e., the Monod constant K_s, and the maximum specific growth rate (μ_m) of the microorganism respectively. An analytic expression to the Monod kinetics does not exist in an explicit form, because in the final analytical solution of Monod kinetics the temporal substrate concentration (S (t)) cannot be expressed explicitly as a time (t) function. Notably, the analytical solution to the Monod kinetics turn into implicit function, i.e., time (t) was expressed in terms of limiting substrate concentration (S(t)) (Rubinow et al., 1975; Segel et al., 1993; Maggi et al., 2016). Moreover, several researchers obtained analytical solution to the Michaelis-Menten kinetics in explicit form using Lambert W function. However, an analytic solution to the Monod kinetics has not been attempted in explicit form.

He et al. (2016) established a kinetic model to illustrate *I. galbana* under varying sodium nitrate concentration in Flat panel photobioreactor. A mathematical model developed by Yang et al. (2011) described the biomass growth, product formation and nutrient consumption of Chlorella minutissima UTEX2341 in a 2L batch bioreactor. Similarly a logistic equation was used to model and simulate the growth pattern of *Chlorella Sorokiana* in bubble column and airlift photobioreactor (Kumar et al., 2012). Regarding limitations, the predictive capabilities of these models have rarely been evaluated. For eg., different sets of model parameters were used to simulate different experiments, even if experiments were performed under same conditions. However, in order to be robust, and exploitable, a model should present a set of parameters that is valid under different operating conditions. A robust process control and mathematical optimization strategies are required to obtain high biomass and lipid concentration simultaneously (Bernard et al., 2016). Thus, it is necessary to develop highly accurate models to predict dynamic behavior of the microalgae inside the photobioreactor. Therefore, Chanona et al. (2017) constructed a dynamic model and embedded an instantly measurable variable (i.e. chlorophyll fluorescence Y(II)) into the

model equation and accurately predicted the real time dynamics of microalgae using same set of parameters in photobioreactor. As suggested by Chanona et al. (2017), for continuous calibration of model and minimizing deviations from experimental data it is necessary to embed instantly measured variables (i.e. Y (II)) into the models. However, in this study, we have introduced light absorption factor (A) as instantly measured variable instead of Y (II), further a new differential equation is developed to estimate the biomass concentration as a function of absorbance factor (A) inside the flat panel airlift photobioreactor.

In the present study, in the first step the approximate solution of Monod kinetics was developed. Further, the explicit solution of the Monod kinetics was coupled with the light evolution kinetic equation to develop a consolidate differential equation for biomass, lipid and nitrate as a function of absorbance factor (A). The present model is based on Lambert-Beer law with varying light intensity in flat panel photobioreactor to develop the mathematical model as a function of light absorbance factor (A) only (i.e. independent of biomass concentration). Hence, the developed mathematical formulations could be used for the real time online monitoring of the algal dynamics in flat panel airlift photobioreactor.

4.2. Material and methods

4.2.1. Microalgae and culture medium

A culture of *B. braunii* was obtained from the Institute of Bioresources and Sustainable Development (IBSD, Takyelpat, Imphal). The microalgae were grown in modified BG-11 medium containing macronutrients such as $NaNO_3$ (1.12 g), $MgSO_4{\cdot}7H_2O$ (75 mg), $K_2HPO_4.\ 3H_2O$ (40 mg), $CaCl_2{\cdot}2H_2O$ (36 mg), Na_2CO_3 (20 mg), EDTA, 2Na-Mg salt (1 mg), citric acid (6 mg), ferric ammonium citrate (6 mg) and micronutrients such as H_3BO_3 (286 µg), $MnCl_2{\cdot}4H_2O$ (181 µg), $ZnSO_4{\cdot}7H_2O$ (22 µg), $Na_2MoO_4{\cdot}2H_2O$ (39 µg), $CuSO_4{\cdot}5H_2O$ (8 µg) and $Co(NO_3)_2{\cdot}6H_2O$ (5 µg) per liter (Khichi et al. 2018). The inoculated medium was incubated at 27 ± 1 °C and 130 rpm in a light incubator shaker. The initial pH of the medium was maintained at 8.

4.2.2. The photobioreactor and experimental design

Airlift Flat Panel photobioreactor was constructed using Borosilicate glass. The dimension of the reactor is (24.13× 29.21 × 7.62 cm) respectively. For air flow porous type sparger was used. The wall thickness was 5 mm and air was introduced into the base by sparger attached at the bottom.

Bubble column was converted into airlift bioreactor by inserting a centre glass plate into them (Fig. 1). During all the experiments room temperature was maintained at 27±2 °C, pH was also maintained to 7.8 during the experiment. The reactor was illuminated by light intensity from the range of 133 μmol m^{-2} s^{-1} by LED Panel placed at one side of the reactor. *B. braunii* was grown in 5.37 liter photobioreactor filled with BG-11 nutrient medium, and operating at 0.3 vvm air flow rate and 5% CO_2.

4.2.3. Determination of biomass concentration

Microalgal biomass was estimated as a function of the optical density (OD) of cell. OD of cells in the circulated liquid was determined using an UV–Visible spectrophotometer (Carry 60, Agilent) at an absorbance of 750 nm (OD_{750}). Dry cell weight (Dwt) was calculated using the following formula generated using OD data and a calibration plot.

C_b (g L^{-1}) = 2.155 OD_{750} (R^2 = 0.99)

where, C_b was the dry weight of biomass and OD_{750} is the optical density measured at 750nm. Therefore, the optical density can be used to precisely determine the dry weight of biomass.

4.2.4. Estimation of nitrate concentration

Nutrient removal was determined by nitrate quantification in the culture medium. To estimate the nitrate concentration 1 ml of sample was taken from the photobioreactorin every 12 h interval. Supernatant was separated by centrifugation at 10,000 rpm for 6 minutes. Nitrate concentration was determined by taking OD at 220 nm using a UV–Visible spectrophotometer (Carry 60 Agilent) according to the method proposed by APHA.

4.2.5. Lipid estimation

Lipid estimation in microalgae samples was performed using the modified rapid colorimetric method based on sulpho-phospho-vanillin (SPV) reaction in the presence of sulphuric acid (Cheng et al., 2011; Byreddy et al., 2016). The vanillin phosphoric acid reagent was prepared by dissolving 120 mg vanillin in 20 ml of distilled water and adjusting the final volume to 100 ml with 85% phosphoric acid. The reagent was stored in dark conditions until further use. SPV reagent was prepared freshly, which results in high activity with lipid samples. A known amount of *B. braunii* sample was taken in test tube and incubated for 100 ºC for 5 min, and allowed to cool for 5 min in an ice bath. Freshly prepared phospho-vanillin reagent (1 ml) was then added to each

test tube. The test tubes were incubated at 37 ºC and 200 rpm for 15 min, and absorbance was measured at 540 nm.

4.3. Model Development (I)

Microalgae growth kinetics is generally illustrated by the Monod kinetics in limiting substrate concentration under light saturating conditions (Lee et al. 2015). To derive the Monod kinetic expression it was assumed that the microalgae biomass i.e X reacted with the substrate S to form a substrate-biomass complex SX (i.e analogous to the Michaelis menten enzyme-substrate complex) and subsequently produce more biomass and product (P). Thus the model reaction can be expressed as Eq. (E4.1).

$$S + X \underset{k_{-1}}{\overset{k_1}{\rightleftharpoons}} SX \xrightarrow{k_2} x_n + P \qquad \text{(E4.1)}$$

In this developed model k_1, k_{-1} and k_2 are defined as the reaction kinetic constants, X_n is new biomass formed and P is the defined as a product. The differential equations derived from the Eq. (1) are difficult to solve, because the analytical solution to these differential equation is not present in the explicit form. Therefore, approximate analytical methods were developed. The mass balance was applied on Eq. (E4.1) and basic growth kinetic differential equations are expressed as

$$\frac{d[S]}{dt} = -k_1[X][S] + k_{-1}\,[SX] \qquad \text{(E4.2)}$$

$$\frac{d[SX]}{dt} = k_1[X][S] - (k_{-1} + k_2)[SX] \qquad \text{(E4.3)}$$

$$\frac{d[X_n]}{dt} = k_2[SX] \qquad \text{(E4.4)}$$

$$\frac{d[P]}{dt} = k_2[SX] \qquad \text{(E4.5)}$$

Where [ ] stand for concentration and the Eq. (E4.6) describes the initial conditions of the system

$$[S_0] = [s_0]_b, \quad [X_0] = [x_0], \quad [SX] = [P] = 0 \qquad \text{(E4.6)}$$

Where s_0 and x_0 denote the initial substrate concentrations and biomass concentration respectively. Here, we assume that the total biomass is sum of the initial biomass (X_0) and biomass substrate complex (SX) and denotes as Eq. (E4.7).

$$[X] = [X_0] + [SX] \qquad \text{(E4.7)}$$

After substituting Eq. (E4.7) into Eq. (E4.2) and Eq. (E4.3)

$$\frac{d[S]}{dt} = -k_1[X_0][S] + (k_{-1} - k_1[S])\,[SX] \qquad \text{(E4.8)}$$

$$\frac{d[SX]}{dt} = -k_1[X_0][S] + (k_{-1} - k_1[S])\,[SX] \qquad \text{(E4.9)}$$

The dimensions variables for system of the Eq. (E4.8) and Eq. (E4.9) are defined as Eq. (E4.10)

$$s(\tau) = \frac{[S]}{s_0}, \qquad c(\tau) = \frac{[SX]}{X_0}, \quad X(\tau) = \frac{[X]}{X_0}, \quad \varepsilon = \frac{X_0}{s_0},$$

$$\lambda = \frac{k_{-1}}{k_1 s_0}, \quad \tau = \frac{k_1 X_0 t}{\varepsilon}, \qquad K = \frac{k_{-1}-k_2}{k_1 s_0} \qquad \text{(E4.10)}$$

In terms of dimensionless variables, Eq. (E4.8) and (E4.9) can be described as

$$\frac{ds}{d\tau} = -\varepsilon s - \varepsilon c s + \lambda \varepsilon c \qquad \text{(E4.11)}$$

$$\frac{dc}{d\tau} = -Kc + s + sc \qquad \text{(E4.12)}$$

4.3.1. Approximate analytical solution by homotopy perturbation method

To describe the concept of homotopy perturbation techniqe, a non-linear differential equation was considered in the following form

$$L(u) + N(u) - f(r) = 0, \qquad r \in \Omega \qquad \text{(E4.13)}$$

With boundary conditions

$$B\left(u, \frac{\partial u}{\partial n}\right) = 0, \quad r \in \Gamma \qquad \text{(E4.14)}$$

Where L is the linear differential operator, N is the nonlinear differential operator and $f(r)$ is defined as known analytic function, B is a boundary operator and Γ is the boundary of the domain Ω.

To solve the differential Eq. (E4.11) and Eq. (E4.12) a homotopy was constructed as

$v(r,p): \Omega \times [0,1] \to \mathbb{R}$, which satisfies

$$H(v,p) = (1-p)[L(v) - L(u_0)] + p\,[L(v) + N(v) - f(r)] = 0, \qquad \text{(E4.15)}$$

Or

$$H(v,p) = L(v) - L(u_0) + pL(u_0) + p[N(v) - f(r)] = 0, \qquad \text{(E4.16)}$$

Where $p\ \varepsilon\ [0,1]$ is an embedding parameter, while u_0 is consider as an initial approximation to the Eq. (E4.15), that can satisfies the boundary conditions, from Eq. (E4.15) and (E4.16) we have

$$H(v,0) = L(v) - L(u_0) = 0 \qquad \text{(E4.17)}$$

$$H(v,1) = L(v) + N(v) - f(r) = 0 \qquad \text{(E4.18)}$$

Thus, at $p = 0$, Eq. (E4.15) and (E4.16) turn into a linear equation, while at $p = 1$ it becomes the original non linear Eq. (E4.13). When the parameter p increase from 0 to 1, the problem $L(v) - L(u_0) = 0$ (i.e. apparently an easy problem) is repeatedly deformed to the (difficult) problem (Vogt et al., 2013).

$$L(v) + N(v) - f(r) = 0 \qquad \text{(E4.19)}$$

According to the homotopy perturbation method, the solution of Eq. (E4.15) and (E4.16) can be expressed as a power series in p

$$v = v_0 + pv_1 + p^2 v_2 + \cdots \qquad \text{(E4.20)}$$

Putting $p = 1$ produces an approximate solution of Eq. (E4.13).

$$u = \lim_{n\to 1} v = v_0 + v_1 + v_2 + \cdots \qquad \text{(E4.21)}$$

The following homotopy has been constructed for Eq. (E4.11) and (E4.12)

$$(1-p)\left(\frac{ds}{d\tau} + \varepsilon s\right) + p\left(\frac{ds}{d\tau} + \varepsilon s + \varepsilon cs - \lambda\varepsilon c\right) = 0, \qquad \text{(E4.22)}$$

$$(1-p)\left(\frac{dc}{d\tau} + Kc\right) + p\left(\frac{dc}{d\tau} + Kc - s - sc\right) = 0, \qquad \text{(E4.23)}$$

Or equivalently,

$$\frac{ds}{d\tau} + \varepsilon s + p(\varepsilon cs - \lambda\varepsilon c) = 0 \qquad \text{(E4.24)}$$

$$\frac{dc}{d\tau} + Kc + p(-s - sc) = 0 \qquad \text{(E4.25)}$$

With initial conditions s(0)=1, c(0)=0, the dimensionless function $s(\tau)$ and $c(\tau)$ are approximated by

$$s = s_0 + ps_1 + p^2 s_2 + \cdots, \quad \text{(E4.26)}$$

$$c = c_0 + pc_1 + p^2 c_2 + \cdots, \quad \text{(E4.27)}$$

Substituting Eq. (E4.26) and (E4.27) into the Eq. (E4.24) and (E4.25) and comparing the coefficient of like powers of p, we obtain the system of differential equations

$$p^0 : \frac{ds_0}{d\tau} + \varepsilon s_0 = 0, \quad \text{(E4.28)}$$

$$p^1 : \frac{ds_1}{d\tau} + \varepsilon s_1 + \varepsilon s_0 c_0 - \lambda\varepsilon c_0 = 0, \quad \text{(E4.29)}$$

$$p^2 : \frac{ds_2}{d\tau} + \varepsilon s_2 + \varepsilon s_0 c_1 + \varepsilon s_1 c_0 - \lambda\varepsilon c_1 = 0, \quad \text{(E4.30)}$$

And

$$p^0 : \frac{dc_0}{d\tau} + K c_0 = 0, \quad \text{(E4.31)}$$

$$p^1 : \frac{dc_1}{d\tau} + K c_1 - s_0 - s_0 c_0 = 0, \quad \text{(E4.32)}$$

$$p^2 : \frac{dc_2}{d\tau} + K c_2 - s_1 - s_0 c_1 - s_1 c_0 = 0, \quad \text{(E4.33)}$$

With initial conditions

$$s_0(0) = 1, c_0(0) = 0, s_i(0) = 0, c_i(0) = 0, i = 1,2, \ldots \quad \text{(E4.34)}$$

Solving Eq. (E4.28) to (E4.33) with initial conditions Eq. (E4.34), we find

$$s_0(\tau) = e^{-\varepsilon\tau} \quad \text{(E4.35)}$$

$$s_1(\tau) = 0 \quad \text{(E4.36)}$$

$$s_2(\tau) = \left[-\frac{1}{K} - \frac{\lambda\varepsilon}{(K-\varepsilon)^2}\right] e^{-\varepsilon\tau} + \frac{\lambda\varepsilon}{(K-\varepsilon)}\, \tau e^{-\varepsilon\tau} + \frac{e^{-2\varepsilon\tau}}{(K-\varepsilon)} - \frac{\varepsilon\, e^{-(\varepsilon+K)\tau}}{K\,(K-\varepsilon)} + \frac{\lambda\varepsilon}{(K-\varepsilon)^2} e^{K\tau} \quad \text{(E4.37)}$$

$$s(\tau) = s_0(\tau) + s_1(\tau) + s_2(\tau) + \cdots \quad \text{(E4.38)}$$

and

$$c_0(\tau) = 0 \quad \text{(E4.39)}$$

$$c_1(\tau) = \frac{e^{-\varepsilon\tau} - e^{K\tau}}{(K-\varepsilon)} \quad \text{(E4.40)}$$

$$c_2(\tau) = -\frac{e^{-K\tau}}{\varepsilon\,(K-2\varepsilon)} + \frac{e^{-2\varepsilon\tau}}{(K-2\varepsilon)(K-\varepsilon)} + \frac{e^{-(\varepsilon+K)\tau}}{\varepsilon\,(K-\varepsilon)} \quad \text{(E4.41)}$$

$$c(\tau) = c_0(\tau) + c_1(\tau) + c_2(\tau) + \cdots \quad \text{(E4.42)}$$

Here, we assumed that the microalgae substrate in light saturating conditions following the zero order kinetics, so that neglecting the higher order terms from the Eq. (E4.38) the final equation for substrate concentration can be expressed as Eq. (E4.43).

$$s(\tau) = e^{-\varepsilon\tau} \quad \text{(E4.43)}$$

After substituting the dimensionless variables from Eq. (E4.10) into the Eq. (E4.43).

$$S(t) = s_0 e^{-k_1 X_0 t} \quad \text{(E4.44)}$$

where S(t) is the temporal substrate concentration (g L^{-1}), s_0 is the initial substrate concentration (g L^{-1}), k_1 is the substrate kinetic constant (L g^{-1} d^{-1}) and X_0 is the initial biomass concentration (g L^{-1}).

4.3.2. Biomass growth model

Microalgae biomass growth model in photobioreactor can be expressed as Eq. (E4.45)

$$\frac{dX}{dt} = \mu \cdot X \quad \text{(E4.45)}$$

The specific growth rate (μ) of the microalgae written as Eq. (E4.46)

$$\mu = \frac{\mu_m\, S(t)}{K_s + S(t)} \quad \text{(E4.46)}$$

After, substituting values of $S(t)$and μ from Eq. (E4.44) and (E4.46) into the Eq. (E4.45) the microalgae biomass growth model can be represent as Eq. (E4.47)

$$\frac{dX}{dt} = \frac{\mu_m \, s_0 e^{-k_1 X_0 t}}{K_s + s_0 e^{-k_1 X_0 t}} \cdot X \qquad \text{(E4.47)}$$

Or Equivalently

$$\frac{dX}{dt} = \frac{\mu_m}{1 + \frac{K_s e^{k_1 X_0 t}}{s_0}} \cdot X \qquad \text{(E4.48)}$$

On separating variables and integration of Eq. (E4.48) produce and explicit analytical solution as

$$X(t) = X_0 e^{\left(\mu_m t - \frac{\mu_m}{k_1 X_0} \ln\left(1 + \frac{K_S}{s_0} e^{k_1 X_0 t}\right)\right)} \qquad \text{(E4.49)}$$

where $X(t)$ is the temporal biomass concentration (g L^{-1}), X_0 is the initial biomass concentration (g L^{-1}), μ_m is the maximum specific growth of the organism (d^{-1}), K_S is the half saturation constant (g L^{-1}), s_0 is the initial substrate concentration (g L^{-1}), and k_1 is the substrate kinetic constant (L g^{-1} d^{-1}).

4.4. Model Development (II)

4.4.1. The light attenuation model

Light attenuation model in a flat panel model is developed previously using the Lambert–Beer law and can be expressed as which speculate that light attenuation per unit distance is proportional to the product of biomass concentration and incident light intensity and can be expressed as Eq. (E4.50).

$$\frac{dI}{dz} = -K_a \cdot I \cdot X \qquad \text{(E4.50)}$$

After Integrating the Eq. (E4.50) from 0 to L results in the following:

$$\ln\left(\frac{I}{I_0}\right) = -K_a X L \qquad \text{(E4.51)}$$

On rearranging Eq. (E4.51), it can be written as Eq. (E4.52)

$$\frac{1}{\mathrm{L}}\ln\left(\frac{I_0}{I}\right) = K_a X \qquad \text{(E4.52)}$$

The left hand side of Eq. (E4.52) was assigned as a new function, called as absorbance factor (A), and the general equation will be described as Eq. (E4.53a) or (E4.53b).

$$\mathrm{A} = K_a \cdot X \qquad \text{(E4.53a)} \qquad \text{(Or)} \quad X = \frac{A}{K_a} \qquad \text{(E4.53b)}$$

Where A is the absorbance factor (m^{-1}) and calculated as Eq. (E4.54).

$$\mathrm{A} = \frac{1}{\mathrm{L}}\ln\left(\frac{I_0}{I}\right) \qquad \text{(E4.54)}$$

In Eq. (E4.53a), K_a is the specific biomass light absorption coefficient ($m^2\ kg^{-1}$); and X is biomass concentration ($g\ L^{-1}$).

4.4.2 Light evolution kinetic model

Based on Lambert–Beer light attenuation model in photobioreactor a differential light kinetic model in flat panel airlift photobioreactor has been developed.

After substituting X from Eq. (E4.49), into the Eq. (E4.53a)

$$A = K_a \cdot \left(X_0 e^{\left(\mu_m t - \frac{\mu_m}{k_1 X_0}\ln\left(1+\frac{K_S}{s_0}e^{k_1 X_0 t}\right)\right)}\right) \qquad \text{(E4.55)}$$

Now, after differentiating A with respect to time

$$\frac{d}{dt}(A) = K_a \cdot X_0 * \frac{d}{dt}\left(e^{\left(\mu_m t - \frac{\mu_m}{k_1 X_0}\ln\left(1+\frac{K_S}{s_0}e^{k_1 X_0 t}\right)\right)}\right) \qquad \text{(E4.56)}$$

$$\frac{dA}{dt} = \frac{K_a \cdot X_0 \cdot \mu_m\ e^{\left(\mu_m t - \frac{\mu_m}{k_1 X_0}\ln\left(1+\frac{K_S}{s_0}e^{k_1 X_0 t}\right)\right)}}{1+\frac{K_S}{s_0}e^{k_1 X_0 t}} \qquad \text{(E4.57)}$$

where A is the absorbance factor (m^{-1}), X_m is the maximum biomass concentration ($g\ L^{-1}$), K_a is the specific biomass light absorption coefficient ($m^2 kg^{-1}$), K_c is the apparent maximum specific growth rate (h^{-1}), X_0 is the initial biomass concentration ($g\ L^{-1}$).

4.5 Consolidate Model I and Model II

4.5.1 Biomass growth kinetics coupled with light evolution kinetic model

Biomass growth of *B. braunii* is affected by the light availability inside the photobioreactor. Thus, the differential equation for biomass growth was expressed as Eq. (E4.48). The dependable variable appears in the right hand side of the Eq. (E4.48) is biomass concentration, which is function of the absorbance factor (A). After substituting value of X form Eq. (E4.53b), into the Eq. (E4.48), the final differential equation of biomass growth rate in terms of light absorbance factor was expressed as Eq. (E4.58).

$$\frac{dX}{dt} = \left(\frac{\mu_m}{1+\frac{K_s e^{k_1 X_0 t}}{s_0}}\right) \cdot \left(\frac{A}{K_a}\right) \qquad \text{(E4.58)}$$

4.5.2. Sodium nitrate consumption kinetics coupled with light evolution kinetic model

Sodium nitrate consumption kinetics in the microalgae is described by the following equation (He et al., 2016).

$$-\frac{dS}{dt} = \frac{1}{Y_{X/S}} \times \frac{dX}{dt} + mX \qquad \text{(E4.59)}$$

Now, after substituting value of $\frac{dX}{dt}$ and X from Eq. (E4.58) and Eq. (E4.53b) respectively into the Eq. (E4.59), the substrate consumption kinetics can be expressed as a function of the light absorbance factor and expressed as Eq. (E4.60).

$$-\frac{dS}{dt} = \frac{1}{Y_{X/S}} \times \left(\frac{\mu_m}{1+\frac{K_s e^{k_1 X_0 t}}{s_0}}\right) \cdot \left(\frac{A}{K_a}\right) + m \cdot \left(\frac{A}{K_a}\right) \qquad \text{(E4.60)}$$

4.5.3. Lipid formation kinetics coupled with light evolution kinetic model

Luedeking-Piret equation was used to predict lipid production in *B. braunii* according to the following equation

$$\frac{dP}{dt} = \alpha . \frac{dX}{dt} + \beta X \qquad \text{(E4.61)}$$

Now, after substituting value of $\frac{dX}{dt}$ and X from Eq. (E4.58) and Eq. (E4.53b) respectively into the Eq. (E4.16), lipid formation kinetics can also be expressed as a function of the light absorbance factor and written as Eq. (E4.62).

$$\frac{dP}{dt} = \alpha \cdot \left(\frac{\mu_m}{1+\frac{K_s e^{k_1 X_0 t}}{s_0}} \right) \cdot \left(\frac{A}{K_a}\right) + \beta \cdot \left(\frac{A}{K_a}\right) \qquad \text{(E4.62)}$$

4.6. Results and discussion

4.6.1. Model calibration

B. braunii behavior in photobioreactor is characterized by biological and physiochemical parameters, so these model parameters must be ingrained into the prospective model to simulate algal dynamics in the photobioreactor. As a result of this, the developed consolidate model retrieved all these model parameters for a base case tested under one specific condition (i.e. 133 µmol m^{-2} s^{-1}, 5% CO_2 and $NaNO_3$=1.125g L^{-1}).

Table 4.1. Best fit model parameters and comparable literature values (adapted from Chapter 5)

Parameters	Best fit value	Comparable values from literature
K_a (m^2 kg^{-1})	65.56	75.2 for *Nanachloropsis* sp.(Gentile and Blanch,2001)
		200 for *Monodus subterraneus* (Bosma et al., 2007)
μ_m (d^{-1})	0.934	μ_m of 0.99 for *Rhizoclonium h*. (pradhan et al., 2015)
		μ_m of 1.2 for *N Salina* (Pegallapati et al., 2012)
		μ_m of 0.94 for *S. obliquus* (Ruiz et al., 2013)
K_1 (L g^{-1} d^{-1})	0.55	Best fit value
K_s (g L^{-1})	0.065	0.058 for *B. braunii* (Nur et al., 2017)
$Y_{X/S}$ (g g^{-1})	3.424	6.92 – 15.18 for *I.galbana* (He et al., 2016)
α (g g^{-1})	0.2063	0.125 for *C. salina* 0.151 for *N. oculata* (Surendhiran et al., 2015)
		3.37×10^{-2} – 7.02×10^{-2} for *I. galbana* (He et al., 2016)
β (g g^{-1})	4×10^{-4}	2×10^{-3} for *C. salina* 6×10^{-4} for *N. oculata* (Surendhiran et al., 2015)
		0.5×10^{-5} – 2.52×10^{-2} for *I. galbana* (He et al., 2016)

Experimental data of light absorbance factor (A), biomass concentration, nitrate removal and lipid concentration in the photobioreactor for every 8h was used to calibrate the model. The model parameters obtained in the calibration step kept fixed for the remaining sets of the experimental data to validate the proposed model. In the calibration step numerical optimization was implemented using the fminsearch routine in Matlab® program with interpolation function (interp1). The model parameters to be obtained were the, biomass specific absorption coefficient (Ka), substrate kinetic constant (K_1), maximum growth rate (μ_{max}), biomass yield constant on nitrate ($Y_{x/s}$), half saturation constant (K_s), growth associated constant for lipid (α), non growth associated constant (β) for lipid and the light extinction coefficient (K_a)

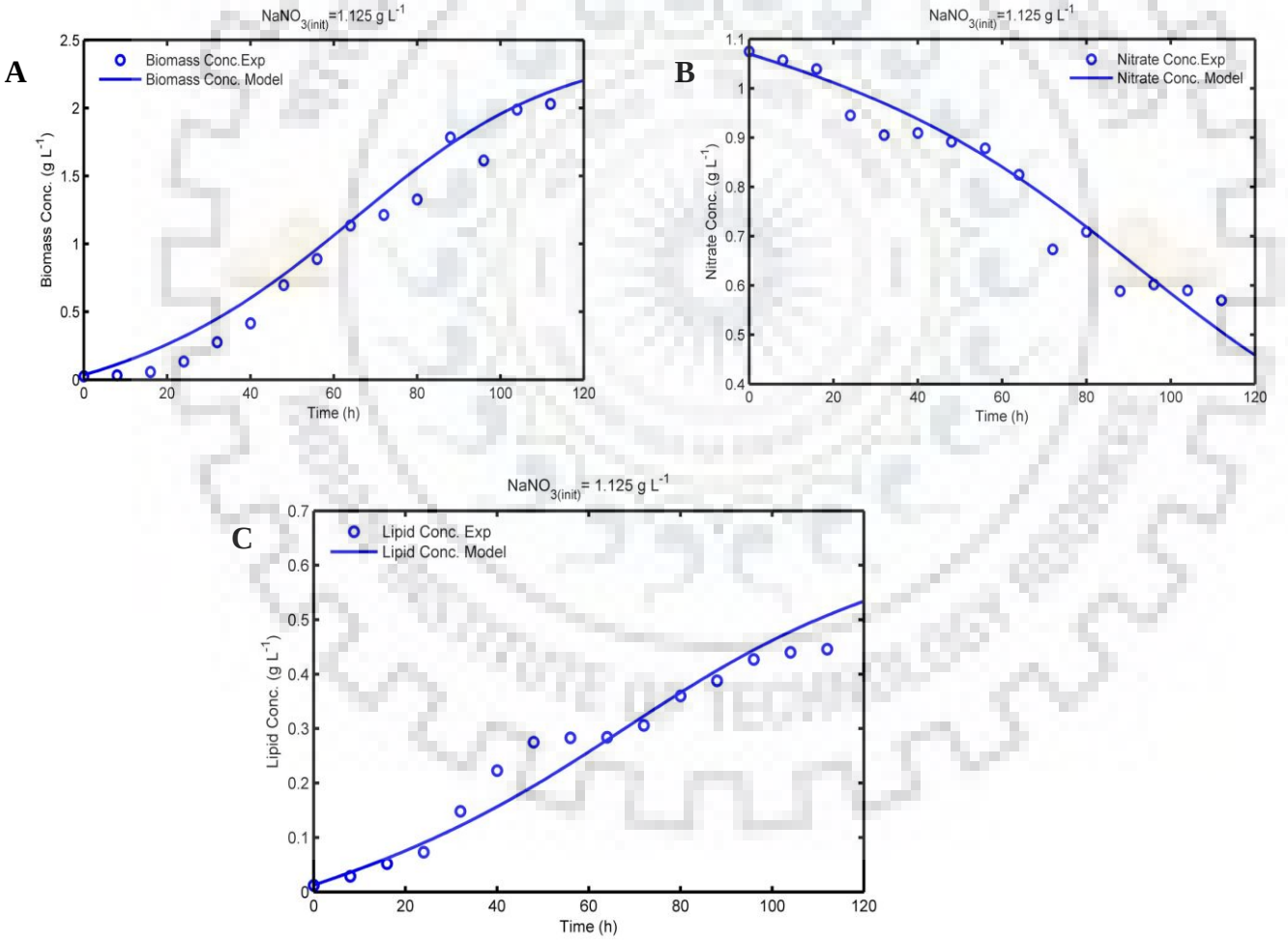

Fig. 4.1. Model Calibration under specific condition of $NaNO_{3\,(init)}^{-}$ = 1.125 g L^{-1}, initial light intensity of 133 µmol $m^{-2}s^{-1}$ and 5% CO2 concentration for (A) Biomass concentration; (B) Nitrate concentration; and (C) lipid concentration respectively.

4.6.2. Model validation

Biomass growth data points of *B. braunii* collected under varying nitrate concentration were fitted as a function of light absorbance factor (A) by Eq. (E4.58). Model validation was confirmed by comparing the experimental data (i.e. biomass) with the simulated values of *B. braunii* under nitrate limiting conditions (i.e. 0.375, 0.75 and 1.125 g L^{-1} nitrate concentration) respectively.

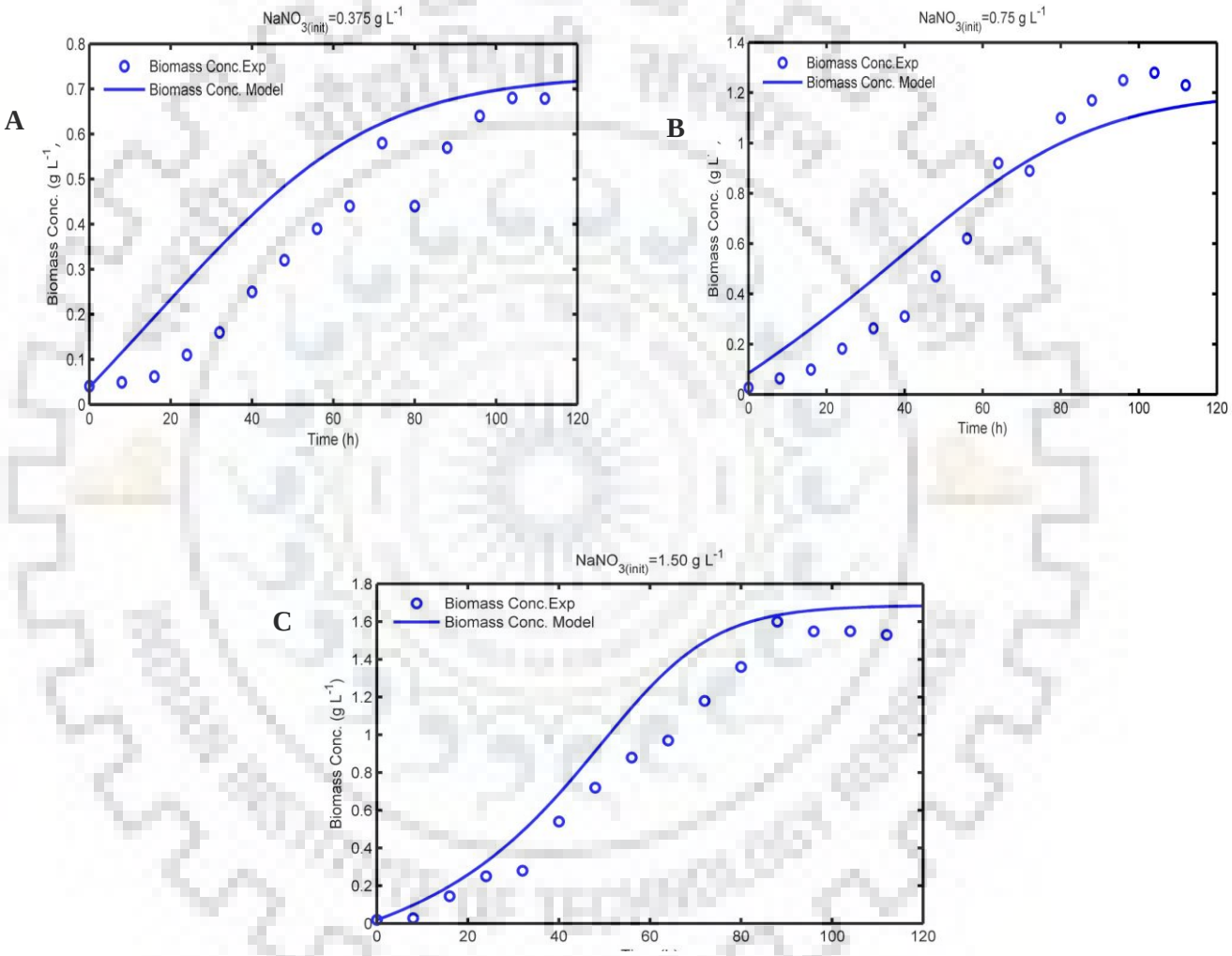

Fig. 4.2. Model validation for biomass concentration as a function of light evolution kinetic model under different nitrate concentration of (A) $NaNO_{3\,(init)}^{-}$= 0.375 g L^{-1}; (B) $NaNO_{3\,(init)}^{-}$= 0.75 g L^{-1}; and (C) $NaNO_{3\,(init)}^{-}$= 1.5 g L^{-1} respectively.

Comparison of model predicted values and experimental data, for biomass in nitrate limiting condition are shown in Fig 4.2. The prediction accuracy of the model was greater than 98% for B.

braunii. This distinctly suggest that this consolidate kinetic model (i.e. Monod kinetic coupled with light evolution model) developed in the study can be adequately used to determine the microalgal biomass in nitrate limiting conditions. Maximum biomass concentration and biomass productivity were 2.03 g L−1 and 0.426 g L−1 d−1, respectively, at nitrate concentration of 1.12 g L-1 after 5 days of cultivation (Fig 4.1 (A)). As shown in (Fig 4.2(A) and 4.2 (B)), the reduction of biomass concentration was observed with decrement in nitrate concentration in culture medium, which suggests that cell growth and metabolic activity of cell slow downed under nitrogen limiting conditions (Wu et al., 2014; Pancha et al., 2014). At higher than optimum nitrate level in the medium (i.e. $NaNO_{3\ (init)}^{-}$= 1.5 g L-1) the biomass concentration further decreased compared to the optimum biomass concentration (i.e. 2.03 g L−1), and the maximum observed biomass concentration was 1.53 g L−1, this indicate that higher nitrate concentration can be detrimental to the algal cell that subsequently reduce the growth of the microalgae (Wu et al., 2014).

Dynamic consumption of nitrate in the nutrient medium under nitrate limiting conditions, as the function of light absorbance factor depicted in (Fig. 4.3A–C), over the ranges of different initial nitrate concentrations and 5% feed gas CO_2 concentration studied. The temporal decrease in nitrate concentration as a function of light absorbance factor (A) under different nitrate concentrations (i.e. 0.375, 0.75 and 1.125 g L^{-1}) was experimentally validated by the output of the model Eq. (E4.60) using the calibrated model parameter values as listed in Table 4.1.

The simulated values produced by the model Eq. (E4.60) were in good agreement with the experimental data under nitrate limiting condition and demonstrate that temporal substrate consumption in FPBR by *B. braunii* could be define very well using Eq. (E4.60).

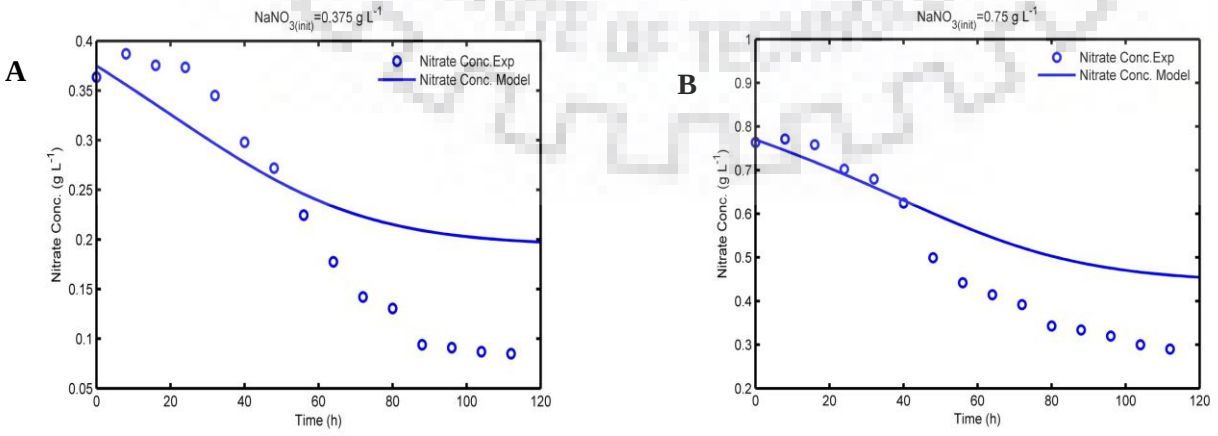

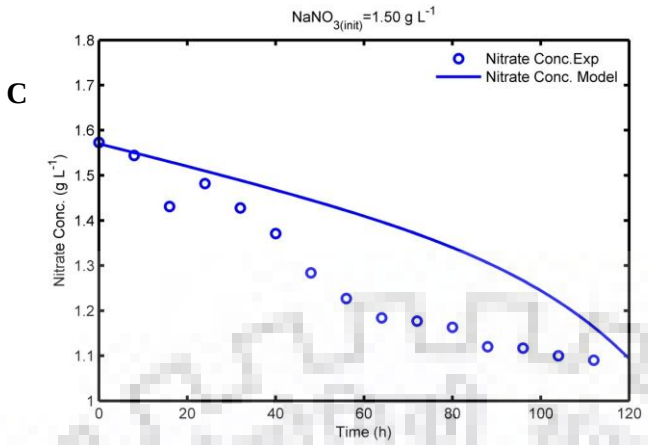

Fig. 4.3. Model validation for residual nitrate concentration as a function of light evolution kinetic model under different nitrate concentration of (A) $NaNO_{3\ (init)}^{-}$= 0.375 g L^{-1}; (B) $NaNO_{3\ (init)}^{-}$= 0.75 g L^{-1}; and (C) $NaNO_{3\ (init)}^{-}$= 1.5 g L^{-1} respectively.

Nitrate removal rate increased linearly with the increase in nitrate concentration in the range of 0.375 to 1.125 g L^{-1}, with the further increment in nitrate concentration (i.e. at $NaNO_{3\ init}$ = 1.5 g L^{-1}) nitrate depletion rate was decreased. Maximum nitrate removal rate of 118.93 mg L^{-1} d^{-1} was observed at $NaNO_{3\ init}$ of 1.125 g L^{-1}. Whilst nitrate removal rate of 62.14, 102.86 and 87.86 mg L^{-1} d^{-1} were observed at the remaining $NaNO_{3\ init}$ of 0.375, 0.75 and 1.5 g L^{-1} respectively.

Biolipid formation kinetics was analyzed by Eq. (E4.62). Based on observation of Fig. 4.4 A–C, the experimental data was fitting well to the model equation, indicating the lipid production in *B. braunii* culture in FPBR can be best described by light coupled lipid Monod kinetics equation. Remarkably, the light coupled lipid Monod kinetic model produces a small overestimation at low level of nitrate concentration (i.e. at $NaNO_{3\ init}$ = 0.375 g L^{-1}) whilst at other nitrate concentration (i.e. at $NaNO_{3\ init}$ = 0.75 L^{-1}) the developed kinetic model produce underestimated outputs. These small variations could be due to the varying nitrate level present in the culture solution, because earlier studies suggests that lipid accumulation within the algal cell is a regulated by external nitrogen source and its concentration (Pancha et al., 2014).

In addition, under nitrogen limiting conditions microalgal cell preferred lipid as a storage molecule because reduced state of biolipids have the ability to be packaged within the cell under stress conditions for their energy requirements. Particularly, the nitrate concentration in the culture solution significantly affects the lipid content of the microalgal cell, and the lower nitrate in nutrient medium triggers the biosynthetic pathway for the lipid production in microalgal cell.

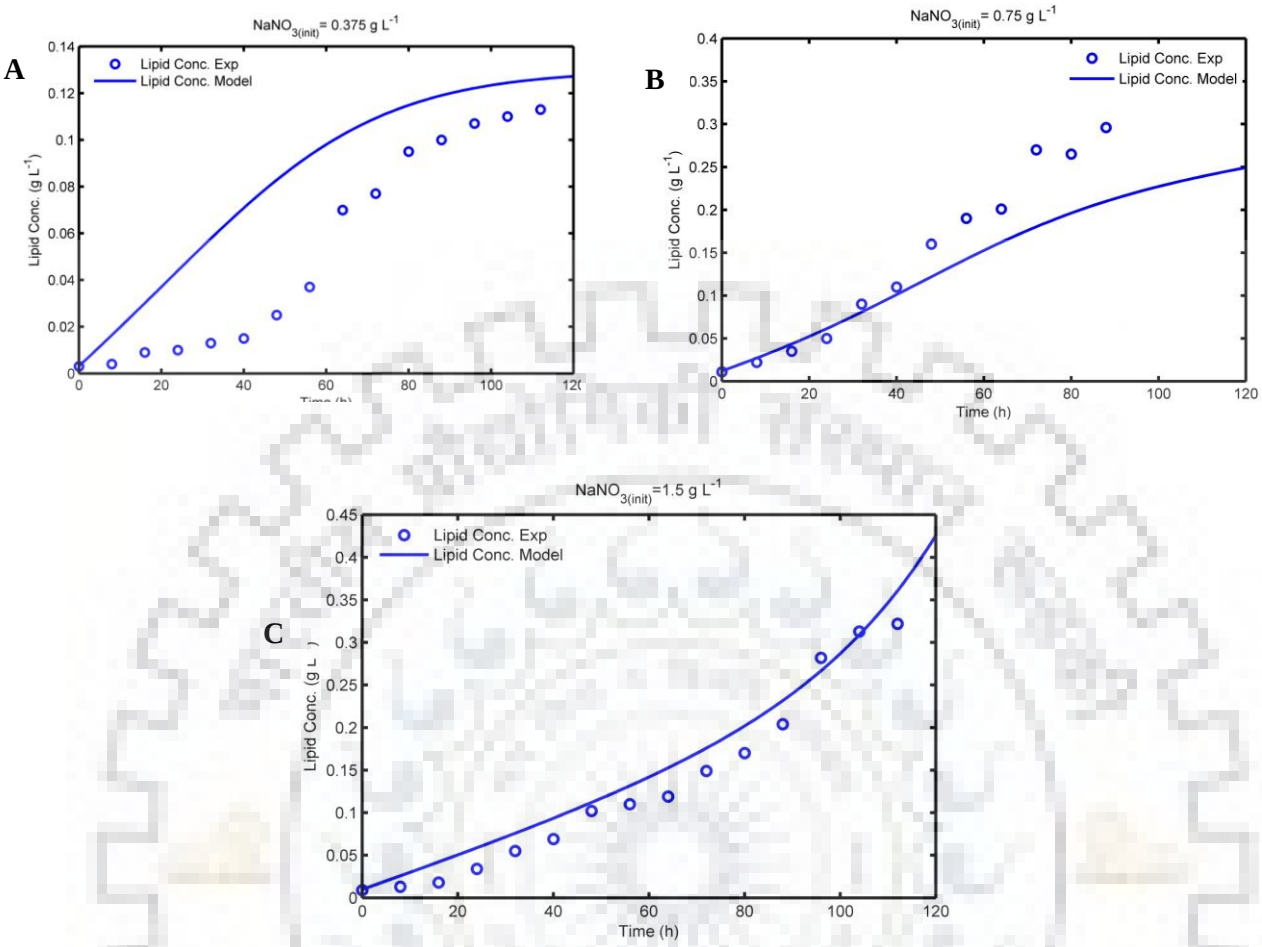

Fig. 4.4. Model validation for biolipid concentration as a function of light evolution kinetic model under different nitrate concentration of (A) $NaNO_{3\ (init)}^{-}$ = 0.375 g L^{-1}; (B) $NaNO_{3\ (init)}^{-}$ = 0.75 g L^{-1}; and (C) $NaNO_{3\ (init)}^{-}$ = 1.5 g L^{-1} respectively.

The biolipid content of the *B. braunii* showed decreasing trend with respect to the increasing nitrate level in the culture solution. The biolipid production trend for B braunii was as follows: 0.375 g L^{-1} (25.29%) > 0.75 g L^{-1} (22.58%) > 1.125 g L^{-1} (18.27%) > 1.5 g L^{-1} (17.42%). The results reported in this study (i.e. biolipid production trend) are consistent with the Wu et al. (2014), who reported quite similar trend of biolipid production (i.e. 0.3 g L−1 (39.16%) > 0.6 g L−1 (36.56%) > 0.9 g L−1 (34.92%) > 1.5 g L−1(32.53%)) for *S. obliquus*. Regarding to the intermediate nitrate level of 1.125 g L^{-1} in the culture solution, the results are in good agreement with the experimental data and suggests that the maintaining the intermediate concentration of nitrate in the nutrient medium is more suitable to produce the high biomass and lipid content for *B. braunii* in flat panel photobioreactor.

4.7. Statistical analysis

The model was further validated by applying the regression analysis for the experimental and predicted profiles of biomass, nitrate and lipid using the Microsoft excel solver. The quality and significance of the fits achieved between measured and predicted data under four different nitrate level concentrations are summarized in Table 4.2, 4.3 and 4.4.

Table 4.2. Regression analysis and goodness of fit between predicted and measured biomass concentration at different nitrate level concentration.

Light Intensity (μmol m^{-2} s^{-1})	R^2	SS	Std Err	F value	Significance F	P value	Adjusted R^2
0.375	0.964	4.02	0.106	345.2488	3.29 E-10	9.59E-11	0.886
0.75	0.967	9.209	0.151	387.958	1.67E-10	4.61E-11	0.891
1.125	0.989	16.25	0.117	1169.041	2.49E-13	4.05E-14	0.917
1.50	0.989	20.57	0.128	1238.719	1.77E-13	2.79E-14	0.912

Table 4.3. Regression analysis and goodness of fit between predicted and measured nitrate concentration at different nitrate level concentration

Light Intensity (μmol m^{-2} s^{-1})	R^2	SS	Std Err	F value	Significance F	P value	Adjusted R^2
0.375	0.905	0.947	0.083	124.21	1.1E-07	5.05E-08	0.828
0.75	0.969	4.758	0.106	407.77	1.25E-10	3.36E-11	0.892
1.125	0.997	9.676	0.044	4841.603	5.16E-17	4.15E-18	0.920
1.50	0.996	27.27	0.084	3811.013	2.16E-16	1.96E-17	0.919

Table 4.4. Regression analysis and goodness of fit between predicted and measured biolipid concentration at different nitrate level concentration

Light Intensity (μmol m^{-2} s^{-1})	R^2	SS	Std Err	F value	Significance F	P value	Adjusted R^2
0.375	0.901	0.12	0.030	121.227	1.25E-07	5.83E-08	0.826
0.75	0.982	0.35	0.020	874.57	1.42E-12	2.61E-13	0.908
1.125	0.984	1.31	0.039	814.75	2.12E-12	4.11E-13	0.907
1.50	0.989	0.49	0.020	1212.19	2.011E-13	3.21E-14	0.912

The regression analysis was illustrated by R^2 values (>0.901) and p values (below 0.0001) for the all validated points. The model appears to reflect the dynamic profile of biomass, nitrate and lipid under varying nitrate concentrations with reasonable accuracy, comparable to that reported by

Ahmed et al. (2016) who investigated the carbon fixation and nutrient removal under various initial concentrations of nitrate, phosphate, CO_2 and light intensities.

4.8. Conclusions

The real time monitoring of algal dynamics using explicit analytical solution of Monod kinetics coupled with the novel light evolution kinetic model in flat panel airlift photobioreactor are addressed in this work. Validation of the model equation was confirmed by predicting the model outputs with the experimental data. The obtained good correlation and statistically significant results suggest that new consolidate differential equation of biomass, lipid and nitrate as a function of absorbance factor (A) can be used as effective tool to monitor the algal dynamics real time.

4.8. References

APHA. 1976. Standard methods for the examination of water and wastewater 14ed. APHA American Public Health Association.

Arbib Z., Ruiz, J., Alvarez-Diaz P., Garrido-Perez C., Perales J. A., 2014. Capability of different microalgae species for phytoremediation processes: wastewater tertiary treatment, CO_2 bio-fixation and low cost biofuels production. Water Research. 49, 465–474.

Bamba B.S.B., Lozano P., Adjé F., Ouattara A., Vian M.A., Tranchant, Lozano Y.,2015. Effects of temperature and other operational parameters on *Chlorella vulgaris* mass cultivation in a simple and low-cost column photobioreactor, Appl. Biochem. Biotechnol. 177, 389-406.

Bernard O., Mairet F., Chachuat B., 2016. Modelling of microalgae culture systems with applications to control and optimization. Adv. Biochem. Engg. Biotechnol. 153, 59–87.

Bosma R., van Zessen E., Reith J. H., Tramper J., Wijffels R. H., 2007. Prediction of volumetric productivity in an outdoor photobioreactor. Biotechnol Bioeng. 97(5), 1108–1120.

Brennan L., Owende P., 2010. Biofuels from microalgae—A review of technologies for production, processing, and extractions of biofuels and co-products. Renewable and Sustainable Energy Reviews, 14(2), 557–577.

Breuer G., Lamers P.P., Martens D.E., Draaisma R.B., Wijffels R.H., 2013. Effect of light intensity, ph, and temperature on triacylglycerol (tag) accumulation induced by nitrogen starvation in *Scenedesmus obliquus*, Bioresour. Technol. 143, 1-9.

Byreddy A. R., Gupta A., Barrow C. J., Puri M., 2016. A quick colorimetric method for total lipid quantification in microalgae. Journal of Microbiological Methods. 125, 28–32.

Cabello J., Cervantes A.T., Sánchez L., Revah S., Morales M., 2015. Effect of the temperature, ph and irradiance on the photosynthetic activity by *Scenedesmus obtusiusculus* under nitrogen replete and deplete conditions, Bioresour. Technol. 181, 128-135.

Chen M., Tang H., Ma H., Holland T.C., Ng K.Y., Salley S.O., 2011. Effect of nutrients on growth and lipid accumulation in the green algae *Dunaliella tertiolecta*. Bioresour. Technol. 102, 1649-1655.

Cheng Y. S., Zheng Y., Gheynst J. V., 2011. Rapid quantitative analysis of lipids using a colorimetric method in a microplate format. Lipids. 46, 95–103.

Chisti Y. 2007. Biodiesel from microalgae. Biotechnol Adv. 25, 294–306.

Converti A., Casazza A. A., Ortiz E. Y., Perego P., Del Borghi M. (2009). Effect of temperature and nitrogen concentration on the growth and lipid content of *Nannochloropsis oculata* and *Chlorella vulgaris* for biodiesel production. Chem. Eng. Process. 48, 1146–1151

Cuellar-Bermudez S.P., Garcia-Perez J.S., Rittmann B.E., Parra-Saldivar R., 2015. Photosynthetic bioenergy utilizing CO_2: an approach on flue gases utilization for third generation biofuels. J.Clean. Prod. 98, 53-65.

Dean A.P., Sigee D.C., Estrada B., Pittman J.K., 2010. Using FTIR spectroscopy for rapid determination of lipid accumulation in response to nitrogen limitation in freshwater microalgae. Bioresour Technol 101, 4499–4507.

del Rio-Chanona E.A., Liu J., Wagner J.L., Zhang D., Meng Y., Xue S., Shah N., 2018. Dynamic modeling of green algae cultivation in a photobioreactor for sustainable biodiesel production. Biotechnol. Bioeng. 115, 359–370.

Gentile M. P., Blanch H. W., 2001. Physiology and xanthophyll cycle activity of *Nannochloropsis gaditana*. Biotechnol. Bioeng. 75, 1-12.

He Y., Chen L., Zhou Y., Chen H., Zhou X., Cai F., Huang J., Wang M., Chen B., Guo Z., 2016. Analysis and model delineation of marine microalgae growth and lipid accumulation in flat-plate photobioreactor. Biochem. Eng. J. 111, 108-116.

Khichi S. S., Anis A., Ghosh S., 2018. Mathematical modeling of light energy flux balance in flat panel photobioreactor for *Botryococcus braunii* growth, CO_2 biofixation and lipid production under varying light regimes. Biochemical Engineering Journal. 134, 44-56.

Kolber Z.S., Zehr J., Falkowski P.G., 1988. Effects of growth irradiance and nitrogen limitation on photosynthetic energy conversion in photosystem II. Plant Physiol. 88,923–929.

Kumar K., Das D., 2012. Growth characteristics of *Chlorella sorokiniana* in airlift and bubble column photobioreactors, Bioresour. Technol. 116, 307-13.

Kunjapur A.M., Eldridge R.B., 2010. Photobioreactor design for commercial biofuel production from microalgae, Ind. Eng. Chem. Res. 49, 3516–3526.

Lee E., Jalalizadeh M., Zhang Q., 2015. Growth kinetic models for microalgae cultivation: a review. Algal Res. 12, 497–512.

Maggi, F., la Cecilia, D., 2016. Implicit analytic solution of Michaelis-Menten-Monod kinetics. ACS Omega 1, 894e89.

Nur M.M.A., Setyoningrum T.M., Budiaman I.G.S., 2017. Potency of *Botryococcus braunii* cultivated on palm oil mill effluent wastewater as a source of biofuel. Enviro. Eng. Res. 22(4), 417–425.

Ördög, V., Stirk, W.A., Bálint, P., van Staden, J., Lovász, C., 2012. Changes in lipid, protein and pigment concentrations in nitrogen-stressed *Chlorella minutissima* cultures. J. Appl. Phycol. 24, 907–914.

Pancha I., Chokshi K., George B., Ghosh T., Paliwal C., Maurya R., Mishra S., 2014. Nitrogen stress triggered biochemical and morphological changes in the microalgae *Scenedesmus* sp. CCNM 1077. Bioresour. Technol. 156, 146–154.

Pegallapati A. N., Nirmalakhandan N., 2012. Modeling algal growth in bubble columns under sparging with CO_2-enriched air. Bioresource Technology. 124, 137– 145.

Pradhan L., Bhattacharjee V., Mitra R., Bhattacharya I., Chowdhury R., 2015. Biosequestration of CO_2 using power plant algae (*Rhizoclonium hieroglyphicum* JUCHE2) in a flat plate photobio-bubble-reactor – experimental and modeling, Chemical Engineering Journal. 275, 381–390.

Rubinow, S. I. Introduction to Mathematical Biology; Wiley: New York, **1975**; p 416.

Ruiz J., Alvarez P., Arbib Z., Garrido C., Barragan J., Perales J. A., 2011. Effect of nitrogen and phosphorus concentration on their removal kinetic in treated urban wastewater by *Chlorella vulgaris*. International Journal of Phytoremediation. 13, 884–896.

Schenk P.M., Thomas-Hall S.R., Stephens E., Marx U.C., Mussgnug J.H., PostenC., Hankamer B., 2008. Second generation biofuels: High-efficiency microalgae for biodiesel production. BioEnergy Research, 1(1), 20–43.

Segel, I. H. *Enzyme Kinetics*; John Wiley: New York, **1993**; p 441.

Sheehan, J., Dunahay, T., Benemann, J. R., & Roessler, P. (1998). A look back at the US Department of Energy's Aquatic Species Program: Biodiesel from Algae. US Department of Energy (US DoE) Office of Fuels Development, Prepared by National Renewable Energy Laboratory (NREL). National Renewable Energy Laboratory Golden, CO.

Surendhiran D., Vijay M., Sivaprakash B., Sirajunnisa A., 2015. Kinetic modeling of microalgal growth and lipid synthesis for biodiesel production. 3 Biotech. 5, 663–669.

Teresa M.M., Antonio A.M., Nidia S.C. 2010. Microalgae for biodiesel production and other applications: A review. Renew Sustain. Energy Rev. 14, 217–232.

Vogt D., 2013. On approximate analytical solutions of differential equations in enzyme kinetics using homotopy perturbation method. J. Math.Chem. 51, 826–842.

Wu H. Q. & Miao X. L. Biodiesel quality and biochemical changes of microalgae *Chlorella pyrenoidosa* and *Scenedesmus obliquus* in response to nitrate levels. Bioresour. Technol. 170, 421–427 (2014).

Yang J., Rasa E., Tantayotai P., Scow K.M., Yuan H., Hristova K.R., 2011. Mathematical model of *Chlorella minutissima* UTEX 2341 growth and lipid production under photoheterotrophic fermentation conditions. Bioresour. Technol. 102 (3), 3077–3082.

Chapter 5

Online Estimation of Biomass, Lipid and Nitrate Dynamic Profile using Innovative Light Evolution Kinetic Model in Flat Panel Airlift Photobioreactor for *Botryococcus braunii* under Varying Light Conditions

5.1. Introduction

Microalgae are unicellular photosynthetic microorganisms that methodically capture CO_2 and store solar energy in complex chemical bonds (Cuellar- Bermudez et al., 2015; Ooms et al., 2016). Microalgae have been considered as a potential feedstock for biofuel and value added metabolites (Slade and Bauen, 2013; Ooms et al., 2016). However, industrial exploitation of microalgae is limited by photobioreactor process productivity (Berteotti et al., 2016). Photobioreactor process productivities are affected by suboptimal light supply, effective light penetration and limiting biological efficiency (Ziffers et al., 2008). Commercial cultivation of microalgae is commonly achieved by open raceway pond (Kunjapur et al., 2010), but open pond system suffers with low light utilization, evaporative losses, diffusion of CO_2 to the atmosphere, contamination, and low mass transfer rates (Mondal et al., 2017). In order to attain large scale and adequate production of microalgae biomass and lipid, photobioreactor can be alternative to open raceway pond. Moreover, there are three different type of most suitable large-scale cultivation reactors are the tubular, column and flat panel (FP) reactors (Kunjapur et al., 2010). However, Flat panel photobioreactors feature important advantages for mass production of photoautotrophic microorganisms and may become a standard reactor type for the mass production of several algal species (Sierra et al., 2008). A Flat Panel photobioreactor can be divided into 3 zones. (i) The region immediately adjacent to the illuminated reactor surface is a photic zone where light saturation and consequently the photo inhibition of algal growth repeatedly occurs (Hankamer et al., 2007). This photo-inhibition leading to decreased photosynthetic efficiency can adversely affect the lipid production in microalgal cell. (ii) In light limited region, at a specific point cell absorption and incident light intensity reached in a balanced state, microalgal cells achieved their maximum growth rate in this region. (iii) Stagnant region is the lowest light intensity zone which is insufficient to sustain the microalgae growth (Wang et al., 2014).

Light distribution inside the photobioreactor is generally illustrated by Lambert – Beer law (Shotipruk et al., 1999). This law estimates the light transport inside the culture, speculating consistent light consumption is proportional to the biomass concentration and light path of the photobioreactor. Lambert – Beer law is based on the assumptions such as, negligible light scattering corresponding to the light absorption due to the culture medium, and a unidirectional luminous intensity while crossing the absorbing medium (Fernandez et al., 1997; Pruvost et al., 2002). Several authors used Lambert – Beer assumptions to model light evolution inside the photobioreactor. Suh & Lee et al. (2003) considered and established a light penetration model for an internally irradiated photobioreactor. A simple monodimensional model was used to estimate the microalgae growth rate in flat panel photobioreactor (Jong et al., 2002), whereas a quasi-collimated one dimensional two-flux model was applied to anticipate the light depletion in torus photobioreactor (Pottier et al., 2005). Light distribution pattern were modelled in cuboidal and cylindrical photobioreactor by Ogbonna et al. (1995), but local light evolution inside the photobioreactor was not explained. Moreover, these models are based on the light absorption only which can be improved by including the scattering light effect (Klok et al., 2013; Blanken et al., 2016).

Lambert – Beer law overestimates the culture real light absorption (Fernandez et al., 1997; Pruvost et al., 2002) Deviation from Lambert – Beer law occurs as a result of differential absorption and light scattering in the culture medium (Csőgör et al., 2001; Pruvost et al., 2006). Regarding limitation, at high cell density cultural conditions Lambert – Beer assumptions are not valid; because scattering effects and light diffusion have significant impact on light transfer at high cell density culture conditions. A number of models have been used with higher complexity for e.g., Packer et al. (2011) applied Lambert – Beer law assumption to model average light intensities in culture medium and validate the model with cell density greater than 7 gL^{-1}. The mathematical model defined by Packer et al. (2011) consists of 10 equations and 12 modelling parameters, whilst model described by Quinn et al. (2011) integrates 7 sub-systems characterized by 16 species-specific modeling parameters. An increase in model complexity improved the predictive capabilities of these models. However, measurements of numerous input model parameters are inconvenient, tedious and require complex mathematical techniques. In order to account for light scattering in dense cultures, it has been proposed to apply Lambert – Beer law using scatter corrected light absorption coefficient (Holland et al., 2011; Huesemann et al., 2013). In fact a thorough formulation with definite depiction of scattering effects can implicate a numerical

simulation with finite difference method, particularly making the light distribution cumbersome and difficult to obtain (Cornet al., 1998), but benefit of applying the Lambert – Beer law which depicts light attenuation with a rather simple equation is lost (Pruvost et al., 2006).

In view of these limitations in Lambert – Beer law, it is objective of this study to modify the Lambert – Beer law by applying differential absorbance in flat panel photobioreactor. In this study, for the first time a new differential equation is proposed to measure the biomass concentration as a function of absorbance factor (A) inside a flat panel airlift photobioreactor. The developed model was calibrated by operating the flat panel photobioreactor under specific condition (i.e. 133 µmol m^{-2} s^{-1} light intensity and 5% CO_2 v/v) and model parameters were numerically optimized. The model validation was done under different light intensities and accuracy of model was verified by statistical and sensitivity analysis. The developed mathematical formulations investigate the temporal biomass, nitrate and lipid profile under varying light conditions. Photobioreactor process productivity can be optimized by dynamically control the light evolution inside the photobioreactor. The model strategy apply here is general one, which can be applicable over any other geometry of the photobioreactor.

5.2. Material and methods

5.2.1. Microalgae and culture medium

B. braunii was provided by Institute of Bioresources and Sustainable Development (IBSD, Takyelpat, Imphal), and maintained in modified BG-11 medium as described by Khichi et al. (2018). In total, four batch experiments were carried out with different initial light intensities as shown in Table 1, and a constant pH of 7.8 and temperature of 27± 1°C were fixed for all the experiments.

5.2.2. Flat Panel Airlift Photobioreactor

Airlift Flat Panel photobioreactor was constructed using borosilicate glass. The dimension of the reactor is (24.13× 29.21 × 7.62 cm) respectively (Fig. 1). For air flow porous type sparger was used. The wall thickness was 5 mm and air was introduced into the base by sparger attached at the bottom. Bubble column was converted into airlift bioreactor by inserting a centre glass plate into them (Fig. 1). The reactor was illuminated by light intensity from the range of (133 to 348 µmol m^{-2} s^{-1}) by LED Panel arranged at one side of the photobioreactor. *B. braunii* was grown in

5.37 liter photobioreactor filled with BG-11 nutrient medium, and operating at 0.3 vvm air flow rate and 5% CO_2 (Table 1).

5.2.3. Analysis of growth, substrate and lipid concentration

Microalgal cell dry weight was measured a function of the cell absorbance at 750 nm (A_{750}) using an UV–Visible spectrophotometer (Carry 60, Agilent). A calibration curve was prepared to determined cell dry weight from the corresponding absorbance using the equation: C_b (g L^{-1}) = 2.155 OD_{750} (R^2 = 0.99) (E5.1). Nitrate concentration was measured by taking absorbance at 220 nm using a UV–Visible spectrophotometer (Carry 60 Agilent) according to the method described by APHA (1976). Lipid concentration in the medium was determined by modified sulpho-phospho-vanillin (SPV) colorimetric method (Cheng et al., 2011; Byreddy et al., 2016).

5.3. Model Development

5.3.1. The light attenuation model

Light attenuation model in a flat panel model is described by Lambert – Beer law which states that light attenuation in microalgae suspension culture occurs as a result of light scattering and absorption properties of microalgae cell, water and growth medium inside the photobioreactor. Light attenuation per unit distance is proportional to the product of biomass concentration and incident light intensity and can be expressed as Eq. (E5.2).

$$\frac{dI}{dz} \propto -I * X \quad \text{(E5.2)}$$

The light attenuation equation Eq. (E5.2) can be rewritten by introducing the proportionality constant (K_a) i.e. specific light absorption coefficient (K_a)

$$\frac{dI}{dz} = -K_a I X \quad \text{(E5.3)}$$

After Integrating the Eq. (E5.3) from 0 to L results in the following:

$$\ln\left(\frac{I}{I_0}\right) = -K_a X L \quad \text{(E5.4)}$$

On rearranging Eq. (E5.4), it can be written as Eq. (E5.5)

$$\frac{1}{L}\ln\left(\frac{I_0}{I}\right) = K_a X \quad \text{(E5.5)}$$

The left hand side of Eq. (E5.5) was assigned as a new function, called as absorbance factor (A), and the general equation will be described as Eq. (E5.6a) or (E5.6b).

$$A = K_a X \qquad \text{(E5.6a)}$$

Or

$$X = \frac{A}{K_a} \qquad \text{(E5.6b)}$$

Where A is the absorbance factor (m^{-1}) and defined as Eq. (E5.7).

$$A = \frac{1}{L} \ln\left(\frac{I_0}{I}\right) \qquad \text{(E5.7)}$$

In Eq. (6a), K_a is the specific biomass light absorption coefficient ($m^2\ kg^{-1}$); and X is biomass concentration ($g\ L^{-1}$).

3.2. Light evolution kinetic model

Based on Lambert – Beer light attenuation model in photobioreactor a differential light kinetic model in flat panel airlift photobioreactor has been developed. Logistic equation of biomass generation in photobioreactor can be expressed as Eq. (E5.8) according to Issarapayup et al. (2009).

$$\frac{dX}{dt} = K_c X \left(1 - \frac{X}{X_{max}}\right) \qquad \text{(E5.8)}$$

On integrating and rearranging Eq. (E5.8), it can be written as Eq. (E5.9).

$$X = \frac{X_{max}}{1 + \left(\frac{X_{max}}{X_0} - 1\right) e^{-K_c t}} \qquad \text{(E5.9)}$$

After substituting X from Eq. (E5.9), into the Eq. (E5.6a)

$$A = K_a * \left(\frac{X_m}{1 + \left(\frac{X_m}{X_0} - 1\right) \exp\left(-K_c t\right)}\right) \qquad \text{(E5.10)}$$

Now, after differentiating A with respect to time

$$\frac{d}{dt}(A) = K_a * \frac{d}{dt}\left(\frac{X_m}{1 + \left(\frac{X_m}{X_0} - 1\right) \exp\left(-K_c t\right)}\right) \qquad \text{(E5.11)}$$

$$\frac{dA}{dt} = \frac{(X_m * K_a * K_c * \exp(-K_c t) * \left(\frac{X_m}{X_0} - 1\right)}{\left(1 + \exp(-K_c t) * \left(\frac{X_m}{X_0} - 1\right)\right)^2} \qquad \text{(E5.12)}$$

where A is the absorbance factor (m^{-1}), X_m is the maximum biomass concentration (g L^{-1}), K_a is the specific biomass light absorption coefficient (m^2 kg^{-1}), K_c is the apparent maximum specific growth rate (h^{-1}), X_0 is the initial biomass concentration (g L^{-1}).

5.3.3. Biomass growth kinetics coupled with light evolution kinetic model

Biomass growth of *B. braunii* is affected by the light availability inside the photobioreactor. Thus, the differential equation for biomass growth was expressed as Eq. (E5.8). The dependable variable appears in the right hand side of the Eq. (E5.8) is biomass concentration, which is function of the absorbance factor (A). After substituting value of X form Eq. (E5.6b), into the Eq. (E5.8), the final differential equation of biomass growth rate in terms of light absorbance factor was expressed as Eq. (E5.13).

$$\frac{dX}{dt} = -\frac{K_c}{X_m {K_a}^2}(A)^2 + \left(\frac{K_c}{K_a}\right) * A \qquad \text{(E5.13)}$$

5.3.4. Sodium nitrate consumption kinetics coupled with light evolution kinetic model

Sodium nitrate consumption kinetics in the microalgae is described by the following equation [33, 46].

$$-\frac{dS}{dt} = \frac{1}{Y_{X/S}} \times \frac{dX}{dt} + mX \qquad \text{(E5.14)}$$

Now, after substituting value of $\frac{dX}{dt}$ and X from Eq. (E5.13) and Eq. (E5.6b) respectively into the Eq. (E5.14), the substrate consumption kinetics can be expressed as a function of the light absorbance factor and expressed as Eq. (E5.15).

$$-\frac{dS}{dt} = \frac{1}{Y_{X/S}} \times \left(-\frac{K_c}{X_m {K_a}^2}(A)^2 + \left(\frac{K_c}{K_a}\right) * A\right) + m\left(\frac{A}{K_a}\right) \qquad \text{(E5.15)}$$

5.3.5 Lipid formation kinetics coupled with light evolution kinetic model

Luedeking-Piret equation was used to predict lipid production in *B. braunii* according to the following equation

$$\frac{dP}{dt} = \alpha . \frac{dX}{dt} + \beta X \qquad \text{(E5.16)}$$

Now, after substituting value of $\frac{dX}{dt}$ and X from Eq. (E5.13) and Eq. (E5.6b) respectively into the Eq. (E5.16), lipid formation kinetics can also be expressed as a function of the light absorbance factor and expressed as Eq. (E5.17).

$$\frac{dP}{dt} = \alpha \times \left(-\frac{K_c}{X_m {K_a}^2}(A)^2 + \left(\frac{K_c}{K_a}\right) * A\right) + \beta\left(\frac{A}{K_a}\right) \qquad \text{(E5.17)}$$

5.4. Results and discussions

5.4.1. Effect of light intensities on biomass, lipid and nitrate profiles

B. braunii were grown in 5.37 L flat panel airlift photobioreactor under peculiar irradiance regimes (Fig. 5.1). After a 5 day cultivation in photobioreactor, the highest biomass concentration and biomass productivity of *B. Braunii* were 2.52 g L^{-1} and 0.630 g L^{-1} d^{-1}, respectively, at light intensity of 261 µmol m^{-2} s^{-1}, but biomass concentration and biomass productivity decreased by 19.44 and 32.38%, 8.33 and 21.43% and 18.25 and 30% under varying light regimes of 133, 174 and 348 respectively. An elevated biomass under the influence of high irradiance was also reported earlier in the studies on *Chlorella* sp. L1, *M. dybowskii* Y1, *M. dybowskii* Y2, and *M. Dybowskii* (Qiaoning et al., 2015) and *Scenedesmus* sp. (Liu et al., 2012).

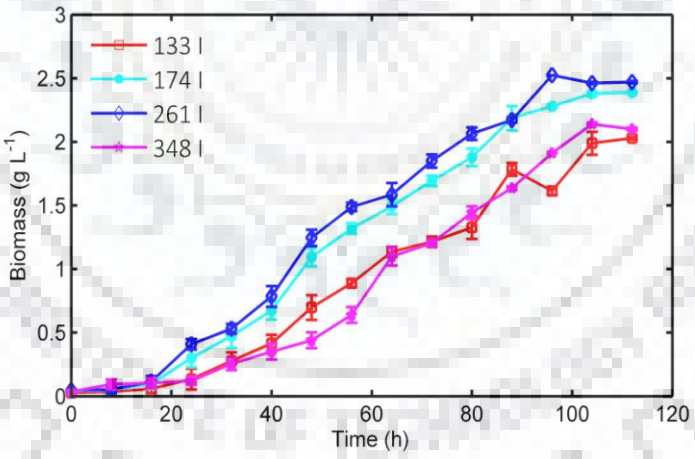

Fig.5.1. Plot of experimental data showing the effect of light intensities (133 to 348 µmol $m^{-2}s^{-1}$) on Total biomass density.

The effects of varying light regimes on microalgal lipid content were analyzed (Fig. 5.2). The maximum lipid content was 19.76%, obtained at light intensities of 261 µmol m^{-2} s^{-1}. At different irradiance regimes of 133, 174 and 348 µmol m^{-2} s^{-1} the lipid content of B. braunii diminished to 18.27%, 18.92% and 12.28% respectively.

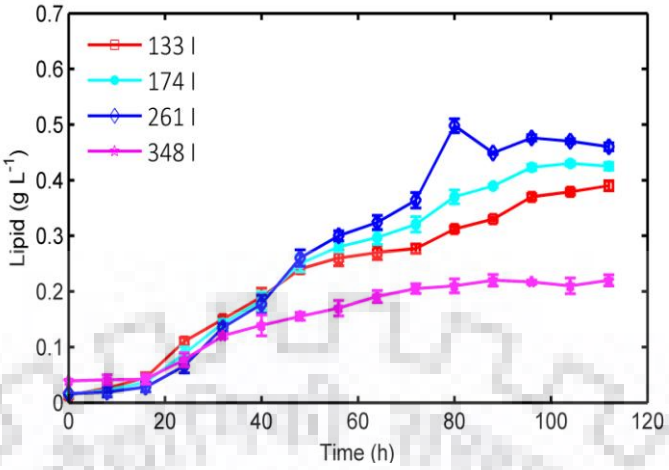

Fig.5.2. Plot of experimental data showing the effect of light intensities (133 to 348 µmol $m^{-2}s^{-1}$) on Total biolipid density.

Saturation irradiance promotes lipid, carbohydrate and protein in microalgal cells (Liu et al., 2012). Whilst at lower than the optimal PPFD microalgal cells allocate their energy to form photosynthetic complexes, chloroplast membrane matrix and cell membrane formation (Khotimchenko et al., 2005; Sommerfeld et al., 2008). Similarly Solovchenko et al. (2008) described that 400 µmol photons m^{-2} s^{-1} light intensity is reasonable for the optimal growth and lipid production in *P. Incise*.

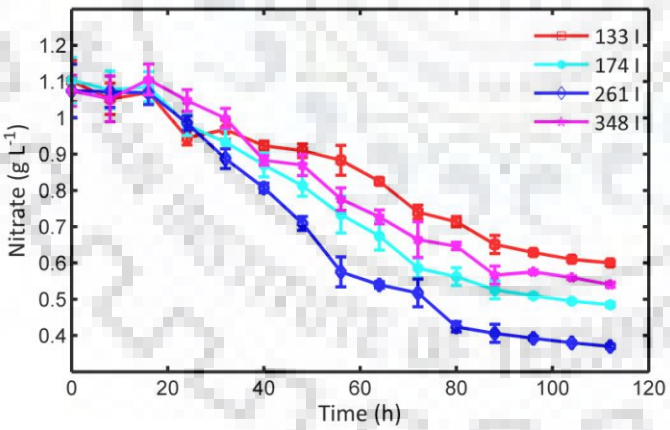

Fig.5.3. Plot of experimental data showing the effect of light intensities (133 to 348 µmol $m^{-2}s^{-1}$) on extracellular nitrate level.

In present study, sodium nitrate consumption profiles under varying light regimes were depicted in (Fig. 5.3). Under low light conditions (i.e. 133 µmol m^{-2} s^{-1}), nitrate removal rate of 107.142 mg L^{-1} d^{-1} was the lowest. As the light intensity increased, corresponding nitrate removal was increased and the highest nitrate removal rate of 150.64 mg L^{-1} d^{-1} was observed at 261 µmol m^{-2} s^{-1}, with

the further increase in light intensity (i.e. at 348 µmol m^{-2} s^{-1}) nitrate removal rate decreased. This illustrates that light intensity adversely affect the nitrate removal rate under the influence of high irradiance. Similarly Gonçalves et al. (2016) described analogous nitrate consumption trend under different light regimes.

5.4.2. Light attenuation in flat panel airlift photobioreactor

A set of experiments was conducted at various incident light intensities and temporal light distribution profile (at z = 0.0762 m) was collected (Fig. 5.4a) using the light sensor (LI-250 A, LI-Core Inc.). Each curve shows light attenuation in photobioreactor at four different incident light intensities (133, 174, 261, 348 µmol m^{-2} s^{-1}), at a particular time and specified biomass concentration. These results are in accordance with Naderi et al. (2017), who investigated effect of light intensities and biomass concentration on light attenuation in cylindrical and rectangular photobioreactors.

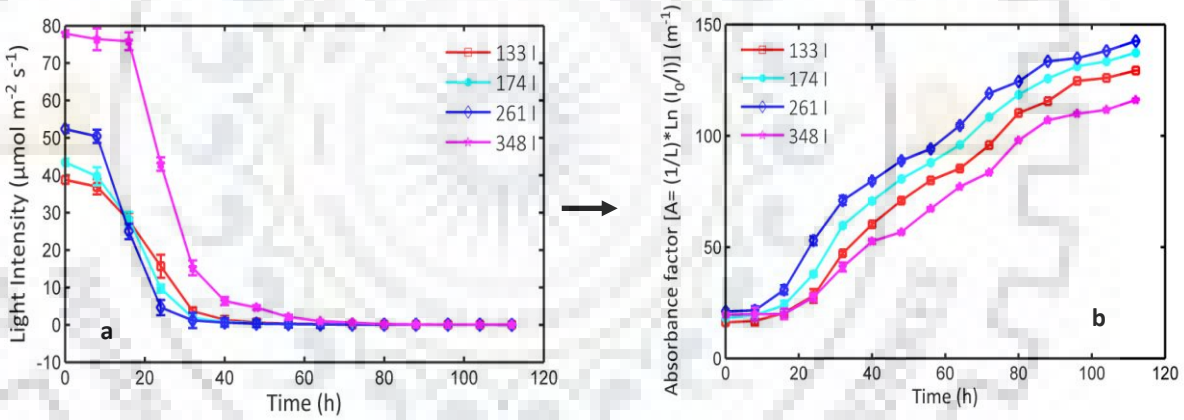

Fig.5.4. Conversion of Light evolution data (5.4a) into the Absorbance factor $[A = \frac{1}{L}\ln\left(\frac{I_0}{I}\right)]$ data (5.4b) for 133 to 348 µmol $m^{-2}s^{-1}$ respectively.

To develop a mathematical model, light evolution data collected in Fig. 3a was converted into the absorbance factor (A) data using the Eq. (E5.7) (Fig. 3b). As shown in (Fig. 5.4b), absorbance factor (A) was increased with increase in incident light intensities up to 261 µmol m^{-2} s^{-1}, but at highest light intensity of 348 µmol m^{-2} s^{-1} lowest evolution of absorbance factor (A) was observed. According to Lambert - Beer law at constant incident light intensity and for a constant light penetration distance, light attenuates as a function of biomass concentration (Naderi et al., 2017). Absorbance factor evolution data collected in Fig. 5.4b was coupled with biomass, nitrate

and lipid kinetics using mathematical methods. The effect of various incident light intensities on coupled dynamic light evolution kinetics was further studied.

5.4.3. Model calibration

The model for light evolution kinetics was calibrated using biomass growth profile collected at the light intensity of 133 µmol m^{-2} s^{-1} and at the CO_2 air ratio of 5% (Fig. 5.5). The calibration process was commenced with typical values for the following parameters obtained from the literature: maximum growth rate (μ_{max}), biomass yield constant on nitrate ($Y_{x/s}$), growth associated constant for lipid (α), non growth associated constant (β) for lipid and the light extinction coefficient (K_a). The model was fitted to the experimental data, and a best fit model generates numerically optimized model parameters. Numerical optimization was performed using the *fminsearch* routine in Matlab® program with interpolation function (interp1).

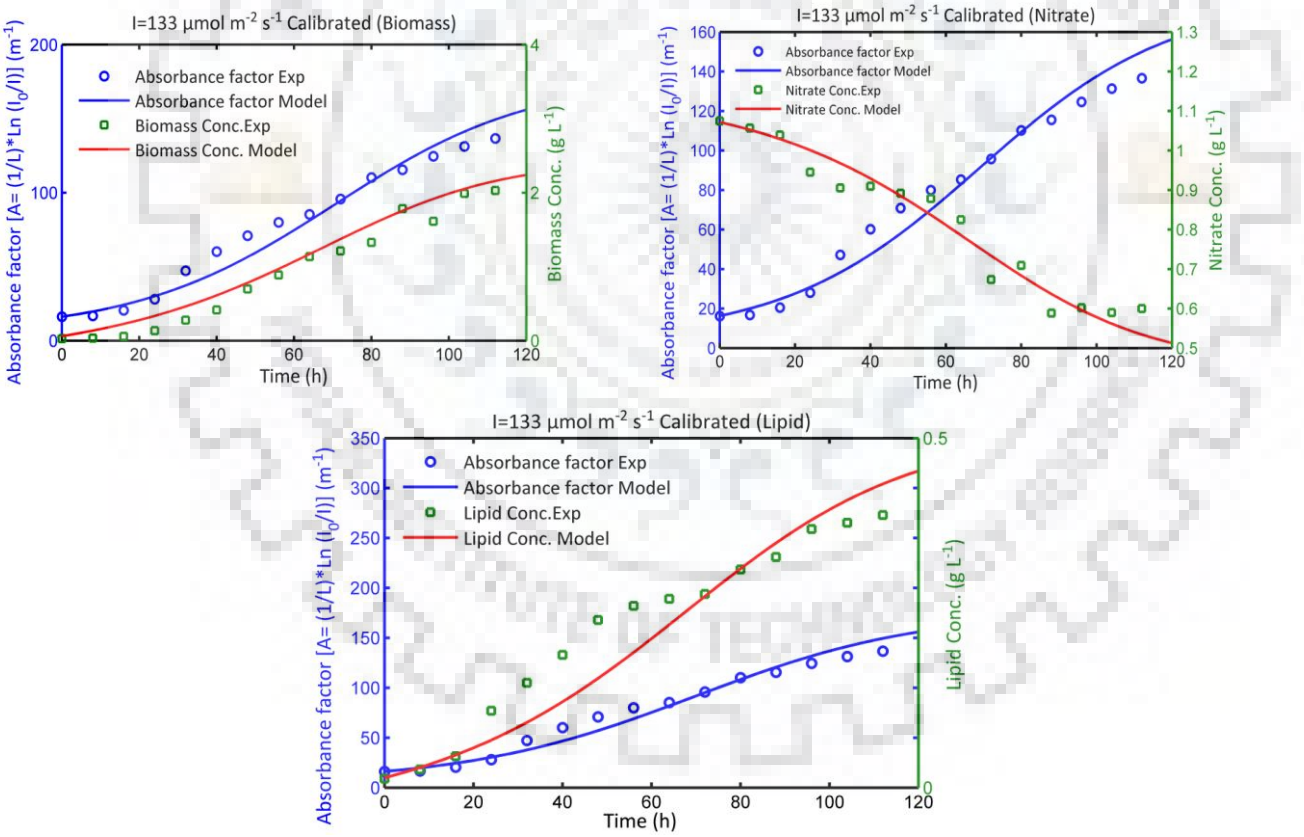

Fig.5.5. Model calibration as function of light absorbance factor at specific light intensity (i.e. 133 µmol $m^{-2}s^{-1}$) for (a) Biomass; (b) extracellular nitrate; (c) lipid

The *fiminsearch* routine in Matlab® program is based on the simplex search algorithm which gives only local solutions, and interpolation function (interp1) of the Matlab®, added new data points within a range of known data points. The numerically optimized values for all parameters established using this exercise are listed in Table 5.1, along with their comparable literature values.

Table 5.1. Best fit model parameters and comparable literature values.

Parameters	Best fit value	Comparable values from literature
K_a (m^2 kg^{-1})	65.56	75.2 for *Nanachloropsis* sp.(Gentile and Blanch,2001)
		200 for *Monodus subterraneus* (Bosma et al., 2007)
K_c (d^{-1})	0.934	μ_m of 0.99 for *Rhizoclonium h*. (pradhan et al., 2015)
		μ_m of 1.2 for *N Salina* (Pegallapati et al., 2012)
		μ_m of 0.94 for *S. obliquus* (Ruiz et al., 2013)
$Y_{X/S}$ (g g^{-1})	3.424	6.92 – 15.18 for *I.galbana* (He et al., 2016)
α (g g^{-1})	0.2063	0.125 for *C. salina* 0.151 for *N. oculata* (Surendhiran et al., 2015)
		3.37×10^{-2} – 7.02×10^{-2} for *I. galbana* (He et al., 2016)
β (g g^{-1})	4×10^{-4}	2×10^{-3} for *C. salina* 6×10^{-4} for *N. oculata* (Surendhiran et al., 2015)
		0.5×10^{-5} – 2.52×10^{-2} for *I. galbana* (He et al., 2016)

The model parameters optimized in the calibration step were kept fixed in the validation step. The observed coupled light evolution profile and biomass growth profiles from the remaining three runs were compared with the model predicted profiles using the numerically optimized parameter values established during the calibration step. The correlation coefficients between the experimental and model outputs of biomass, nitrate and lipid profiles for the calibration data set were r2 = (0.99, 0.97 and 0.97) respectively. Significance of fits also assessed by determining the p values, and the p values were below 0.0001 (i.e. significant) for the all calibrated points (Supplementary Table S1, S2 and S3).

5.4.4. Experimental validation of novel light evolution model in flat panel airlift photobioreactor

To test the predictive model capability, the estimated model parameters were used to simulate the novel light evolution model Eq. (E5.12). Simulation and validation of the mathematical model was performed at z = 0.0762 m on the other side of the photobioreactor. The local light absorbance factor (A) at the end of the reactor was calculated using Eq. (E5.12), and the experimental values of light evolution factor were measured using the temporal light evolution data from the photobioreactor using Eq. (E5.7). Fig. 5.6 a–c (i.e. the blue line), represent the comparison of model results with the experimental data in terms of temporal light evolution. As shown in Fig. 5.6 a–c (i.e. the blue line), the sigmoidal profiles of light absorption factor from Eq. (E5.12) were overlapping with the experimental data which signifies that mathematical model is close enough to the observed values. Light absorbance at z = 0.0762 m, of the flat panel photobioreactor increased with increase in cell growth rate. Whilst at stationary phase of microalgae growth, saturation in the absorbance factor (A) was also observed. After 24 hour of cultivation when microalgae cell enters the exponential phase of cultivation light attenuation phenomena exist in photobioreactor in which self shading of microalgae cell curtailed the adequate light infiltration beyond the light limited region of the reactor. This results in exponential increase in absorbance factor in the photobioreactor. The results reported here are in accordance with (Naderi et al., 2017; Kumar et al., 2013), which reported similar trend of light distribution in photobioreactor at higher biomass concentration. The light attenuation is also correlated with width of the photobioreactor which suggests that the specific growth rate of microalgae reduced at higher panel width (Naderi et al., 2017; Kumar et al., 2013).

5.4.5. Kinetic studies

5.4.5.1. Biomass growth kinetics coupled with light evolution kinetic model

Biomass concentrations of *B. braunii* as a function of light absorbance factor (A) under different irradiance level were predicted by Eq. (E5.13). This innovative model was validated by comparing the predicted and experimental biomass growth profiles of *B. braunii* in the flat panel airlift photobioreactor under different light conditions from 174, 261 and 348 μmol m^{-2} s^{-1} respectively (Fig 5.6). As expected the biomass concentration increase with increase in light absorbance factor (A) under the varying light condition of 133, 174 and 261 μmol m^{-2} s^{-1}. Whist at high light

intensity of 348 µmol m^{-2} s^{-1} the biomass concentration decreased from their optimal value. This might be due to the photoinhibition phenomena exist in the photobioreactor at high light intensity. This indicating that biomass yield on light energy is not consistent but reached to its optimal value at sub saturating light regimes and reduced at high light intensity (Huesemann et al., 2013; Wagenen et al., 2012). For example, 1.96-times increment in initial light intensity from 133 to 261 µmol m^{-2} s^{-1} resulted in 1.48 fold and 1.24 fold increase in the volumetric biomass productivity and lipid productivity from 0.426 to 0.630 g L^{-1} d^{-1} and 92.75 to 114.92 mg L^{-1} d^{-1} respectively

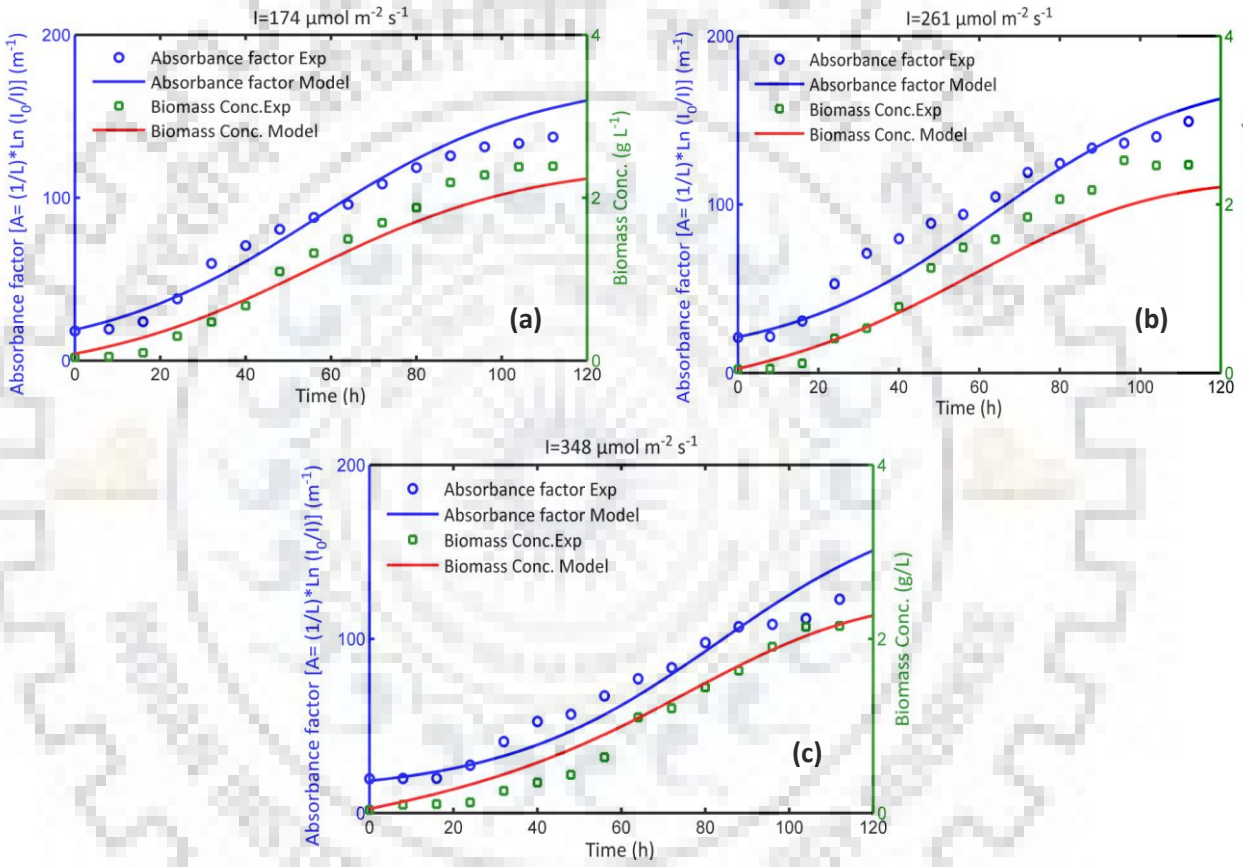

Fig.5.6. Model validation for biomass as a function of light absorbance factor at different light intensities of (a) 174 µmol $m^{-2}s^{-1}$; (b) 261 µmol $m^{-2}s^{-1}$; (c) 348 µmol $m^{-2}s^{-1}$.

These observations suggest that increasing incident light intensity is not a competent approach for promoting photosynthesis in opaque cultures. As shown in Table 5.1, the numerically optimized value of specific biomass light absorption coefficient (K_a) was compared with the literature reported value. The value of K_a is similar to the light absorption coefficient of 75.2 m^2 kg^{-1} that was measured by Gentile and Blanch (2001) for nanochloropsis. Although, several other authors

reported higher values of K_a, in the range of 75.2 to 200 m^2 kg^{-1} for different algal strains (Table 3). The variation in light absorption coefficient K_a is expected, as different species and strain of microalgae might have different degree and types of pigmentation (Huesemann et al., 2013).

5.4.5.2. Nitrate consumption kinetics coupled with light evolution kinetic model

The evolution of sodium nitrate uptake as a function of light absorbance factor (A) was modelled and the output of the model Eq. (E5.15) was compared with experimental data. The predictions of the established model were in good agreement with experimental data at different light conditions and suggested that nitrate removal in FPBR by B. braunii could be well explained by Eq. (E5.15). The batch test data at 133 µmol m^{-2} s^{-1}, (NaNO3, init=1.1 gL-1) and CO_2 concentration (5% v/v) were used to calibrate the model (Fig. 5.7). Nitrate removal rate under different light intensities of 174, 261 and 348 µmol m^{-2} s^{-1}were validated using the calibrated model parameters as listed in Table 5.1, the results of the model validation sets are illustrated

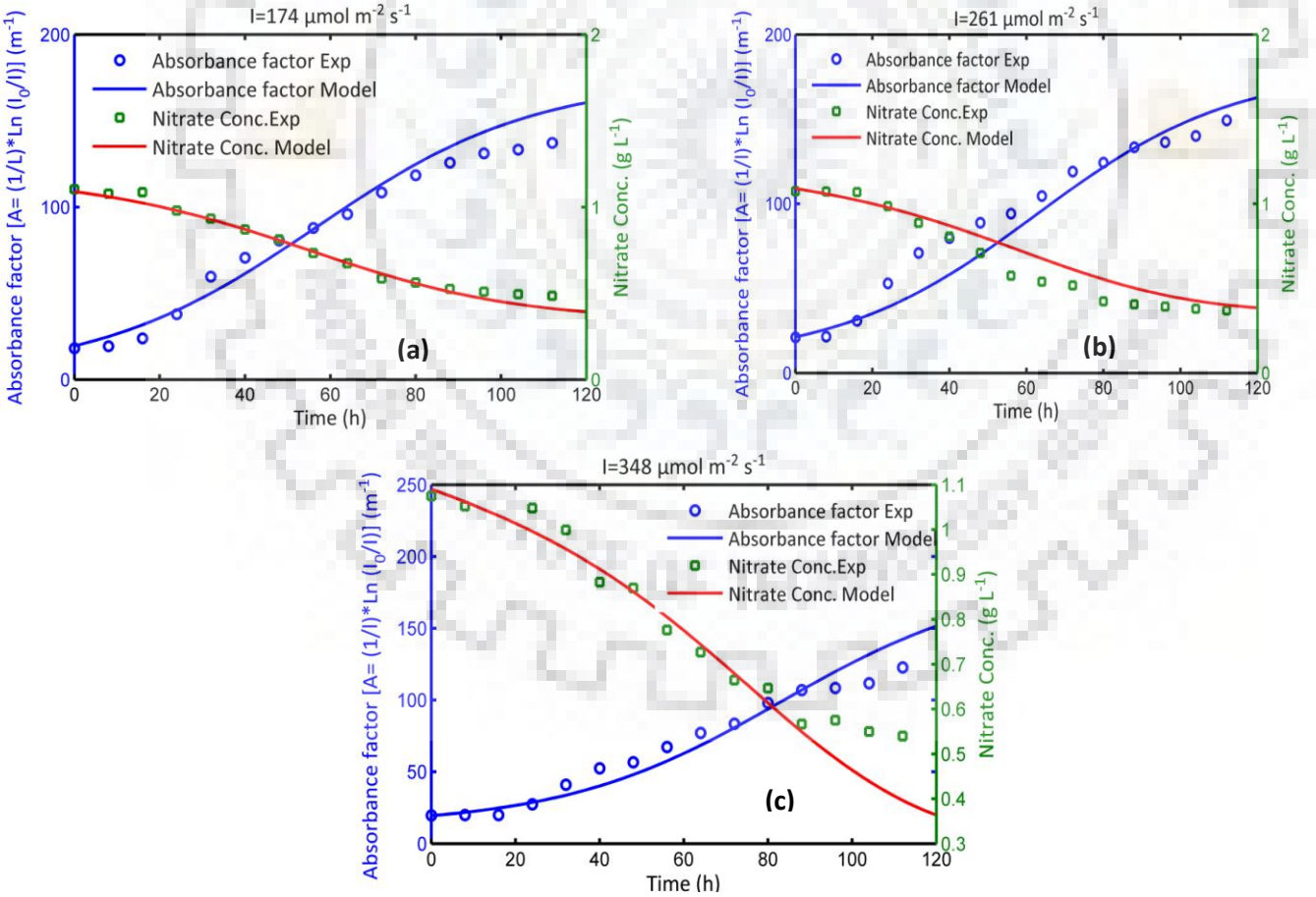

Fig.5.7. Model validation for extracellular nitrate concentrations as a function of light absorbance factor at different light intensities of (a) 174 µmol $m^{-2}s^{-1}$; (b) 261 µmol $m^{-2}s^{-1}$; (c) 348 µmol $m^{-2}s^{-1}$.

The results of the model validation sets are illustrated in (Fig. 5.7). Nitrate removal rate increased as the light intensities in the FPBR increased from 133 to 261 μmol m^{-2} s^{-1}, with the further increase in light intensity reduced the nitrate removal rate. Highest nitrate removal efficiency of 65.42% were recorded after 5 days for light intensity of 261, whilst only 45.56% and 49.53% of the nitrate removal was observed after 5 days of cultivation, at 133 and 348 μmol m^{-2} s^{-1} respectively. The developed model appropriately predicts the dynamic depletion of nitrate in the cultivation medium, along with light absorbance factor (Fig. 5.7), over the ranges of initial light intensities and 5% feed gas CO_2 concentration studied.

5.4.5.3. Lipid formation kinetics coupled with light evolution kinetic model

The lipid production kinetics was evaluated by Eq. (E5.17). Based on observation of Fig. 5.8, the measured values lipid profile agreed well to the model outputs, suggested that the lipid formation in *B. braunii* culture in FPBR can be best described by light coupled lipid kinetic equation. In general it has been observed that the light coupled lipid kinetic model produces a small overestimation of the lipid production under different light conditions of 348 μmol m^{-2} s^{-1}. This small variation could be due to lower level of lipid accumulation at high light intensity (i.e. 348 μmol m^{-2} s^{-1}) as algal growth is halted under higher than saturation light intensity which also reduced lipid production.

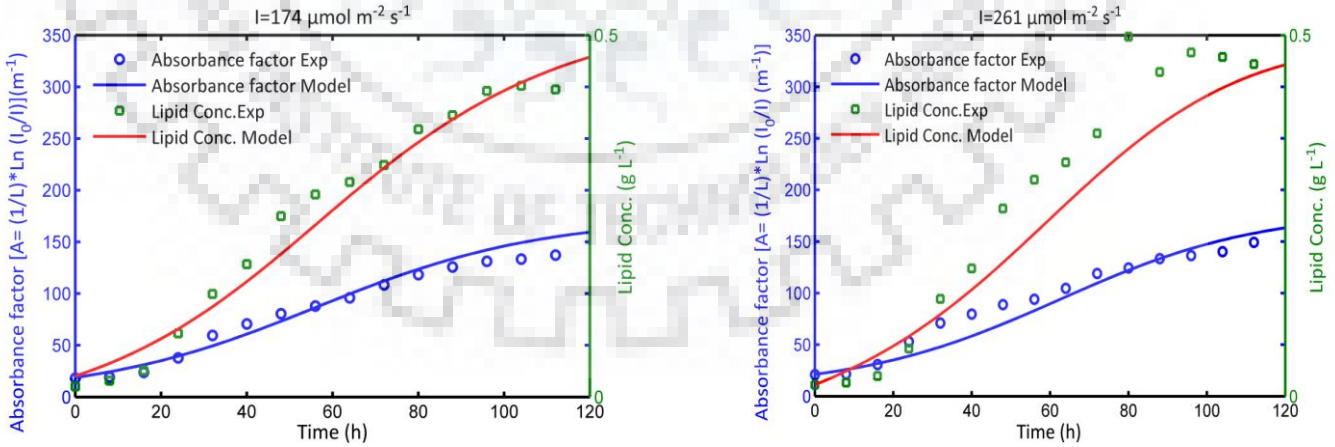

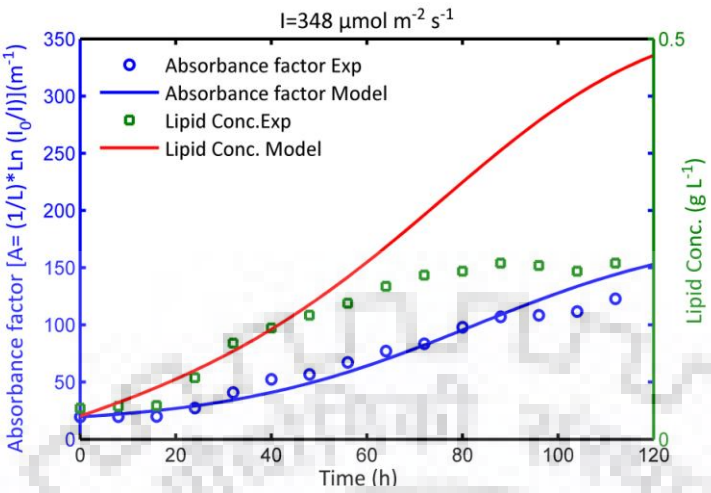

Fig.5.8. Model validation for extracellular nitrate concentrations as a function of light absorbance factor at different light intensities of (a) 174 µmol $m^{-2}s^{-1}$; (b) 261 µmol $m^{-2}s^{-1}$; (c) 348 µmol $m^{-2}s^{-1}$.

Since the high irradiance level augmented the growth of microalgae, the microalgae might use synthesized energy to divide themselves rather accumulate it in lipid form (Cheirsilp et al., 2012). Regarding to the intermediate light conditions of 133 and 261 µmol m^{-2} s^{-1} light intensity, the results are in good agreement with the experimental data. The results are in accordance with Ho et al. (2012) as their study suggested that higher irradiance (> 420 µmol m^{-2} $s^{-}1$) reduced the lipid content and lipid yield in *S. obliquus* CNW-N.

5.5. Conclusions

The novel light evolution kinetic modelling, simulation and validation in flat panel airlift photobioreactor are addressed in this work. The dynamic light attenuation in photobioreactor cannot be described accurately by Lambert-Beer law. Therefore, it has been proposed to apply Lambert-Beer law with corrected differential absorbance in photobioreactor. In this study, a light absorption factor (A) was introduced as instantly measured variable. First, the logistic growth model of microalgae ingrained into general equation to develop the novel light evolution kinetic model, further a new differential equation is proposed to estimate the biomass concentration as a function of absorbance factor (A) inside the flat panel airlift photobioreactor. As a result of this the consolidated logistic equation becomes independent of biomass concentration. Our prospective model couples biomass, nitrate and lipid kinetics with the light evolution kinetic equation. The calibrated model has been successfully validated for the prediction of *B. braunii* growth, nitrate consumption and lipid production within the photobioreactor as a function of absorbance factor

(A). Hence, the consolidated modelling strategy implements an explicit and inclusive tool for microalgae growth in flat panel airlift photobioreactor, which can be used as a reasonable and adequate bioreactor design criteria and for large-scale biomass production.

5.6. References

APHA. 1976. Standard Methods for the Examination of Water and Wastewater 14ed. APHA American Public Health Association.

Arbib Z., Ruiz, J., Alvarez-Diaz P., Garrido-Perez C., Perales J. A., 2014. Capability of different microalgae species for phytoremediation processes: wastewater tertiary treatment, CO_2 bio-fixation and low cost biofuels production. Water Research. 49, 465–474.

Berteotti S., Ballottari M., Bassi R., 2016. Increased biomass productivity in green algae by tuning non-photochemical quenching. Sci Rep, 6, 21339.

Blanken W., Postma P. R., de Winter L., Wijffels R. H., Janssen M., 2016. Predicting microalgae growth. Algal Research. 14, 28-38.

Bosma R., van Zessen E., Reith J. H., Tramper J., Wijffels R. H., 2007. Prediction of volumetric productivity in an outdoor photobioreactor. Biotechnol. Bioeng. 97(5), 1108–1120.

Byreddy A. R., Gupta A., Barrow C. J., Puri M., 2016. A quick colorimetric method for total lipid quantification in microalgae. Journal of Microbiological Methods. 125, 28–32.

Chang H. X., Huang Y., Fu Q., Liao Q., Zhu X., 2016. Kinetic characteristics and modeling of microalgae *Chlorella vulgaris* growth and CO_2 biofixation considering the coupled effects of light intensity and dissolved inorganic carbon. Bioresource Technology. 206, 231–238.

Cheirsilp, B., Torpee, S., 2012. Enhanced growth and lipid production of microalgae under mixotrophic culture condition: Effect of light intensity, glucose concentration and fed-batch cultivation. Bioresource Technology. 110, 510-516.

Cheng Y. S., Zheng Y., Gheynst J. V., 2011. Rapid quantitative analysis of lipids using a colorimetric method in a microplate format. Lipids. 46, 95–103.

Csőgör Z., Herrenbauer M., Schmidt K., Posten C., 2001. Light distribution in a novel photobioreactor- modelling for optimization. Journal of Applied Phycology. 13(4), 325-333.

Cornet, J. F., Dussap, C. G., Gros, J. B., 1998. Kinetics and energetics of photosynthetic micro-organisms in photobioreactors: application to *Spirulina* growth. Adv Biochem Eng. Biotechnol. 59, 155–224.

Cuellar-Bermudez S. P., Garcia-Perez J. S., Rittmann B. E., Parra-Saldivar R., 2015. Photosynthetic bioenergy utilizing CO_2: an approach on flue gases utilization for third generation biofuels. J. Cleaner Prod. 98, 53-65.

Fernandez F. G., Camacho F. G., Perez J. A., Sevilla J. M., Molina-Grima E., 1997. A model for light distribution and average solar irradiance inside outdoor tubular photobioreactors for the microalgal mass culture. Biotechnol. Bioeng.. 55 (5), 701–714.

Gentile M. P., Blanch H. W., 2001. Physiology and xanthophyll cycle activity of *Nannochloropsis gaditana*. Biotechnol. Bioeng.. 75, 1-12.

Gonçalves A.L., Pires J.C.M., Simões M., 2016. The effects of light and temperature on microalgal growth and nutrient removal: an experimental and mathematical approach. RSC Adv. 6, 22896-22907.

Hankamer B., Lehr F., Rupprecht J., Mussgnug J. H., Posten C., Kruse O., 2007. Photosynthetic biomass and H_2 production by green algae: from bioengineering to bioreactor scale-up. Physiologia Plantarum. 131(1), 10-21.

He Y., Chen L., Zhou Y., Chen H., Zhou X., Cai F., Huang J., Wang M., Chen B., Guo Z., 2016. Analysis and model delineation of marine microalgae growth and lipid accumulation in flat-plate photobioreactor, Biochem Eng. J. 111, 108-116.

Ho S. H., Chen, C. Y., Chang, J. S., 2012. Effect of light intensity and nitrogen starvation on CO_2 fixation and lipid/carbohydrate production of an indigenous microalga *Scenedesmus obliquus* CNW-N. Bioresource Technol.113, 244-252.

Holland A. D., Wheeler D. R., 2011. Intrinsic autotrophic biomass yield and productivity in algae: modeling spectral and mixing-rate dependence. Biotechnol. J. 6(5), 584-99.

Hu Q., Sommerfeld M., Jarvis E., Ghirardi M, Posewitz M., Seibert M., Darzins A., 2008. Microalgal triacylglycerols as feedstocks for biofuel production: perspectives and advances. Plant J. 54, 621–639.

Huang Q., Yao L., Liu T., Yang J., 2012. Simulation of the light evolution in an annular photobioreactor for the cultivation of *Porphyridium cruentum*. Chem. Eng. Sci. 84, 718-726.

Huesemann M. H., Van Wagenen J., Miller T., Chavis A., Hobbs S., Crowe B., 2013. A screening model to predict microalgae biomass growth in photobioreactors and raceway ponds. Biotechnol. Bioeng. 110(6), 1583-94.

Issarapayup K., Powtongsook S., Pavasant P., 2009. Flat panel airlift photobioreactors for cultivation of vegetative cells of microalga *Haematococcus pluvialis*. J. biotechnol. 142(3), 227-232.

Jong K. N., Suh I. S., Hur B.K., Lee C. G., 2002. Simple monodimensional model for linear growth rate of photosynthetic microorganisms in flat-plate photobioreactors. J. Microbiol. . Biotechnol. 12(6), 962–971.

Khichi S. S., Anis A., Ghosh S., 2018. Mathematical modeling of light energy flux balance in flat panel photobioreactor for *Botryococcus braunii* growth, CO_2 biofixation and lipid production under varying light regimes. Biochem. Eng. J. 134, 44-56.

Khotimchenko S.V., Yakovleva I.M., 2005. Lipid composition of the red alga *Tichocarpus crinitus* exposed to different levels of photon irradiance. Phytochemistry. 66, 73–79.

Klok A. J., Verbaanderd J. A., Lamers P. P., Martens D. E., Rinzema, A., Wijffels, R. H., 2013. A model for customising biomass composition in continuous microalgae production. Bioresour. Technol.. 146, 89-100.

Kong B., Vigil R. D., 2014. Simulation of photosynthetically active radiation distribution in algal photobioreactors using a multidimensional spectral radiation model. Bioresour. Technol.. 158, 141-148.

Kumar K., Sirasale A., Das D., 2013. Use of image analysis tool for the development of light distribution pattern inside the photobioreactor for the algal cultivation. Bioresour. Technol. 143, 88-95.

Kumar K., Das D., 2012. Growth characteristics of *Chlorella sorokiniana* in airlift and bubble column photobioreactors, Bioresour. Technol. 116, 307-313.

Kunjapur A. M., Eldridge R. B., 2010. Photobioreactor design for commercial biofuel production from microalgae. Industrial and Engineering Chemistry Research. 49, 3516–3526.

Liu J., Yuan C., Hu G., Li F., 2012. Effects of light intensity on the growth and lipid accumulation of microalga *Scenedesmus* sp. 11-1 under nitrogen limitation. Appl. Biochem. Biotechnol. 166, 2127–2137.

Mondal M., Goswami S., Ghosh A., Oinam G., Tiwari O. N., Das P., Gayen K., Mandal M. K., Halder G. N., 2017. Production of biodiesel from microalgae through biological carbon capture: a review. 3 Biotech. 7(2), 99.

Naderi G., Znad H., Tade M. O., 2017.Investigating and modelling of light intensity distribution inside algal photobioreactor. Chemical Engineering & Processing: Process Intensification. 122, 530–537.

Ogbonna J. C., Yada H., Tanaka H. 1995. Light supply coefficient: a new engineering parameter for photobioreactor design. J. Fermen Bioeng. 80 (4), 369-376.

Ooms M. D., Dinh C. T., Sargent E. H., Sinton D., 2016. Photon management for augmented photosynthesis. Nature Communications. 7, 12699.

Packer A., Li Y., Andersen T., Hu Q., Kuang Y., Sommerfeld M., 2011. Growth and neutral lipid synthesis in green microalgae: a mathematical model. Bioresour. Technol. 102(1), 111-117.

Pegallapati A. N., Nirmalakhandan N., 2012. Modeling algal growth in bubble columns under sparging with CO_2-enriched air. Bioresour. Technol. 124, 137– 145.

Pottier L., Pruvost J., Deremetz J., Cornet J. F., Legrand J., Dussap C. G., 2005. A fully predictive model for one-dimensional light attenuation by *Chlamydomonas reinhardtii* in a torus photobioreactor. Biotechnol. Bioeng. 91(5), 569-582.

Pradhan L., Bhattacharjee V., Mitra R., Bhattacharya I., Chowdhury R., 2015. Biosequestration of CO_2 using power plant algae (*Rhizoclonium hieroglyphicum* JUCHE2) in a flat plate photobio-bubble-reactor – experimental and modeling, Chem.Eng. J. 275, 381–390.

Pruvost J., Legrand J., Legentilhomme P., Muller-Feuga A., 2002. Simulation of microalgae growth in limiting light conditions: flow effect. AIChE Journal. 48, 1109–1120.

Pruvost J., Pottier L., Legrand J., 2006. Numerical investigation of hydrodynamic and mixing conditions in a torus photobioreactor. Chem. Eng. Sci. 61(14), 4476-4489.

Qiaoning H., Haijian Y., Lei W., Chunxiang H., 2015. Effect of light intensity on physiological changes, carbon allocation and neutral lipid accumulation in oleaginous microalgae. Bioresour. Technol. 191, 219-228.

Quinn J., de Winter L., Bradley T., 2011. Microalgae bulk growth model with application to industrial scale systems. Bioresour. Technol. 102(8), 5083-92.

Ruiz J., Alvarez P., Arbib Z., Garrido C., Barragan J., Perales J. A., 2011. Effect of nitrogen and phosphorus concentration on their removal kinetic in treated urban wastewater by *Chlorella vulgaris*. Int. J. Phytorem. 13, 884–896.

Shotipruk A., Kaufman P. B., Wang H. Y.1999.Conceptual design of led-based hydroponic photobioreactor for high-density plant cultivation. Biotechnol. Prog. 15, 1058-1064.

Sierra E., Acién F. G., Fernández J. M., García J. L., González C., Molina E., 2008. Characterization of a flat plate photobioreactor for the production of microalgae. Chem. Eng. J. 138(1-3), 136-147.

Slade R., Bauen A., 2013. Micro-algae cultivation for biofuels: Cost, energy balance, environmental impacts and future prospects. Biomass Bioenergy, 53, 29-38.

Solovchenko A.E., Khozin-Goldberg I., Didi-Cohen S., Cohen Z., Merzlyak M.N., 2008. Effects of light intensity and nitrogen starvation on growth, total fatty acids and arachidonic acid in the green microalga *Parietochloris incise*. J. Appl. Phycol. 20, 245-251.

Suh I.S., Lee S. B., 2003. A light distribution model for an internally radiating photobioreactor. Biotechnol. Bioeng. 82(2), 180-189.

Surendhiran D., Vijay M., Sivaprakash B., Sirajunnisa A., 2015. Kinetic modeling of microalgal growth and lipid synthesis for biodiesel production. 3 Biotech. 5, 663–669.

Van Wagenen J., Miller T. W., Hobbs S., Hook P., Crowe B., Huesemann M. H., 2012. Effects of light intensity and temperature on fatty acid composition in *Nannochloropsis salina*. Energies. 5, 731–740.

Wang S. K., Stiles A. R., Guo C., Liu C. Z., 2014. Microalgae cultivation in photobioreactors: An overview of light characteristics. Eng. Life Sci. 14(6), 550-559.

Zijffers J. W., Janssen M., Tramper, J., Wijffels, R. H., 2008. Design process of an area-efficient photobioreactor. Marine Biotechnol. 10(4), 404-15.

Chapter 6

Specific Uptake Kinetics of Glucose and Nitrate in Carbon-Limited and Nitrogen-Limited C:N ratio under Photoheterotrophic Cultural Conditions for Botryococcus braunii Growth and Lipid Production

6.1. Introduction:

Microalgae are simple aquatic organism that photosynthesizes the solar energy to produce carbohydrate and small amount of liquid biofuel under autotrophic conditions. However, the autotrophic conditions are not sufficient to produce high biomass titer and biolipids. To conquer the limitations of autotrophic conditions, microalgae should be grown in heterotrophic, photoheterotrophic and/or mixotrophic cultivations. In particular, the biolipid content and growth of the microalgae in affected by carbon and nitrogen source in the nutrient medium under heterotrophic, photoheterotrophic and mixotrophic cultivations (Isleten-Hosoglu et al., 2012). However, in this study we have focused on photoheterotrophic cultivation of microalgae to analyze the role of carbon and nitrogen, on the uptake of each other.

The photoheterotrophic cultivation of microalgae requires light and organic substrate for their growth in which light and organic substrate act as energy source and carbon source respectively. In addition, the photoheterotrophic microalgal growth rate depends on the strain and culture conditions. Particularly, the carbon source uptake in photoheterotrophic culture conditions is regulated by the diffusion or transport of carbon source across the cellular membrane, which requires different enzymatic activities for assimilation of these carbon sources into the central carbon metabolic pathways (Morales-Sánchez et al., 2017).

Carbon and nitrogen metabolism in microorganisms is generally linked by the α-KG intermediate of the TCA cycle (Bren et al., 2016). In particular, the carbon metabolism in microalgae is highly affected by the nitrogen source and its concentration in the nutrient medium (Gopalkrishnan et al., 2015). Remarkably, in nitrogen limiting (carbon sufficient) conditions the accumulation of α-KG intermediate inhibits the Enzyme I (i.e the first step of the phosphotransferase system) which subsequently blocks the glucose uptake ability of the microorganism (Doucette et al., 2011). Although, in nitrogen limiting (carbon sufficient) conditions excess ATP is determined this inhibits

the glycolytic pathway and reduces glucose assimilation efficiency of the microalgae (Pagnanelli et al., 2014). Moreover, in these conditions the relative activity of PPP is found higher than the glycolysis, reflecting excess NADPH requirements for lipid biosynthesis (Xiong et al., 2010). Notably, it is evident that the pentose phosphate pathway (PPP) is preferred for glucose metabolism in nitrogen limiting (carbon sufficient) conditions. Whilst glycolytic pathway is favored over PPP for glucose metabolism in nitrogen sufficient (carbon limited) conditions (Gopalkrishnan et al., 2015). Furthermore, in carbon limited (nitrogen sufficient) conditions the relative activity of Phosphoenolpyruvate Carboxylase (PEPCase) has increased which assist glucose consumption through TCA cycle and subsequently favors carbon skeleton generation for improved carbon and nitrogen assimilation into protein synthesis. It also provides reducing equivalents to meet growth demands (Gopalkrishnan et al., 2015).

Nitrogen utilization pathway is affected by a regulatory molecule (i.e. αKG) which serves as both as a TCA intermediate and as the carbon backbone of glutamate and glutamine. In addition, α KG together with the glutamine regulates the nitrogen assimilation system (Bren et al., 2016). Moreover, nitrogen assimilation (nitrate or/and nitrite) in green microalgae is regulated at three levels: (1) the activity and capacity of nitrate and nitrite transport systems, (2) the activity of nitrate reductase and nitrite reductase, and (3) the amount of nitrate and nitrite reductases in the cells (Fernandez and Cardenas, 1989). Furthermore, Nitrate uptake rate is also stimulated in the presence of glucose, and 5 fold increased in NUR of *Chlorella vulgaris* was observed when the cells were preincubated with glucose (Schlee et al., 1985).

To date, our understanding of the substrate (i.e. glucose and nitrate) uptake kinetics in C- limited and N-limited photoheterotrophic cultivation condition is limited. While previous research manifested that *B. braunii* can grown under different organic carbon source and inorganic nitrogen source, little is known about the role of carbon and nitrogen on the specific uptake rates of each other, in C- limited and N-limited photoheterotrophic cultivation conditions. Therefore, we have compared specific uptake kinetics of *B. braunii* in C- limited medium with sufficient NO_3^- as the sole source of N, with the N- limited medium supplied with sufficient glucose as the sole C source. In addition, the effect of individual C:N ratio on biomass growth, chlorophyll formation and lipid accumulation were also studied in these conditions.

6.2. Material and methods

6.2.1. Microalgae and culture medium

B. braunii was provided by Institute of Bioresources and Sustainable Development (IBSD, Takyelpat, Imphal), and maintained in modified BG-11 medium as described by Khichi et al. (2018). The inoculated medium was incubated at 27 ± 1 °C and 130 rpm in the light incubator shaker and initial pH of the medium was maintained at 8.

To prepare C-limited and N-limited phothetrotrophic nutrient medium glucose and nitrate in modified BG – 11 medium were added according to Table 6.1 and Table 6.2 respectively. Furthermore, the nutrient medium was inoculated with a 10% v/v freshly grown *B. braunii* (i.e. 4-5 days old) and incubated at 27 °C on an orbital shaker at 150 rpm, that is, equipped with the fluorescent lamps. Two control experiments (control 1 and control 2) were also performed. In control 1 glucose was completely absent (Table 1) whilst in control 2 nitrate was completely absent (Table 2). All the experiments were conducted in triplicates.

Table 6.1. Showing the Glucose Limited (GL) C:N ratio

GL C:N ratio	Glucose Conc. (g L^{-1})	Nitrate Conc. (g L^{-1})
13:1	4.015	0.75
21:1	6.49	0.75
29:1	8.96	0.75
37:1	11.43	0.75
61:1	18.84	0.75
Control 1	-	0.75

Table 6.2. Showing the Nitrate Limited (NL) C:N ratio.

NL C:N ratio	Glucose Conc. (g L^{-1})	Nitrate Conc. (g L^{-1})
13:1	6.49	1.211
21:1	6.49	0.75
29:1	6.49	0.54
37:1	6.49	0.43
61:1	6.49	0.26
Control 2	6.49	-

6.2.2. Determination of biomass concentration

Microalgal cell dry weight was measured a function of the cell absorbance at 750 nm (A750) using an UV–Visible spectrophotometer (Carry 60, Agilent). A calibration curve was prepared to determined cell dry weight from the corresponding absorbance using the Eq. (E.6.1).

C_b (g L-1) = 2.84 OD_{750} (R^2 = 0.99) (E.6.1)

in which C_b is the dry weight of biomass and OD_{750} is the optical density measured at 750 nm. Therefore, the optical density can be used to precisely determine the dry weight of biomass.

6.2.3. Maximum Specific growth rate

Maximum specific growth rate of *B. braunii* in batch growth was calculated by applying the biomass mass balance

$$\frac{dM_x}{dt} = \mu^{max} M_x \qquad \text{(E.6.2)}$$

Biomass mass balance can be solved firstly by separation of variables and then integrated

$$\ln\left(\frac{M_x}{M_{x0}}\right) = \mu^{max} t \qquad \text{(E.6.3)}$$

A plot between $\ln\left(\frac{M_x}{M_{x0}}\right)$ vs t gives the slope as μ^{max} which is the maximum specific growth rate of microalgae.

6.2.4. Maximum Specific Substrate uptake rates

Substrate uptake kinetics was measured by applying the substrate mass balance in batch growth of *B. braunii.*

$$\frac{dM_s}{dt} = q_s^{max} M_x \qquad \text{(E.6.4)}$$

Where $\frac{dM_s}{dt}$ is the total consumption rate of Carbon or Nitrogen, t is fermentation time, q_s^{max} is maximum specific substrate consumption rate, M_x is biomass concentration at time t. M_x can be expressed as $M_{x0}.\exp(\mu^{max} t)$ by applying mass balance on biomass in batch growth. After substituting M_x in equation (3)

$$\frac{dM_s}{dt} = q_s^{max} M_{x0}.\exp(\mu^{max} t) \qquad \text{(E.6.5)}$$

Integrating equation (2) from t=0 to t and M_{s0} to $M_s(t)$

$$M_s(t) - M_{s0} = \frac{q_s^{max} M_{x0}}{\mu^{max}}.[\exp(\mu^{max}.t) - 1]$$

$$M_s(t) - M_{s0} = \frac{q_s^{max}}{\mu^{max}}.[M_x(t) - M_{x0}] \qquad \text{(E.6.6)}$$

A plot between $[M_s(t) - M_{s0}]$ vs $[M_x(t) - M_{x0}]$ were drawn whose slope is $\left(\frac{q_s^{max}}{\mu^{max}}\right)$, Where M_{s0} is the initial concentration of Carbon or Nitrogen , $M_s(t)$ is substrate concentration at different times, M_{x0} is initial biomass concentration and $M_x(t)$ is biomass concentration at different time.

6.2.5. Estimation of sugar consumption by DNS method

Residual sugars were estimated by modified DNS method (Miller et al., 1959). To estimate the residual glucose concentration 1 ml of sample was taken from the each flask in every 12 h interval. Supernatant was separated by centrifugation at 10,000 rpm for 6 minutes. Furthermore, 100 µl of diluted supernatant were added to 900 µl of deionized water, 1ml of DNS and 333 µl of Rochelle's salt (40% w/v). The mixture was then heated in boiling water bath for 5 minutes and cooled to room temperature, and the absorbance of the sample was measured at 540nm against the blank.

6.2.6. Estimation of Nitrate concentration-

Nutrient removal was determined by nitrate quantification in the culture medium. To estimate the nitrate concentration 1 ml of sample was taken from the photobioreactor in every 12 h interval. Supernatant was separated by centrifugation at 10,000 rpm for 6 minutes. Nitrate concentration was determined by taking OD at 220 nm using a UV–Visible spectrophotometer (Carry 60 Agilent) according to the method proposed by APHA (1976).

6.2.8.. Lipid extraction and estimation

Extraction of lipid was done by modified Bligh and dyer method with chloroform and methanol as solvents, and water as co-solvent (Bligh and Dyer, 1959). The cells were harvested by centrifugation at 10,000 rpm for 10 min at 4°C. After centrifugation the pellet was dried in oven for 2 h at 80°C. The chloroform/methanol (2:1 v/v) solvent system was used to extract the lipid from dried algal cells. The layers were separated by centrifugation for 10 min at 2000 rpm. The lower layer was separated and the procedure was again repeated with the pellet. The lipid content was measured gravimetrically and expressed as a dry weight percentage. The lipid productivity was calculated by the following equation

$$P_{\text{lipid}} = \frac{C_{\text{lipid}} \text{ X DCW}}{Time} \quad \text{(E.6.8)}$$

Where P_{lipid} is lipid productivity in g l^{-1} d^{-1}, C_{lipid} is lipid content of cells or lipid yield of the cells in g/g, DCW is dry cell weight g/l, and Time is the cultivation period in days.

6.3. Results

6.3.1. Algal growth

B. braunii growth in two sets (GL (Set I, i.e., fixed $NaNO_3^-$ = 0.75 g L^{-1}, with varying glucose) and NL (Set II, i.e., fixed Glucose = 6.49 g L^{-1}, with varying nitrate)) of five different C:N ratios (13:1, 21:1, 29:1, 37:1 and 61:1) under photohetertrophic conditions were studied in 250 ml flask respectively.

In GL C:N ratio (i.e. Set I), the maximum biomass concentration, maximum biomass productivity and maximum specific growth rate of 4.44 g L^{-1}, 1.11 g L^{-1} d^{-1} and 0.073 h^{-1}, observed respectively, at 29:1 C:N ratio on 4th of day of cultivation. At GL C:N ratio of 13:1, 21:1, 37:1, 61:1 maximum biomass concentration, maximum biomass productivity and maximum specific growth rate were 2.76 g L^{-1} 0.69 g L^{-1} d^{-1} and 0.063 h^{-1}, 4.20 g L^{-1}, 1.05 g L^{-1} d^{-1} and 0.069 h^{-1}, 4.04 g L^{-1}, 1.01 g L^{-1} d^{-1} and 0.072 h^{-1}, 3.57 g L^{-1}, 0.89 g L^{-1} d^{-1} and 0.071 h^{-1} respectively (Table 6.3).

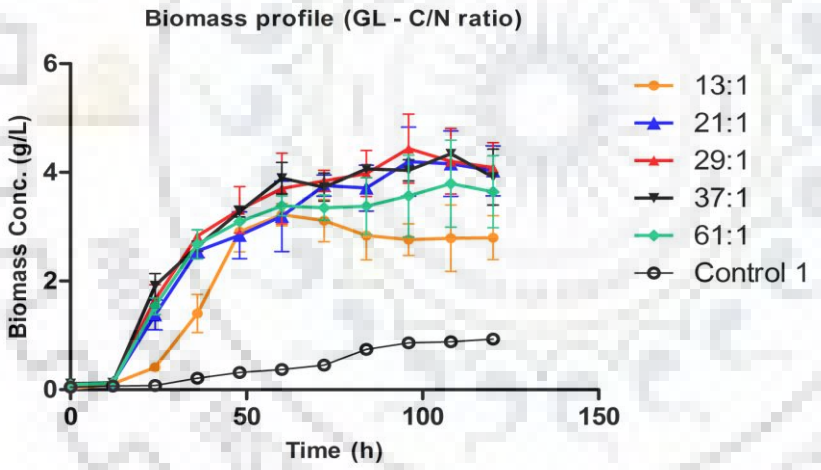

Fig. 6.1. Growth profile of *Botrycoccus braunii* in Glucose-Limited C:N

In this study, as depicted in Fig 6.1, the algal growth was increased with the increment in C:N ratio, in the range of 13:1 to 29:1 (i.e. 2.76 to 4.44 g L^{-1}), however, further increase in GL C:N ratio a gradual decline in biomass was observed for 37:1 (4.04 g L^{-1}) and 61:1 (3.57 g L^{-1}) GL C:N ratios respectively. This study suggests that at higher than optimum glucose concentration (i.e. organic carbon source) microalgae growth reduced significantly. Similar effects of varying glucose concentration on biomass growth profile were recorded previously by Zhang et al. (2011) and Yeesang et al. (2014).

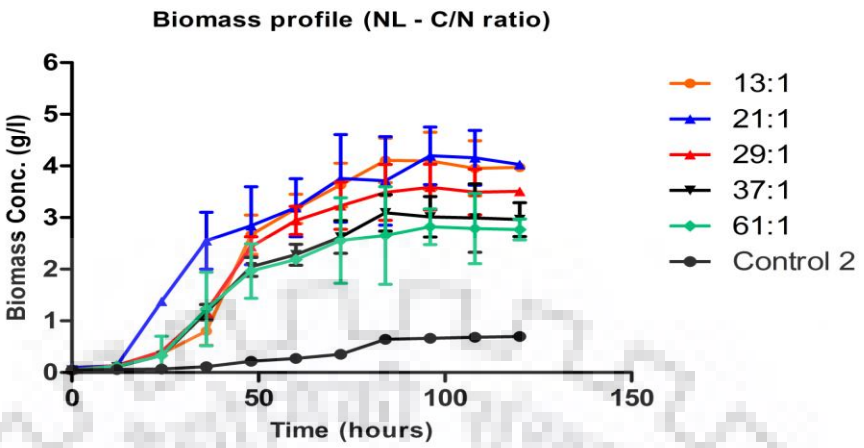

Fig. 6.2. Growth profile of *Botrycoccus braunii* in Nitrate-Limited C:N ratio

Notably, In NL C:N ratio (i.e. Set II), a moderate increase in algal growth was observed with initial increase in NL C:N ratio from 13:1 (4.10 g L^{-1}) to 21:1 (4.20 g L^{-1}) respectively (Fig 6.2). However, with the further increase in NL C:N ratio consequently reduces the microalgae growth. In this case (i.e. Set II) the maximum biomass concentration, maximum biomass productivity and maximum specific growth rate of 4.20 g L^{-1}, 1.05 g L^{-1} d^{-1} and 0.069 h^{-1}, obtained at 21:1 NL C:N ratio on 4th of day of cultivation. At GL C:N ratio of 13:1, 29:1, 37:1, 61:1 maximum biomass concentration, maximum biomass productivity and maximum specific growth rate were 4.10 g L^{-1} 1.02 g L^{-1} d^{-1} and 0.060 h^{-1}, 3.59 g L^{-1}, 0.90 g L^{-1} d^{-1}. and 0.061 h^{-1}, 3.01 g L^{-1}, 0.75 g L^{-1} d^{-1} and 0.057 h^{-1}, 2.82 g L^{-1}, 0.71 g L^{-1} d^{-1} and 0.056 h^{-1} respectively (Table 4). These findings are in accordance with Zhang et al. (2011), which showed the decrease in biomass concentration with increase in nitrogen concentration from 0.4 to 1.6 g L^{-1}.

Table 6.3. Showing the kinetic parameters of *B. braunii* in Glucose Limited C:N ratio (i.e.Maximum biomass (X_{max}), maximum specific growth rate (μ_{max}), Maximum specific glucose uptake rate (q_G^{max}) and Maximum specific Nitrate uptake rate (q_N^{max})).

GL C:N ratio	**X_{max} (g L^{-1})**	**μ_{max} (h^{-1})**	**q_G^{max} (GUR) (mM g_b^{-1} h^{-1})**	**q_N^{max} (NUR) (mM g_b^{-1} h^{-1})**
13:1	2.76	0.063	0.44	0.168
21:1	4.20	0.069	0.56	0.160
29:1	4.44	0.073	0.59	0.150
37:1	4.04	0.072	0.65	0.153
61:1	3.57	0.071	0.46	0.187
Control	0.66	0.014	-	0.094

Table 6.4. Showing the kinetic parameters of *B. braunii* in Nitrate Limited C:N ratio (i.e.Maximum biomass (X_{max}), maximum specific growth rate (μ_{max}), Maximum specific glucose uptake rate (q_G^{max}) and Maximum specific Nitrate uptake rate (q_N^{max})).

NL C:N ratio	X_{max} (g L^{-1})	μ_{max} (h^{-1})	q_G^{max} (GUR) (mM g_b^{-1} h^{-1})	q_N^{max} (NUR) (mM g_b^{-1} h^{-1})
13:1	4.10	0.06	0.57	0.178
21:1	4.20	0.069	0.56	0.160
29:1	3.59	0.061	0.49	0.130
37:1	3.014	0.057	0.48	0.115
61:1	2.82	0.056	0.41	0.074
Control 2	0.35	0.023	0.021	-

Table 6.5. Effect of GL C:N ratio on biomass productivity, lipid productivity, lipid Content, and lipid yield on glucose ($Y_{P/Glu}$).

GL C:N ratio	Biomass Productivity (g L^{-1} d^{-1})	Lipid Productivity (g L^{-1} d^{-1})	Lipid Content (g g^{-1})	$Y_{P/Glu}$
13:1	0.69	0.16	0.23	0.172
21:1	1.059	0.35	0.33	0.23
29:1	1.11	0.39	0.35	0.225
37:1	1.01	0.38	0.38	0.219
61:1	0.89	0.28	0.31	0.159
Control 1	0.17	0. 03	0.18	-

Table 6.6. Effect of NL C:N ratio on biomass productivity, lipid productivity, lipid Content, and lipid yield on glucose ($Y_{P/Glu}$).

NL C:N ratio	Biomass Productivity (g L^{-1} d^{-1})	Lipid Productivity (g L^{-1} d^{-1})	Lipid Content (g g^{-1})	$Y_{P/S}$
13:1	1.02	0.38	0.28	0.249
21:1	1.05	0.35	0.33	0.230
29:1	0.90	0.31	0.34	0.250
37:1	0.75	0.26	0.35	0.226
61:1	0.71	0.30	0.43	0.340
Control 2	0.09	0.023	0.26	-

6.3.2. Specific glucose uptake kinetics

The residual glucose pattern under GL C:N ratio were recorded in photoheterotrophic cultivation mode (Fig 6.3). To quantitatively analyze the effect of GL C:N ratio on glucose consumption, the maximum specific uptake rate of glucose (q_G^{max}) was calculate by Eq. (E.6.6). As shown in Table 6.3, the elevation in the maximum specific glucose uptake rate (q_G^{max}) was observed with the increment in GL C:N ratio in the range of 13:1 to 37:1 ratio. The highest value of q_G^{max} was 0.65 mM g_b^{-1} h^{-1} obtained at GL C:N ratio of 37:1, whilst at the GL C:N ratio of 61:1 the lowest value of q_G^{max} (i.e. 0.46 mM g_b^{-1} h^{-1}) was observed. This observation, suggests that the GUR is proportional to the glucose level present in the nutrient medium in the range of 13:1 to 37:1 GL C:N ratio in phototrophic mode, and the glucose consumption was decreased at higher than optimum glucose level in culture solutions.

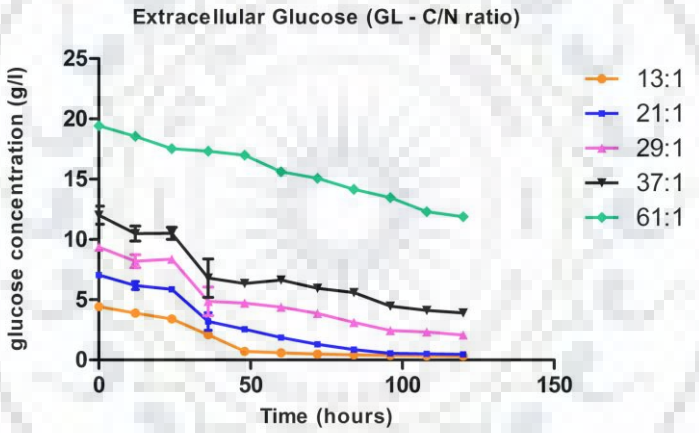

Fig 6.3. Glucose consumption profile in Glucose Limited C:N ratio

In this research, the glucose consumption pattern in GL C/N ratio indicated that increase in carbon concentration, the glucose consumption of 91.41%, 92.68%, 76.84%, 65.88% and 36.94% were observed for 13:1, 21:1, 29:1, 37:1 and 61:1 respectively. These results are in accordance with Yang et al. (2011), who reported similar decrease in sugar consumption pattern using glycerin as a carbon source for *Chlorella minutissima.*

Extracellular glucose profile in NL C:N ratio was also obtained under photoheterotrophic culture conditions (Fig.6.4). Although, in NL culture conditions the glucose concentration was kept fixed (i.e. 6.49 g L^{-1}) whilst the nitrate concentrations were retain differ in each flask from 1.21 to 0.26 g L^{-1} (i.e.,$NaNO_3^-$) to achieve the analogous C:N ratio (i.e. 13:1, 21:1, 29:1, 37:1 and 61:1) in the

culture solution. Similarly, the GUR rate was calculated by Eq. (E.6.6), and the affect of extracellular nitrate on GUR in NL C:N ratio was analyzed.

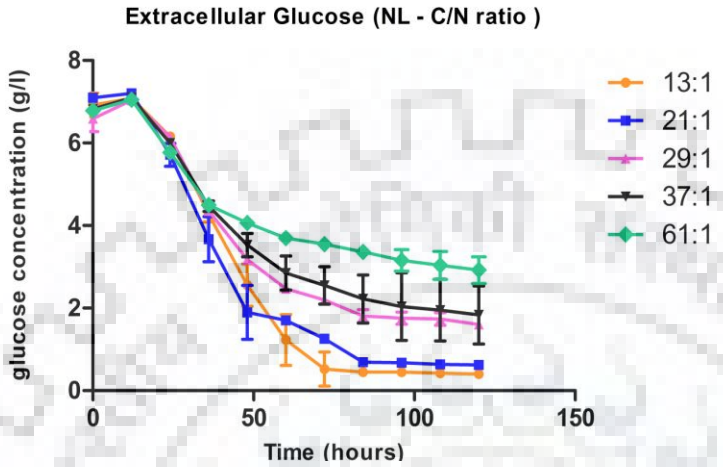

Fig 6.4. Glucose consumption profile in Nitrate Limited C:N ratio

Remarkably, the GUR is highly dependent on the external nitrate concentration available in the culture solution. In particular, the GUR was decreased with the increase (i.e. decrease in nitrate concentration) in NL C:N ratio. Maximum specific glucose uptake rate (q_G^{max}) of 0.57 mM g_b^{-1} h^{-1} was observed under 13:1 NL C:N ratio. At NL C:N ratio of 21:1, 29:1, 37:1 and 61:1 the observed q_G^{max} was 0.56 mM g_b^{-1} h^{-1}, 0.49 mM g_b^{-1} h^{-1}, 0.48 mM g_b^{-1} h^{-1} and 0.41 mM g_b^{-1} h^{-1} respectively (Table 6.4). This study suggests, that the lower nitrogen content in nutrient medium disturbs the metabolic flow of glucose and emphasizing the consumption of glucose from PPP rather than to glycolytic pathway (Gopalkrishnan et al., 2015), which subsequently reduce the glucose consumption, in lower nitrogen containing nutrient medium.

6.3.3. Specific nitrate uptake kinetics

Nitrogen depletion pattern in GL C:N ratio was also observed. As shown in Fig. 6.5, the extracellular nitrate concentration exponentially decreased after 24 h of cultivation. The perceptible change in nitrate depletion was quantified by specific nitrate uptake rate (NUR) by Eq.(E.6.6). Notably, as depicted in Table 6.3, the regulation of nitrate uptake was governed by the extracellular glucose present in the culture solution. Particularly, the NUR was decreased with increase in GL C:N ratio in the of 13:1 to 29:1 (i.e. from 0.168 mM $g_b^{-1}h^{-1}$ to 0.150 mM $g_b^{-1}h^{-1}$) (Table 6.3), with the further increase in GL C:N ratio an elevation in NUR was observed for 37:1

C:N ratio (153 mM $g_b^{-1}h^{-1}$), whilst at 61:1 GL C:N ratio the highest value (i.e.,187 mM $g_b^{-1}h^{-1}$) of NUR was observed.

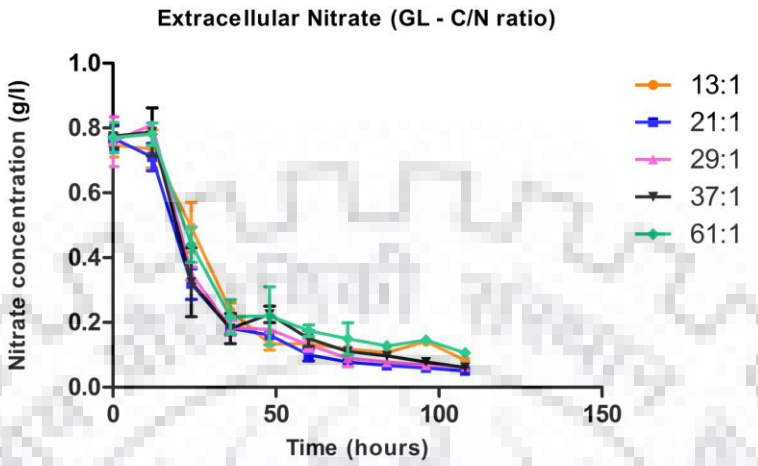

Fig 6.5. Nitrate consumption profile in Glucose Limited C:N ratio

In addition, it has been previously reported that addition of glucose in the culture solution induces nitrogen transport systems (i.e. shortchain neutral amino acids, basic amino acids) microalgal cells (Schlee et al., 1985). These results are also in accordance with Yan et al. (2013) and observed the highest TN removal efficiency of 92.85% in C limited C:N (5:1) ratio for *Chlorella vulgaris*.

Nitrate consumption pattern (Fig 6.6) and nitrate uptake rate (Table 6.4) in NL C:N ratio was also recorded. Maximum NUR of 0.178 mM g_b^{-1} h^{-1} was observed for 13:1 NL C:N ratio (i.e. $NaNO_3^-$ = 1.21 g L^{-1}). At other NL C:N ratio 21:1 (i.e. $NaNO_3^-$ = 0.75 g L^{-1}), 29:1 (i.e. $NaNO_3^-$ = 0.54 g L^{-1}), 37:1 (i.e. $NaNO_3^-$ = 0.43 g L^{-1}), 61:1 (i.e. $NaNO_3^-$ = 0.26 g L^{-1}) the observed maximum NUR was 0.160 mM g_b^{-1} h^{-1}, 0.130 mM g_b^{-1} h^{-1}, 0.115 mM g_b^{-1} h^{-1}, 0.074 mM g_b^{-1} h^{-1} respectively.

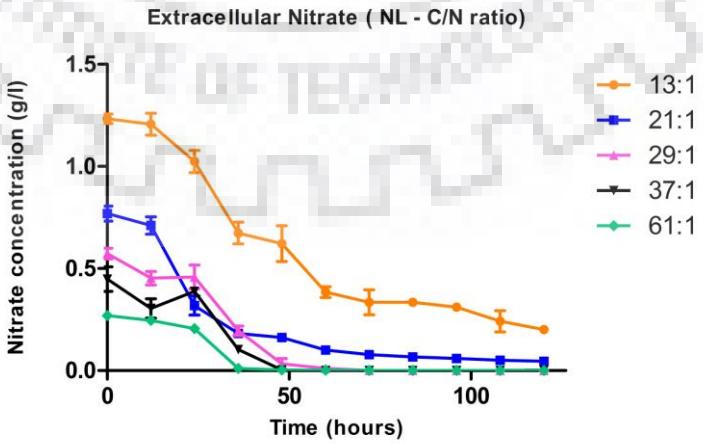

Fig 6.6. Nitrate consumption profile in Nitrate Limited C:N ratio

The obtained result advice that the NUR in NL C:N ratio is regulated by the external nitrate concentration available in the culture solution. In addition, as the nitrate concentration was decreased from 1.21 to 0.26 g L^{-1} (i.e. 78.51% decrease), the significant reduction (i.e. 58.43% reduction) in NUR was observed (i.e 0.178 mM $g_b^{-1}h^{-1}$ to 0.074 mM $g_b^{-1}h^{-1}$).

6.3.4. Lipid productivities

Lipid content in GL C:N ratio was examined and represented in Fig. 6.7. Noteworthy, an upsurge in the lipid content was noticed in the range of GL C:N ratio of 13:1 to 37:1, whilst above than optimal glucose concentration (i.e. 61:1 C:N ratio) a decrease in trend for lipid content was observed. Although, the maximum lipid content of 0.38 g g^{-1} was attained at 37:1 GL C:N ratio but the maximum lipid productivity of 0.39 g L^{-1} d^{-1} (lipid content = 0.35 g g^{-1}) was achieved at 29:1 GL C:N ratio. However, this observation demonstrate that the lipid content was increased with increase in glucose concentration (i.e. up to 11.43 g L^{-1} or 37:1 C:N ratio) in the culture solution. Remarkably, despite the fact that the highest lipid content was observed for 37:1 C:N ratio, the lipid productivity was higher for 29:1 GL C:N ratio (Table 6.5).

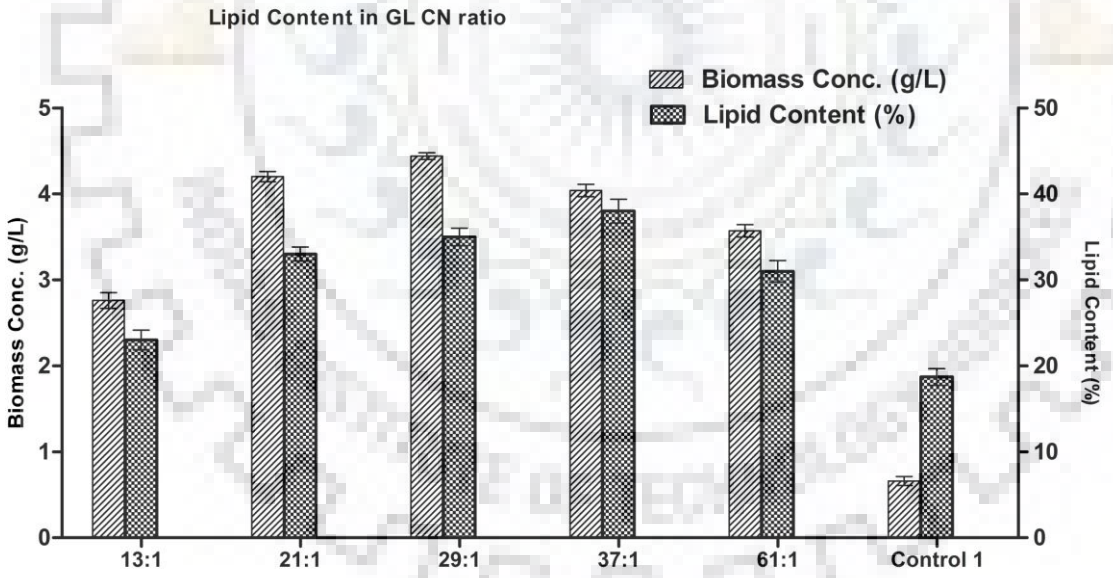

Fig 6.7. Maximum Biomass and Lipid Content in Glucose-Limited C:N ratio

In addition, it must be noted that the lipid productivity is considered as a function of biomass productivity which subsequently increase with increase in biomass productivity whilst the lipid content of the microalgal cell is related to the external carbon source present in the GL photohetertrophic cultivation. So that, the external glucose concentration (11.43 g L^{-1} or 37:1 C:N

ratio) increases the lipid content but remarkably decrease the biomass productivity (i.e. 1.01 g L^{-1} d^{-1}, Table 6.5) which consequently reduce the overall lipid productivity at high GL C:N ratio of 37:1 (11.43 g L^{-1} glucose concentration).

Table 6.7 Comparable literature values of biomass productivity and lipid productivity under different C:N ratios

Microalgae	C: N ratio	Biomass productivity (g $L^{-1}day^{-1}$)	Lipid productivity (g $L^{-1}day^{-1}$)	Data	Reference
B. braunii	47.35	0.13	-	Calculated	Zhang et al., 2011
B.braunii	72.85	0.163	0.0645	Provided	Yeesang and Cheirsilp., 2014
N.oleoabundans	17	0.344	0.0826	Provided	Sánchez et al., 2013
N.oleoabundans	278	1.022	0.528	Provided	Sánchez et al., 2013
B.braunii (GL)	29	1.11	0.39	Calculated	Present studies
B.braunii (NL)	21	1.05	0.35	Calculated	Present studies

The lipid content and lipid productivity of 0.23 g g^{-1} and 0.16 g L^{-1} d^{-1}, 0.33 g g^{-1} and 0.35 g L^{-1} d^{-1}, 0.31 g g^{-1} and 0.28 g L^{-1} d^{-1} were observed for 13:1, 21:1, 61:1 respectively. In present studies, lipid productivities obtained under different C:N ratios were compared with the literature reported values. Moreover, the lipid productivities obtained under GL C:N ratio of 29:1 (i.e. 0.35 g L^{-1} d^{-1}) higher than the other B braunii strains for different C:N ratios (Table 6.7). However, the lipid productivity of *N.oleoabundans* under C:N ratio of 278 was higher than the present studies, this might be due to the different type of strains and/or different cultivation system used for the production of biomass and lipid was adopted in their studies.

In NL C:N ratio the trend for lipid content in Fig. 6.8, and lipid productivity of *B. branui* in Table 6.6 were exemplified. As depicted in Table 6.6, the elevation in lipid content was observed with increase (i.e. decrease in nitrate concentration) in NL C:N ratio in culture solution. Remarkably, the trend for maximum lipid productivity was found exactly reverse to the lipid content trend (i.e. lipid productivity decreased with increase in NL C:N ratio). In addition, it must be noteworthy that the lower nitrate concentration present in the culture solution reduces the biomass productivity whilst it influences the lipid accumulation in microalgal cells in NL photohetertrophic cultivation.

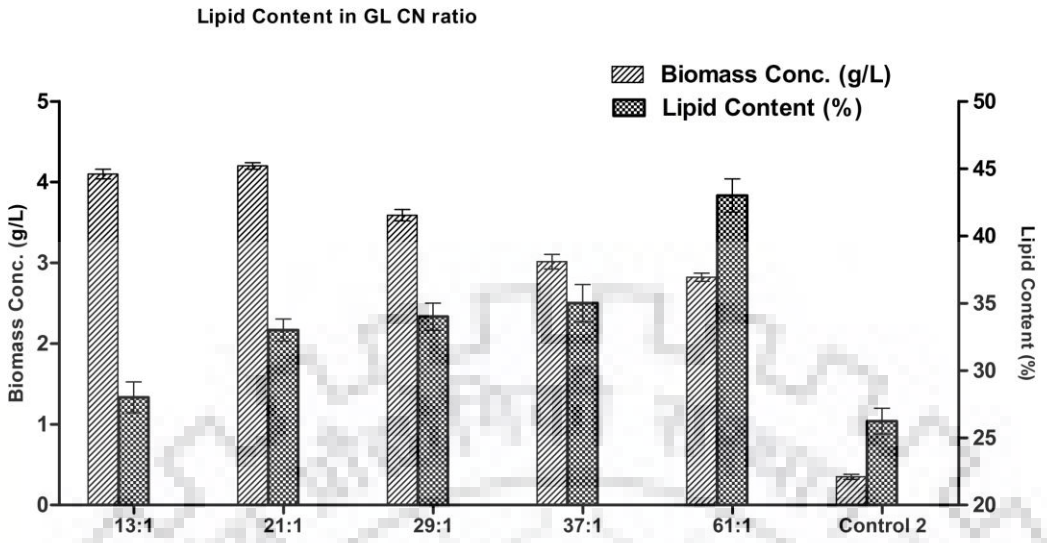

Fig 6.8. Maximum Biomass and Lipid Content in Nitrate-Limited C:N

In NL C:N ratio the lipid productivity increase with decrease in nitrate concentration (i.e increase in NL C:N ratio) and maximum lipid yield of 0.43 g g^{-1} was found for the NL C:N ratio of 61:1. The lipid content decrease with decrease in NL C:N ratio and the values of 0.347±0.013, 0.343±0.021, 0.33±0.027 and 0.28±0.016 was observed at 37:1, 29:1, 21:1 and 13:1 respectively (Fig. 10).

6.4. Conclusion

Carbon and nitrogen sources are most significant elements for photoheterotrophic cultivation of *B. braunii*. Moreover, carbon and nitrogen metabolic pathways are linked with each other and their metabolic activity is regulated by the availability of the carbon or nitrogen source in the culture solution. In this study, we have measured the specific uptake rate of carbon and nitrogen for B braunii in GL and NL photoheterotrophic cultivation conditions. Further, we have studied the role of the each source (i.e. either 'C' or 'N') on the specific uptake rate of each other. This study suggests that carbon uptake ability of the B braunii is majorly regulated by the external nitrate level in the nutrient medium whilst the nitrogen uptake rate is associated with the external carbon source in the culture solution. The significance of this study ensures that both the sources (i.e. 'C' or 'N') are equally important for the lipid production, hence the optimum level of these sources are required for efficient growth, lipid and large-scale biomass production

6.5. References:

APHA., Standard methods for the examination of water and wastewater 14ed. APHA American Public Health Association (1976).

Bligh EG and Dyer WJ, 1959. A rapid method of total lipid extraction and purification. Canadian J. Biochemistry physiol. 37,911-917.

Bren A, Park J.O, Towbin B.D., Dekel E, Rabinowitz J.D. and Alon U., 2016. Glucose becomes one of the worst carbon sources for E. coli on poor nitrogen sources due to suboptimal levels of cAMP. Sci. rep. 2016, 6.

Doucette C.D., Schwab D.J., Wingreen N.S., Rabinowitz J.D., 2011. α-Ketoglutarate coordinates carbon and nitrogen utilization via enzyme I inhibition. Nat. chem.biol. 7, 894-901.

Fernandez E., Cardenas J., 1989. Genetics and regulatory aspects of nitrate assimilation in algae. Molecular and genetic aspects of nitrate assimilation/edited by John L Wray and James R Kinghorn.

Gopalakrishnan S., Baker J., Kristoffersen L., Betenbaugh M.J., 2015. Redistribution of metabolic fluxes in Chlorella protothecoides by variation of media nitrogen concentration. Metabol. Eng.Commun. 2,124-131.

Isleten-Hosoglu M., Gultepe I. and Elibol M., 2012. Optimization of carbon and nitrogen sources for biomass and lipid production by *Chlorella saccharophila* under heterotrophic conditions and development of Nile red fluorescence based method for quantification of its neutral lipid content. Biochem. Eng J. 61,11-19.

Miller G.L., Blum R., Glennon W.E., Burton A.L., 1960. Measurement of carboxymethylcellulase activity. Analytical Biochemistry. 1,127-132.

Morales-Sánchez D., Tinoco-Valencia R., Kyndt J., Martinez A., 2013. Heterotrophic growth of *Neochloris oleoabundans* using glucose as a carbon source. Biotechnol. for biofuels. 6,1.

Pagnanelli F., Altimari P., Trabucco F., Toro L., 2014. Mixotrophic growth of *Chlorella vulgaris* and *Nannochloropsis oculata*: interaction between glucose and nitrate. J. Chemi. Technol. Biotechnol. 89, 652-661.

Schlee J., Cho B-H., Komor E., 1985. Regulation of nitrate uptake by glucose in *Chlorella*. Plant sci. 39,25-30.

Xiong W., Liu L., Wu C., Yang C., Wu Q., 2010. 13C-tracer and gas chromatography-mass spectrometry analyses reveal metabolic flux distribution in the oleaginous microalga Chlorella protothecoides. Plant Physiol. 154,1001-1011.

Yan C., Zhang L., Luo X., Zheng Z., 2013. Effects of various LED light wavelengths and intensities on the performance of purifying synthetic domestic sewage by microalgae at different influent C/N ratios. Ecological Eng. 51, 24-32.

Yang J., Rasa E., Tantayotai P., Scow K.M., Yuan H., Hristova K.R., 2011. Mathematical model of *Chlorella minutissima* UTEX2341 growth and lipid production under photoheterotrophic fermentation conditions. Bioresour. Technol. 102, 3077-3082.

Yeesang C., Cheirsilp B., 2014. Low-cost production of green microalga *Botryococcus braunii* biomass with high lipid content through mixotrophic and photoautotrophic cultivation. Appl. Biochem. Biotechnol. 174,116-129.

Zhang H., Wang W., Li Y., Yang W., Shen G., 2011. Mixotrophic cultivation of *Botryococcus braunii*. Biomass Bioenergy. 35,1710-1715.

Chapter 7

Single Stage Two Phase Fed-Batch cultivation of *Botryococcus braunii* in Flat Panel Airlift Photobioreactor under Mixotrophic Cultivation Conditions

7.1. Introduction

The quest for alternative fossil fuels has been driven by global interest because of rapid depletion of natural resources and greenhouse gas emissions. Biodiesels are considered as a possible revolutionary energy resource because it has ability to curtail 57−86% greenhouse gas emissions (Sun et al., 2014). Currently, the oil crops (soybeans, corns, jatropha, etc.), animal fat, and waste cooking oil are the main sources for the biodiesel production. However, large scale production of biodiesels from these sources seems distant from fulfilling the demand as alternative fuels (Lin et al., 2011; Liu et al., 2008). Microalgae are a decisive source of biodiesel production that can satisfy the global demand, due to their eco-friendliness, rapid growth, excessive lipid content, and low prerequisite for cultivated land (Chisti, 2007; Xie et al., 2012). Furthermore, microalgal biodiesel is considered as highly biodegradable and nontoxic (Sun et al., 2014). Moreover, microalgae have the ability to grow in autotrophic (i.e. in light only), heterotrophic (i.e. in organic substrate only) or mixotrophic (i.e. in light, CO_2 and organic substrate). Heterotrophic or mixotrophic cultivation of microalgae in bioreactor offers higher specific growth rates in comparison to photoautotrophic cultivation and resulted in substantiate biomass and lipid productivities which subsequently minimized the process harvesting cost (Brennan and Owende, 2010). However, mixotrophic cultivation of microalgae is attractive, because light limitation is no longer issue in mixotrophic conditions (Ogbonna and Tanaka 2000). In mixotrophic cultivation system organic substrate and inorganic carbon (i.e. CO_2) both provides the carbon source for microalgae growth whilst light is required for energy source to carry out photosynthesis. In mixotrophic cultivation, microalgae can efficiently obtain high cell density, growth rate, and lipid content (Qiao et al., 2009). Moreover, the application of mixotrophic mode of nutrition (i.e. glucose, CO_2 and light) in microalgal photofermentation is potentially an extensive addition to biodiesel production (Kong et al., 2013; Scott et al., 2010). The culture mode affects microalgal growth and lipid accumulation. Notably, the microalgae growth and lipid production are two mutually exclusive phenomena in photofermentation (Muthuraj et al., 2014; Kumar et al., 2014).

Therefore, it is not necessary that optimized growth conditions may also suitable for lipid production. In particular, high biomass production and lipid accumulation is achieved under two-stage cultivation strategies (Karemore et al., 2013), but imitations of this process includes additional processs harvesting cost and replenishment of nutrient medium (Xia et al., 2014). Hence, single-stage cultivation in a single bioreactor will provide high biomass titer in lipid rich microalgal cell under control environment.

In addition, an effective culture mode, that is, single stage two-phase fed-batch culture is an efficient way to enhance microalgal biomass and lipid accumulation. Microalgal cells are first cultivated in a phototrophic mode using CO_2 and light as the carbon source and energy source respectively to reach high cell density; the cells are then stimulated to accumulate lipids by the addition of glucose. A series of experiments were conducted for *B. braunii* to determine the critical substrate concentration for growth and/or lipid production. In this study, the combined effects of organic substrate and nitrogen on the growth and lipid production on B. braunii were explored. Finally, a single-stage two phase fed-batch cultivation process was developed. The growth and lipid production of *B. braunii*, in the single-stage two phase cultivation process were investigated.

7.2. Material and methods

7.2.1. Microalgae and culture medium

A culture of *B. braunii* was obtained from the Institute of Bioresources and Sustainable Development (IBSD, Takyelpat, Imphal). The microalgae were grown in modified BG-11 medium containing macronutrients such as $NaNO_3$ (1.12 g), $MgSO_4.7H_2O$ (75 mg), K_2HPO_4. $3H_2O$ (40 mg), $CaCl_2.2H_2O$ (36 mg), Na_2CO_3 (20 mg), EDTA, 2Na-Mg salt (1 mg), citric acid (6 mg), ferric ammonium citrate (6 mg) and micronutrients such as H_3BO_3 (286 µg), $MnCl_2.4H_2O$ (181 µg), $ZnSO_4.7H_2O$ (22 µg), $Na_2MoO_4.2H_2O$ (39 µg), $CuSO_4.5H_2O$ (8 µg) and $Co(NO_3)_2.6H_2O$ (5 µg) per liter. The inoculated medium was incubated at 27 ± 1 °C and 130 rpm in a light incubator shaker. The initial pH of the medium was maintained at 8.

7.2.2. Flat Panel Airlift Photobioreactor

Airlift Flat Panel photobioreactor was constructed using borosilicate glass. The dimension of the reactor is (24.13× 29.21 × 7.62 cm) respectively (Fig. 1). For air flow porous type sparger was used. The wall thickness was 5 mm and air was introduced into the base by sparger attached at the bottom. Bubble column was converted into airlift bioreactor by inserting a centre glass plate into

them (Fig. 1). The reactor was illuminated by light intensity from the range of (133 to 348 μmol m^{-2} s^{-1}) by LED Panel arranged at one side of the photobioreactor. *B. braunii* was grown in 5.37 liter photobioreactor filled with BG-11 nutrient medium, and operating at 0.3 vvm air flow rate and 5% CO_2 (Table 1).

7.2.3. Determination of biomass concentration

Microalgae Biomass was estimated as a function of optical density of cell. The Optical density (OD) of cells in the circulated liquid was determined using an UV–Visible spectrophotometer (Carry 60Varian) at an absorbance of 680 nm (OD_{680}). Dry cell weight (Dwt) was calculated using following formula generated using OD data and a calibration plot.

C_b (g/l) = 1.115 OD_{680} (R^2 = 0.99)

in which C_b is the dry weight of biomass and OD_{680} is the optical density measured at 680 nm. Therefore, the optical density can be used to precisely determine the dry weight of biomass.

7.2.4. Estimation of sugar consumption by DNS method

Residual sugars were estimated by modified DNS method (Miller et al., 1959). To estimate the residual glucose concentration 1 ml of sample was taken from the each flask in every 12 h interval. Supernatant was separated by centrifugation at 10,000 rpm for 6 minutes. Furthermore, 100 μl of diluted supernatant were added to 900 μl of deionized water, 1ml of DNS and 333 μl of Rochelle‘s salt (40% w/v). The mixture was then heated in boiling water bath for 5 minutes and cooled to room temperature, and the absorbance of the sample was measured at 540nm against the blank.

7.2.5. Estimation of Nitrate concentration

Nutrient removal was determined by nitrate quantification in the culture medium. To estimate the nitrate concentration 1 ml of sample was taken from the photobioreactor in every 12 h interval. Supernatant was separated by centrifugation at 10,000 rpm for 6 minutes. Nitrate concentration was determined by taking OD at 220 nm using a UV–Visible spectrophotometer (Carry 60 Agilent) according to the method proposed by APHA (1976).

7.2.6. Lipid estimation

Lipid estimation in microalgae samples was performed using the modified rapid colorimetric method based on sulpho-phospho-vanillin (SPV) reaction in the presence of sulphuric acid (Cheng

et al., 2011; Byreddy et al., 2016). The vanillin phosphoric acid reagent was prepared by dissolving 120 mg vanillin in 20 ml of distilled water and adjusting the final volume to 100 ml with 85% phosphoric acid. The reagent was stored in dark conditions until further use. SPV reagent was prepared freshly, which results in high activity with lipid samples. A known amount of *B. braunii* sample was taken in test tube and incubated for 100 ºC for 5 min, and allowed to cool for 5 min in an ice bath. Freshly prepared phospho-vanillin reagent (1 ml) was then added to each test tube. The test tubes were incubated at 37 ºC and 200 rpm for 15 min, and absorbance was measured at 540 nm.

7.3 Results and discussion

7.3.1. Effect of various carbon sources on biomass growth and lipid (flask cultivation)

In first step, effect of seven different carbon sources (i.e., glucose, fructose, mannose, arabinose, xylose, sucrose and glycerine) on biomass production and lipid accumulation were studied and represented in Fig 1. In addition, the nitrate concentration was remained constant fixed at 0.75 g L^{-1} whilst the carbon source concentration was adjusted accordingly to bring the optimum GL C:N ratio of 29:1 in the culture solution. The shake flask studies suggest that glucose is the most favored carbon source for lipid induction and high biomass production. Maximum biomass concentration and lipid content of 4.44 g L^{-1} and 0.35 g g^{-1} was obtained using glucose as a sole carbon source in photoheterotrophic cultivation conditions.

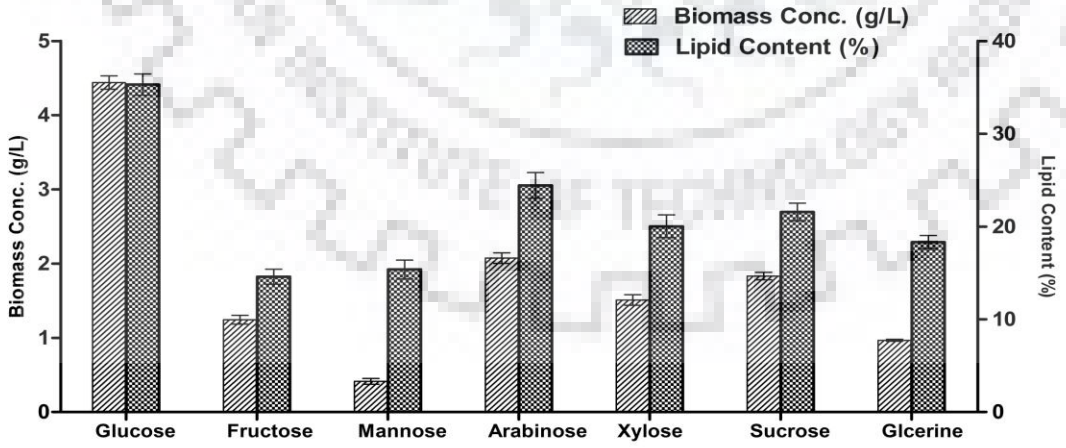

Fig. 7.1. Effect of different carbon sources on biomass and lipid content with constant C:N ratio of 29:1.

However, at other carbon sources such as fructose, mannose, arabinose, xylose,sucrose, glycerine the maximum biomass concentration and lipid content of 1.243 g L^{-1} and 0.146 g g^{-1}, 0.414 g L^{-1} and 0.154 g g^{-1}, 2.075 g L^{-1} and 0.244 g g^{-1}, 1.51 g L^{-1} and 0.201 g g^{-1}, 1.832 g L^{-1} and 0.22 g g^{-1}, 0.967 g L^{-1} and 0.183 g g^{-1} were obtained respectively. The lower biomass concentration and lipid content in other carbon sources (i.e. excluding glucose) might be due to discrete events that are associated with carbon transport activity such as inadequate catabolic activity of several enzymes, lower oxidizing capacity for carbon sources (excluding glucose) or the non-availability of relevant permeases in the microalgal cell membrane (Morales-Sánchez et al., 2013).

7.3.2. Effect of Trace and micro elements (TME) on *B. braunii* growth (flask cultivation)

Furthermore, effect of TME on specific growth rate of B braunii was evaluated for different (0.3, 0.5, 2, 3 and 1 as control) units L-1 of TME. The study was conducted in optimized GL C:N ratio of 29:1 with unique amount of TME in each flask under photoheterotrophic cultivation condition in batch mode. The stock concentration of TME was prepared according to Table 7.1.

Table 7.1 Stock Solution Concentration of TME

Trace Elements	Composition (g L^{-1})	Micro elements	Composition (mg L^{-1})
$MgSO_4.7H_2O$	75	H_3BO_3	286
$CaCl_2.2H_2O$	36	$MnCl_2.H_2O$	181
Na_2CO_3	20	$ZnSO_4.7H_2O$	22
Citric Acid	6	$CuSO_4.5H_2O$	8
Ferric ammonium citrate	6	$Na_2MoO_4.2H_2O$	39
EDTA	1	$Co(NO_3)_2.6H_2O$	5

In particular, 1 ml of TME stock solution added in the 1 L culture solution is considered as 1 unit of TME per liter. Similarly to prepare 0.3, 0.5, 2 and 3 units of TME per liter, the required amount of TME stock solution were 300 µl, 500 µl, 2 ml and 3 ml in per liter of culture solution respectively. Further, the specific growth of B. braunii was quantified by measuring the algal growth at regular intervals under different amount of TME.

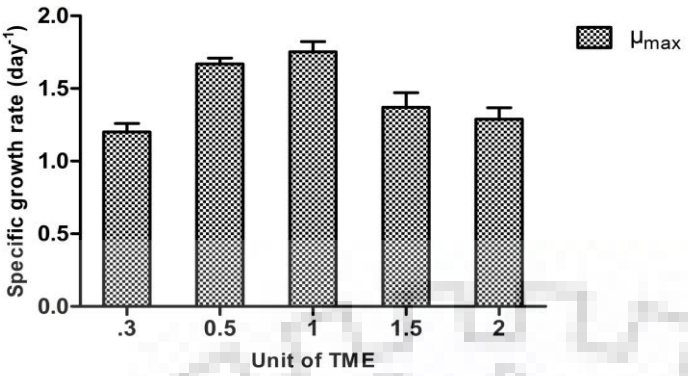

Fig. 7.2. Effect of different units of TME on specific growth of *B. braunii*.

As shown in Fig, the 1 unit of TME per liter culture solution the maximum specific growth rate of B braunii reached to 1.752 d^{-1} and supports biomass generation up to 4.44 g L^{-1} without perplexing the B. braunii growth. Hence, this study implied that approximately 225.23 µl of TME stock solution is required to generate 1 g of B braunii biomass. The results obtained in this study are relevant and confirming in manner with Basavraj et al. (2016), who described that 1 unit of TME produces 5.17 g of biomass for *Chlorella* sp. FC2 IITG.

7.3.3. Effect of glucose concentration on biomass growth and lipid production under mixotrophic cultivation conditions (photobioreactor batch cultivation)

Effects of three different glucose concentrations on biomass growth of *B. braunii* were studied using 5.37 L PSI flat panel photobioreactor in batch mode under mixotrophic cultivation conditions. Maximum biomass concentration and biomass productivity were 5.33 g L^{-1} and 1.99 g L^{-1} d^{-1}, respectively, at glucose concentration of 20 g L^{-1} after 96 h of cultivation. At glucose concentration of 10 and 30 g L^{-1} the maximum biomass concentration and maximum biomass productivity rate were 4.37 g L^{-1} and 1.311 g L^{-1} $d^{-1}$and 2.73 g L^{-1} and 0.55 g L^{-1} d^{-1}respectively. Similar effects of varying glucose concentration on growth pattern of B. braunii were reported by Yeesang et al. 2014. Effect of varying glucose concentration on lipid content and lipid productivities were assessed for mixotrophic batch cultivation. Maximum lipid content and maximum lipid productivity of 29.47% and 0.589 g L^{-1} d^{-1} were observed at 20 g L^{-1} glucose concentration and 133 µmol m^{-2} s^{-1} light intensities respectively.

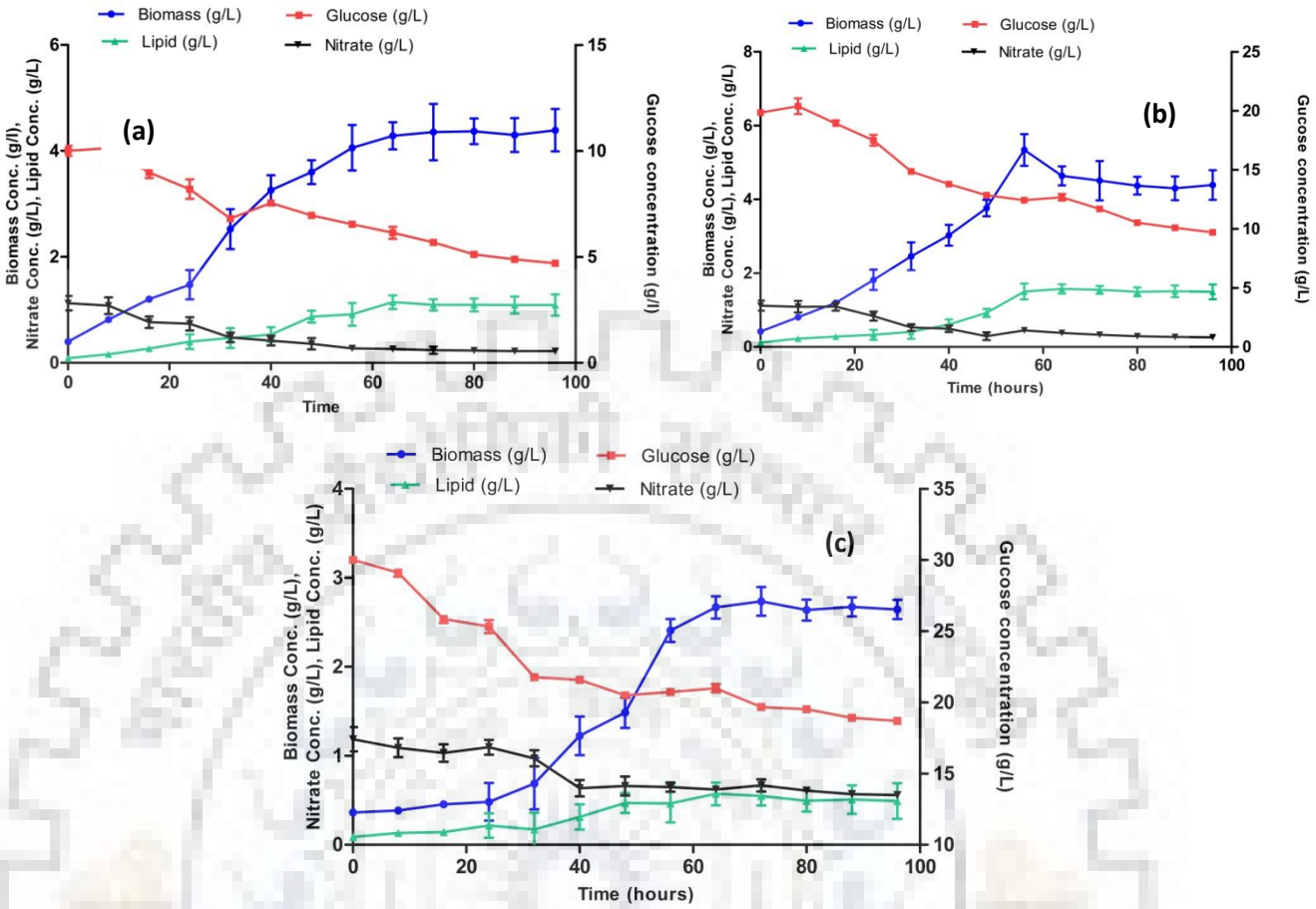

Fig. 7.3. Biomass, gucose, nitrate and lipid profiles under different initial glucose concentrations of (a) 10 g L^{-1}; (b) 20 g L^{-1} and (c) 30 g L^{-1} respectively.

Whilst at other glucose concentration of 10 g L^{-1} and 30 g L^{-1} the lipid content of B. braunii decreased to 25.03% and 20.15% respectively (Table 3). Hence, the algal lipid content could be stimulated by raising the glucose concentration from 10 to 20 g L^{-1} in the culture solution; however, further increment in glucose concentration reduced the lipid formation.

Table 7.1. Maximum biomass and lipid concentration, Lipid content, Biomass and Lipid productivity under varying light regimes.

Glucose Conc. (g L^{-1})	X_{max} (g L^{-1})	P_{max} (g L^{-1})	Biomass Productivity (g L^{-1} d^{-1})	Lipid Productivity (g L^{-1} d^{-1})	Lipid Content (%)
10	4.37	1.094	1.311	0.327	25.03
20	5.34	1.57	1.99	0.589	29.45
30	2.73	0.55	0.819	0.165	20.15

In present study, sodium nitrate consumption profiles under varying glucose concentration were illustrated in Fig (1,2,3). As shown in Fig 3 (i.e. at 30 g L−1 glucose concentration) the lowest nitrate removal rate of 141. 46 mg L^{-1} d^{-1} was obtained under mixotrophic batch mode of operation in flat panel photobioreactor. Whilst the nitrate removal rate of B braunii under other glucose concentrations of 10 g L^{-1} and 20 g L^{-1} were found nearly same (i.e. 216.23 mg L^{-1} d−1 and 226.39 mg L^{-1} d^{-1}) respectively. This illustrates that higher carbon source concentration (i.e. ≤ 30 g L^{-1}) adversely affect the nitrate removal rate in mixotrophic cultivation conditions.

7.3.4. Single-stage two phase mixotrophic fed-batch cultivation (photobioreactor)

A single-stage two phase fed-batch approach was applied for the production high biomass titer and lipid-enriched microalgal cells under mixotrophic condition. The experiments was performed in 5.37 L flat panel airlift photobioreactor with working volume of 2.87 L and the growth control parameters (i.e. temperature, pH, light, CO2% and airflow rate) remains same as that of the mixotrophic batch experiments as represented in the above section. In first step, single stage single phase fed batch (i.e. primary fed batch) was studied in phototrophic mode only. In first step, single stage single phase fed batch (i.e. primary fed batch) was studied in phototrophic mode only. In primary fed batch cultivation (single stage-single phase) only nitrate concentration was maintained in proper range under phototrophic cultivation mode.

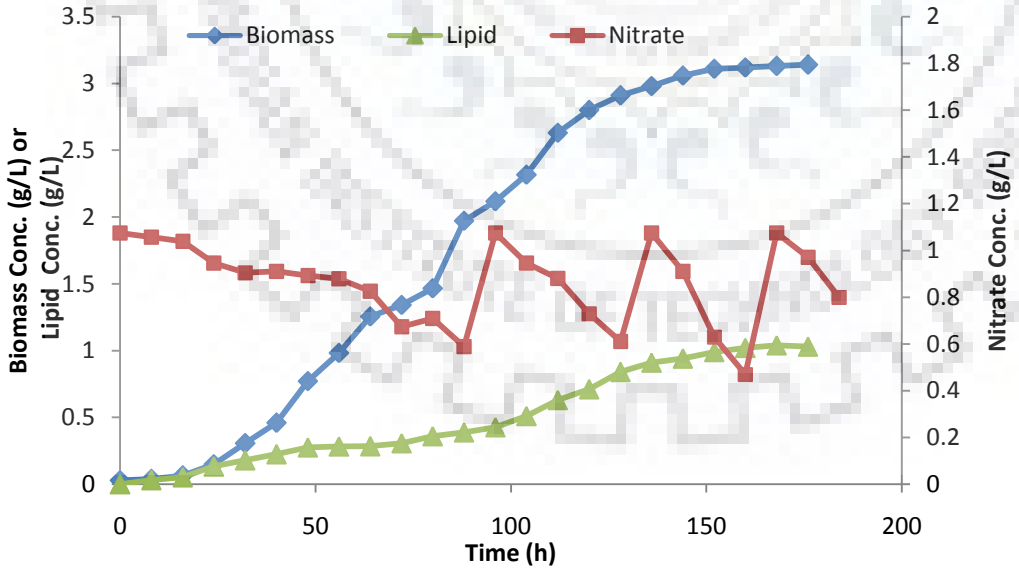

Fig. 7.4. Biomass, nitrate and lipid profiles of *B. braunii* in primary fed batch cultivation (Single stage single phase) under photoautotrohic conditions.

As depicted in Fig the temporal profile for biomass, lipid and nitrate was illustrated and shown that after 176 h cultivation, 3.14 g L^{-1}biomass and 1.04 g L^{-1} lipid were produced with the productivity of 0.495 g L^{-1} d^{-1} and 0.149 g L^{-1} d^{-1} respectively. Although, the obtained algal biomass concentration was comparatively higher with our earlier batch experiments (i.e. $NaNO_{3\ ini}$ (1.125 g L^{-1}), X_{max} = 2.03 g L^{-1}), but the observed lipid accumulation was only 33.12% in this study by concomitant feeding of nitrate at fixed CO_2 (5% v/v) concentration. Thus, to improve lipid yield, in the second set of experiment a single stage two phase fed batch strategy was adopted to enhance the lipid content within the algal cell.

Single stage two phase fed batch operation comprised of two phases: the first phase was used to acclimatize the microalgae cell in phototrophic mode, whilst the second phase was targeted to increase the lipid accumulation within the microalgal cell. In first phase of the single stage, only nitrogen and TME sources were fed to the culture together, after 40h of cultivation the carbon substrate (i.e. glucose) was fed into the reactor. Nitrate was used as the nitrogen source and optimal pH was maintained to 7.8. As shown in Fig 7.5, a single stage two phase growth profile, the first phase (0-40 h) and the second phase (40- 120 h), was illustrated for B braunii.

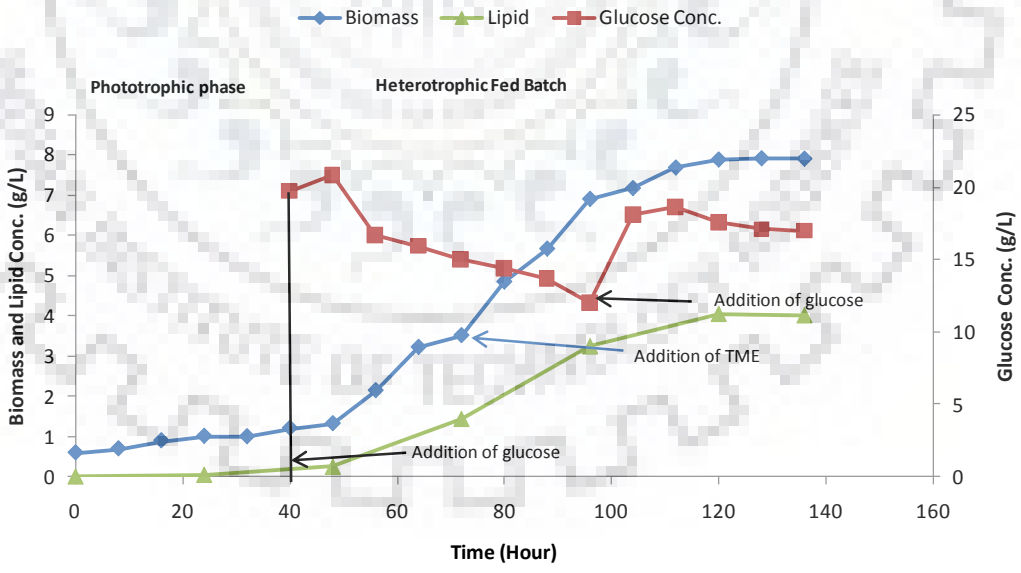

Fig. 7.5. Biomass, glucose and lipid profiles of *B. braunii* in Single stage two phase fed batch cultivation under mixotrophic conditions.

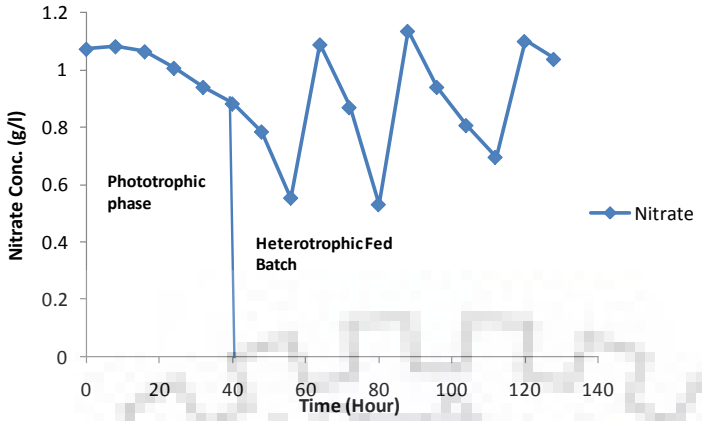

Fig. 7.5. Nitrate consumption profiles of *B. braunii* in Single stage two phase fed batch cultivation under mixotrophic conditions.

A linear increase in the algal biomass was observed i.e. from 0.6 g L^{-1} to 1.32 g L^{-1} in the first phase of the single stage cultivation conditions with the biomass productivity of 0.432 g L^{-1} d^{-1}. However, in this stage only 15.37% (0.2 g L^{-1}) of lipid accumulation was observed. Further, the glucose was introduced after 40 h of cultivation into the reactor and the second phase of the single stage cultivation was begun. Initially in the second phase of single stage an exponential increase in biomass concentration was observed within first 20 h of the second phase. This increasing exponential pattern continues until the 130 h of cultivation after that B braunii growth reached to the stationary phase. It must be noted that during the intermittent feeding of glucose and nitrate, the concentrations of these nutrients keep above the half of their maximal value. Whilst the intermittent feeding of TME was based on the biomass yield coefficient of TME (Yx/TME), that is, when the biomass concentration in the reactor was reached to the 4.4 g L^{-1}, 1 unit of TME was added into the reactor. Once the second phase set in, the introduced glucose triggers the lipid accumulation pathway of the microalgae which in turn enhance the lipid content of the microalgal cell, this phenomena was observed after the addition of the glucose into the reactor. Thus, an exponential increase in lipid concentration was also observed in the second phase of this process. The maximum lipid concentration and lipid productivity of 4.4 g L^{-1} and 1.32 g L^{-1} d^{-1} were achieved respectively at the end of fed batch process. The advantage of the single stage two phase cultivation processes is the augmentation of lipid content within the microalgal cell. Remarkable, it has been noted that, once microalgae cell enters into the second phase of cultivation process (i.e. after 40 h of cultivation) the external nitrate concentration available in the nutrient medium is above 0.88 g L^{-1}, this ensures that rate of glucose uptake will be enhanced which in turn trigger the

lipid synthetic pathway in microalgae. In addition, at the later stage of the cultivation the nitrate concentration was always kept above the half of the maximum concentration (< 0.55 g L^{-1}) in the culture solution to maintain the optimum glucose uptake rate for B. braunii in single stage two phase fed batch cultivation. The higher lipid productivity (i.e. 1.32 g L^{-1} d^{-1}) in single stage two phase fed batch cultivation indicates that lipid biosynthesis was the major activity for B. braunii in the second phase of single stage fed batch cultivation process.

Table 7.2. Comparison of different parameters obtained under single stage single phase and single stage two phase respectively. (*BP (Biomass Productivity), *LP (Lipid Productivity).

Parameters	Single Stage Single Phase Fed Batch	Single Stage Two Phase Fed Batch
X_{max} (g L^{-1})	3.14	7.9
P_{max} (g L^{-1})	1.04	4.04
*BP (g L^{-1} d^{-1})	0.495	2.07
*LP (g L^{-1} d^{-1})	0.149	1.32
Lipid Content (%)	33.12	51.13

Table 7.3. Comparison of mixotrophic lipid productivity using *B. braunii* with the literature reported values

Trophic condition	Lipid productivity (g L^{-1}day^{-1})	Cultivation mode	Data	Reference
Mixotrophic	0.0645	Batch	Provided	Yeesang et al., 2014
Heterotrophy	0.118	Semi-continuous	Provided	Yeesang et al., 2014
Phototrophy	0.271	Batch	Calculated	Ozkan et al., 2012
Photoautotrophy	0.09	Fed-batch	Calculated	Ling Xu et al., 2012
wastewater	0.082	Batch	Provided	Rafael Órpez et al., 2009
Mixotrophic	1.326	Fed Batch	Calculated	Present studies

After 128 h, the biomass and lipid concentration reached to stationary phase. It must be noteworthy, that concentration of glucose in the culture solution was above 15 g L^{-1}, the reason to maintain the higher level of glucose concentration in the culture solution was to ensure that carbon source could not be the limiting factor for the further biomass enhancement.

The final biomass concentration of 7.9 g L^{-1}, and lipid content of 51.13% were obtained for B. braunii in this study. The results produced in this study are similar to the earlier reported values (Table 7.3). As shown in the Table 7.3 the obtained results for B. braunii was comparatively higher from the previous studies (Table 7.4). That is, the present study shown 2.52 fold and 3.42 fold increase in the biomass concentration compared to the single stage single phase fed batch and mixotrophic batch cultivation. This suggests that, in comparison to the single stage single phase fed batch and mixotrophic batch experiment the single stage- two phase fed-batches with the intermittent feeding of the limiting nutrients nitrate, glucose and TME has resulted in 60.25% and 32.53% increase in maximum biomass concentration.

7.3.5 . Conclusion

In this study, both mixotrophic batch and fed batch cultivation strategies could yield high biomass concentration and productivities. The lower lipid content in mixotrophic batch and single stage single phase phototrophic fed batch culture conditions suggest the requirement of an alternative strategy. Thus, single-stage two phase fed-batch mixotrophic cultivation was applied to obtain lipid-enriched high biomass that eventually produced higher biomass titer (7.9 g L^{-1}) with lipid content and lipid productivity of 51.13% (w/w DCW) and 1.32 g L^{-1} day^{-1} respectively.

7.3.6. References

APHA, Standard methods for the examination of water and wastewater 14ed. APHA American Public Health Association (1976).

Brennan L., Owende P., 2010. Biofuels from microalgae—A review of technologies for production, processing, and extractions of biofuels and co-products. Renew. Sustain. Energy Rev., 14(2), 557–577.

Byreddy, A.R., Gupta, A., Barrow, C.J., Puri M. 2016. A quick colorimetric method for total lipid quantification in microalgae. J. Microbiol. Methods. 125, 28–32.

Cheng, Y.S., Zheng, Y., VanderGheynst, J., 2011. Rapid quantitative analysis of lipids using a colorimetric method in a microplate format. Lipids, 46, 95–103.

Chisti Y. 2007. Biodiesel from microalgae. Biotechnol Adv. 25, 294–306.

Karemore, A., Pal, R., Sen, R., 2013. Strategic enhancement of algal biomass and lipid in *Chlorococcum infusionum* as bioenergy feedstock. Algal Res. 2 (2), 113–121.

Kong, W.B., Yang, H., Cao, Y.T., Song, H., Hua, S.F., Xia, C.G., 2013. Effect of glycerol and glucose on the enhancement of biomass, lipid and soluble carbohydrate production by *Chlorella vulgaris* in mixotrophic culture. Food Technol. Biotechnol. 51 (1), 62–69.

Kumar, V., Muthuraj, M., Palabhanvi, B., Ghoshal, A.K., Das, D., 2014. High cell density lipid rich cultivation of a novel microalgal isolate *Chlorella sorokiniana* FC6 IITG in a single-stage fed-batch mode under mixotrophic condition. Bioresour. Technol. 170, 115–124.

Lin, J.T., Shen, H.W., Tan, H.D., Zhao, X., Wu, S.G., Hu, C.M., Zhao, Z.B.K., 2011. Lipid production by Lipomyces starkeyi cells in glucose solution without auxiliary nutrients. J. Biotechnol. 152, 184–188.

Liu, Z.Y., Wang, G.C., Zhou, B.C., 2008. Effect of iron on growth and lipid accumulation in *Chlorella vulgaris*. Bioresour. Technol. 99, 4717– 4722.

Morales-Sánchez D, Tinoco-Valencia R, Kyndt J and Martinez A, Heterotrophic growth of *Neochloris oleoabundans* using glucose as a carbon source. Biotechnol. Biofuels 2013,6,1.

Muthuraj, M., Kumar, V., Palabhanvi, B., Das, D., 2014. Evaluation of indigenous microalgal isolate *Chlorella* sp. FC2 IITG as a cell factory for biodiesel production and scale up in outdoor conditions. J. Ind. Microbiol. Biotechnol. 41, 499–511

Ogbonna J.C., Yada H., Tanaka H., 1995. Light supply coefficient: a new engineering parameter for photobioreactor design, J. Ferment. Bioeng. 80, 369-376.

Orpez R., Martinez M.E., Hodaifa G., El Yousfi F., Jbari N., Sanchez S., 2009. Growth of the microalga *Botryococcus braunii* in secondarily treated sewage. Desalination. 246, 625–630.

Ozkan A., Kinney K., Katz L., Berberoglu H., 2012. Reduction of water and energy requirement of algae cultivation using an algae biofilm photobioreactor. Bioresour. Technol. 114, 542–548.

Palabhanvi B., Muthuraj M., Mukherjee M., Kumar V., Das D., 2016. Process engineering strategy for high cell density-lipid rich cultivation of *Chlorella* sp.FC2 IITG via model guided feeding recipe and substrate driven pH control. Algal Res. 16, 317–329.

Qiao, H., Wang, G., 2009. Effect of carbon sources on growth and lipid accumulation in *Chlorella sorokiniana* GXNN01. Chin. J. Oceanol. Limnol. 27, 762–768.

Scott S.A., Davey M.P., Dennis J.S., Horst I., Howe C.J., Lea-Smith D.J., Smith A., 2010. Biodiesel from algae: challenges and prospects. Curr. Opin. Biotechnol. 21, 277–86.

Sun, Y., Liu, J., Xie, T., Xiong, X., Liu, W., Liang, B., Zhang, Y., 2014. Enhanced lipid accumulation by *Chlorella vulgaris* in a two-stage fed-batch culture with glycerol. Energy Fuels 28 (5), 3172–3177.

Xia, L., Rong, J., Yang, H., He, Q., Zhang, D., Hu, C., 2014. NaCl as an effective inducer for lipid accumulation in freshwater microalgae *Desmodesmus abundans*. Bioresour. Technol. 161, 402–409.

Xie, T., Sun, Y., Du, K., Liang, B., Cheng, R., Zhang, Y., 2012. Optimization of heterotrophic cultivation of *Chlorella* sp. for oil production. Bioresour. Technol. 118, 235–242.

Xu L., Wang F., Guo C., Liu C.-Z., 2012. Improved algal oil production from *Botryococcus braunii* by feeding nitrate and phosphate in an airlift bioreactor. Eng. Life Sci. 12, 171–177.

Yeesang C., Cheirsilp B. 2014. Low-cost production of green microalga *Botryococcus braunii* biomass with high lipid content through mixotrophic and photoautotrophic cultivation. Appl Biochem Biotechnol. 174, 116–12

Chapter 8

Photosynthetic Characterization of Flat Panel Photobioreactor using Dynamic Light Response Curve to Determine the Effective Cultivation Parameters for *Botryococcus braunii* Growth and Lipid production

8.1. Introduction

Microalgae are extensive source for CO_2 sequestration and renewable bioenergy; and their biofixation efficiency is higher than terrestrial plants (Cuellar-Bermudez et al., 2015). An efficient photosystem requires balance growth conditions to minimize the adverse effect caused by light energy, temperature, light quality and aeration (Gargano et al., 2015; Jeon et al., 2005; Jodłowska & Śliwińska, 2014; Serôdio et al., 2012). Microalgae mass cultivation limited by light, aeration, temperature and light quality. The photosynthetic activity of microalgae is strongly reduced under stress conditions (Benvenuti et al., 2015).

Photosynthetic activity (PA) of microalgae can be determined by oxygen production rates inside the photobioreactor (Brindley et al., 2010). PA of microalgae is an effective parameter for the developing the kinetic expression for specific oxygen production rate and photosynthetic efficiency (PE) inside the photobioreactor (Costache et al., 2013).

Photosynthesis–irradiance curves determine the performance of the photosynthetic apparatus as a function of luminous intensity using O_2 or CO_2 gas exchange measurements. P-I curve have three different regions: the light limited, the light saturated and photoinhibited region (Ralph & Gademann, 2005; Schreiber et al., 1997). Photosynthetic efficiency (PE) can be expressed as quantum yield of oxygen evolution (i.e., mole of oxygen produced per mole of PAR photons absorbed). Effective quantum yield in light limited region is defined as α ((maximum light capture efficiency) (nmol O_2 μmol_{ph}^{-1} g^{-1} m^2)) and light saturation coefficient (Ek) calculated by finding the interception of α with the maximum photosynthetic rate (Sakshaug et al., 1997). The P-I curve optimized the maximum light utilization efficiency (α) and Light saturation coefficient (Ek) under different culturing conditions.

Hence PA and PE can become effective parameters for pursuing maximum photosynthetic productivity inside the photobioreactor. PA and PE of microalgae significantly altered at

inadequate temperature, aeration and light wavelength. It was assumed that cultural conditions which are maximizing the PA and PE of microalgae in photobioreactor will also favorable for maximizing the biomass productivity of microalgae inside the photobioreactor. Temperature, light quality and aeration rate inside the photobioreactor significantly affect the process productivity. These photosynthetic parameters can be characterized by the P-I curve and PA activity of *Botrycoccus braunii* in Flat panel photobioreactor.

The optimum temperature range for effective growth is in the range of 20 °C to 30 °C for different algae species (Singh & Singh, 2015). Microalgae growth rate can be alter by temperature fluctuations and the seasonal temperature variations reduce the photosynthetic efficiency. To counter the effect the high temperature stress microalgae deploy energy re-balancing and cell shrinkage strategies (Ras et al., 2013).

Light quality is also a key factor for controlling the growth and polysaccharide production(You & Barnett, 2004). Moreover, previous studies suggest that the red light is more effectively utilized for photosynthetic activity than green light; probably microalgae have wavelength-specific pigment for light harvesting (Jeon et al., 2005). A chromatic spectrum of different light is usually used to enhance growth and product formation. Red light is considered as the optimal light wavelength for microalgae growth, biogas upgrading, and digestate nutrient reduction (Zhao et al., 2013). Light wavelength, intensity and the interaction between light wavelength and intensity significantly affected biomass growth rate and nutrient removal efficiency of microalgae (Yan & Zheng, 2013). Efficient light transfer was the most important parameters in optimizing the mass culture of the photosynthetic organism.

The influence of mixing rate on productivity and photosynthetic efficiency significantly increased as algal concentration is increased. At very high mixing rate cell damage and reduction in product rate was observed (Qiang & Richmond, 1996). Aeration rate enhanced specific growth rate and gamma-linolenic acid (GLA) in spirulina (Ronda et al., 2012). It has been suggested that optimal aeration rate also enhanced microalgae growth.

The aim of this study was to measure the PE and PA of *B. braunii* on photosynthetic parameters (i.e. temperature, light quality and aeration rate) in photobioreactor. Based on PE and PA the most effective and optimum operating cultural conditions were selected to grow microalgae in flat panel photobioreactor in further experiments. The significance of study suggested that PE and PA can be used as effective tool to determine the effective cultivation parameter for the growth of the microalgae in flat panel photobioreactor using oxygen measurements only.

8.2. Material and methods

8.2.1. Microalgae and culture medium

A culture of *B. braunii* was obtained from the Institute of Bioresources and Sustainable Development (IBSD, Takyelpat, Imphal). The microalgae were grown in modified BG-11 medium containing macronutrients such as $NaNO_3$ (1.12 g), $MgSO_4.7H_2O$ (75 mg), K_2HPO_4. $3H_2O$ (40 mg), $CaCl_2.2H_2O$ (36 mg), Na_2CO_3 (20 mg), EDTA, 2Na-Mg salt (1 mg), citric acid (6 mg), ferric ammonium citrate (6 mg) and micronutrients such as H_3BO_3 (286 µg), $MnCl_2.4H_2O$ (181 µg), $ZnSO_4.7H_2O$ (22 µg), $Na_2MoO_4.2H_2O$ (39 µg), $CuSO_4.5H_2O$ (8 µg) and $Co(NO_3)_2.6H_2O$ (5 µg) per liter. The inoculated medium was incubated at 27 ± 1 °C and 130 rpm in a light incubator shaker. The initial pH of the medium was maintained at 8.

8.2.2. The photobioreactor and experimental design

The flat panel photobioreactor (Model, PSI Photon System Instruments (PSI, Brno, Czech Republic) was used for the experimental studies. The dimensions of the reactor were (0.75 m × 0.59 m × 0.068 m). For maintaining air flow a porous sparger was used. The temperature and pH of the system were precisely controlled (Fig. 1). The reactor was illuminated by high-power light emitting diodes (LEDs) placed at one side of the reactor. The irradiance could be dynamically modulated by the instrument control unit. The reactor was illuminated by light intensity from the range of (100-to 2000) µmol m^{-2} s^{-1} by LED Panel placed at one side of the reactor.

B. braunii were grown in 30 liter photobioreactor filled with BG-11 nutrient media. Photobioreactor was exposed to 150 µ mol m^{-2} s^{-1} light intensity, and once the growth of the *B. braunii* reached to the extent of the exponential phase (i.e. early stationary phase), the batch mode operation of the reactor was shifted to the turbidostat mode of operation (i.e. turbidity was maintained constant) to study the dynamic response curve under different operating conditions (i.e. temperature, aeration, light quality). The P-I curve was implied to maximize the photosynthetic efficiency of *B. braunii* at different parameters in the reactor.

8.2.3. Oxygen Concentration Measurement

The oxygen concentration in liquid medium was calculated according to hennery law constant.

$$H = \frac{C_a}{p}$$

Here H is hennery constant and this constant depends upon the temperature, C_a is concentration of oxygen, p is partial pressure of oxygen.

$$H(T) = H^{\Theta} \times \exp\left(\frac{-\Delta_{sol}\, H}{R}\left(\frac{1}{T} - \frac{1}{T^{\theta}}\right)\right) \quad \text{(E8.1)}$$

H^{Θ} = 1.2 x 10^{-5} mol/m^3 pa (Sander, 2015; Warneck & Williams, 2012) T^{θ}= 298.15K, $\frac{-\Delta_{sol}\, H}{R}$ = 1700 K.

8.2.4. Photosynthetic- irradiance curve

The effect of photosynthetic parameters on photosynthetic oxygen production are best described by Photosynthetic irradiance curve (P-I curve) (Jassby & Platt, 1976; Vejrazka et al., 2013). Initial slope of P-I curve defined as photosynthetic efficiency and maximum oxygen evolution rate.

$$P_{O_2,n} = \left(\left(P_{O_2,n}^{max} + R_{ms}\right)\right).\tanh\left(\frac{\alpha.PFD}{P_{O_2,n}^{max} + R_{ms}}\right) - R_{ms} \quad \text{(E8.2)}$$

$P_{O_2,n}$ is the rate of oxygen production (nmol g^{-1} min^{-1}), $P_{O_2,n}^{max}$ maximum rate of photosynthetic oxygen evolution (nmol g^{-1} min^{-1}). R_{ms} is maintenance respiration rate (nmol g^{-1} min^{-1}) , α is effective light utilization coefficieint (nmol O_2 μmol_{ph}^{-1} g^{-1} m^2), PFD is photosynthetic active radiation (µmol/m^2/sec).

8.2.5. Maintenance respiration rate

Maintenance respiration rate of microalgae can be calculated with equation (2) by plotting the B. braunii respiration rate in dark and oxygen evolution during light time.

$$R = R_{ms} + c_R \,.\, P_{O_{2,n}} \quad \text{(E8.3)}$$

R (nmol g^{-1} min^{-1}) is respiration rate of *B. braunii* during dark period, c_R is growth associated respiration coefficient.

8.2.6. Gross oxygen production

Gross oxygen production rate can be calculated by following equation

$$P_{O_{2,g}} = R + P_{O_{2,n}} \quad \text{(E8.4)}$$

$P_{O_{2,g}}$ is defined as gross oxygen production rate (nmol g^{-1} min^{-1}).

8.2.9. Photosynthetic activity

Photosynthetic activity of B braunii was calculated by taking the initial slope of O_2 v/s time graph and divided by the cell concentration.

$$\text{PA} = r_{O_2} = \frac{1}{C_b}\frac{dC_{O_2}}{dt} \qquad \text{(E8.5)}$$

PA is photosynthetic activity (mg O2 g^{-1}biomass h^{-1}), C_{O_2} is O_2 concentration in liquid phase (mg/L). where N_2 and N_1were the biomass concentration at days $t_2$and t_1 respectively. Net specific growth rate was taken in exponential phase.

8.3. Results and discussion

8.3.1. Effect of Aeration on PI curve and photosynthetic activity

B. braunii was cultured in modified BG–11 enriched nutrient medium in which $NaNO_3$ was sol nitrogen source in flat panel photobioreactor. Microalgae culture was incubated for 4-5 days before running light curve experiments. To evaluate the effect of different cultivation parameter on photosynthetic efficiency; photosynthetic response curve were generated. PI curve were measured under continuous illumination with varying light intensity from (100 to 2000 µmol $m^{-2}sec^{-1}$) and steady state was maintained by operating the reactor in turbidostat cultivation module. Dissolved oxygen was measured for each response and correlates each light curve to each culture conditions. Two main parameters PA and quantum efficiency (α) were chosen for optimal photosynthetic cultivation parameters.

Photosynthetic activity of *B.braunii* was measured at different light intensities with different aeration rate (1 LPM to 10 LPM) as presented in Fig (8.1). Photosynthetic oxygen evolution was increased initially with increase in light intensity and inhibited above 1200 µmol $m^{-2}sec^{-1}$. PA and α were significantly affected by the aeration rate inside the phtobioreactor. Maximum PA and effective quantum efficiency (α) were found to be 7.72 nmol O_2 g^{-1} min^{-1} and 0.0034 ±.00042 nmol O_2 μmol_{ph}^{-1} g^{-1} m^2 respectively at 10 LPM aeration rates. The highest value of maximum photosynthetic oxygen (i.e. $PO_{2,\,max}$) evolution was 74.38 ± 2.85 nmol g^{-1} min^{-1} also achieved at 10 LPM aeration. Model parameters were estimated by fitting the experimental values in equation 1, and are summarized in table (2). Our observation suggests that values of PA and PE increased with increase in air flow rate. At lowest air flow rate of 1 LPM the minimum value of PA 5.12 nmol O_2

g^{-1} min^{-1} was observed, and 5 fold and 10 fold increase in air flow rate increased the PA up to 24.59% and 33.68% respectively.

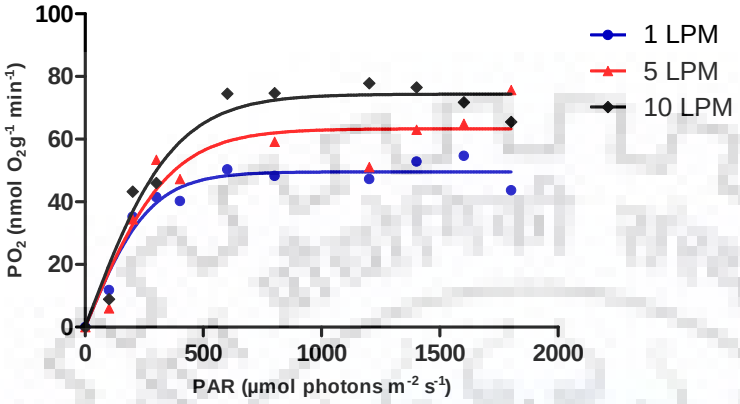

Fig.8.1. P-I curve of *B.braunii* under different aeration rate in flat panel photobioreactor.

Similarly at low aeration rate no significant effect on α and the values of 0.0030 and 0.0029 nmol O_2 μmol_{ph}^{-1} g^{-1} m^2 observed at 1 LPM and 5 LPM respectively (Table 8.1). Whilst at maximum flow rate of 10 LPM the maximum value of PA and α were 7.72 nmol O_2 g^{-1} min^{-1} and 0.0034 nmol O_2 μmol_{ph}^{-1} g^{-1} m^2 obtained respectively.

Table 8.1. Simulated values of P_{max} nmol g^{-1} min^{-1}, α (nmol O_2 μmol_{ph}^{-1} g^{-1} m^2 x 10^{-2}) and PA (nmol O_2 g^{-1} min^{-1}) of P-I curve under different aeration rate with their R^2 values in flat panel photobioreactor.

Aeration (LPM)	P_{max} (nmol O_2 g^{-1} min^{-1})	α (nmol O_2 μmol_{ph}^{-1} g^{-1} m^2)x 10^{-2}	PA (nmol O_2 g^{-1} min^{-1})	R^2
1	49.57±1.733	0.3016±.035	5.12	0.95
5	63.32±3.855	0.299±.053	6.78	0.90
10	74.38±2.86	0.3350±.042	7.72	0.96

This study suggests that effective flow rate increases the mixing efficiency of nutrients inside the photobioreactor which allows microalgal cells to effectively utilize the light energy or growth medium for higher photosynthetic efficiencies. The effect of aeration rate on the microalgae growth rate was previously reported and show that the increase in aeration rate from 0.2 to 2.5 *vvm* significantly enhanced the specific growth rate of *Spirulina plantesis* in bubble column reactor (Ronda et al., 2012). Similarly in the light limited range of PAR of 300 µE m^{-2} s^{-1}, specific

growth rate of red microalga *Porphyridium Sp* increasd from 0.012 to 0.022 h^{-1}, when the air flow rate in the bubble column reactor was increased from 1 ml min^{-1} to 5 ml min^{-1} respectively (Merchuk et al., 1998).

Table 8.2. Simulated values of P_{max} nmol g^{-1} min^{-1}, α (nmol O_2 μmol_{ph}^{-1} g^{-1} m^2 x 10^{-2}) and PA (nmol O_2 g^{-1} min^{-1}) of P-I curve under different Temperature region with their R^2 values in flat panel photobioreactor

Temperature (ºC)	P_{max} (nmol O_2 g^{-1} min^{-1})	α (nmol O_2 μmol_{ph}^{-1} g^{-1} m^2)x 10^{-2}	PA (nmol O_2 g^{-1} min^{-1})	R^2
17	91.64±3.084	0.2257±.036	5.79	0.89
22	93.36± 2.97	0.2763± 0.049	6.19	0.93
27	75.26±3.97	0.3898±.063	7.72	0.91
33	91.02±4.18	0.2546±.053	5.94	0.85

Table 8.3. Simulated values of P_{max} nmol g^{-1} min^{-1}, α (nmol O_2 μmol_{ph}^{-1} g^{-1} m^2 x 10^{-2}) and PA (nmol O_2 g^{-1} min^{-1}) of P-I curve under different light wavelength regions with their R^2 values in flat panel photobioreactor.

Wavelength	P_{max} (nmol O_2 g^{-1} min^{-1})	α (nmol O_2 μmol_{ph}^{-1} g^{-1} m^2)x 10^{-2}	PA (nmol O_2 g^{-1} min^{-1})	R^2
Red Light	80.08±7.06	0.2487±.023	5.70	0.97
White Light	76.90±9.31	0.2406±.03	5.18	0.94
Red & White	80.48±7.3	0.3728±.061	7.72	0.92

8.3.2. Effect of Temperature on PI curve and photosynthetic activity

The effect of temperatures on Photosynthetic activity of *B.braunii* was observed at different light intensities with temperature range of (17 ºC to 32 ºC) Fig (8.2). PA and quantum efficiency (α) initially increased with increase in temperature in the range of 27 ºC, and further increase in temperature (i.e. at 33 ºC) both of these values decreased. Maximum PA and maximum quantum efficiency were 7.72 nmol O_2 g^{-1} min^{-1} and 0.0038 ± 0.00063 nmol O_2 μmol_{ph}^{-1} g^{-1} m^2 observed at 27 ºC (Table 2). The values of PA and α were decreased at inadequate temperatures. At 17 ºC, 22 ºC, 32 ºC, the values of PA and α were 5.79 nmol O_2 g^{-1} min^{-1} and 0.0023 ± .00036 nmol O_2 μmol_{ph}^{-1} g^{-1} m^2, 6.19 nmol O_2 g^{-1} min^{-1} and 0.002763± .00049, 5.94 nmol O_2 g^{-1} min^{-1} and 0.0025± .00053 nmol O_2 μmol_{ph}^{-1} g^{-1} m^2 were observed respectively (Table 8.2).

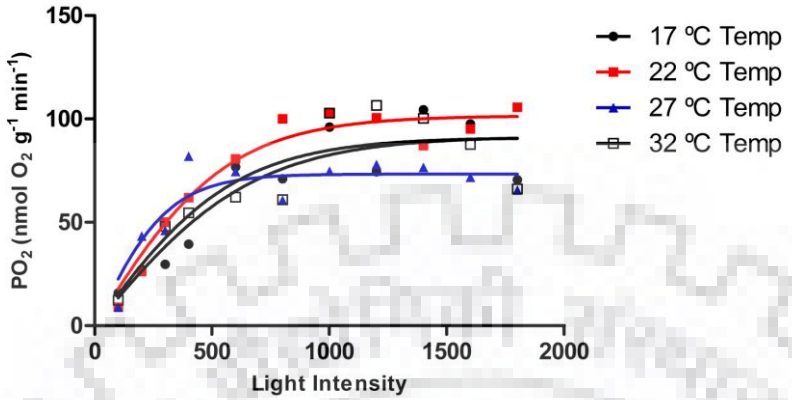

Fig.8.2. P-I curve of *B.braunii* under different temperatures in flat panel photobioreactor.

As shown in the Table 8.2, the effective quantum yield of *B. braunii* was reduced at high temperature. In addition, the lower quantum yield at high temperature was a result of poor efficiency in the use of separated charge at the photosystem II reaction center (Jursinic & Pearcy, 1988). Particularly high temperatures and high irradiance decreased the PA of microalgae due to photoinhibition which eventually inactivates metabolic enzymes of the microalgae (Cabello et al., 2015). In case of *B. braunii*, initially the PA was increased linearly with increase in irradiance in the range of 100–400 µmol m^{-2} s^{-1} at all temperatures. Above this range, photoinhibition was observed at (1000-1500 µmol m^{-2} s^{-1}). The previous study suggests that *B. braunii* strain Showa can not grow at 5 °C and above 35 °C under any irradiance levels (Yoshimura et al., 2013) whilst at supraoptimal temperature of (32˚C) considerable inhibition in the synthesis of nearly all intracellular lipids was observed (Kalacheva et al., 2002). These results are in accordance with our results as we have achieved the maximum PA and α at 27˚C optimum temperature.

8.3.3. Development of Thermodynamic Model for *B.braunii*

Oxygen evolution during photosynthesis is highly influenced by light intensity and temperature. Light energy conversion from CO_2 to sugar and O_2 is critical step of the photosynthesis. The effects of varying temperature treatment on the oxygen yield and the rate constant of the light reaction for *B. braunii* have been investigated.

It is assumed that rate of change of oxygen evolution directly proportional to oxygen concentration and it follows the first order kinetics. The corresponding rate equation can be expressed as

$\frac{dC}{dt} = KC$ -(E8.6)

$k = \frac{\ln(\frac{C_2}{C_1})}{t_2 - t_1}$ (E8.7)

C_2= oxygen concentration at time t_2

C_1= oxygen concentration at time t_1

K= rate constant of light reaction

According to Arrhenius rate constant of any reaction will be function of temperature. So the rate constant can also be expressed as

$k = Ae^{(-\frac{E}{RT})}$ (E8.8)

Plot between ln k and 1/T were used to measure the frequency factor (A) and activation energy (E). Activation energy calculated from Arrhenius plot were used to measure the enthalpy of the reaction.

$\Delta H = E - RT$ (E8.9)

where ΔH is enthalpy of activation

The photosynthetic efficiency and PA of the process depends on temperature and evolved photosynthetic O_2 concentration. The rate constant of the reaction depends upon the temperature. Enthalpy of the activation decreased with increase in temperature whilst the negative values of enthalpies indicate the reaction is exothermic in nature (Table 8.4).

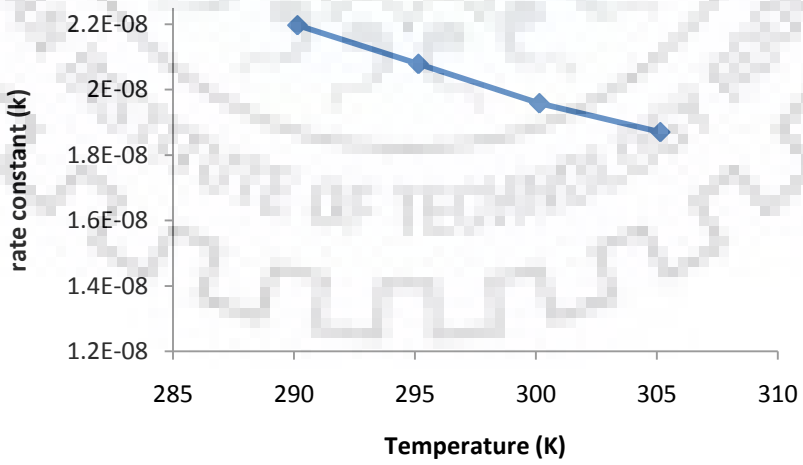

Fig.8.3. Photosynthetic O_2 evolution rate constant vs temperature curve.

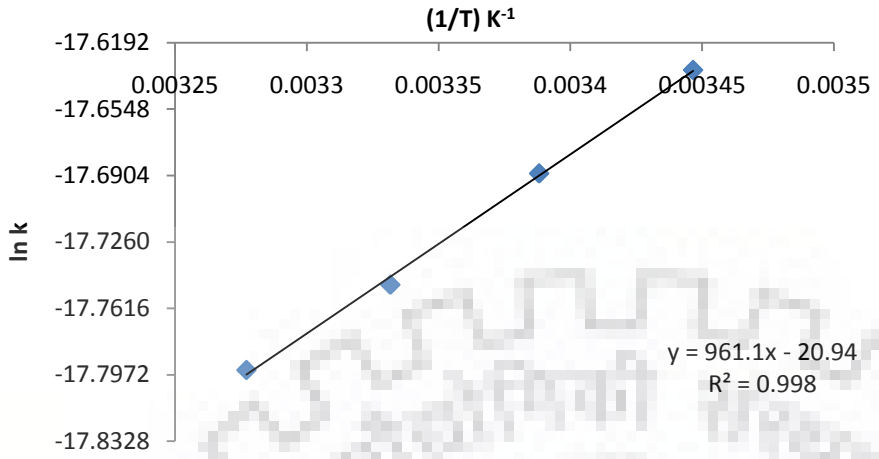

Fig.8.4. ln(k) vs (1/T) curve

Rate constant of the reaction and enthalpy of activation were used to measure the entropies of the activation and calculated by Eyring equation.

$$e^{\Delta S/R} = \frac{h}{K_b T}\left(ke^{\left(\frac{\Delta H}{RT}\right)}\right) \quad \text{(E8.10)}$$

where ΔS are entropy of activation and k is reaction rate constant.

The values of entropy of the reaction decreased with increase in temperature (Table 8.4). This suggests the stability of the process increased with the rise in temperature. The Gibbs free energy (ΔG) for photosynthetic O_2 evolution is obtained by using equation:

$$\Delta G = \Delta H - T\Delta S \quad \text{(E8.11)}$$

The Gibbs free energy of the system under different temperatures condition was calculated and the values are given in Table (8.4). The positive values of Gibbs free energy suggest the photosynthetic O_2 evolution reaction will be non- spontaneous in nature.

Table 8.4. Thermodynamic parameters of photosynthetic Oxygen evolution of Botrycoccus braunii under different temperature regions

Temperature	Activation energy (KJ/mol)	RT (J/mol)	ΔH (KJ/mol)	ΔS (KJ/K/mol)	ΔG (KJ/mol)
290.15	-13.88438	2445.563	-16.3299431	-0.4255	108.8313
295.15	-13.88438	2470.505	-16.3548851	-0.42605	110.2448
300.15	-13.88438	2495.447	-16.3798271	-0.42663	111.672
305.15	-13.88438	2545.331	-16.4297111	-0.42768	114.5032

The values of ΔG increased with rise in temperature. It was observed from the experimental results that at 17ºC temperature the lowest values of ΔG, PA and α were 108.8313 kJ mol^{-1}, 5.79 nmol O_2 g^{-1} min^{-1} 0.0023 nmol O_2 μmol_{ph}^{-1} g^{-1} m^2 observed respectively. Further, when the process was operated at 22 ºC, there was 1.28% rise in the Gibbs free energy was observed at this temperature which leads to only 6.4% and 18.31% increase in PA and α respectively, from the lowest reported value. Whilst at 27 ºC, further 1.28% increment in the Gibbs free energy resulted in 25% and 42.10% increase in the values of PA and α was observed respectively, from the lowest reported value. Remarkably, at 32ºC the value of ΔG was found maximum 114.50 kJ mol^{-1} and the PA and α decreased significantly. This study suggests that the process is not thermodynamically efficient at 32ºC temperature. So it can be evaluated from the study that 27 º C temperatures is the optimum process temperature for maximum PA and photosynthetic efficiency.

8.3.4 Effect of light wavelength on photosynthetic activity

To evaluate the effect of different wavelength on PA and PE three different light sources were used (actinic red, white and R&W combination) for photosynthetic O_2 evolution. The effect of light source was observed in Fig (8.3); if the single light source is used; the red light was more effectively utilized photons and have higher value of α 0.0025 ± 0.00023 nmol O_2 μmol_{ph}^{-1} g^{-1} m^2 than white light which has value of 0.0024 ±0.00031 nmol O_2 μmol_{ph}^{-1} g^{-1} m^2. But when equal combination of red and white light was used it shows maximum value of α and PA 0.0037 ± 0.00064 nmol O_2 μmol_{ph}^{-1} g^{-1} m^2 and 7.72 nmol O_2 g^{-1} min^{-1} respectively.

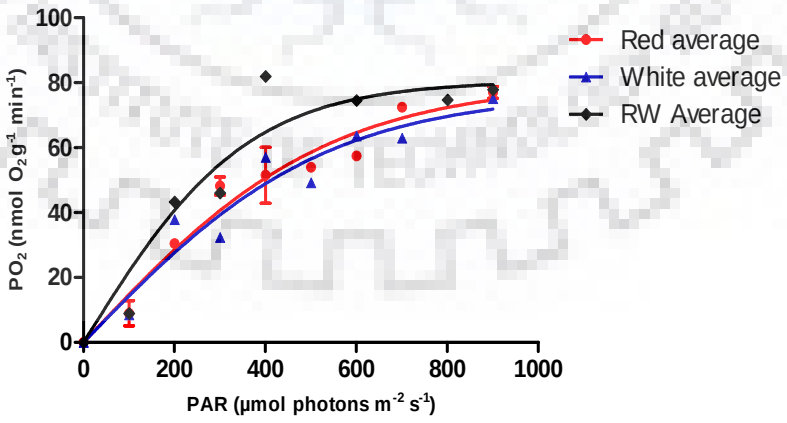

Fig.8.3. P-I curve of *B.braunii* under different light wavelength in flat panel photobioreactor.

The $PO_{2,\ max}$ decreased at single specific wavelength than to be combined light wavelength. The maximum value of $PO_{2,\ max}$ was 80.48 nmol O_2 g^{-1} min^{-1} achieved at equal combination of Red and white light; whereas $PO_{2,\ max}$ decreased at single wavelength and values of 76.90 and 80.08 nmol O_2 g^{-1} min^{-1} were observed at single white and red wavelength respectively (Table 8.3). This was probably due to the wavelength specific major pigment of *B braunii* which absorbs red light more efficiently over white light and the equal combination of each light enhanced the efficiency of light utilization over single specific light.

The higher photosynthetic efficiency achieved at red LEDs over the single white light LED because chlorophyll absorption peak of microalgae perfectly fit with red wavelengths (Darko et al., 2014; Schoefs, 2002). The combination of white and red provide better excitation of the different types of photoreceptors, which allowed the higher photosynthetic activity than that under either monochromatic light (Sabzalian et al., 2014). These results are in accordance with our study which showed the higher photosynthetic activity in red+white (7.72 nmol O_2 g^{-1} min^{-1}) combination over the single specific red (5.70 nmol O_2 g^{-1} min^{-1}) or white (5.18 nmol O_2 g^{-1} min^{-1}) monochromatic light wavelength.

8.4. Conclusion

B. braunii growth is significantly affected by the cultural conditions (i.e. aeration, temperature and light wavelength) inside the photobioreactor. The Photosynthetic response curve experiments were performed to study the effect of photosynthetic parameters on the rate of photosynthesis, PE and PA. In aeration/temperature/wavelength limited cultivation of Botrycoccus braunii in flat panel PBR the maximum PA and PE were 7.72 nmol O_2 g^{-1} min^{-1} and 0.0038 nmol O_2 μmol_{ph}^{-1} g^{-1} m^2, were obtained at 10LPM, 27 ºC and RW combination. This study suggests that the temperature, light wavelength and aeration rate affects the light utilization capacity of microalgae which alters the photosynthetic yield of the microalgae. In addition, this study also suggests that photosynthetic irradiance based model can be used to determine the effective cultivation parameters of the microalgae in photobioreactor.

8.5.References:

Benvenuti G., Bosma R., Cuaresma M., Janssen M., Barbosa M.J., WijffelsR.H., 2015. Selecting microalgae with high lipid productivity and photosynthetic activity under nitrogen starvation. J. Appl. Phycol., 27, 1425-1431.

Brindley C., Acién F.G., Fernández-Sevilla J.M., 2010. The oxygen evolution methodology affects photosynthetic rate measurements of microalgae in well-defined light regimes. Biotechnol. Bioeng. 106(2), 228-237.

Cabello J., Toledo-Cervantes A., Sánchez L., Revah S., Morales M., 2015. Effect of the temperature, pH and irradiance on the photosynthetic activity by *Scenedesmus obtusiusculus* under nitrogen replete and deplete conditions. Bioresour. Technol. 181, 128-135.

Costache T., Fernández F.G.A., Morales M., Fernández-Sevilla J., Stamatin, I., Molina E., 2013. Comprehensive model of microalgae photosynthesis rate as a function of culture conditions in photobioreactors. App. Microbiol. Biotechnol. 97(17), 7627-7637.

Cuellar-Bermudez S.P., Garcia-Perez J.S., Rittmann B.E., Parra-Saldivar R., 2015. Photosynthetic bioenergy utilizing CO_2: an approach on flue gases utilization for third generation biofuels. J. Cleaner Prod. 98, 53-65.

Darko E., Heydarizadeh P., Schoefs B., Sabzalian M.R., 2014. Photosynthesis under artificial light: the shift in primary and secondary metabolism. Phil. Trans. R. Soc. B. 369 (1640), 20130243.

Gargano I., Olivieri G., Spasiano D., Andreozzi R., Pollio A., Marotta R., D'Ambrosio N., Marzocchella A., 2015. Kinetic characterization of the photosynthetic reaction centres in microalgae by means of fluorescence methodology. J. Biotechnol. 212, 1-10.

Jassby A.D., Platt T., 1976. Mathematical formulation of the relationship between photosynthesis and light for phytoplankton. Limnol. Oceanography. 21(4), 540-547.

Jeon Y.-C., Cho C.-W., Yun Y.-S., 2005. Measurement of microalgal photosynthetic activity depending on light intensity and quality. Biochem.Eng. J. 27(2), 127-131.

Jodłowska S., Śliwińska S., 2014. Effects of light intensity and temperature on the photosynthetic irradiance response curves and chlorophyll fluorescence in three picocyanobacterial strains of *Synechococcus*. Photosynthetica. 52(2), 223-232.

Jursinic P.A., Pearcy R.W., 1988. Determination of the rate limiting step for photosynthesis in a nearly isonuclear rapeseed (Brassica napus L.) biotype resistant to atrazine. Plant Physiol. 88(4), 1195-1200.

Kalacheva, G., Zhila, N., Volova, T., Gladyshev, M. 2002. The effect of temperature on the lipid composition of the green alga *Botryococcus*. Microbiology. 71(3), 286-293.

Merchuk J., Ronen M., Giris S., Arad S., 1998. Light/dark cycles in the growth of the red microalga Porphyridium sp. Biotechnol.Bioeng. 59(6), 705-713.

Murphy T.E., Berberoglu H., 2014. Flux balancing of light and nutrients in a biofilm photobioreactor for maximizing photosynthetic productivity. Biotechnol. Prog. 30(2), 348-59.

Qiang H., Richmond A., 1996. Productivity and photosynthetic efficiency ofSpirulina platensis as affected by light intensity, algal density and rate of mixing in a flat plate photobioreactor. J. Appl. Phycol. 8(2), 139-145.

Ralph P.J., Gademann R., 2005. Rapid light curves: a powerful tool to assess photosynthetic activity. Aquatic Botany. 82(3), 222-237.

Ras M., Steyer J.-P., Bernard O., 2013. Temperature effect on microalgae: a crucial factor for outdoor production. Rev. Environ. Sci. Biotechnol. 12(2), 153-164.

Ronda S.R., Bokka C.S., Ketineni C., Rijal B., Allu P.R., 2012. Aeration effect on *Spirulina platensis* growth and γ-linolenic acid production. Brazilian J. Microbiol. 43(1), 12-20.

Sabzalian M.R., Heydarizadeh P., Zahedi M., Boroomand A., Agharokh M., Sahba M.R., Schoefs, B., 2014. High performance of vegetables, flowers, and medicinal plants in a red-blue LED incubator for indoor plant production. Agro. Sustain. Dev. 34(4), 879-886.

Sakshaug E., Bricaud A., Dandonneau Y., Falkowski P.G., Kiefer D.A., Legendre L., Morel, A., Parslow J., Takahashi M., 1997. Parameters of photosynthesis: definitions, theory and interpretation of results. J. Plankton Res. 19(11), 1637-1670.

Sander R., 2015. Compilation of Henry's law constants (version 4.0) for water as solvent. Atmospheric Chemistry Physics. 15(8).

Schoefs B., 2002. Chlorophyll and carotenoid analysis in food products. Properties of the pigments and methods of analysis. Trends Food Sci.Technol. 13(11), 361-371.

Schreiber U., Gademann R., Ralph P., Larkum A., 1997. Assessment of photosynthetic performance of Prochloron in *Lissoclinum patella* in hospite by chlorophyll fluorescence measurements. Plant Cell Physiol. 38(8), 945-951.

Serôdio J., Ezequiel J., Barnett A., Mouget J.-L., Méléder V., Laviale M., Lavaud, J., 2012. Efficiency of photoprotection in microphytobenthos: role of vertical migration and the xanthophyll cycle against photoinhibition. Aquatic Microbial Ecol. 67, 161-175.

Singh S., Singh P. 2015. Effect of temperature and light on the growth of algae species: a review. Renew. Sustain. Energy Rev. 50, 431-444.

Vejrazka C., Janssen M., Benvenuti G., Streefland M., Wijffels R.H., 2013. Photosynthetic efficiency and oxygen evolution of *Chlamydomonas reinhardtii* under continuous and flashing light. Appl. Microbiol.Biotechnol. 97(4), 1523-1532.

Warneck P., Williams J., 2012. The Atmospheric Chemist's Companion: Numerical Data for Use in the Atmospheric Sciences. Springer Science & Business Media.

Yan C., Zheng Z., 2013. Performance of photoperiod and light intensity on biogas upgrade and biogas effluent nutrient reduction by the microalgae *Chlorella* sp. Bioresour.Technol. 139, 292-299.

Yoshimura T., Okada S., Honda M., 2013. Culture of the hydrocarbon producing microalga Botryococcus braunii strain Showa: Optimal CO_2, salinity, temperature, and irradiance conditions. Bioresour. Technol. 133, 232-239.

You T., Barnett S.M., 2004. Effect of light quality on production of extracellular polysaccharides and growth rate of Porphyridium cruentum. Biochem. Eng. J. 19(3), 251-258.

Zhao Y., Wang J., Zhang H., Yan C., Zhang Y., 2013. Effects of various LED light wavelengths and intensities on microalgae-based simultaneous biogas upgrading and digestate nutrient reduction process. Bioresour. Technol. 136, 461-46.

Chapter 9

Mathematical Modeling of Light Energy Flux Balance in Flat Panel Photobioreactor for *Botryococcus braunii* Growth, CO_2 Biofixation and Lipid Production under Varying Light Regimes

9.1. Introduction

Microalgae cultivation in photobioreactor is gaining attention for scale-up of biomass and lipid productivity (Huerlimann et al., 2010). Microalgae growth in photobioreactor is affected by several photosynthetic parameters such as light intensity, air flow rate, temperature, and pH (Breuer et al., 2013; Bamba et al., 2015; Cabello et al., 2015). Among those, the light intensity is considered as the most significant parameter to determine the biomass composition, growth rate and product yield in photobioreactor (Fernandes et al., 2010; Zhao et al., 2013; Wang et al., 2015). The photobioreactor is an efficient technical device to process photosynthetic microalgae for biomass, photo-hydrogen or biofuel production (Brennan et al., 2010; Gajda et al., 2015). Photosynthetic engineering is nowadays recognized as a possible solution to the exhaustion of fossil resources and global warming because it enables CO_2 mitigation and sustainable energy production efficiently (Brennan et al., 2010; Dauchet et al., 2015).

Optimization of light availability to the microorganism in PBR is a crucial aspect of biomass production and process productivity (Kandilian et al., 2014). The microalgal growth is highly influenced by light intensity, duration, and the wavelength inside the PBR (Carvalho et al., 2010). Inadequate light supply reduces the microalgae growth while excessive light intensity causes photo-oxidative damage to PSII unit of microalgae (Murata et al., 2007; Carvalho et al., 2010; Kandilian et al., 2014). Optimum light penetration and supply inside the photobioreactor is the most challenging task (Kandilian et al., 2014). Therefore, it is necessary to predict accurate light distribution profile inside the photobioreactor for optimum process productivity.

The radiative transfer theory was originally developed by Chandrasekhar in astrophysics and the application of radiative transfer theory has been successfully applied to model effective light transfer in photobioreactors (Cornet et al., 1995).

Several authors applied radiative transfer model to different geometries of the photobioreactor to predict light attenuation profile. Pioneering work of light transfer model in rectangular photobioreactor was based on a monodimensional equation of Schuster (Cornet et al., 1992). In this light limited model, the radiative transfer equation (RTE) was coupled with photosynthetic kinetics to represent the light attenuation profile inside the photobioreactor as a function of photosynthetic parameters (Cornet et al., 1995). In comparison with the light limited model, Berberoglu et al. (2007) applied RTE in a bubble sparged photobioreactor containing gas bubble and suspension culture of *cynobacteria* and *anabaena*. They used Mie theory to estimate the scattering phase function of the gas bubble and microalgae to solve RTE (Berberoglu et al., 2007). An accurate prediction of radiative transfer model requires absorption, scattering coefficient, and scattering phase function of microalgae in photobioreactor (Lee et al., 2014). Optical properties (i.e. size and shape distribution) of microalgae and growth medium can be calculated using the Mie theory (Kong et al., 2014; Pottier et al., 2005). Light diffusion across the photobioreactor mainly depends on the absorption and scattering phenomena of microalgal cell (Csogor et al., 2001; Pruvost et al., 2006).

In recent years the classical radiative transfer equation was solved majorly by discrete ordinate method (DOM) and finite volume method (FVM). Both of these methods are widely applicable and require low computer and memory cost (Huang et al., 2012). The other method, e.g. Monte Carlo method which is based on probability theory and a random number generator, is used and solved the RTE using multiple scattering simulations. Whilst the diffusion method, which is based on the diffusion approximation (DA) and obtains analytical solutions of light propagation in the optically thick medium for several geometries (Limert et al., 2013). It is difficult to predict the light distribution in PBR accurately with polychromatic light due to the fact that the absorption coefficient and the scattering coefficient are both spectrally dependent.

In the present study, light energy flux balance across the flat panel photobioreactor was applied to develop the mathematical model as a function of light intensity and microalgal growth rate. The present model is based on the radiative transfer equation with varying light intensity in flat panel photobioreactor for effective utilization of light energy. The RTE equation was solved by the MATLAB bvp4c solver. The developed mathematical formulations could be used for investigating the light distribution profile inside a photobioreactor. Biomass, lipid and nitrate kinetics under varying light regimes were also investigated; which paved the path for developing new

photobioreactor designing criteria with effective mixing to maximize the biomass and lipid productivities.

9.2. Mathematical Model and Basic Assumptions

9.2.1. Mathematical formulations

The radiative transfer equation (RTE) with monochromatic light is an energy balance on light energy in absorbing and scattering medium at position $\hat{r}$ and $\hat{s}$ direction which can be written as (Huang et al., 2012; Murphy et al., 2014).

$$\hat{s}.\ \nabla I_{c,\lambda}\ (\hat{r},\hat{s}) = -\beta_{eff,\lambda} I_{c,\lambda}(\hat{r},\hat{s}) \qquad \text{(E9.1)}$$

Where $\beta_{eff,\lambda}$ is the effective extinction coefficient expressed as

$$\beta_{eff,\lambda} = \mathrm{K}_{eff,\lambda} + \sigma_{eff,\lambda} \qquad \text{(E9.2)}$$

The steady state RTE for the diffuse intensity can be written as

$$\frac{dI_\lambda}{dz} = -\mathrm{K}_{eff,\lambda} I_\lambda - \sigma_{eff,\lambda} I_\lambda + \frac{\sigma_{eff,\lambda}}{4\pi} \int I_\lambda \phi_\lambda \qquad \text{(E9.3)}$$

The parameters $\mathrm{K}_{eff,\lambda}$ and $\sigma_{eff,\lambda}$ are the effective absorption and scattering coefficient of the photobioreactor in (m^{-1}) and can be written as

$$\mathrm{K}_{eff,\lambda} = \mathrm{k}_{L,\lambda}(1 - X\mathrm{v}_x) + \mathrm{A}_{abs,\lambda} X \qquad \text{(E9.4)}$$

$$\sigma_{eff,\lambda} = \mathrm{S}_{sca,\lambda} X \qquad \text{(E9.5)}$$

Where X is the microorganism concentration (kg m^{-3}) and $\mathrm{k}_{L,\lambda}$ is absorption coefficient of the medium surrounding the cells (m^{-1}), which was assumed to be equal to that of the water. The spectral absorption coefficient of water can be written as

$$\mathrm{k}_{L,\lambda} = \frac{4\pi \mathrm{k}_\lambda^{'}}{\lambda} \qquad \text{(E9.6)}$$

where $\mathrm{k}_\lambda^{'}$ is the absorption index of water (1.96×10^{-9}) reported by Murphy et al., 2014. In Eq. (E9.4), the parameter v_x is the specific volume of the microorganisms, assumed to be equal to

0.001 m^3 kg^{-1} (Murphy et al., 2014). The mass absorption and scattering cross sections, $A_{abs,\lambda}$ and $S_{sca,\lambda}$, respectively, are both expressed in m^2 kg^{-1}. The final equation will be expressed as follows:

$$\frac{dI_\lambda}{dz} = -\left(k_{L,\lambda}(1 - X v_X) + A_{abs,\lambda} X\right) * I_\lambda - S_{sca,\lambda} X * I_\lambda + \frac{\sigma_{eff,\lambda}}{4\pi} \int I_\lambda \phi_\lambda \quad \text{(E9.7)}$$

9.2.2. Boundary conditions

To solve this Eq. (E9.7) two boundary conditions are required,

At z = 0, $I_\lambda = I_{\lambda 0}$; and

at z = w, $\frac{dI_\lambda}{dz} = 0$;

9.2.3. Fluence rate

The incident fluence rate in PBR at any spatial position from all the direction is defined as (Pilon et al., 2011; Lee et al., 2014).

$$G_\lambda = \int_{\Omega=0}^{\Omega=4\pi} I_\lambda(\vec{r}\ \vec{s}) d\Omega \quad \text{(E9.8)}$$

The one dimensional RTE was solved previously using two flux approximation and the solution accounted for anisotropic in-scattering terms in the RTE equation (Pottier et al., 2005; Modest et al., 2013; Kandilian et al., 2016). The analytical solution for local fluence rate G_λ in transparent PBR with back wall reflectance ρ_λ is defined as (Pottier et al., 2005).

$$G_\lambda(z) = 2q_{in,\lambda} \frac{\left[\rho_\lambda(1+\alpha_\lambda)e^{-\delta_\lambda L} - (1-\alpha_\lambda)e^{e^{-\delta_\lambda L}}\right]e^{\delta_\lambda z} + [1+\alpha_\lambda)e^{\delta_\lambda L} - \rho_\lambda(1-\alpha_\lambda)e^{\delta_\lambda L}]e^{-\delta_\lambda z}}{(1+\alpha_\lambda)^2 e^{\delta_\lambda L} - (1-\alpha_\lambda)^2 e^{-\delta_\lambda L} - \rho_\lambda(1-\alpha_\lambda^2)e^{\delta_\lambda L} + \rho_\lambda(1-\alpha_\lambda^2)e^{-\delta_\lambda L}} \quad \text{(E9.9)}$$

Where the parameters α_λ and δ_λ are expressed as (Pottier et al., 2005) [19].

$$\alpha_\lambda = \sqrt{\frac{\bar{A}_{abs,\lambda}}{\bar{A}_{abs,\lambda} + 2b_\lambda \bar{S}_{abs,\lambda}}} \quad \text{(E9.10)} \qquad \delta_\lambda = \sqrt{\bar{A}_{abs,\lambda}(\bar{A}_{abs,\lambda} + 2b_\lambda \bar{S}_{abs,\lambda})} \quad \text{(E9.11)}$$

Here, b_λ denoted as the backward scattering fraction for axisymmetric phase function; as microalgae suspension in photobioreactors forward scattering predominates over backward

scattering, then assumed b_λ tends to zero and α_λ approaches to unity. Thus the above expression can be simplified according to Lee et al. (2014).

$$G_\lambda(z) = q_{in,\lambda} e^{-\bar{A}_{abs,\lambda} Xz} + \rho_\lambda q_{in,\lambda} e^{-\bar{A}_{abs,\lambda} X(2L-z)} \qquad \text{(E9.12)}$$

The simplified expression for fluence rate in PBR are given by Eq. (E9.12) depends only on mass absorption cross section $\bar{A}_{abs,\lambda}$ of microalgae suspension, this is slightly differ from the Beer-Lambert law which is based on extinction coefficient $\beta_\lambda = (\bar{A}_{abs,\lambda} + \bar{S}_{abs,\lambda})X$ and always over estimates the local fluence rate inside the photobioreactor.

9.3. Material and methods

9.3.1. Microalgae and culture medium

A culture of B. braunii was obtained from the Institute of Bioresources and Sustainable Development (IBSD, Takyelpat, Imphal). The microalgae were grown in modified BG-11 medium containing macronutrients such as NaNO3 (1.12 g), MgSO4.7H2O (75 mg), K2HPO4. 3H2O (40 mg), CaCl2.2H2O (36 mg), Na2CO3 (20 mg), EDTA, 2Na-Mg salt (1 mg), citric acid (6 mg), ferric ammonium citrate (6 mg) and micronutrients such as H3BO3 (286 µg), MnCl2.4H2O (181 µg), ZnSO4.7H2O (22 µg), Na2MoO4.2H2O (39 µg), CuSO4.5H2O (8 µg) and Co(NO3)2.6H2O (5 µg) per liter. The inoculated medium was incubated at 27 ± 1 °C and 130 rpm in a light incubator shaker. The initial pH of the medium was maintained at 8.

9.3.2. The photobioreactor and experimental design

The flat panel photobioreactor (Model, PSI Photon System Instruments (PSI, Brno, Czech Republic) was used for the experimental studies. The dimensions of the reactor were (0.75 m × 0.59 m × 0.068 m). For maintaining air flow a porous sparger was used. The temperature and pH of the system were precisely controlled (Fig. 9.1). The reactor was illuminated by high-power light emitting diodes (LEDs) placed at one side of the reactor.The irradiance could be dynamically modulated by the instrument control unit. All the experiments were conducted in control environment (i.e. 27 ºC temperature and 1% CO_2) under the light intensity range of (150 to 1000 µmol m^{-2} s^{-1}) by LED Panel. *B. braunii* was grown in 30 liter photobioreactor filled with BG-11 nutrient medium, and operating at 0.33 vvm air flow rate and 1% CO_2.

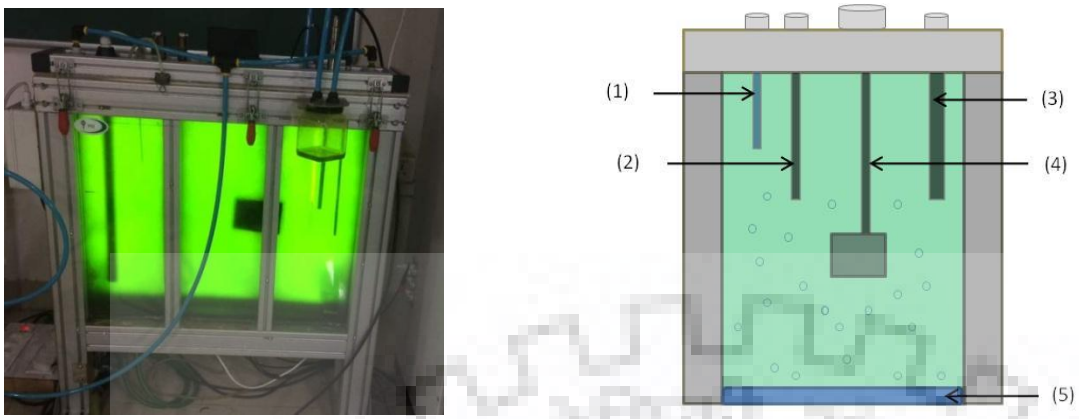

Fig. 9.1. (a) Experimental set up of a flat panel photobioreactor. (b) Schematic diagram of flat panel photobioreactor and the nomenclature as follows (1) pH probe, (2) Temperature probe, (3) Heating or cooling coil, (4) Online biomass monitor, (5) Porous type sparger.

9.3.3. Determination of biomass concentration

Microalgal biomass was estimated as a function of the optical density (OD) of cell. OD of cells in the circulated liquid was determined using an UV–Visible spectrophotometer (Carry 60, Agilent) at an absorbance of 750 nm (OD_{750}). Dry cell weight (Dwt) was calculated using the following formula generated using OD data and a calibration plot.

C_b (g L^{-1}) = 2.155 OD_{750} (R^2 = 0.99)

where, C_b was the dry weight of biomass and OD_{750} is the optical density measured at 750 nm. Therefore, the optical density can be used to precisely determine the dry weight of biomass.

3.4. Net specific growth rate

The net specific growth rate was calculated from Eq. (E9.13) (Issarapayup et al., 2009) [28] as follows:

$$\mu_{net} = \frac{(ln N_2 - ln N_1)}{(t_2 - t_1)} \qquad \text{(E9.13)}$$

where, N_2 and N_1 were the biomass concentrations (g L^{-1}) at days t_2 and t_1, respectively. Net specific growth rate was taken in exponential phase.

9.3.4. Biomass growth rate using logistic model

Modeling and simulation of the microalgal growth profile were obtained using the following logistic equation (Gilbert et al., 2011; Kumar et al., 2012).

$$\frac{dX}{dt} = K_c X \left(1 - \frac{X}{X_{max}}\right) \qquad \text{(E9.14)}$$

After integrating and rearranging Eq. (E9.14), it was written as Eq. (E9.15) as follows:

$$X = \frac{X_{max}}{1+\left(\frac{X_{max}}{X_0}-1\right)e^{-K_c t}} \qquad \text{(E9.15)}$$

where, X_{max} is the maximum concentration of microalgae (g L^{-1}), X_0 is the initial concentration of microalgae (g L^{-1}), and K_c is apparent specific growth rate (h^{-1}).

9.3.5. Sodium nitrate consumption kinetics

Sodium nitrate is consumed by microalgae to maintain cellular metabolism and synthesize products. Thus, the equation for sodium nitrate consumption can be expressed as follows:

$$-\frac{dS}{dt} = \frac{1}{Y_{X/S}} \times \frac{dX}{dt} + mX \qquad \text{(E9.16)}$$

where, $\frac{dS}{dt}$ is the consumption rate of sodium nitrate; $Y_{X/S}$ is the maximum microalgae growth coefficient g g^{-1}; $Y_{P/S}$ is the maximum lipid production coefficient g g^{-1}; m is maximum maintenance coefficient g g^{-1} h^{-1}.At t = 0, the sodium nitrate content is given by initial sodium nitrate content ($S = S_0$). After integration, Eq. (E9.16) becomes:

$$S = S_0 - \frac{1}{Y_{X/S}} \times \left(\frac{X_m\, X_0\, e^{\mu_m t}}{X_m - X_0 + X_0\, e^{\mu_m t}} - X_0\right) - \frac{m\, X_m}{\mu_m} \times ln\left(\frac{X_m - X_0 + X_0\, e^{\mu_m t}}{X_m}\right) \qquad \text{(E9.17)}$$

9.3.6. Maximum specific substrate uptake rates

Specific substrate uptake kinetics was measured by applying the substrate mass balance to a batch culture of *B. braunii*.

$$\frac{dM_s}{dt} = q_s^{max} M_x \qquad \text{(E9.18)}$$

where, $\frac{dM_s}{dt}$ is the total consumption rate of nitrogen, t is the fermentation time, q_s^{max} is maximum specific substrate consumption rate, M_x is biomass concentration at time t.

Biomass formation kinetics can be expressed as Eq. (E9.19).

$$\frac{dM_x}{dt} = \mu_{max} M_x \quad \text{(E9.19)}$$

After integrating Eq. (E9.19), it was written as Eq. (E9.20) as follows

$$M_x = M_{x0}.\exp(\mu_{max}\, t) \quad \text{(E9.20)}$$

After substituting M_x in Eq. (E9.18)

$$\frac{dM_s}{dt} = q_s^{max} M_{x0}.\exp(\mu_{max}\, t) \quad \text{(E9.21)}$$

Integrating Eq. (E9.21) from t = 0 to t and M_{s0} to $M_s(t)$

$$M_s(t) - M_{s0} = \frac{q_s^{max} M_{x0}}{\mu_{max}}.[\exp(\mu_{max}.t) - 1]$$

$$M_s(t) - M_{s0} = \frac{q_s^{max}}{\mu_{max}}.[M_x(t) - M_{x0}] \quad \text{(E9.22)}$$

A plot between $[M_s(t) - M_{s0}]$ vs $[M_x(t) - M_{x0}]$ was drawn, whose slope was $\left(\frac{q_s^{max}}{\mu_{max}}\right)$, where M_{s0} was the initial concentration of nitrogen (g L-1) , $M_s(t)$ was substrate concentration at different time (g L-1), M_{x0} was initial biomass concentration and $M_x(t)$ was biomass concentration at different time points.

9.3.7. Lipid formation kinetics

The Luedeking-Piret model was employed to estimate lipid production in *B. braunii* using the following equation:

$$\frac{dP}{dt} = \alpha\, \frac{dX}{dt} + \beta X \quad \text{(E9.23)}$$

where, $\frac{dP}{dt}$ is the rate of product formation; P is the product concentration in (mg L^{-1}); α is the growth associated coefficient (g g^{-1}) ; β is non-growth associated coefficient (g g^{-1}).

Product formation kinetics is divided into the following 3 classes: Class 1, when $\alpha \neq 0$ and $\beta = 0$, then product formation is microalgae growth associated; Class 2, when $\alpha = 0$ and $\beta \neq 0$ the product is not related to microalgae growth, Class 3, when $\alpha \neq 0$ and $\beta \neq 0$, product is partially growth associated. As shown in (Fig.9.6 A to F) the lipid accumulation was initially slow in early stage of microalgal growth, whereas majority of lipid accumulated when microalgal cell entered in stationary phase. In addition other studies also suggested that lipid formation in microalgae is partially growth associated (He et al., 2016). Thus, class 3 may better fit the lipid production of microalgae. When t = 0, the product content is given by the initial product content ($P = P_0$). After integration Eq. (E9.23) becomes:

$$P = P_0 - \alpha X_0 + \alpha \frac{X_0 * X_m * e^{\mu_m t}}{X_m - X_0 + X_0\, e^{\mu_m t}} + \beta \frac{X_m}{\mu_m} \ln\left(\frac{X_m - X_0 + X_0\, e^{\mu_m t}}{X_m}\right) \qquad \text{(E9.24)}$$

9.3.8. Estimation of nitrate concentration

Nutrient removal was determined by nitrate quantification in the culture medium. To estimate the nitrate concentration 1 ml of sample was taken from the photobioreactor in every 12 h interval. Supernatant was separated by centrifugation at 10,000 rpm for 6 minutes. Nitrate concentration was determined by taking OD at 220 nm using a UV–Visible spectrophotometer (Carry 60 Agilent) according to the method proposed by APHA (APHA, 1976).

9.3.9. Chlorophyll estimation

To estimate chlorophyll content in cell, 1 ml of microalgae sample was collected and centrifuged at 10,000 rpm for 10 minutes and the pellet was resuspended in 600 µl methanol. After that samples were heated for 5 minutes in water bath and cooled down to room temperature, then volume of the sample was made upto 1 ml by adding methanol, and chlorophyll content was calculated according to following equation (Aslan et al., 2006).

chl a (mg L^{-1}) = (16.5 x A_{665}) - (8.3 x A_{650}) (E9.25)

9.3.10. CO_2 fixation rate

The CO_2 fixation rate was determined from the carbon content of algal cells and the growth rate as follows (Yun et al., 1997) [34].

$$R_{CO_2} = C_C \times \mu_L \times (\frac{M_{CO_2}}{M_C}) \qquad \text{(E9.26)}$$

Where, R_{CO_2} and μ_L are the fixation rate (mg L^{-1} d^{-1}) and the volumetric growth rate (mg L^{-1} d^{-1}), of *B. braunii* respectively, in the linear growth phase. M_{CO_2} and M_C represented the molecular weights of CO_2 and elemental carbon, respectively. The average C_C carbon content was 0.63 g carbon per g dry cell weight. The algal growth rate was determined in the linear growth phase because most of the algal growth occurred during this phase.

9.3.11. Lipid estimation

Lipid estimation in microalgae samples was performed using the modified rapid colorimetric method based on sulpho-phospho-vanillin (SPV) reaction in the presence of sulphuric acid (Cheng et al., 2011; Byreddy et al., 2016). The vanillin phosphoric acid reagent was prepared by dissolving 120 mg vanillin in 20 ml of distilled water and adjusting the final volume to 100 ml with 85% phosphoric acid. The reagent was stored in dark conditions until further use. SPV reagent was prepared freshly, which results in high activity with lipid samples. A known amount of *B. braunii* sample was taken in test tube and incubated for 100 ºC for 5 min, and allowed to cool for 5 min in an ice bath. Freshly prepared phospho-vanillin reagent (1 ml) was then added to each test tube. The test tubes were incubated at 37 ºC and 200 rpm for 15 min, and absorbance was measured at 540 nm.

9.4. Results and discussion

9.4.1. Radiation characteristics of *B. braunii*

The RTE equation given by Eq. (7) was solved by MATLAB (R2013a, MathWorks, Inc., USA). To apply the RTE equation a number of model parameters must be known. For that, most of the model parameters were retrieved from the literature while others have been experimentally determined, as detailed below. The optical properties of *B. braunii* $\bar{C}_{ext,\lambda}$, $\bar{C}_{abs,\lambda}$ and $\bar{C}_{sca,\lambda}$ were reported previously and values were 1.68 x 10^{-10}, 1.84 x 10^{-11} and 1.500 x 10^{-10} (m^2 $cell^{-1}$) respectively (Berberoglu et al., 2009).

The average minor and major diameter of *B. braunii* microalgae cell were 10.3 and 13.3 µm respectively (Berberoglu et al., 2007). The average single scattering albedo (ω) was about 0.89, and their asymmetry factor g was 0.986, in the 400-800 nm spectral range (Berberoglu et al., 2009;

Berberoglu et al., 2008). These two parameters were dimensionless, and were independent of cell concentration.

Thus, it is more convenient to introduce the spectral mass extinction and absorption cross section denoted by $E_{ext,\lambda}$ and $A_{abs,\lambda}$ respectively. They are defined as (Pilon et al., 2011).

$$E_{ext,\lambda} = \frac{\beta_\lambda}{X} \quad \text{(E9.27)} \quad \text{and} \quad A_{abs,\lambda} = \frac{\kappa_\lambda}{X} \quad \text{(E9.28)}$$

The extinction coefficient β_λ (m^{-1}) is obtained from normal- normal transmittance measurements of dilute suspensions. Moreover, the measurement of absorption coefficient κ_λ(m^{-1}) can be retrieved by using integrating sphere technique (Berberoglu et al., 2008). In this article the optical parameters of *B. braunii* including the extinction coefficient, spectral mass cross section ($\bar{C}_{abs,\lambda}$) were taken from the literature (Berberoglu et al., 2009). The effective absorption coefficient κ_λ of polydisperse microalgae suspension is related to the average absorption cross section, denoted by $\bar{C}_{abs,\lambda}$, as (Pilon et al., 2011).

$$\kappa_\lambda = \bar{C}_{abs,\lambda} N_T \quad \text{(E9.29)}$$

similarly κ_λ is correlated with mass spectral cross section area, denoted as following (Berberoglu et al., 2009),

$$\kappa_\lambda = A_{abs,\lambda} X \quad \text{(E9.30)}$$

and by using simple correlation between average absorption cross section ($\bar{C}_{abs,\lambda}$ (m^2 $cell^{-1}$)) of microalgae and the mass spectral cross section $A_{abs,\lambda}$ (m^2 kg^{-1}) can be expressed as

$$\bar{C}_{abs,\lambda} N_T = A_{abs,\lambda} X \quad \text{(E9.31)}$$

The value of $\bar{C}_{abs,\lambda}$ was 1.84 x 10^{-11} (m^2 $cell^{-1}$) reported for *B. braunii* (Berberoglu et al., 2009). The cell density N_T in each dilution was counted in Petroff-Hausser counting chamber. The resulting calibration curves were $N_T = 11.17 \times 10^{12}$ OD_{750} and X = 2.155 OD_{750} with correlation coefficient R^2 of 0.99 for both calibrations, where N_T is total cell number expressed in (cell m^{-3}) and X is biomass concentration expressed as (kg m^{-3}), using all the values of coefficients and microalgae parameters, the value of $A_{abs,\lambda}$ was calculated from the Eq. (31) and the observed value

of $A_{abs,\lambda}$ was 95.37 (m^2 kg^{-1}). Once determined the mass spectral absorption cross section ($A_{abs,\lambda}$); $S_{sca,\lambda}$ can be calculated according to (Pilon et al., 2011).

$$E_{ext,\lambda} = A_{abs,\lambda} + S_{sca,\lambda} \qquad \text{and} \qquad S_{sca,\lambda} = E_{ext,\lambda} - A_{abs,\lambda}$$

Similarly the mass spectral scattering cross section was calculated and the value of $S_{sca,\lambda}$ was found to be 771.65 (m^2 kg^{-1}).

9.4.2. Effect of light intensities on biomass growth and CO_2 fixation

Effects of six different light intensities on biomass growth of *B. braunii* were studied using 30 L PSI flat panel photobioreactor. Maximum biomass concentration and maximum specific growth rate were 1.8 g L^{-1} and 1.344 d^{-1}, respectively, at light intensity of 800 µmol m^{-2} s^{-1} after 5 days of cultivation. As shown in (Fig. 9.2), at lower- than-optimal PPFD levels the growth of *B. braunii* may have been light-limited due to a suboptimal supply of electrons for photosynthesis (Jacob-lopes et al., 2009; Ketseoglou et al., 2013). At high light intensities the microalgae growth reached in saturation phase. Thus, considerably less increase in growth was observed. Notably, low light intensities did not support biomass growth or lipid accumulation in microalgal cells. At light intensity of 150, 300, 450, 600, 1000 µmol m^{-2} s^{-1} maximum biomass concentration and maximum specific growth rate were 0.62 g L^{-1} and 0.74 d^{-1}, 1.09 g L^{-1} and 1.128 d^{-1}, 1.52 g L^{-1} and 1.152 d^{-1}, 1.78 g L^{-1} and 1.32 d^{-1}, 1.17 g L^{-1} and 1.25 d^{-1} respectively. Similar effects of varying light intensities on growth pattern were reported by Converti et al. (2006) and Kumar et al., (2013).

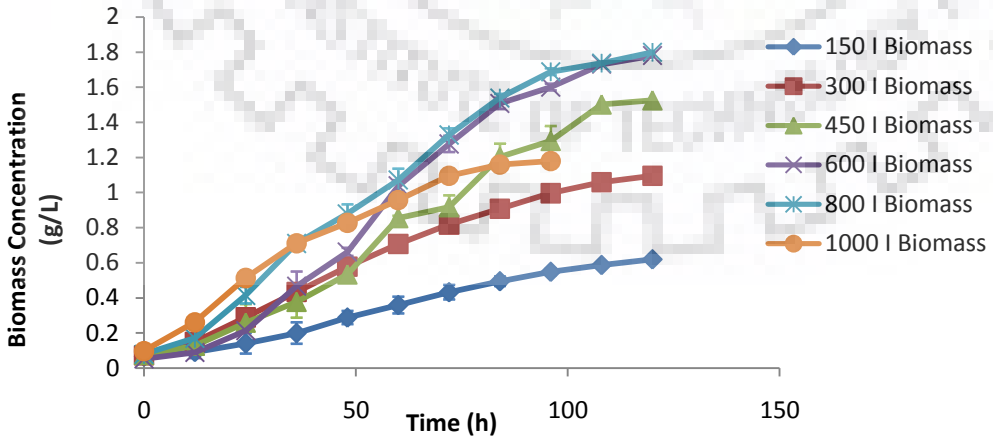

Fig. 9.2. Growth pattern of *B. braunii* in flat panel photobioreactor at different light intensities.

To quantitatively analyze the effect of light intensities on the performance of carbon dioxide removal, the CO_2 fixation rate of *B. braunii* was calculated based on Eq. (E9.26). The rate of CO_2 fixation is proportional to the biomass growth rate. The maximum CO_2 fixation rate of 826.98 mg L^{-1} d^{-1} was observed at 800 μmol m^{-2} s^{-1}. At light intensities of 150, 300, 450, 600 and 1000 μmol m^{-2} s^{-1} the CO_2 fixation rate were 286.44, 503.58, 702.24, 822.36 and 540.54 mg L^{-1} d^{-1} respectively (Table 9.2).

Thus, the maximum biomass productivity of 358 mg L^{-1} d^{-1} was observed at a light intensity of 800 μmol m^{-2} s^{-1} with the highest CO_2 fixation rate of 826.98 mg L^{-1} d^{-1}. In Table 9.2, this biomass productivity and CO_2 fixation rate is higher that obtained from other *Botryococcus sp.* such as 181.78 mg L^{-1} d^{-1} and 419.91 mg L^{-1} d^{-1} (Yeesang et al., 2011), 92.37 mg L^{-1} d^{-1} and 213.37 mg L^{-1} d^{-1} (Ge et al., 2011), 26.55 mg L^{-1} d^{-1} and 61.33 mg L^{-1} d^{-1} (Yoo et al., 2010), 222.90 mg L^{-1} d^{-1} and 514.90 mg L^{-1} d^{-1} (Yeesang et al., 2014), 186 mg L^{-1} d^{-1} and 429.66 mg L^{-1} d^{-1} (Sydney et al., 2010), 173.29 and 400.30 mg L^{-1} d^{-1} (Perez-Mora et al., 2016) respectively. The results obtained in present studies indicate that optimum light intensity level inside the photobioreactor significantly enhanced the biomass productivity and CO_2 biofixation rate in *B. braunii*. Light evolution and light dynamics inside the PBR can be best described by the RTE equation. The effect of cell concentration and light path on RTE and light distribution pattern were further studied.

9.4.3. Light intensity profile in flat panel photobioreactor

The mathematical model of light intensity profile inside the flat panel photobioreactor was solved by bvp4c solver of the MATLAB (R2013a, MathWorks, Inc., USA); this solver can solve boundary value problems in one spatial dimension. The light intensity profile at various biomass concentrations under different irradiance level are shown in (Fig. 9.3A-F). Light distribution inside the flat panel photobioreactor decreased with increase in cell concentration and at higher cell concentration a steeper decrease in light intensity profile was observed. As the cell concentration increases; self shading of the microalgae cells has been increased which reduces the light penetration inside the photobioreactor. These results are in accordance with Kumar et al. (2013), and reported similar decrease in light penetration at higher cell concentration.

This observation is also associated with light path of the reactor which signifies the lower specific growth rate of microalgae at higher light path (Ogbonna et al., 2000; Huang et al., 2012; Kumar et al., 2013).

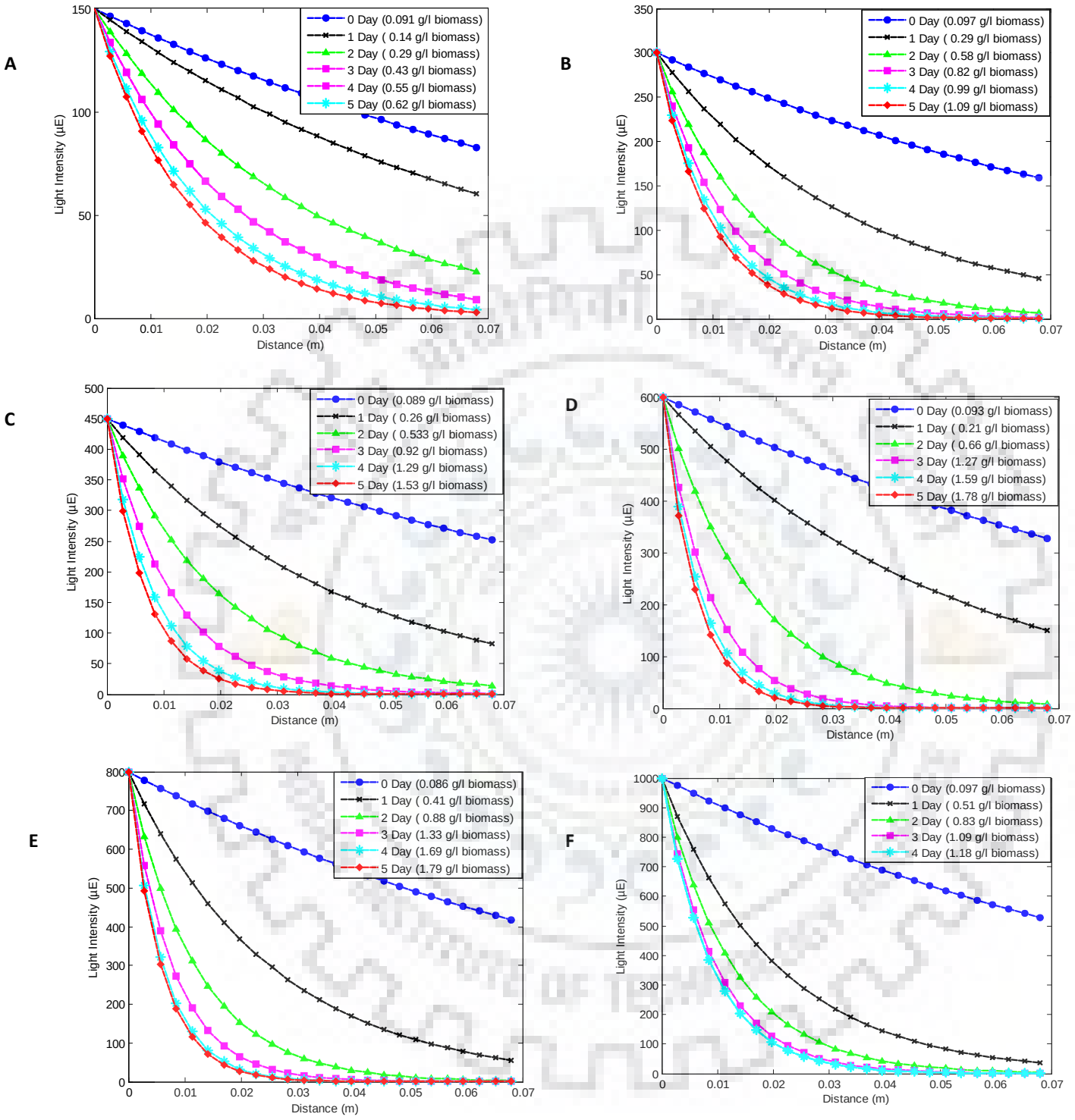

Fig. 9.3. Plot of light distribution pattern vs. light path distance at given light intensity of (A) 150 µmol m^{-2} s^{-1}, (B) 300 µmol m^{-2} s^{-1}, (C) 450 µmol m^{-2} s^{-1}, (D) 600 µmol m^{-2} s^{-1}, (E) 800 µmol m^{-2} s^{-1}, (F) 1000 µmol m^{-2} s^{-1}, at different cell density at different point location inside flat panel photobioreactor.

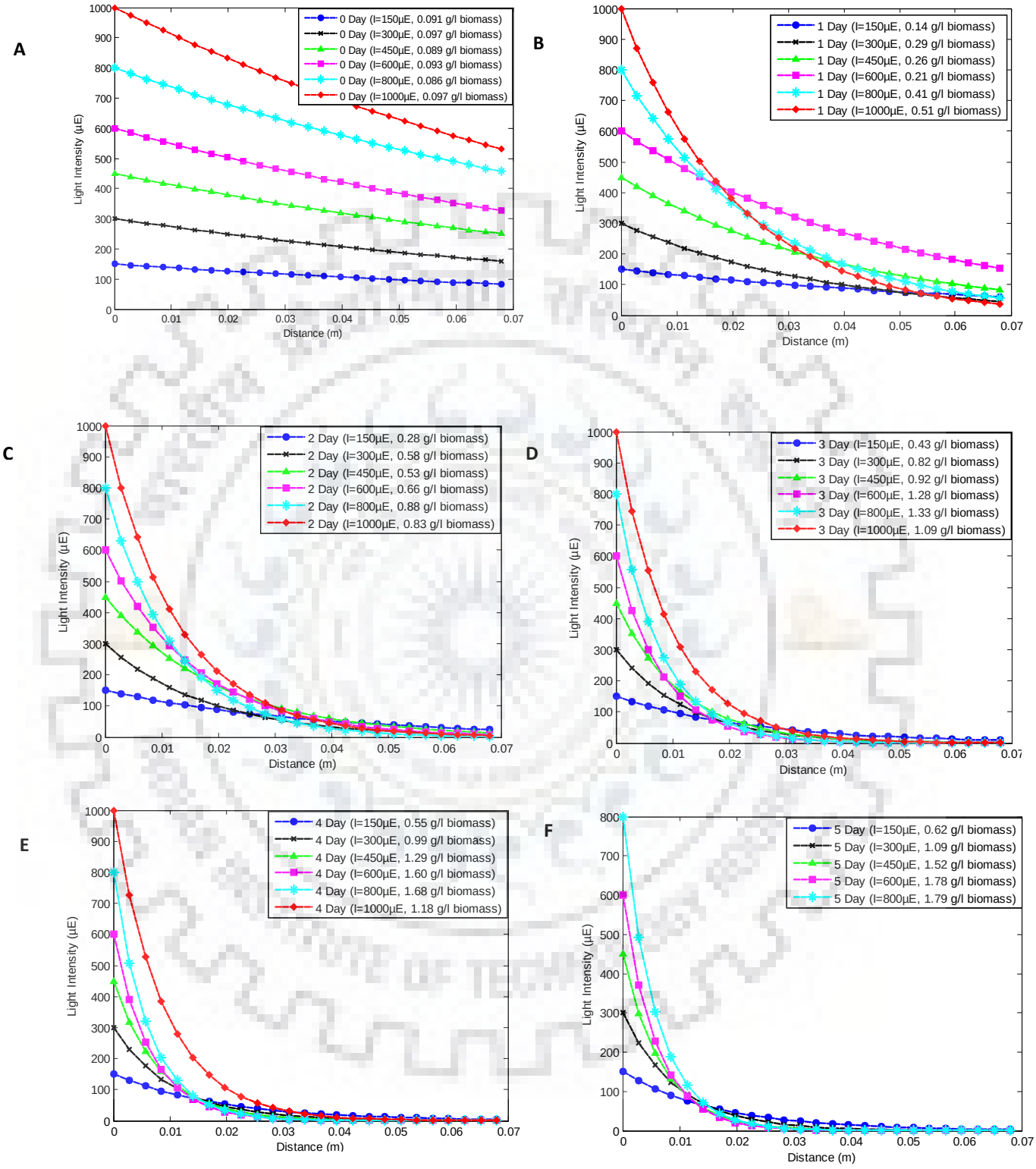

Fig. 9.4. Comparison plot of light distribution pattern vs. light path distance at varying light intensity (from 150 to 1000 µmol m^{-2} s^{-1}) (A) Day 0, (B) Day 1, (C) Day 2, (D) Day 3, (E) Day 4, (F) Day 5, at different cell density at different point location inside flat panel photobioreactor.

The effect of cell concentration on light distribution profile in photobioreactor at different cultivation days are shown in Fig. 9.4A-F, when microorganism growth reached stationary phase the light distribution profile nearly overlapped with each other on 4^{th} and 5^{th} day of cultivation in photobioreactor.

In Fig. 9.4A-F, the RTE equation was also simulated from zero to fifth day of cultivation with different intensities and different cell concentrations. As shown in Fig. 9.4B, the light distribution profile comparatively reduced more at higher light intensity due to increase in cell concentration at 0.41 g L^{-1} and 0.51 g L^{-1} for 800 and 1000 μmol m^{-2} s^{-1} light intensity respectively after 1^{st} day of cultivation. This indicates that at cell concentration (> 0.41 g L^{-1}) multiple scattering and diffusive reflections reduced the light penetration. A close inspection of Fig.9.4 D-F reveals that at high cell concentration effective light penetration inside photobioreactor reached upto 3 cm of the panel width and almost all light patterns except (1000 μmol m^{-2} s^{-1}) overlapping each other, which signifies the occurrence of saturation in specific growth occur at higher light intensities. At the higher- than-optimal PPFD levels i.e. 1000 μmol m^{-2} s^{-1} caused photo-oxidative damage to microalgae cell which lower the specific growth rate of microalgae. In Fig. 9.4E on 4^{th} day of cultivation microalgae cells were reached their maximum growth at different cultivation lights. The exponential decay was observed in light intensities upto 3 cm width of the photobioreactor. Beyond 3 cm the light distribution profile in photobioreactor is nearly constant and becomes independent of light intensities for cell concentration above (> 0.83g L^{-1}; Fig. 9.4C).

Therefore, it can be inferred that increasing the panel width or light intensity may not significantly enhance the microalgae growth. These results are in accordance with (Huang et al., 2012; Kumar et al., 2013) which reported similar light distribution profile in phototobioreactor.

It can therefore be inferred that algal cell growth may not be significantly affected by high light intensities because of two reasons; firstly, beyond nearly 3 cm of photobioreactor width the light intensity is fairly constant and secondly increase in cell concentration causes the self shading and multiple forward light scattering or diffusive reflection by the cells which results into significant decrease in incident light intensity at the first layer of the cells than that of outer surface of vessel glass (Kumar et al., 2013).

9.4.4. Effect of light intensities on chlorophyll content

It is known that light intensity directly influences microalgal cell growth and photosynthesis. Therefore, the effect of light intensity on chlorophyll concentrations was assessed under

phototrophic cultivation, with varying light intensity ranging from 150 to 1000 µmol m^{-2} s^{-1} and a constant photoperiod (24:0). The chlorophyll concentration were initially increased with increase in light intensity and the maximum chlorophyll concentration of 97.23 mg L^{-1} was observed at the light intensity of 800 µmol m^{-2} s^{-1} on the fifth day of cultivation (Fig. 9.5). Further increase in light intensity leads to decrease in chlorophyll concentration.

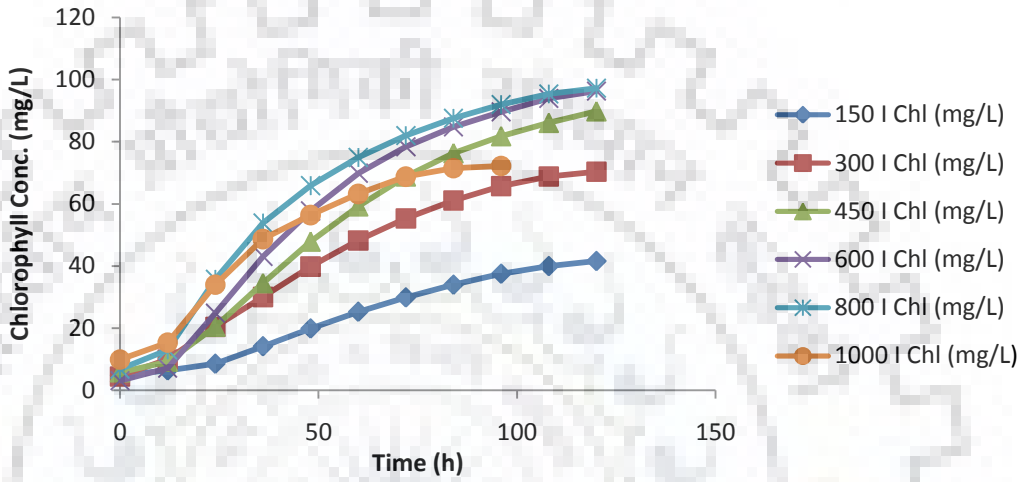

Fig. 9.5. Chlorophyll concentration of *B. braunii* in flat panel photobioreactor at different light intensities

The chlorophyll concentration was highly inhibited at higher light intensity of 1000 µmol m^{-2} s^{-1} and approximately 25.79% reduction in chlorophyll concentration (72.15 mg L^{-1}) was observed from the maximum chlorophyll concentration. At light intensities of 150, 300, 450, 600 µmol m^{-2} s^{-1} maximum observed chlorophyll concentration were 41.59, 70.34, 89.83, 96.34 mg L^{-1} respectively. It is noteworthy that light intensity did not have a significant impact on cell growth but stimulated chlorophyll content in cells remarkably at higher light intensity (Table 9.5). The results were consistent with (Gim et al., 2016; Takache et al., 2012), as their optimal range of light intensities were 80 to 150 µmol m^{-2} s^{-1} and 100 to 200 µmol m^{-2} s^{-1} respectively suitable for higher chlorophyll content (g g^{-1}). In this study the optimal range for higher pigment content was also lies in this region (Table 9.5). The pigment content in microalgae cells are significantly affected by incident PFD by a well known phenomenon, called photoacclimation, which can be induced by light intensities, leading to decrease in pigment contents with increasing PPFD (Takache et al., 2012).

9.4.5. Effect of light intensities on lipid productivities

Effect of varying light conditions on lipid content and lipid productivities were evaluated. Maximum lipid content and maximum lipid productivity of 27.37% and 86.4 mg L^{-1} d^{-1} were observed at light intensities of 450 μmol m^{-2} s^{-1} and 600 μmol m^{-2} s^{-1} respectively. At high light intensities of 600, 800 and 1000 μmol m^{-2} s^{-1} the lipid content of B. braunii decreased to 24.27%, 22.23% and 19.74% respectively. At low light intensities of 150 and 300 μmol m^{-2} s^{-1} low levels of lipid accumulation corresponding to 10.65% and 20.18%, respectively, were observed (Table 9.1). However, the lipid content and yield in culture were considerably lower at low light intensities than at intermediate light intensities. Thus, lipid accumulation could be promoted by increasing the light intensity from 150 to 450 μmol m^{-2} s^{-1} ; however, further increase in light intensity reduced lipid formation.

An intermediate light intensity was observed to be more suitable for lipid accumulation than high light intensities. Since high light intensities enhanced the microalgal growth, the microalgae might use synthesized energy to divide themselves, rather than store it as lipid (Cheirsilp et al., 2012). Moreover, Guedes et al. (2010) reported that lipid content decreased while light intensity increased because lipids were major components of chloroplasts, so an increase in light intensity overcomes the need for a high chloroplastidial activity.

Table 9.1. Maximum biomass, lipid concentration, lipid content, biomass and lipid productivity under varying light regimes.

Light Intensity (μmol m^{-2} s^{-1})	**X_{max} (g L^{-1})**	**P_{max} (g L^{-1})**	**Lipid Content (%)**	**Biomass Productivity (mg L^{-1} d^{-1})**	**Lipid Productivity (mg L^{-1} d^{-1})**
150	0.62	0.066	10.65	124	13.2
300	1.09	0.22	20.18	218	44.0
450	1.52	0.416	27.37	304	83.2
600	1.78	0.432	24.27	356	86.4
800	1.79	0.398	22.23	358	79.6
1000	1.17	0.231	19.74	292.5	57.75

Table 9.2 Comparison of phototrophic growth and lipid production using *B. braunii* with the literature reported values. [a] Calculated values from the given data from literatures.

Medium type	Type of cultivation	Biomass Productivity (mg L^{-1} d^{-1})	CO_2fixation rate (mg L^{-1} d^{-1})	Lipid Content (%)	Lipid Productivity (mg L^{-1} d^{-1})	Reference
Chu-13	Erlenmeyer Flask	181.78	419.91	25.8	46.9	Yeesang et al. (2011)
BG-11	Tubular Photobioreactor	92.37	213.37	12.71	11.74[a]	Ge et al. (2011)
Chu-13	Bioreactor	26.55	61.33	20.75	5.51	Yoo et al. (2010)
Wastewater	CSTR PBR	222.90	514.90	31	69.1	Yeesang et al. (2014)
Chlorella medium	Glass flask with continuous illumination	28.63	66.14	54.69	15.66[a]	Ruangsomboon, 2012
3N-MBM	CSTR PBR	186	429.66	33	61.38	Sydney et al.(2010)
Chu-13	Tubular PBR	173.29	400.30	33.7	58.40[a]	Perez-Mora et al.(2016)
BG-11	Flat Panel Photobioreactor	358	826.98	22.23	79.6	Present study
BG-11	Flat Panel Photobioreactor	304	702.24	27.37	83.2	Present study

However, Ho et al. (2012) reported that no significant variations occurred in lipid content of S. obliquus CNW-N with respect to light intensity. Sukenik et al. (1989; 1991) reported that the lipid content of *Nannochloropsis* sp. and *Isochrysis galbana* increased with increase in light intensity, whereas Chrismadha et al. (1994) did not detect any effect of irradiance on the lipid content of *Phaeodactylum tricornutum*, and concluded that the correlation of light intensity and lipid content is usually species- specific (Ho et al., 2012; Chrismadha et al., 1994).

In present study, the production of lipids, (86.4 mg $L^{-1}d^{-1}$) was observed to be higher than that observed in the previous studies: 46.90 mg L^{-1} d^{-1} (Yeesang et al., 2011), 11.74 mg L^{-1} d^{-1} (Ge et al., 2011), 5.51 mg L^{-1} d^{-1} (Yoo et al., 2010), 69.1 mg L^{-1} d^{-1} (Yeesang et al., 2014), 15.66 mg L^{-1} d^{-1} (Ruangsomboon et al., 2012), 61.38 mg L^{-1} d^{-1} (Sydney et al., 2010), 58.40 mg L^{-1} d^{-1} (Perez-Mora et al., 2016) (Table 9.2). Lipid content was also compared to the data reported previously. It was observed that lipid content (27.37%) measured in the present study was slightly lower than previously reported values such as 54.69% (Ruangsomboon et al., 2012), 33.7% (Perez-Mora et al., 2016) and 33% (Sydney et al., 2010) (Table 9.2).

It must be noted that the results can vary according to methodology used for determination of lipid content. Moreover, lipid accumulation also changes according to the strain and culture conditions used, such as nitrogen deprivation which generally increases algal lipid content (Zhang et al., 2011). Although, results suggests that mid level light intensity is optimum for higher lipid accumulation in microalgae.

9.4.6. Kinetic studies

9.4.6.1. Growth kinetics under different light intensities

Biomass concentrations of *B. braunii* under different light intensities were fitted by Eq. (E9.15). As shown in Fig. 9.6, the model fits well to the experimental data. The model parameter i.e. (X_0, X_m and K_c) were evaluated by logistic rate equation and presented in Table 9.3.

As depicted in Table 9.4, the increasing light intensity in photobioreactor, the value of X_m was increased in the range of (150 to 800 μmol m^{-2} s^{-1}) light intensity, but the K_c was decreased when light intensity was higher than 600 μmol m^{-2} s^{-1}. This indicated that a higher light intensity negatively affected the algal growth rate which was also reported by Chen et al., 2010. Yoshimura et al. (2013) found that the maximum specific growth rate for *B. braunii* was 0.50 d^{-1} at 850 μmol m^{-2} s^{-1}. Similar results were reported by Sasi et al., 2011 who pointed that higher PAR density (> 44.2 mW L^{-1}) in circulating loop photobioreactor for *Chlorella* did negatively affect the specific growth rate. In this work, the maximum specific growth rate shows a strong dependency on irradiance; the maximal specific growth at 800 μmol m^{-2} s^{-1} is up to 1.344 d^{-1}. The maximum specific growth rate revealed in this study is, to our best knowledge, the highest specific growth rate for *B. braunii* reported in the previous studies (Table 9.3).

Table 9.3. Comparison of specific growth rate of *B. braunii* with the literature reported values.[a] Calculated values from the given data in literatures.

Light Intensity (μmol m^{-2} s^{-1})	%CO_2	Specific growth rate(d^{-1})	Reference
850	1	0.50	Yoshimura et al.(2013)
250	0.3	0.42	Wolf et al. (1985)
1.2 klux	2	0.07[a]	Rao et al. (2007)
150	20	0.13[a]	[45]
200	0	0.10[a]	Ruangsomboon, (2012)
800	1	1.344	Present Study

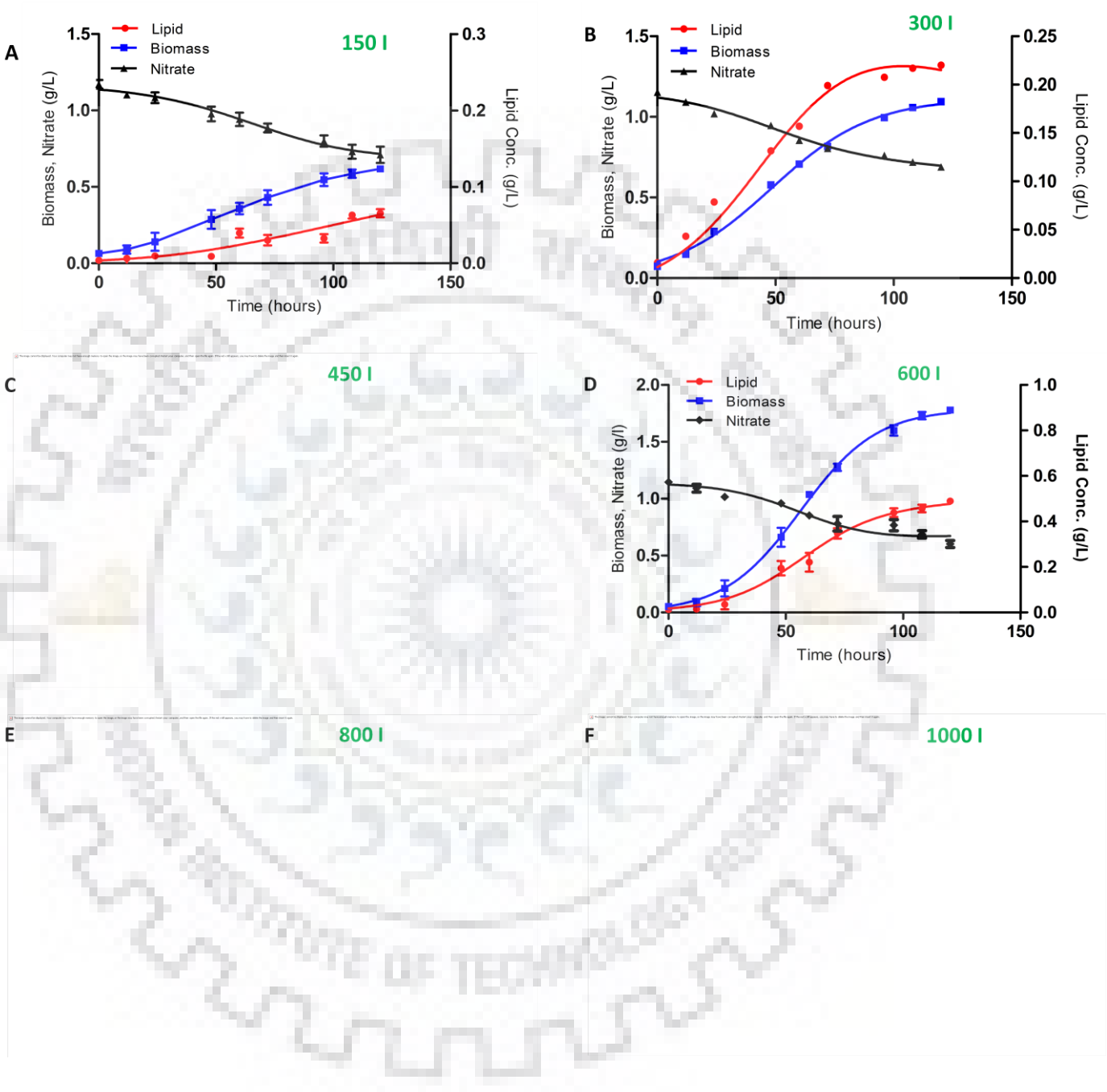

Fig. 9.6. (A to F) Experimental and simulated biomass, lipid and nitrate profile of *B. braunii* in flat panel photobioreactor at light intensities of (150 to 1000 µmol m^{-2} s^{-1}) respectively.

Table 9.4. K_c is the apparent specific growth rate of the microalgae; X_0 is the initial biomass concentration; X_m is the maximum biomass concentration of microalgae; P_0 is the initial lipid content; α is the growth correlation coefficient; β is the non-growth correlation coefficient; S_0 is the sodium nitrate concentration; $Y_{X/S}$ is the maximum microalgal growth coefficient; and m is the maximum maintenance coefficient.

Parameters	150 µmol m^{-2} s^{-1}	300 µmol m^{-2} s^{-1}	450 µmol m^{-2} s^{-1}	600 µmol m^{-2} s^{-1}	800 µmol m^{-2} s^{-1}	1000 µmol m^{-2} s^{-1}
Biomass						
K_c (h^{-1})	0.0404	0.047	0.0483	0.0614	0.050	0.047
X_0 (g L^{-1})	0.061	0.113	0.114	0.101	0.178	0.17
X_m (g L^{-1})	0.66	1.118	1.518	1.614	1.697	1.20
R^2	0.9982	0.9959	0.9975	0.9931	0.9912	0.9925
Lipid						
P_0 (g L^{-1})	0.013	0.0263	0.038	0.04	0.029	0.0325
α (g g^{-1})	0.022	0.274	0.5353	0.226	0.1761	0.1637
β (g g^{-1})	1.75×10^{-4}	-1.2×10^{-3}	-7.2×10^{-4}	3.7×10^{-4}	7.3×10^{-4}	1.2×10^{-4}
R^2	0.87	0.99	0.99	0.99	0.986	0.935
Nitrate						
S (g L^{-1})	1.173	1.163	1.08	1.141	1.14	1.21
$Y_{X/S}$ (g g^{-1})	1.779	1.897	1.982	4.642	4.12	4.79
m (g g^{-1} h^{-1})	2.2×10^{-3}	-1.66×10^{-3}	-1.4×10^{-3}	5.8×10^{-4}	4.4×10^{-4}	-1.23×10^{-3}
R^2	0.986	0.985	0.94	0.959	0.975	0.977

9.4.6.2. Nitrate uptake kinetics and specific nitrate uptake rates under different light intensities.

Sodium nitrate consumption kinetics under different irradiance level was calculated by using Eq. (E9.17). The experimental data was fitted in the Eq. (E9.18) and the estimated parameter values of S_0, $Y_{X/S}$ and m are listed in Table (9.4). A good correlation with the model equation indicated that nitrate consumption in FPBR by *B. braunii* could be well described using Eq. (E9.18). In addition, the values of $Y_{X/S}$ at 150, 300 and 450 µmol m^{-2} s^{-1} light intensities were similar, but lower than those observed at 600, 800 and 1000 µmol m^{-2} s^{-1} (Table 9.4). This suggested that intermediate light intensity was more suitable compared to high or low light intensity. The values of maintenance coefficient (m) in all cultures were either very low or negative, which potentially indicated that a small amount of light in culture was required to maintain the metabolic activity of microalgal cell.

Table 9.5. Effect of light intensity on chlorophyll content, maximum specific nitrate uptake rate (q_s^{max}), maximum specific growth rate (μ_{max}) and CO_2 consumption rate. (**Note**: negative values of q_s^{max} indicates that substrate is consuming with respect to time).

Light Intensity µmol m^{-2} s^{-1}	**Chlorophyll Content (%)**	q_s^{max} **(g g_b h^{-1})**	μ_{max} **(h^{-1})**	R_{CO_2} **(mg L^{-1} d^{-1})**
150	6.68	-0.03131	0.031	286.44
300	6.45	-0.02872	0.047	503.58
450	5.91	-0.02174	0.048	702.24
600	5.41	-0.0165	0.055	822.36
800	5.43	-0.01568	0.056	826.98
1000	6.16	-0.01404	0.052	540.54

The values of $Y_{X/S}$ as shown in Table 9.4, continuously increased with an increase in light intensity upto the 600 µmol m^{-2} s^{-1}, however, further increase in light intensity reduced the values of $Y_{X/S}$, this indicates that high light intensity negatively affect the nitrate consumption rate and biomass yield on nitrate under the influence on high irradiance.

To quantitatively analyze the effect of light intensities on nitrate removal, the specific nitrate uptake rate (q_s^{max}) of *B. braunii* was calculated based on Eq. (E.22). Under low light conditions (150 µmol m^{-2} s^{-1}), it was observed that specific nitrate uptake rate 0.0313 g g_b^{-1} h^{-1} was the highest. As the light intensity increased, corresponding q_s^{max} decreased and the lowest value of q_s^{max} was 0.0140 g g_b^{-1} h^{-1} observed at 1000 µmol m^{-2} s^{-1} (Table 9.5). The nitrate uptake mechanism in phytoplanktons is not completely understood, although it is assumed that active transport of nitrate across the cell membrane is an energy intensive process (Anderson, 1981). At the moment, the fact that algae had a higher value of $Y_{X/S}$ and lower values of q_s^{max} under the higher light intensities, cannot be explained and needs to be investigated further. These results are in accordance to Gonçalves et al. (2016) who reported similar trend of nitrogen removal under the influence of high light intensity, and shown that increase in light intensity from 105 to 180 µmol m^{-2} s^{-1} the two species of microalgae, *Chlorella vulgaris* and *Synechocystis salina* reduced nitrogen removal rate from 2.78 to 2.43 mg L^{-1} d^{-1} and 2.54 to 1.97 mg L^{-1} d^{-1} respectively. The

results reported in present study has also shown similar trend of nitrate consumption under different level of irradiance.

9.4.6.3. Lipid formation kinetics under different light intensities

Lipid formation kinetics was analyzed using Luedeking-Piret Eq. (E9.23). The experimental data was fitted in the Eq. (E9.24) and the parameters values were listed in Table 9.4. Based on observation of Fig. 9.6, and correlation coefficient in Table 9.4, the experimental data was fitting well to the model equation, indicating the lipid production in *B. braunii* culture in FPBR can be best described by Luedeking-Piret equation. As depicted in Table 9.4, the growth associated coefficient (α) increased with increase in the biomass concentration upto the 450 μmol m^{-2} s^{-1} light intensity, suggesting that lipid accumulation is growth associated in this range (150 to 450 μmol m^{-2} s^{-1}), further increase in light intensity from (600 to 1000 μmol m^{-2} s^{-1}) value of α decreased, indicating that high light intensity negatively affect the lipid accumulation in *B. braunii*. The results are consistent with Ho et al. (2012) as their study indicated that higher light intensity (> 420 μmol m^{-2} s^{-1}) reduced the lipid content and lipid yield in *S. obliquus* CNW-N. The non-growth associated coefficient (β) was found negative for 300 and 450 μmol m^{-2} s^{-1} light intensity, but under low light (150 μmol m^{-2} s^{-1}) and high light intensities (600 to 1000 μmol m^{-2} s^{-1}) the value of β varied from (1.2 to 7.3×10^{-4} g g^{-1}), suggesting that lipid formation under this range of light intensity is partially growth associated (Class 3). Although the kinetic parameters obtained in this study suggested that optimal range of light intensity for maximum lipid production lied between 300 to 450 μmol m^{-2} s^{-1}. This could be explained further by the lipid yield on light energy.

9.4.7. Effect of light intensities on biomass and lipid yield

The effect of light intensity on biomass yield and lipid yield of *B. braunii* were summarized in Fig. 9.7. Biomass yield on light energy was decreased from 0.65 to 0.23 g mol $photons^{-1}$ in a linear mode. This suggests that higher algal growth at high light intensities reduced the effective light penetration inside the photobioreactor and results in lower biomass yield. The similar results were also reported by Zijffers et al. (2010) who explained that increase in biomass concentration at high light intensity may decreased the light utilization efficiency of microalgae.

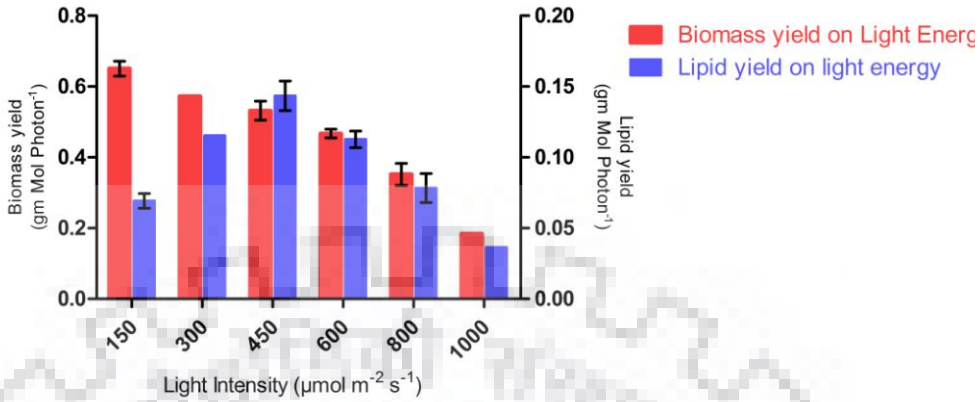

Fig. 9.7. Showing the effect of light intensities on biomass and lipid yield

The results of the present studies were compared with the other photobioreactor systems in which *B. braunii* were cultivated, such as Cheng et al. (2013) reported biomass yield on light energy had value of 0.75 g mol photons^{-1} at 100 µmol m^{-2} s^{-1}. In addition, the lipid yields on light energy (Fig. 9.7) increased from 0.069 to 0.146 g mol photons^{-1} for the light intensity range of 150 to 450 µmol m^{-2} s^{-1}, further increase in light intensity, a steeper decrease in lipid yield was observed at 600 µmol m^{-2} s^{-1} and follows the similar trend when the light intensity beyond the 450 µmol m^{-2} s^{-1}. These results indicate that mid level light intensities up to the 450 µmol m^{-2} s^{-1} in flat panel photobioreactor is optimum for higher lipid productivities.

9.5. Conclusions

In the present study, the effect of varying light regimes on light dynamics, biomass growth and lipid kinetics in flat panel photobioreactor has been evaluated. Simulation of light energy flux balance across the panel width showed the light distribution pattern inside the photobioreactor. Self shading of the microalgae cell reduced the effective light penetration beyond the 3 cm width of the photobioreactor irrespective of the incident light intensity at high biomass concentration. The lowest value of biomass and lipid yield on light energy was 0.23 and 0.045 g mol photons^{-1} achieved at 1000 µmol m^{-2} s^{-1}. The maximum lipid yield and lipid content of 0.146 g mol photons^{-1} and 27.37% w/w was achieved at 450 µmol m^{-2} s^{-1} light intensity. Growth kinetics and lipid kinetics models were found to give reasonably good fit with experimental data. It is concluded that *B. braunii* shows optimum biomass and lipid productivities with mid level light intensities region (300 to 600 µmol m^{-2} s^{-1}) and higher light intensities produced the photooxidative damage to the

microalgae cell. Suitable light distribution pattern facilitate its application in improved design of photobioreactor productivity system in flat panel photobioreactor.

9.6.References

Anderson., 1981. Effects of Light Intensity on Nitrate and Nitrite Uptake and Excretion by Chaetoceros curvisetus. Marine Biology. 62, 257-261.

APHA. 1976. Standard methods for the examination of water and wastewater 14ed. APHA American Public Health Association.

Aslan S., Kapdan I.K., 2006. Batch kinetics of nitrogen and phosphorus removal from synthetic wastewater by algae. Ecol. Eng. 28(1), 64-70.

Bamba B.S.B., Lozano P., Adjé F., Ouattara A., Vian M.A., Tranchant C., Lozano Y., 2015. Effects of Temperature and Other Operational Parameters on *Chlorella vulgaris* Mass Cultivation in a Simple and Low-Cost Column Photobioreactor. Appl. Biochem. Biotechnol. 177(2), 389-406.

Berberoglu H., Gomez P.S., Pilon L., 2009. Radiation characteristics of *Botryococcus braunii*, *Chlorococcum littorale*, and *Chlorella* sp. used for fixation and biofuel production. J. Quant. Spectr. Rad.Tran. 110(17), 1879-1893.

Berberoglu H., Pilon L., 2007. Experimental measurements of the radiation characteristics of Anabaena variabilis ATCC 29413-U and Rhodobacter sphaeroides ATCC 49419. Int. J. Hydrogen Energy. 32(18), 4772-4785.

Berberoglu H., Pilon L., Melis A., 2008. Radiation characteristics of *Chlamydomonas reinhardtii* CC125 and its truncated chlorophyll antenna transformants tla1, tlaX and tla1-CW+. Int. J. Hydrogen Energy. 33(22), 6467-6483.

Berberoglu H., Yin J., Pilon L., 2007. Light transfer in bubble sparged photobioreactors for H2 production and CO_2 mitigation. Int. J. Hydrogen Energy. 32(13), 2273-2285.

Brennan L., Owende P., 2010. Biofuels from microalgae—A review of technologies for production, processing, and extractions of biofuels and co-products. Renew. Sustain Energy Rev. 14(2), 557-577.

Breuer G., Lamers P.P., Martens D.E., Draaisma R.B., Wijffels R.H., 2013. Effect of light intensity, pH, and temperature on triacylglycerol (TAG) accumulation induced by nitrogen starvation in *Scenedesmus obliquus*. Bioresour. Technol. 143, 1-9.

Byreddy A.R., Gupta A., Barrow C.J., Puri M., 2016. A quick colorimetric method for total lipid quantification in microalgae. J. Microbiol. Methods. 125, 28–32.

Cabello J., Toledo-Cervantes A., Sánchez L., Revah S., Morales M., 2015. Effect of the temperature, pH and irradiance on the photosynthetic activity by *Scenedesmus obtusiusculus* under nitrogen replete and deplete conditions. Bioresour. Technol. 181, 128-135.

Carvalho A.P., Silva S.O., Baptista J.M., Malcata F.X., 2010. Light requirements in microalgal photobioreactors: an overview of biophotonic aspects. Appl. Microbiol. Biotechnol. 89(5), 1275-1288.

Cheirsilp B., Torpee S., 2012. Enhanced growth and lipid production of microalgae under mixotrophic culture condition: Effect of light intensity, glucose concentration and fed-batch cultivation. Bioresour. Technol. 110, 510-516.

Cheng P., Ji B., Gao L., Zhang W., Wang J., Liu T., 2013. The growth, lipid and hydrocarbon production of *Botryococcus braunii* with attached cultivation. Bioresour Technol. 138, 95-100.

Cheng Y.S., Zheng Y., Vander-Gheynst J., 2011. Rapid quantitative analysis of lipids using a colorimetric method in a microplate format. Lipids. 46, 95–103.

Converti A., Lodi A., Del Borghi A., Solisio C., 2006. Cultivation of *Spirulina platensis* in a combined airlift-tubular reactor system. Biochem. Eng. J. 32(1), 13-18.

Cornet J.F., Dussap C. G., Gros J.B., 1995. A simplified monodimensional approach for modeling coupling between radiant light transfer and growth kinetics in photobioreactors. Chemical Eng. Sci. 50,1489-1500.

Csőgör Z., Herrenbauer M., Schmidt K., Posten C., 2001. J. Appl. Phycol. 13(4), 325-333.

Dauchet J., Blanco S., Cornet J.-F., Fournier R., 2015. Calculation of the radiative properties of photosynthetic microorganisms. J. Quant. Spectr.Rad Tran. 161, 60-84.

Fernandes B.D., Dragone G.M., Teixeira J.A., Vicente A.A., 2010. Light regime characterization in an airlift photobioreactor for production of microalgae with high starch content. Appl. Biochem. Biotechnol. 161(1-8), 218-226.

Gajda I., Greenman J., Melhuish C., Ieropoulos I., 2015. Self-sustainable electricity production from algae grown in a microbial fuel cell system. Biomass Bioenergy, 82, 87-93.

Gilbert J.J., Ray S., Das D. 2011. Hydrogen production using *Rhodobacter sphaeroides* (O.U. 001) in a flat panel rocking photobioreactor. Int. J. Hydro. Energy. 36(5), 3434-3441.

Gim G.H., Jaewon Ryu J., Kim M. J., Kim P. I., Kim S.W., 2016. Effects of carbon source and light intensity on the growth and total lipid production of three microalgae under different culture conditions. J Ind Microbiol Biotechnol. 43, 605–616.

Guedes A.C., Meireles L.A., Amaro H.M., Malcata F.X., 2010. Changes in Lipid Class and Fatty Acid Composition of Cultures of *Pavlova lutheri*, in Response to Light Intensity. J. American Oil Chem. Soc. 87(7), 791-801.

He Y., Chen L., Zhou Y., Chen H., Zhou X., Cai F., Huang J., Wang M., Chen B., Guo Z., 2016. Analysis and model delineation of marine microalgae growth and lipid accumulation in flat-plate photobioreactor. Biochem. Eng. J. 111, 108-116.

Ho S.-H., Chen C.-Y., Chang J.-S., 2012. Effect of light intensity and nitrogen starvation on CO_2 fixation and lipid/carbohydrate production of an indigenous microalga *Scenedesmus obliquus* CNW-N. Bioresour.Technol.113, 244-252.

Huang Q., Yao L., Liu T., Yang J., 2012. Simulation of the light evolution in an annular photobioreactor for the cultivation of *Porphyridium cruentum*. Chemical Eng. Sci. 84, 718-726.

Huerlimann R., de Nys R., Heimann K., 2010. Growth, lipid content, productivity, and fatty acid composition of tropical microalgae for scale-up production. Biotechnol.Bioeng. 107(2), 245-257.

Issarapayup K., Powtongsook S., Pavasant P., 2009. Flat panel airlift photobioreactors for cultivation of vegetative cells of microalga *Haematococcus pluvialis.* J. Biotechnol. 142(3), 227-232.

Jacob-Lopes E., Revah S., Hernández S., Shirai K., Franco T.T., 2009. Development of operational strategies to remove carbon dioxide in photobioreactors. Chemical Eng. J. 153(1-3), 120-126.

Kandilian R., Tsao T.-C., Pilon L., 2014. Control of incident irradiance on a batch operated flat-plate photobioreactor. Chemical Eng. Sci. 119, 99-108.

Kandilian R., Soulies A., Rousseau B., Pruvost J., Legrand J., Pilon L., 2016. Simple method to measure spectral absorption cross-section of microalgae. Chem Eng Sci, 146, 357–368.

Ketseoglou I., Bouwer G., 2013. Optimization of photobioreactor growth conditions for a cyanobacterium expressing mosquitocidal *Bacillus thuringiensis* Cry proteins. J Biotechnol. 167(1), 64-71.

Kong B., Vigil R.D., 2014. Simulation of photosynthetically active radiation distribution in algal photobioreactors using a multidimensional spectral radiation model. Bioresour. Technol. 158, 141-148.

Kumar K., Das D., 2012. Growth characteristics of *Chlorella sorokiniana* in airlift and bubble column photobioreactors. Bioresour Technol. 116, 307-13.

Kumar K., Sirasale A., Das D., 2013. Use of image analysis tool for the development of light distribution pattern inside the photobioreactor for the algal cultivation. Bioresour Technol, 143, 88-95.

Lee E., Pruvost, J., He X., Munipalli R., Pilon L., 2014. Design tool and guidelines for outdoor photobioreactors. Chemical Eng. Sci. 106, 18-29.

Leupold, M., Hindersin, S., Kerner, M., Hanelt, D., 2013. The effect of discontinuous airlift mixing in outdoor flat panel photobioreactors on growth of *Scenedesmus obliquus.* Bioprocess Biosys. Eng. 36(11), 1653-1663.

Liemert A., Kienle A., 2013. Exact and efficient solution of the radiative transport equation for the semi-infinite medium. Sci Rep, 3, 2018.

Modest, M.F., 2013. Radiative Heat Transfer, third ed. Elsevier, Oxford, UK.

Murakami M., Ikenouchi M., 1997. The biological CO_2 fixation and utilization project by rite (2)-screening and breeding of microalgae with high capability in fixing CO_2. Energy Convers. Mgmt. 38. 493-497.

Murata N., Takahashi S., Nishiyama Y., Allakhverdiev S.I., 2007. Photoinhibition of photosystem II under environmental stress. Biochimica et Biophysica Acta (BBA) - Bioenergetics, 1767(6), 414-421.

Murphy T.E., Berberoglu H., 2014. Flux balancing of light and nutrients in a biofilm photobioreactor for maximizing photosynthetic productivity. Biotechnol. Prog, 30(2), 348-59.

Ogbonna J.C., Tanaka H. 2000. Light requirement and photosynthetic cell cultivation Development of processes for efficient light utilization in photobioreactors. J. Appl. Phycol. 12, 207–218.

Ozkan A., Kinney K., Katz L., Berberoglu H., 2012. Reduction of water and energy requirement of algae cultivation using an algae biofilm photobioreactor. Bioresour. Technol. 114, 542-8.

Pilon L., Berberoğlu H., Kandilian R., 2011. Radiation transfer in photobiological carbon dioxide fixation and fuel production by microalgae. J. Quant. Spectr. Rad. Trans. 112(17), 2639-2660.

Pottier L., Pruvost J., Deremetz J., Cornet J.F., Legrand J., Dussap C.G., 2005. A fully predictive model for one-dimensional light attenuation by*Chlamydomonas reinhardtii* in a torus photobioreactor. Biotechnol.Bioeng. 91(5), 569-582.

Pruvost J., Pottier L., Legrand J., 2006. Numerical investigation of hydrodynamic and mixing conditions in a torus photobioreactor. Chemical Eng. Sci. 61(14), 4476-4489.

Sydney E.B., Sturm W., de Carvalho J.C., Thomaz-Soccol V., Larroche C., Pandey A., Soccol C.R., 2010. Potential carbon dioxide fixation by industrially important microalgae. Bioresour. Technol. 101(15), 5892-6.

Takache H., Pruvost J., Cornet J.-F., 2012. Kinetic modeling of the photosynthetic growth of *Chlamydomonas reinhardtii* in a photobioreactor. Biotechnol. Prog. 28(3), 681-692.

Wang, J., Liu, J., Liu, T. 2015. The difference in effective light penetration may explain the superiority in photosynthetic efficiency of attached cultivation over the conventional open pond for microalgae. Biotechnol. Biofuels. 8(1).

Yun Y. S., Lee S. B., Jong Moon Park J.M., Lee C.I., Yang J.W., 1997. Carbon Dioxide Fixation by Algal Cultivation Using Wastewater Nutrients. J. Chem. T ech. Biotechnol. 69, 451-455.

Zhao Y., Wang J., Zhang H., Yan C., Zhang Y. 2013. Effects of various LED light wavelengths and intensities on microalgae-based simultaneous biogas upgrading and digestate nutrient reduction process. Bioresour. Technol. 136, 461-468.

10. Conclusions

This study investigates the studies of lipid production for biodiesel production in Flat Panel Photobioreactor.

- One of the objectives was to study the effect of varying CO_2 concentration on biomass and lipid productivity of *B. braunii* in flat panel airlift photobioreactor. The developed process (i.e. pH stat) significantly enhanced the process productivity of *B. braunii* and the maximum biomass and CO_2 consumption rate was achieved at 20% CO_2 concentration using the pH stat cultivation strategy.
- A novel light evolution kinetic equation was developed to study the B braunii dynamics is flat panel photobioreactor. Furthermore, the light evolution kinetic equation was coupled with the *B. braunii* growth dynamics. In addition, the developed novel consolidate equation were capable of to monitor algal dynamics in real time. This study also suggests that 1.125 g L^{-1} nitrate is most appropriate conditions for higher biomass and lipid productivity.
- Physical parameters (i.e. Light intensity) effects on biomass and lipid production of *B. braunii* were also identified in flat panel airlift photobioreactor system. The study concluded that 261 µmol m^{-2} sec^{-1} light intensity for flat panel airlift photobioreactor (5.13 L) is optimum for *B. braunii* growth and lipid production.
- In Heterotrophic cultivation conditions first of all effective C:N ratio was identified for optimum growth, and the study suggest that 21:1 C:N ratio is optimum for growth.
- In flat panel photobioreactor 20 g L^{-1} glucose is optimum for biomass and lipid productivity under mixotrophic batch cultivation
- Single stage and two-phase fed batch cultivation for microalgae biomass is a promising strategy to boost lipid accumulation and productivity in flat panel PBR. Importantly, during two-phase fed batch cultivation for *B. braunii* the biomass was increased to 7.9 g/L, and the lipid productivity was increased from 0.536 g L^{-1} d^{-1} to 1.32 g L^{-1} d^{-1} compared to single stage heterotrophic batch cultivation
- In addition, B braunii was also cultivated in a fully controlled commercial flat Panel Bubble column PBR (30 L volume), and the study suggests that the 450 µmol m^{-2} sec^{-1}light intensity, 27 ºC temperature and 1:1 (white:red) wavelength ratio is optimum for growth and lipid production.

11. Future Prospective

- The developed novel light evolution kinetic model can be exploited to develop online process monitoring systems.
- Real time bioprocess control system (software) can also be developed using this equation.
- Mixotrophic cultivation studies in photobioreactor
- Continuous and different fed Batch cultivation strategies for *B. braunii* biomass and lipid production in flat Panel Photobioreactor.
- Wastewater and lignocellulosic hydrolysate can be used for cost effective cultivation.
- Model predictive control and flux balance analysis studies in flat panel photobioreactor can also be tested.

Publications

Khichi S.S., Anis A. and Ghosh S., Mathematical modeling of light energy flux balance in flat panel photobioreactor for *Botryococcus braunii* growth, CO_2 biofixation and lipid production under varying light regimes, Biochem. Eng. J. 134 (2018) 44-56.

Khichi S.S., Gehlot K., Dutta B.C. and Ghosh S., Online Estimation of Biomass, Lipid and Nitrate Dynamic Profile using Innovative Light Evolution Kinetic Model in Flat Panel Airlift Photobioreactor for Botryococcus braunii under Varying Light Conditions **(Ms. Ref. No.: BEJ-D-18-00835 (Under Review).**

Khichi S.S. and Ghosh S. Real Time Monitoring of Algal Dynamics using Explicit Analytical Solution of Monod Kinetics Coupled with the Light Evolution Kinetic Model in Flat Panel Airlift Photobioreactor under Nitrate Limiting Conditions (To be submitted)

Khichi S.S. and Ghosh S. Specific Uptake Kinetics of Glucose and Nitrate in Carbon-Limited and Nitrogen-Limited C:N ratio under Photoheterotrophic Cultural Conditions for Botryococcus braunii Growth and Lipid Production (Manuscript in preparation)

Khichi S.S. and Ghosh S. Optimization of Photosynthetic parameters of photobioreactor using Photosynthetic Efficiency and Photosynthetic Activity of light response curve as function of biomass productivity

Poster /Abstract Presented

Khichi S.S., Gehlot K., Singh P., Kumar S., and Ghosh S., (2018). Real Time Monitoring of Algal Dynamics using Novel Light Evolution Kinetic Model in Flat Panel Airlift Photobioreactor. DBT National Workshop on Bioenergy, July 2018, IIT Roorkee.

Khichi S.S. and Ghosh S., (2017). Process Engineering for Improved Biosequestration of CO_2 Using Two Stage Sequential Photobioreactor System- Experimental and Modeling. BESCON-2017, Delhi.

Khichi S.S., Singh P. and Ghosh S., (2016). Mathematical Modeling and Simulation of Light Energy Flux Balancing for Maximizing Photosynthetic Productivity of *B. braunii* in Flat Panel Photobioreactor. 3rd International conference on new frontiers in Biotechnology Science, Health and Medicine, Genopro 2016, Bareilly.

Khichi S.S., Singh P. and Ghosh S., (2016). Mathematical Modeling of CO_2 Diffusion in *B. braunii* under pH Stat Condition. 3rd International conference on new frontiers in Biotechnology Science, Health and Medicine, Genopro 2016, Bareilly.

Khichi S.S., Singh P. and Ghosh S., (2016). Metabolic flux Balance Analysis of *B. braunii* in C-Limited and N- Limited Heterotrophic Culture Conditions. Bioprocessing India 2016, Mohali.

Khichi S. S., Choudhary G., Mishra A. and Ghosh S., (2013). CO_2 sequesteration and Bidirectional Production of Biodiesel and Biofuels from Microalgal Photobioreactor.

Organized by Association of Biochemical Engineers and Food Technologists, March 2013, HBTI, Kanpur.

Choudhary G., Singh L.K., **Khichi S. S**., Mishra A. and Ghosh S., (2013). Algal Biomass Potential source for the ecofriendly fuel of the future. Organized by Association of Biochemical Engineers and Food Technologists, March 2013, HBTI, Kanpur.

Choudhary G., Singh L.K., **Khichi S. S**., Mishra A. and Ghosh S., (2013). Co Culture study of *Zymomonas Mobilis* and *Schffersoomyces stiptis* for fuel ethanol production from mixed sugars.8thInternational conference on Recent Advances in Biotechnology & Biodiversity Conservation and environment Management Research.

Oral Presentation

Khich S.S. and Sanjoy Ghosh (2017). Mathematical Modeling of Light Energy Flux Balance in Flat Panel Photobioreactor for B. braunii Growth, CO_2 Biofixation and Lipid Production under Varying Light Regimes. BES Foundation day 2017, IIT Roorkee, Roorkee.

Workshop

Optimization Techniques for Solving Industrial Problems (OTSIP-2016). Organized by Mathematical colloquium, Department of Mathematics, IIT Roorkee, Roorkee.

Prizes/ Awards

Secured 1st position in Industry Academia Meet 2017 for presenting innovative idea on the topic "A novel solid state fermentation Bioreactor. IIT Roorkee, Roorkee.

Secured 3rd position in Biotechnology Day-2017 for presenting the "Cool Biotechnology Idea". IIT Roorkee, Roorkee.

Biochemical Engineering Journal 134 (2018) 44–56

Contents lists available at ScienceDirect

Biochemical Engineering Journal

journal homepage: www.elsevier.com/locate/bej

Mathematical modeling of light energy flux balance in flat panel photobioreactor for *Botryococcus braunii* growth, CO_2 biofixation and lipid production under varying light regimes

Shailendra Singh Khichi, Afifa Anis, Sanjoy Ghosh *

Department of Biotechnology, Indian Institute of Technology, Roorkee, 247667, India

ARTICLE INFO

Article history:
Received 23 June 2017
Received in revised form 20 February 2018
Accepted 3 March 2018
Available online 7 March 2018

Keywords:
Light energy flux
Photobioreactor
Botryococcus braunii
Growth and lipid model
Mathematical model

ABSTRACT

Light is the most significant parameter for microalgal growth and light distribution inside the flat panel photobioreactor is critical to assess the photosynthetic productivity of *Botryococcus braunii*. In algal photobioreactors, self shading of the microalgal cells reduces the effective light penetration. The local light intensity inside the photobioreactor is essential for efficient designs. In this study *B. braunii* was grown in flat panel photobioreactor under varying light intensity. Maximum biomass concentration and maximum specific growth rate were 1.8 g L^{-1} and 1.344 d^{-1} respectively at light intensity of 800 μmol m^{-2} s^{-1}. The maximum lipid content and lipid yield were 27.37% and 0.146 g mol photons^{-1} respectively at 450 μmol m^{-2} s^{-1} light intensity. The results reported in this study is used with the radiative transport equation (RTE) to accurately predict and optimize light transport in photobioreactors for biomass and lipid production. Finally, simulation of RTE in flat panel photobioreactor also suggests, at cell concentration (>0.41 g L^{-1}) multiple scattering and diffusive reflections reduced the light penetration. Based on these results, optimal conditions for lipid production were found to be at mid level light intensity i.e. 450 μmol m^{-2} s^{-1} which allows maximizing the use of light energy by the cells to produce maximum lipid.

1. Introduction

Microalgae cultivation in photobioreactor is gaining attention for scale-up of biomass and lipid productivity [1]. Microalgae growth in photobioreactor is affected by several photosynthetic parameters such as light intensity, air flow rate, temperature, and pH [2–4]. Among those, the light intensity is considered as the most significant parameter to determine the biomass composition, growth rate and product yield in photobioreactor [5–7]. The photobioreactor is an efficient technical device to process photosynthetic microalgae for biomass, photo-hydrogen or biofuel production [8,9]. Photosynthetic engineering is nowadays recognized as a possible solution to the exhaustion of fossil resources and global warming because it enables CO_2 mitigation and sustainable energy production efficiently [9,10].

Optimization of light availability to the microorganism in PBR is a crucial aspect of biomass production and process productivity [11]. The microalgal growth is highly influenced by light intensity, duration, and the wavelength inside the PBR [12]. Inadequate light supply reduces the microalgae growth while excessive light intensity causes photo-oxidative damage to PSII unit of microalgae [11,13]. Optimum light penetration and supply inside the photobioreactor is the most challenging task [11]. Therefore, it is necessary to predict accurate light distribution profile inside the photobioreactor for optimum process productivity.

Light penetration in photobioreactor is affected by the absorption, emission and scattering processes. Light interaction with matter is based on the particle description of light and is best described by the radiative transfer theory. The radiative transfer theory was originally developed by Chandrasekhar in astrophysics and the application of radiative transfer theory has been successfully applied to model effective light transfer in photobioreactors [14].

Several authors applied radiative transfer model to different geometries of the photobioreactor to predict light attenuation profile. Pioneering work of light transfer model in rectangular photobioreactor was based on a monodimensional equation of Schuster

Abbreviations: FPBR, flat panel photobioreactor; PBR, photobioreactor; PFD, photon flux density; PPFD, photosynthetic photon flux density; RTE, radiative transfer equation.

* Corresponding author.
E-mail address: ghoshfbs@iitr.ac.in (S. Ghosh)

https://doi.org/10.1016/j.bej.2018.03.001
1369-703X/

Nomenclature

$I_{c,\lambda}$	Incident light energy (μmol m^{2} s^{-1})
$\beta_{eff,\lambda}$	Effective extinction coefficient of microalgae (m^{-1})
$K_{eff,\lambda}$	Effective absorption coefficient of microalgae (m^{-1})
$\sigma_{eff,\lambda}$	Effective scattering coefficient of microalgae (m^{-1})
$A_{abs,\lambda}$	Mass absorption cross section of microalgae (m^2 kg^{-1})
$S_{sca,\lambda}$	Mass scattering cross section of microalgae (m^2 kg^{-1})
$\bar{C}_{ext,\lambda}$	Average extinction cross section of microalgae cell (m^2 cell^{-1})
$\bar{C}_{abs,\lambda}$	Average absorption cross section of microalgae cell (m^2 cell^{-1})
$\bar{C}_{sca,\lambda}$	Average scattering cross section of microalgae cell (m^2 cell^{-1})
$k_{L,\lambda}$	Absorption coefficient of the medium (m^{-1})
k'_{λ}	Absorption index of water (dimensionless)
ϕ_{λ}	Phase function (dimensionless)
$\hat{r}$	Position vector (dimensionless)
$\hat{s}$	Direction (dimensionless)
X	Biomass concentration (g L^{-1})
μ	Specific growth rate (d^{-1})
X_m	Maximum biomass concentration (g L^{-1})
X_0	Initial biomass concentration (g L^{-1})
K_c	Apparent specific growth rate (d^{-1})
q_S^{max}	Maximum specific substrate consumption rate (g g$_b$ h^{-1})
μ_{max}	Maximum specific growth rate (d^{-1})
P	Lipid concentration (g L^{-1})
α	Growth associated coefficient (g g^{-1})
β	Non growth associated coefficient (g g^{-1})
M_{CO_2}	Molecular weight of CO_2
M_c	Molecular weight of carbon
C_c	Carbon content of the cell
P_{areal}	Areal biomass productivity (g m^{-2} h^{-1})
V	Volume of the photobioreactor (L)
A	Illuminated surface area of photobioreactor (m^2)
$Y_{X,E}$	Biomass yield on light energy (g mol photons^{-1})
R^2	Coefficient of determination (−)

[15]. In this light limited model, the radiative transfer equation (RTE) was coupled with photosynthetic kinetics to represent the light attenuation profile inside the photobioreactor as a function of photosynthetic parameters [14]. In comparison with the light limited model, Berberoglu et al. [16] applied RTE in a bubble sparged photobioreactor containing gas bubble and suspension culture of *cynobacteria* and *anabaena*. They used Mie theory to estimate the scattering phase function of the gas bubble and microalgae to solve RTE [16].

An accurate prediction of radiative transfer model requires absorption, scattering coefficient, and scattering phase function of microalgae in photobioreactor [17]. Optical properties (i.e. size and shape distribution) of microalgae and growth medium can be calculated using the Mie theory [18,19]. Light diffusion across the photobioreactor mainly depends on the absorption and scattering phenomena of microalgal cell [20,21].

In recent years the classical radiative transfer equation was solved majorly by discrete ordinate method (DOM) and finite volume method (FVM). Both of these methods are widely applicable and require low computer and memory cost [22]. The other method, e.g. Monte Carlo method which is based on probability theory and a random number generator, is used and solved the RTE using multiple scattering simulations. Whilst the diffusion method, which is based on the diffusion approximation (DA) and obtains analytical solutions of light propagation in the optically thick medium for several geometries [23]. It is difficult to predict the light distribution in PBR accurately with polychromatic light due to the fact that the absorption coefficient and the scattering coefficient are both spectrally dependent.

In the present study, light energy flux balance across the flat panel photobioreactor was applied to develop the mathematical model as a function of light intensity and microalgal growth rate. The present model is based on the radiative transfer equation with varying light intensity in flat panel photobioreactor for effective utilization of light energy. The RTE equation was solved by the MATLAB bvp4c solver. The developed mathematical formulations could be used for investigating the light distribution profile inside a photobioreactor. Biomass, lipid and nitrate kinetics under varying light regimes were also investigated; which paved the path for developing new photobioreactor designing criteria with effective mixing to maximize the biomass and lipid productivities.

2. Mathematical model and basic assumptions

2.1. Mathematical formulations

The radiative transfer equation (RTE) with monochromatic light is an energy balance on light energy in absorbing and scattering medium at position $\hat{r}$ and $\hat{s}$ direction which can be written as [22,24].

$$\hat{s}.\nabla I_{c,\lambda}\left(\hat{r},\hat{s}\right) = -\beta_{eff,\lambda} I_{c,\lambda}\left(\hat{r},\hat{s}\right) \quad (1)$$

Where $\beta_{eff,\lambda}$ is the effective extinction coefficient expressed as

$$\beta_{eff,\lambda} = K_{eff,\lambda} + \sigma_{eff,\lambda} \quad (2)$$

The steady state RTE for the diffuse intensity can be written as

$$\frac{dI_\lambda}{dz} = -K_{eff,\lambda} I_\lambda - \sigma_{eff,\lambda} I_\lambda + \frac{\sigma_{eff,\lambda}}{4\pi}\int I_\lambda \phi_\lambda \quad (3)$$

The parameters $K_{eff,\lambda}$ and $\sigma_{eff,\lambda}$ are the effective absorption and scattering coefficient of the photobioreactor in (m^{-1}) and can be written as

$$K_{eff,\lambda} = k_{L,\lambda}(1 - Xv_x) + A_{abs,\lambda} X \quad (4)$$

$$\sigma_{eff,\lambda} = S_{sca,\lambda} X \quad (5)$$

Where X is the microorganism concentration (kg m^{-3}) and $k_{L,\lambda}$ is absorption coefficient of the medium surrounding the cells (m^{-1}), which was assumed to be equal to that of the water. The spectral absorption coefficient of water can be written as

$$k_{L,\lambda} = \frac{4\pi k'_\lambda}{\lambda} \quad (6)$$

where k'_λ is the absorption index of water (1.96×10^{-9}) reported by Murphy et al. [24]. In Eq. (4), the parameter v_x is the specific volume of the microorganisms, assumed to be equal to 0.001 m^3 kg^{-1} [24]. The mass absorption and scattering cross sections, $A_{abs,\lambda}$ and $S_{sca,\lambda}$, respectively, are both expressed in m^2 kg^{-1}. The final equation will be expressed as follows:

$$\frac{dI_\lambda}{dz} = -\left(k_{L,\lambda}(1 - Xv_X) + A_{abs,\lambda} X\right) * I_\lambda - S_{sca,\lambda} X * I_\lambda + \frac{\sigma_{eff,\lambda}}{4\pi}\int I_\lambda \phi_\lambda \quad (7)$$

2.2. Boundary conditions

To solve this Eq. (7) two boundary conditions are required,

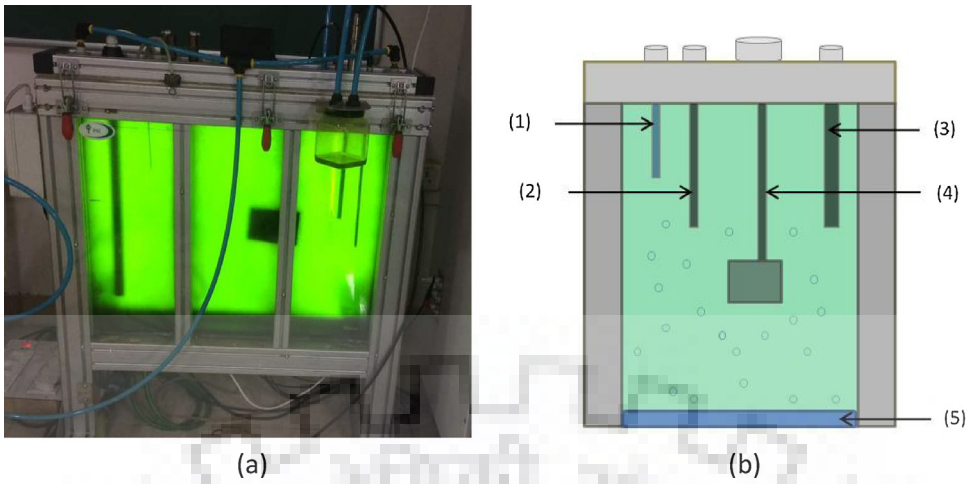

Fig. 1. (a) Experimental set up of a flat panel photobioreactor. (b) Schematic diagram of flat panel photobioreactor and the nomenclature as follows (1) pH probe, (2) Temperature probe, (3) Heating or cooling coil, (4) Online biomass monitor, (5) Porous type sparger.

At z = 0, $I_\lambda = I_{\lambda 0}$; and
at z = w, $\frac{dI_\lambda}{dz} = 0$;

2.3. Fluence rate

The incident fluence rate in PBR at any spatial position from all the direction is defined as [17,25].

$$G_\lambda = \int_{\Omega=0}^{\Omega=4\pi} I_\lambda(\vec{r}\vec{s})d\Omega \tag{8}$$

The one dimensional RTE was solved previously using two flux approximation and the solution accounted for anisotropic in-scattering terms in the RTE equation [19,26,27]. The analytical solution for local fluence rate G_λ in transparent PBR with back wall reflectance ρ_λ is defined as [19].

$$G_\lambda(z) = 2q_{in,\lambda}\frac{[\rho_\lambda(1+\alpha_\lambda)e^{-\delta_\lambda L} - (1-\alpha_\lambda)e^{e^{-\delta_\lambda L}}]e^{\delta_\lambda z} + [1+\alpha_\lambda)e^{\delta_\lambda L} - \rho_\lambda(1-\alpha_\lambda)e^{\delta_\lambda L}]e^{-\delta_\lambda z}}{(1+\alpha_\lambda)^2 e^{\delta_\lambda L} - (1-\alpha_\lambda)^2 e^{-\delta_\lambda L} - \rho_\lambda(1-\alpha_\lambda^2)e^{\delta_\lambda L} + \rho_\lambda(1-\alpha_\lambda^2)e^{-\delta_\lambda L}} \tag{9}$$

Where the parameters α_λ and δ_λ are expressed as [19].

$$\alpha_\lambda = \sqrt{\frac{\bar{A}_{abs,\lambda}}{\bar{A}_{abs,\lambda} + 2b_\lambda \bar{S}_{abs,\lambda}}} \tag{10}$$

$$\delta_\lambda = \sqrt{\bar{A}_{abs,\lambda}(\bar{A}_{abs,\lambda} + 2b_\lambda\ \bar{S}_{abs,\lambda})} \tag{11}$$

Here, b_λ denoted as the backward scattering fraction for axisymmetric phase function; as microalgae suspension grow in photobioreactors forward scattering predominates over backward scattering, then assumed b_λ tends to zero and α_λ approaches to unity. Thus the above expression can be simplified according to Lee et al. [17].

$$G_\lambda(z) = q_{in,\lambda}e^{-\bar{A}_{abs,\lambda}Xz} + \rho_\lambda q_{in,\lambda}e^{-\bar{A}_{abs,\lambda}X(2L-z)} \tag{12}$$

The simplified expression for fluence rate in PBR are given by Eq. (12) depends only on mass absorption cross section $\bar{A}_{abs,\lambda}$ of microalgae suspension, this is slightly differ from the Beer- Lambert law which is based on extinction coefficient $\beta_\lambda = \left(\bar{A}_{abs,\lambda} + \bar{S}_{abs,\lambda}\right)X$ and always over estimates the local fluence rate inside the photobioreactor.

3. Material and methods

3.1. Microalgae and culture medium

A culture of *B. braunii* was obtained from the Institute of Bioresources and Sustainable Development (IBSD, Takyelpat, Imphal). The microalgae were grown in modified BG-11 medium containing macronutrients such as $NaNO_3$ (1.12 g), $MgSO_4{\cdot}7H_2O$ (75 mg), $K_2HPO_4.3H_2O$ (40 mg), $CaCl_2{\cdot}2H_2O$ (36 mg), Na_2CO_3 (20 mg), EDTA, 2Na-Mg salt (1 mg), citric acid (6 mg), ferric ammonium citrate (6 mg) and micronutrients such as H_3BO_3 (286 μg), $MnCl_2{\cdot}4H_2O$ (181 μg), $ZnSO_4{\cdot}7H_2O$ (22 μg), $Na_2MoO_4{\cdot}2H_2O$ (39 μg), $CuSO_4{\cdot}5H_2O$ (8 μg) and $Co(NO_3)_2{\cdot}6H_2O$ (5 μg) per liter. The inoculated medium was incubated at 27 ± 1 °C and 130 rpm in a light incubator shaker. The initial pH of the medium was maintained at 8.

3.2. The photobioreactor and experimental design

The flat panel photobioreactor (Model, PSI Photon System Instruments (PSI, Brno, Czech Republic) was used for the experimental studies. The dimensions of the reactor were (0.75 m × 0.59 m × 0.068 m). For maintaining air flow a porous sparger was used. The temperature and pH of the system were precisely controlled (Fig. 1). The reactor was illuminated by high-power light emitting diodes (LEDs) placed at one side of the reactor. The irradiance could be dynamically modulated by the instrument control unit. All the experiments were conducted in control environment (i.e. 27 °C temperature and 1% CO_2) under the light intensity range of (150–1000 μmol m^{-2} s^{-1}) by LED Panel. *B. braunii* was grown in 30 l photobioreactor filled with BG-11 nutrient medium, and operating at 0.33 vvm air flow rate and 1% CO_2 (Table 1).

3.3. Determination of biomass concentration

Microalgal biomass was estimated as a function of the optical density (OD) of cell. OD of cells in the circulated liquid was determined using an UV–visible spectrophotometer (Carry 60, Agilent)

Table 1
Photobioreactor parameters selected for the experimental setup. V_L is the total volume of the photobioreactor (L), V_w is the working volume of the photobioreactor (L), H_R is the height of photobioreactor column (cm), L_R is the length of the photobioreactor column (cm), W_R is the width of the photobioreactor column (cm), A_r is the illuminated surface area of the photobioreactor (m^2).

Parameters	Symbol	Value
Total volume (L)	V_L	30
Working volume (L)	V_w	28.57
Column height (cm)	H_R	58.68
Column length (cm)	L_R	75.18
Column width (cm)	W_R	6.8
Surface Area (m^2)	A_r	0.42
Air Flow rate (vvm)		0.3
CO_2 (%)		1
Inoculum Size (L)		2.86

at an absorbance of 750 nm (OD_{750}). Dry cell weight (Dwt) was calculated using the following formula generated using OD data and a calibration plot.

$$C_b(g\,L^{-1}) = 2.155OD_{750}(R^2 = 0.99)$$

where, C_b was the dry weight of biomass and OD_{750} is the optical density measured at 750 nm. Therefore, the optical density can be used to precisely determine the dry weight of biomass.

3.4. Net specific growth rate

The net specific growth rate was calculated from Eq. (13) [28] as follows:

$$\mu_{net} = \frac{(lnN_2 - lnN_1)}{(t_2 - t_1)} \tag{13}$$

where, N_2 and N_1 were the biomass concentrations ($g\,L^{-1}$) at days t_2 and t_1, respectively. Net specific growth rate was taken in exponential phase.

3.5. Biomass growth rate using logistic model

Modeling and simulation of the microalgal growth profile were obtained using the following logistic equation [29,30].

$$\frac{dX}{dt} = K_c X\left(1 - \frac{X}{X_{max}}\right) \tag{14}$$

After integrating and rearranging Eq. (14), it was written as Eq. (15) as follows:

$$X = \frac{X_{max}}{1 + \left(\frac{X_{max}}{X_0} - 1\right)e^{-K_c t}} \tag{15}$$

where, X_{max} is the maximum concentration of microalgae ($g\,L^{-1}$), X_0 is the initial concentration of microalgae ($g\,L^{-1}$), and K_c is apparent specific growth rate (h^{-1}).

3.6. Sodium nitrate consumption kinetics

Sodium nitrate is consumed by microalgae to maintain cellular metabolism and synthesize products. Thus, the equation for sodium nitrate consumption can be expressed as follows:

$$-\frac{dS}{dt} = \frac{1}{Y_{X/S}} \times \frac{dX}{dt} + mX \tag{16}$$

where, $\frac{dS}{dt}$ is the consumption rate of sodium nitrate; $Y_{X/S}$ is the maximum microalgae growth coefficient $g\,g^{-1}$; $Y_{P/S}$ is the maximum lipid production coefficient $g\,g^{-1}$; m is maximum maintenance coefficient $g\,g^{-1}\,h^{-1}$.

At t = 0, the sodium nitrate content is given by initial sodium nitrate content ($S = S_0$). After integration, Eq. (16) becomes:

$$S = S_0 - \frac{1}{Y_{X/S}} \times \left(\frac{X_m X_0 e^{\mu_m t}}{X_m - X_0 + X_0 e^{\mu_m t}} - X_0\right) - \frac{mX_m}{\mu_m} \times ln\left(\frac{X_m - X_0 + X_0 e^{\mu_m t}}{X_m}\right) \tag{17}$$

3.7. Maximum specific substrate uptake rates

Specific substrate uptake kinetics was measured by applying the substrate mass balance to a batch culture of *B. braunii*.

$$\frac{dM_s}{dt} = q_s^{max} M_x \tag{18}$$

where, $\frac{dM_s}{dt}$ is the total consumption rate of nitrogen, t is the fermentation time, q_s^{max} is maximum specific substrate consumption rate, M_x is biomass concentration at time t.

Biomass formation kinetics can be expressed as Eq. (19).

$$\frac{dM_x}{dt} = \mu_{max} M_x \tag{19}$$

After integrating Eq. (19), it was written as Eq. (20) as follows

$$M_x = M_{x0}.\exp(\mu_{max} t) \tag{20}$$

After substituting M_x in Eq. (18)

$$\frac{dM_s}{dt} = q_s^{max} M_{x0}.\exp(\mu_{max} t) \tag{21}$$

Integrating Eq. (21) from t = 0 to t and M_{s0} to $M_s(t)$

$$M_s(t) - M_{s0} = \frac{q_s^{max} M_{x0}}{\mu_{max}}.[\exp(\mu_{max}.t) - 1]$$

$$M_s(t) - M_{s0} = \frac{q_s^{max}}{\mu_{max}}.[M_x(t) - M_{x0}] \tag{22}$$

A plot between $[M_s(t) - M_{s0}]$ vs $[M_x(t) - M_{x0}]$ was drawn, whose slope was $\left(\frac{q_s^{max}}{\mu_{max}}\right)$, where M_{s0} was the initial concentration of nitrogen ($g\,L^{-1}$), $M_s(t)$ was substrate concentration at different time ($g\,L^{-1}$), M_{x0} was initial biomass concentration and $M_x(t)$ was biomass concentration at different time points.

3.8. Lipid formation kinetics

The Luedeking-Piret model was employed to estimate lipid production in *B. braunii* using the following equation:

$$\frac{dP}{dt} = \alpha\frac{dX}{dt} + \beta X \tag{23}$$

where, $\frac{dP}{dt}$ is the rate of product formation; P is the product concentration in ($mg\,L^{-1}$); α is the growth associated coefficient ($g\,g^{-1}$); β is non-growth associated coefficient ($g\,g^{-1}$).

Product formation kinetics is divided into the following 3 classes: Class 1, when $\alpha \neq 0$ and $\beta = 0$, then product formation is microalgae growth associated; Class 2, when $\alpha = 0$and $\beta \neq 0$ the product is not related to microalgae growth, Class 3, when $\alpha \neq 0$ and $\beta \neq 0$, product is partially growth associated. As shown in (Fig. 5A–F) the lipid accumulation was initially slow in early stage of microalgal growth, whereas majority of lipid accumulated when microalgal cell entered in stationary phase. In addition other studies also suggested that lipid formation in microalgae is partially growth associated [31]. Thus, class 3 may better fit the lipid production of microalgae.

When t = 0, the product content is given by the initial product content ($P = P_0$). After integration Eq. (23) becomes:

$$P = P_0 - \alpha X_0 + \alpha \frac{X_0 * X_m * e^{\mu_m t}}{X_m - X_0 + X_0 e^{\mu_m t}} + \beta \frac{X_m}{\mu_m} \ln\left(\frac{X_m - X_0 + X_0 e^{\mu_m t}}{X_m}\right) \quad (24)$$

3.9. Estimation of nitrate concentration

Nutrient removal was determined by nitrate quantification in the culture medium. To estimate the nitrate concentration, 1 ml of sample was taken from the photobioreactor in every 12 h interval. Supernatant was separated by centrifugation at 10,000 rpm for 6 min. Nitrate concentration was determined by taking OD at 220 nm using a UV–visible spectrophotometer (Carry 60 Agilent) according to the method proposed by APHA [32].

3.10. Chlorophyll estimation

To estimate chlorophyll content in cell, 1 ml of microalgae sample was collected and centrifuged at 10,000 rpm for 10 min and the pellet was resuspended in 600 μl methanol. After that samples were heated for 5 min in water bath and cooled down to room temperature, then volume of the sample was made upto 1 ml by adding methanol, and chlorophyll content was calculated according to following equation [33].

$$\text{chla}(\text{mg L}^{-1}) = (16.5\,\text{xA}_{665}) - (8.3\,\text{xA}_{650}) \quad (25)$$

3.11. CO_2 fixation rate

The CO_2 fixation rate was determined from the carbon content of algal cells and the growth rate as follows [34].

$$R_{CO_2} = C_C \times \mu_L \times \left(\frac{M_{CO_2}}{M_C}\right) \quad (26)$$

Where, R_{CO_2} and μ_L are the fixation rate ($\text{mg L}^{-1}\ \text{d}^{-1}$) and the volumetric growth rate ($\text{mg L}^{-1}\ \text{d}^{-1}$), of *B. braunii* respectively, in the linear growth phase. M_{CO_2} and M_C represented the molecular weights of CO_2 and elemental carbon, respectively. The average C_C carbon content was 0.63 g carbon per g dry cell weight. The algal growth rate was determined in the linear growth phase because most of the algal growth occurred during this phase.

3.12. Lipid estimation

Lipid estimation in microalgae samples was performed using the modified rapid colorimetric method based on sulpho-phospho-vanillin (SPV) reaction in the presence of sulphuric acid [35,36]. The vanillin phosphoric acid reagent was prepared by dissolving 120 mg vanillin in 20 ml of distilled water and adjusting the final volume to 100 ml with 85% phosphoric acid. The reagent was stored in dark conditions until further use. SPV reagent was prepared freshly, which results in high activity with lipid samples. A known amount of *B. braunii* sample was taken in test tube and incubated for 100 °C for 5 min, and allowed to cool for 5 min in an ice bath. Freshly prepared phospho-vanillin reagent (1 ml) was then added to each test tube. The test tubes were incubated at 37 °C and 200 rpm for 15 min, and absorbance was measured at 540 nm.

3.13. Areal biomass productivity

The areal productivity of *B. braunii* can be calculated from Eq. (27). P_{areal} is the areal productivity (g m^{-2} PBR surface) determined for the time period (h) between two sampling times and the area of irradiated PBR surface (m^2).

$$P_{areal} = \frac{X_2 - X_1}{t_2 - t_1} \times \frac{V}{A} \left(\text{g m}^{-2}\ \text{h}^{-2}\right) \quad (27)$$

where, X_1 and X_2 are cell dry weight (g L^{-1}) of *B. braunii* at time t_1 and t_2, respectively. V is the working volume (m^3) and A is the illuminated surface area (m^2) of the FPBR.

3.14. Biomass yield on light energy

Biomass yield on light energy was calculated by following equation [37].

$$Y_{X,E} = \frac{P_{areal}\left(\text{g m}^{-2}\ \text{h}^{-1}\right)}{PFD_{in}\left(\mu\text{mol photons m}^{-2}\ \text{h}^{-1}\right)} \quad (28)$$

where P_{areal} was the areal biomass productivity and PFD_{in} was the average light intensity on the surface of flat panel photobioreactor.

4. Results and discussion

4.1. Radiation characteristics of B. braunii

The RTE equation given by Eq. (7) was solved by MATLAB (R2013a, MathWorks, Inc., USA). To apply the RTE equation a number of model parameters must be known. For that, most of the model parameters were retrieved from the literature while others have been experimentally determined, as detailed below.

The optical properties of *B. braunii* $\bar{C}_{ext,\lambda}$, $\bar{C}_{abs,\lambda}$ and $\bar{C}_{sca,\lambda}$ were reported previously and values were 1.68×10^{-10}, 1.84×10^{-11} and 1.500×10^{-10} ($\text{m}^2\ \text{cell}^{-1}$) respectively [38].

The average minor and major diameter of *B. braunii* microalgae cell were 10.3 and 13.3 μm respectively [16]. The average single scattering albedo (ω) was about 0.89, and their asymmetry factor g was 0.986, in the 400–800 nm spectral range [38,39]. These two parameters were dimensionless, and were independent of cell concentration.

Thus, it is more convenient to introduce the spectral mass extinction and absorption cross section denoted by $E_{ext,\lambda}$ and $A_{abs,\lambda}$ respectively. They are defined as [25].

$$E_{ext,\lambda} = \frac{\beta_\lambda}{X} \quad \text{and} \quad A_{abs,\lambda} = \frac{\kappa_\lambda}{X}$$

The extinction coefficient β_λ (m^{-1}) is obtained from normal-normal transmittance measurements of dilute suspensions. Moreover, the measurement of absorption coefficient κ_λ(m^{-1}) can be retrieved by using integrating sphere technique [39]. In this article the optical parameters of *B. braunii* including the extinction coefficient, spectral mass cross section ($\bar{C}_{abs,\lambda}$) were taken from the literature [38]. The effective absorption coefficient κ_λ of polydisperse microalgae suspension is related to the average absorption cross section, denoted by $\bar{C}_{abs,\lambda}$, as [25].

$$\kappa_\lambda = \bar{C}_{abs,\lambda} N_T \quad (29)$$

similarly κ_λ is correlated with mass spectral cross section area, denoted as following [38],

$$\kappa_\lambda = A_{abs,\lambda} X \quad (30)$$

and by using simple correlation between average absorption cross section ($\bar{C}_{abs,\lambda}$($\text{m}^2\ \text{cell}^{-1}$)) of microalgae and the mass spectral cross section $A_{abs,\lambda}$ ($\text{m}^2\ \text{kg}^{-1}$) can be expressed as

$$\bar{C}_{abs,\lambda} N_T = A_{abs,} X \quad (31)$$

The value of $\bar{C}_{abs,\lambda}$ was 1.84×10^{-11} ($\text{m}^2\ \text{cell}^{-1}$) reported for *B. braunii* [38]. The cell density N_T in each dilution was counted in

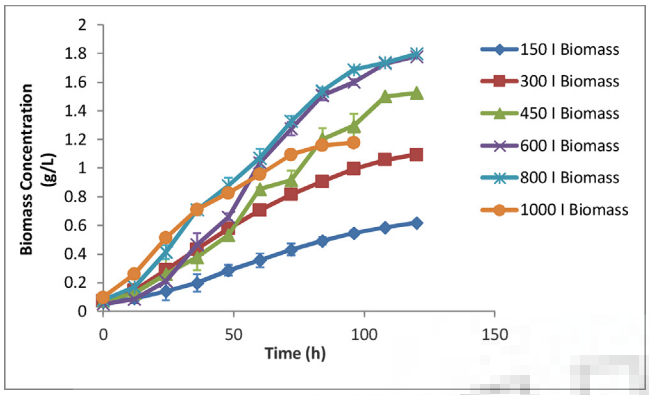

Fig. 2. Growth pattern of *B. braunii* in flat panel photobioreactor at different light intensity.

Petroff-Hausser counting chamber. The resulting calibration curves were $N_T = 11.17 \times 10^{12}$ OD_{750} and $X = 2.155$ OD_{750} with correlation coefficient R^2 of 0.99 for both calibrations, where N_T is total cell number expressed in (cell m^{-3}) and X is biomass concentration expressed as (kg m^{-3}), using all the values of coefficients and microalgae parameters, the value of $A_{abs,\lambda}$ was calculated from Eq. (31) and the observed value of $A_{abs,\lambda}$ was 95.37 (m^2 kg^{-1}). Once determined the mass spectral absorption cross section ($A_{abs,\lambda}$); $S_{sca,\lambda}$ can be calculated according to [25].

$$E_{ext,\lambda} = A_{abs,\lambda} + S_{sca,\lambda} \text{ and } S_{sca,\lambda} = E_{ext,\lambda} - A_{abs,\lambda}$$

Similarly the mass spectral scattering cross section was calculated and the value of $S_{sca,\lambda}$ was found to be 771.65 (m^2 kg^{-1}).

4.2. Effect of light intensities on biomass growth and CO_2 fixation

Effects of six different light intensities on biomass growth of *B. braunii* were studied using 30 l PSI flat panel photobioreactor. Maximum biomass concentration and maximum specific growth rate were 1.8 g L^{-1} and 1.344 d^{-1}, respectively, at light intensity of 800 μmol m^{-2} s^{-1} after 5 days of cultivation. As shown in (Fig. 2), at lower- than-optimal PPFD levels the growth of *B. braunii* may have been light-limited due to a suboptimal supply of electrons for photosynthesis [40,41]. At high light intensities the microalgae growth reached in saturation phase. Thus, considerably less increase in growth was observed. Notably, low light intensities did not support biomass growth or lipid accumulation in microalgal cells. At light intensity of 150, 300, 450, 600, 1000 μmol m^{-2} s^{-1} maximum biomass concentration and maximum specific growth rate were 0.62 g L^{-1} and 0.74 d^{-1}, 1.09 g L^{-1} and 1.128 d^{-1}, 1.52 g L^{-1} and 1.152 d^{-1}, 1.78 g L^{-1} and 1.32 d^{-1}, 1.17 g L^{-1} and 1.25 d^{-1} respectively. Similar effects of varying light intensities on growth pattern were reported by Converti et al. [42] and Kumar et al. [43].

To quantitatively analyze the effect of light intensities on the performance of carbon dioxide removal, the CO_2 fixation rate of *B. braunii* was calculated based on Eq. (26). The rate of CO_2 fixation is proportional to the biomass growth rate. The maximum CO_2 fixation rate of 826.98 mg L^{-1} d^{-1} was observed at 800 μmol m^{-2} s^{-1}. At light intensities of 150, 300, 450, 600 and 1000 μmol m^{-2} s^{-1} the CO_2 fixation rate were 286.44, 503.58, 702.24, 822.36 and 540.54 mg L^{-1} d^{-1} respectively (Table 4).

Thus, the maximum biomass productivity of 358 mg L^{-1} d^{-1} was observed at a light intensity of 800 μmol m^{-2} s^{-1} with the highest CO_2 fixation rate of 826.98 mg L^{-1} d^{-1}. In Table 5, this biomass productivity and CO_2 fixation rate is higher that obtained from other *Botryococcus* sp. such as 181.78 mg L^{-1} d^{-1} and 419.91 mg L^{-1} d^{-1} [44], 92.37 mg L^{-1} d^{-1} and 213.37 mg L^{-1} d^{-1} [45], 26.55 mg L^{-1} d^{-1} and 61.33 mg L^{-1} d^{-1} [46], 222.90 mg L^{-1} d^{-1} and 514.90 mg L^{-1} d^{-1} [47], 186 mg L^{-1} d^{-1} and 429.66 mg L^{-1} d^{-1} [48], 173.29 and 400.30 mg L^{-1} d^{-1} [49] respectively. The results obtained in present studies indicate that optimum light intensity level inside the photobioreactor significantly enhanced the biomass productivity and CO_2 biofixation rate in *B. braunii*. Light evolution and light dynamics inside the PBR can be best described by the RTE equation. The effect of cell concentration and light path on RTE and light distribution pattern were further studied.

4.3. Light intensity profile in flat panel photobioreactor

The mathematical model of light intensity profile inside the flat panel photobioreactor was solved by bvp4c solver of the MATLAB (R2013a, MathWorks, Inc., USA); this solver can solve boundary value problems in one spatial dimension. The light intensity profile at various biomass concentrations under different irradiance level are shown in (Fig. 3A–F). Light distribution inside the flat panel photobioreactor decreased with increase in cell concentration and at higher cell concentration a steeper decrease in light intensity profile was observed. As the cell concentration increases; self shading of the microalgae cells has been increased which reduces the light penetration inside the photobioreactor. These results are in accordance with Kumar et al. [43], and reported similar decrease in light penetration at higher cell concentration. This observation is also associated with light path of the reactor which signifies the lower specific growth rate of microalgae at higher light path [22,43,50]. The effect of cell concentration on light distribution profile in photobioreactor at different cultivation days are shown in Fig. 3A–F, when microorganism growth reached stationary phase the light distribution profile nearly overlapped with each other on 4th and 5th day of cultivation in photobioreactor.

In Fig. 4A–F, the RTE equation was also simulated from zero to fifth day of cultivation with different intensities and different cell concentrations. As shown in Fig. 4B, the light distribution profile comparatively reduced more at higher light intensity due to increase in cell concentration at 0.41 g L^{-1} and 0.51 g L^{-1} for 800 and 1000 μmol m^{-2} s^{-1} light intensity respectively after 1st day of cultivation. This indicates that at cell concentration (>0.41 g L^{-1}) multiple scattering and diffusive reflections reduced the light penetration. A close inspection of Fig. 4D–F reveals that at high cell concentration effective light penetration inside photobioreactor reached upto 3 cm of the panel width and almost all light patterns except (1000 μmol m^{-2} s^{-1}) overlapping each other, which signifies the occurrence of saturation in specific growth occur at higher light intensities. At the higher- than-optimal PPFD levels i.e. 1000 μmol m^{-2} s^{-1} caused photo-oxidative damage to microalgae cell which lower the specific growth rate of microalgae.

In Fig. 4E on 4th day of cultivation microalgae cells were reached their maximum growth at different cultivation lights. The exponential decay was observed in light intensities upto 3 cm width of the photobioreactor. Beyond 3 cm the light distribution profile in photobioreactor is nearly constant and becomes independent of light intensities for cell concentration above (>0.83 g L^{-1}; Fig. 4C). Therefore, it can be inferred that increasing the panel width or light intensity may not significantly enhance the microalgae growth. These results are in accordance with [22,43] which reported similar light distribution profile in phototobioreactor.

It can therefore be inferred that algal cell growth may not be significantly affected by high light intensities because of two reasons; firstly, beyond nearly 3 cm of photobioreactor width the light intensity is fairly constant and secondly increase in cell concentration causes the self shading and multiple forward light scattering or diffusive reflection by the cells which results into significant decrease in incident light intensity at the first layer of the cells than that of outer surface of vessel glass [43].

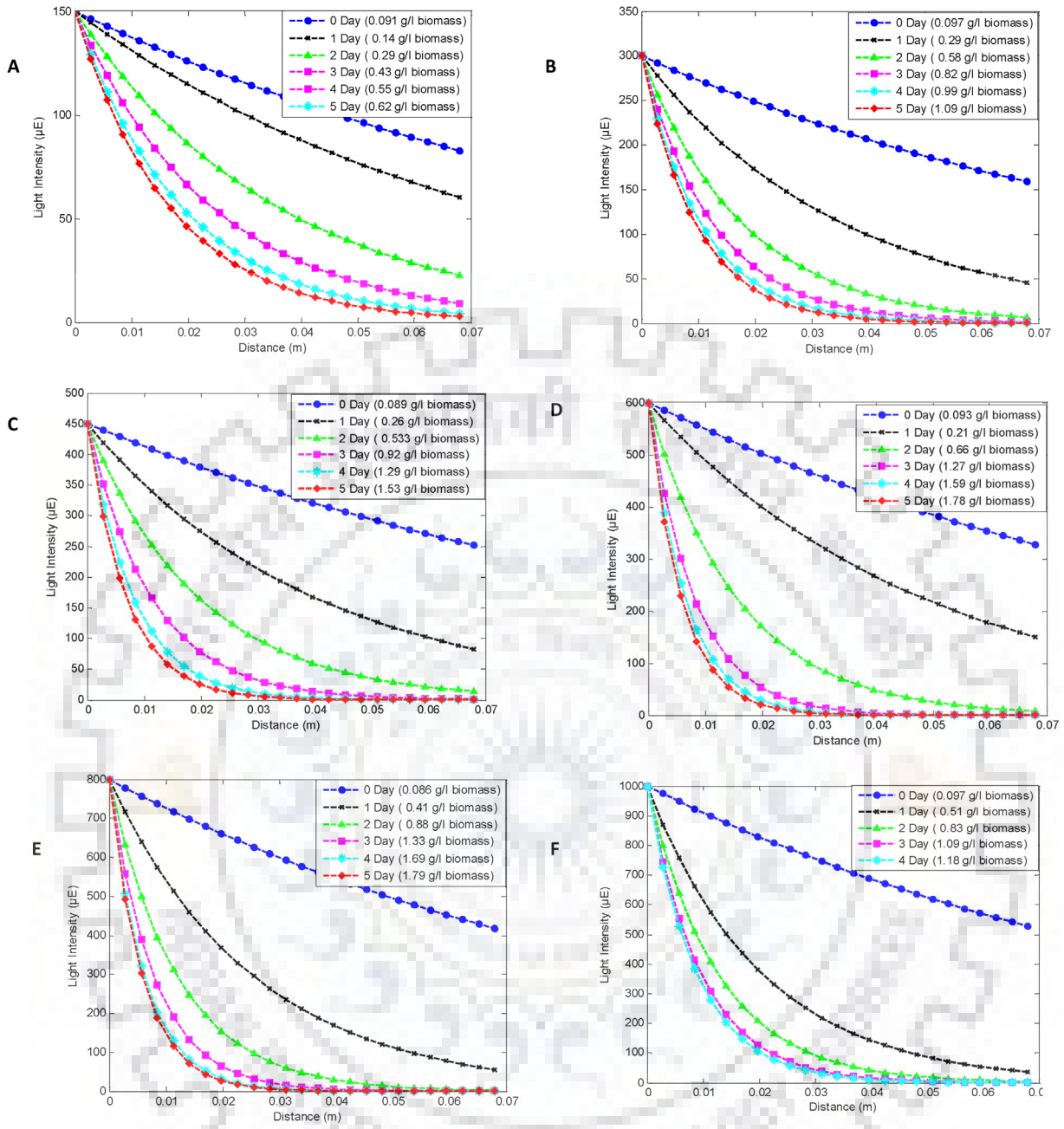

Fig. 3. Plot of light distribution pattern vs. light path distance at given light intensity of (A) 150 µmol m^{-2} s^{-1}, (B) 300 µmol m^{-2} s^{-1}, (C) 450 µmol m^{-2} s^{-1}, (D) 600 µmol m^{-2} s^{-1}, (E) 800 µmol m^{-2} s^{-1}, (F) 1000 µmol m^{-2} s^{-1}, at different cell density at different point location inside flat panel photobioreactor.

4.4. *Effect of light intensities on chlorophyll content*

It is known that light intensity directly influences microalgal cell growth and photosynthesis. Therefore, the effect of light intensity on chlorophyll concentrations was assessed under phototrophic cultivation, with varying light intensity ranging from 150 to 1000 µmol m^{-2} s^{-1} and a constant photoperiod (24:0). The chlorophyll concentration were initially increased with increase in light intensity and the maximum chlorophyll concentration of 97.23 mg L^{-1} was observed at the light intensity of 800 µmol m^{-2} s^{-1} on the fifth day of cultivation (Fig. 6). Further increase in light intensity leads to decrease in chlorophyll concentration. The chlorophyll concentration was highly inhibited at higher light intensity of 1000 µmol m^{-2} s^{-1} and approximately 25.79% reduction in chlorophyll concentration (72.15 mg L^{-1}) was observed from the maximum chlorophyll concentration. At light intensities of 150, 300, 450, 600 µmol m^{-2} s^{-1} maximum observed chlorophyll concentration were 41.59, 70.34, 89.83, 96.34 mg L^{-1} respectively. It is noteworthy that light intensity did not have a significant impact on cell growth but stimulated chlorophyll content in cells remarkably at higher light intensity (Table 4). The results were consistent with [51,52], as their optimal range of light intensities were 80–150 µmol m^{-2} s^{-1} and 100–200 µmol m^{-2} s^{-1} respectively suitable for higher chlorophyll content (g g^{-1}). In this study the optimal range for higher pigment content was also lies in this region (Table 4). The pigment content in microalgae cells are significantly affected by incident PFD by a well known phenomenon, called photoacclimation, which can be induced by light intensities, leading to decrease in pigment contents with increasing PPFD [52].

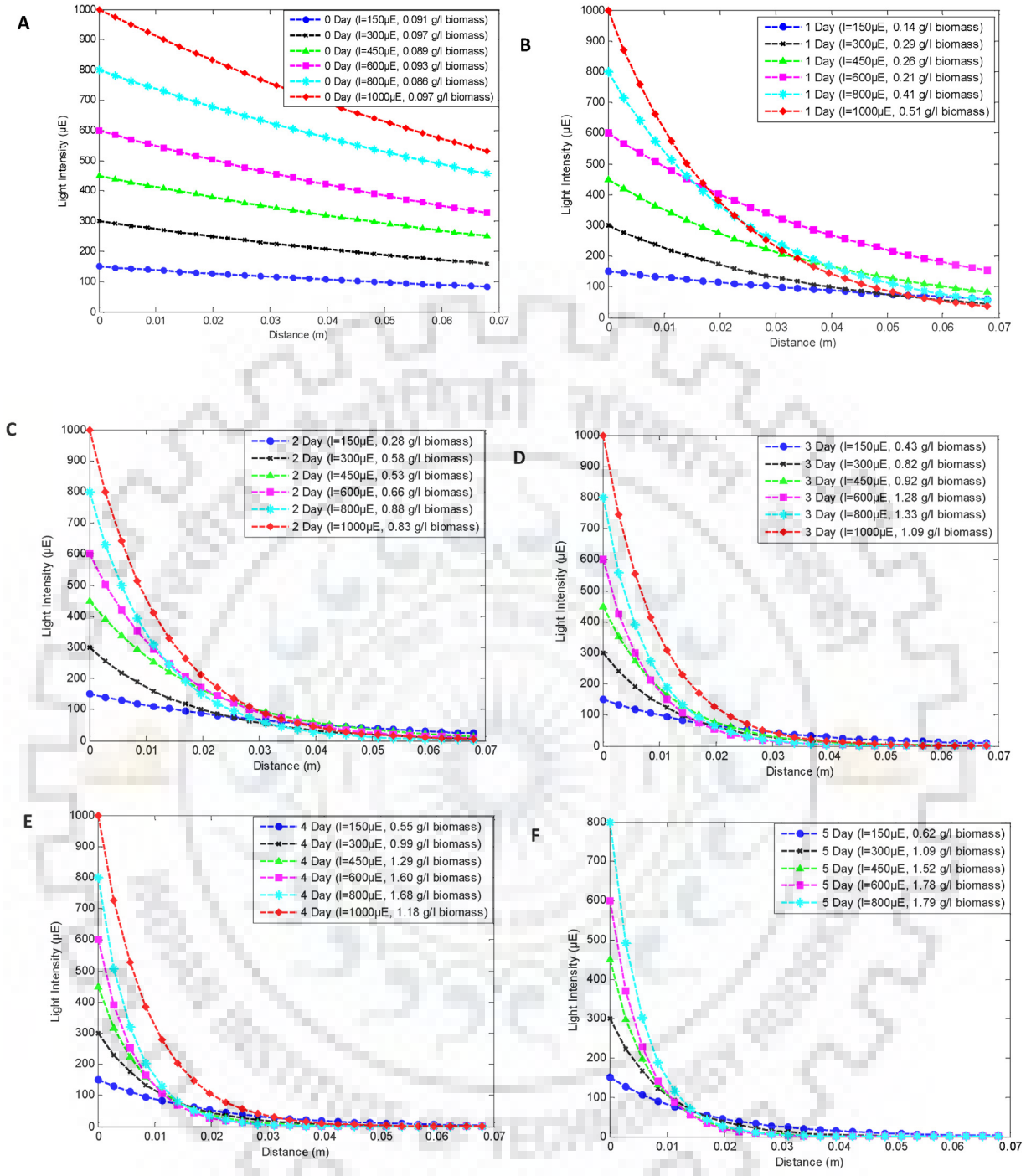

Fig. 4. Comparison plot of light distribution pattern vs. light path distance at varying light intensity (from 150 to 1000 $\mu mol\, m^{-2}\, s^{-1}$) (A) Day 0, (B) Day 1, (C) Day 2, (D) Day 3, (E) Day 4, (F) Day 5, at different cell density at different point location inside flat panel photobioreactor.

4.5. *Effect of light intensities on lipid productivities*

Effect of varying light conditions on lipid content and lipid productivities were evaluated. Maximum lipid content and maximum lipid productivity of 27.37% and 86.4 $mg\, L^{-1}\, d^{-1}$ were observed at light intensities of 450 $\mu mol\, m^{-2}\, s^{-1}$ and 600 $\mu mol\, m^{-2}\, s^{-1}$ respectively. At high light intensities of 600, 800 and 1000 $\mu mol\, m^{-2}\, s^{-1}$ the lipid content of *B. braunii* decreased to 24.27%, 22.23% and 19.74% respectively. At low light intensities of 150 and 300 $\mu mol\, m^{-2}\, s^{-1}$ low levels of lipid accumulation corresponding to 10.65% and 20.18%, respectively, were observed (Table 3). However, the lipid content and yield in culture were considerably lower at low light intensities than at intermediate light intensities. Thus, lipid accumulation could be promoted by increasing the light intensity from 150 to 450 $\mu mol\, m^{-2}\, s^{-1}$; however, further increase in light intensity reduced lipid formation.

An intermediate light intensity was observed to be more suitable for lipid accumulation than high light intensities. Since high light intensities enhanced the microalgal growth, the microalgae might use synthesized energy to divide themselves, rather than store it as lipid [53]. Moreover, Guedes et al. [54] reported that lipid content decreased while light intensity increased because lipids were major components of chloroplasts, so an increase in light intensity overcomes the need for a high chloroplastidial activ-

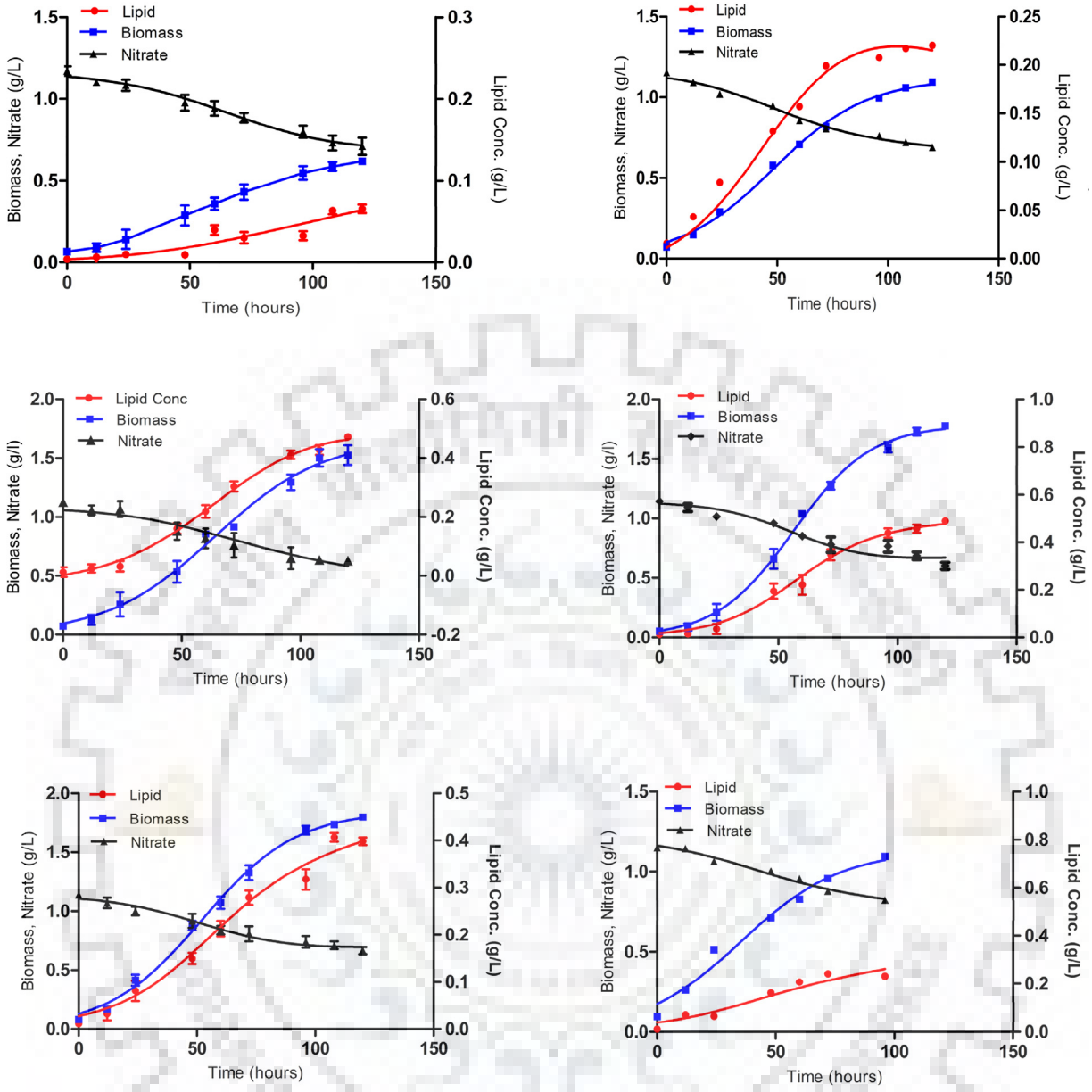

Fig. 5. (A–F) Experimental and simulated biomass, lipid and nitrate profile of *B. braunii* in flat panel photobioreactor at light intensities of (150–1000 μmol m^{-2} s^{-1}) respectively.

ity. However, Ho et al. [55] reported that no significant variations occurred in lipid content of *S. obliquus* CNW-N with respect to light intensity. Sukenik et al. [67,68] reported that the lipid content of *Nannochloropsis* sp. and *Isochrysis galbana* increased with increase in light intensity, whereas Chrismadha et al. [69] did not detect any effect of irradiance on the lipid content of *Phaeodactylum tricornutum*, and concluded that the correlation of light intensity and lipid content is usually species- specific [55,69].

In present study, the production of lipids, (86.4 mg L^{-1} d^{-1}) was observed to be higher than that observed in the previous studies: 46.90 mg L^{-1} d^{-1} [44], 11.74 mg L^{-1} d^{-1} [45], 5.51 mg L^{-1} d^{-1} [46], 69.1 mg L^{-1} d^{-1} [47], 15.66 mg L^{-1} d^{-1} [57], 61.38 mg L^{-1} d^{-1} [48], 58.40 mg L^{-1} d^{-1} [49] (Table 5). Lipid content was also compared to the data reported previously. It was observed that lipid content (27.37%) measured in the present study was slightly lower than previously reported values such as 54.69% [57], 33.7% [49] and 33% [48] (Table 5). It must be noted that the results can vary according to methodology used for determination of lipid content. Moreover, lipid accumulation also changes according to the strain and culture conditions used, such as nitrogen deprivation which generally increases algal lipid content [56]. Although, results suggests that mid level light intensity is optimum for higher lipid accumulation in microalgae.

4.6. Kinetic studies

4.6.1. Growth kinetics under different light intensities

Biomass concentrations of *B. braunii* under different light intensities were fitted by Eq. (15). As shown in Fig. 7a and b, the model fits well to the experimental data. The model parameter i.e. (X_0, X_m and K_c) were evaluated by logistic rate equation and presented in Table 2. As depicted in Table 2, the increasing light intensity in photobioreactor, the value of X_m was increased in the range of (150–800 μmol m^{-2} s^{-1}) light intensity, but the K_c was decreased when light intensity was higher than 600 μmol m^{-2} s^{-1}. This indicated that a higher light intensity negatively affected the algal

Table 2
K_c is the apparent specific growth rate of the microalgae; X_0 is the initial biomass concentration; X_m is the maximum biomass concentration of microalgae; P_0 is the initial lipid content; α is the growth correlation coefficient; β is the non-growth correlation coefficient; S_0 is the sodium nitrate concentration; $Y_{X/S}$ is the maximum microalgal growth coefficient; and m is the maximum maintenance coefficient.

Parameters	150 μmol m^{-2} s^{-1}	300 μmol m^{-2} s^{-1}	450 μmol m^{-2} s^{-1}	600 μmol m^{-2} s^{-1}	800 μmol m^{-2} s^{-1}	1000 μmol m^{-2} s^{-1}
Biomass						
K_c (h^{-1})	0.0404	0.047	0.0483	0.0614	0.050	0.047
X_0 (g L^{-1})	0.061	0.113	0.114	0.101	0.178	0.17
X_m (g L^{-1})	0.66	1.118	1.518	1.614	1.697	1.20
R^2	0.9982	0.9959	0.9975	0.9931	0.9912	0.9925
Lipid						
P_0 (g L^{-1})	0.013	0.0263	0.038	0.04	0.029	0.0325
α (g g^{-1})	0.022	0.274	0.5353	0.226	0.1761	0.1637
β (g g^{-1})	1.75×10^{-4}	-1.2×10^{-3}	-7.2×10^{-4}	3.7×10^{-4}	7.3×10^{-4}	1.2×10^{-4}
R^2	0.87	0.99	0.99	0.99	0.986	0.935
Nitrate						
S (g L^{-1})	1.173	1.163	1.08	1.141	1.14	1.21
$Y_{X/S}$ (g g^{-1})	1.779	1.897	1.982	4.642	4.12	4.79
m (g g^{-1} h^{-1})	2.2×10^{-3}	-1.66×10^{-3}	-1.4×10^{-3}	5.8×10^{-4}	4.4×10^{-4}	-1.23×10^{-3}
R^2	0.986	0.985	0.94	0.959	0.975	0.977

Table 3
Maximum biomass, lipid concentration, lipid content, biomass and lipid productivity under varying light regimes.

Light Intensity (μmol m^{-2} s^{-1})	X_{max} (g L^{-1})	P_{max} (g L^{-1})	Lipid Content (%)	Biomass Productivity (mg L^{-1} d^{-1})	Lipid Productivity (mg L^{-1} d^{-1})
150	0.62	0.066	10.65	124	13.2
300	1.09	0.22	20.18	218	44.0
450	1.52	0.416	27.37	304	83.2
600	1.78	0.432	24.27	356	86.4
800	1.79	0.398	22.23	358	79.6
1000	1.17	0.231	19.74	292.5	57.75

Table 4
Effect of light intensity on chlorophyll content, maximum specific nitrate uptake rate (q_s^{max}), maximum specific growth rate (μ_{max}) and CO_2 consumption rate. (**Note**: negative values of q_s^{max} indicates that substrate is consuming with respect to time).

Light Intensity μmol m^{-2} s^{-1}	Chlorophyll Content (%)	q_s^{max} (g g_b h^{-1})	μ_{max} (h^{-1})	R_{CO_2} (mg L^{-1} d^{-1})
150	6.68	−0.03131	0.031	286.44
300	6.45	−0.02872	0.047	503.58
450	5.91	−0.02174	0.048	702.24
600	5.41	−0.0165	0.055	822.36
800	5.43	−0.01568	0.056	826.98
1000	6.16	−0.01404	0.052	540.54

Table 5
Comparison of phototrophic growth and lipid production using *B. braunii* with the literature reported values.

Medium type	Type of cultivation	Biomass Productivity (mg L^{-1} d^{-1})	CO_2 fixation rate (mg L^{-1} d^{-1})	Lipid Content (%)	Lipid Productivity (mg L^{-1} d^{-1})	Reference
Chu-13	Erlenmeyer Flask	181.78	419.91	25.8	46.9	[44]
BG-11	Tubular Photobioreactor	92.37	213.37	12.71	11.74[a]	[45]
Chu-13	Bioreactor	26.55	61.33	20.75	5.51	[46]
Wastewater	CSTR PBR	222.90	514.90	31	69.1	[47]
Chlorella medium	Glass flask with continuous illumination	28.63	66.14	54.69	15.66[a]	[57]
3N-MBM	CSTR PBR	186	429.66	33	61.38	[48]
Chu-13	Tubular PBR	173.29	400.30	33.7	58.40[a]	[49]
BG-11	Flat Panel Photobioreactor	358	826.98	22.23	79.6	Present study
BG-11	Flat Panel Photobioreactor	304	702.24	27.37	83.2	Present study

[a] Calculated values from the given data from literatures.

growth rate which was also reported by Chen et al. [58]. Yoshimura et al. [59] found that the maximum specific growth rate for *B. braunii* was 0.50 d^{-1} at 850 μmol m^{-2} s^{-1}. Similar results were reported by Sasi et al. [60] who pointed that higher PAR density (>44.2 mW L^{-1}) in circulating loop photobioreactor for *Chlorella* did negatively affect the specific growth rate. In this work, the maximum specific growth rate shows a strong dependency on irradiance; the maximal specific growth at 800 μmol m^{-2} s^{-1} is up to 1.344 d^{-1}. The maximum specific growth rate revealed in this study is, to our best knowledge, the highest specific growth rate for *B. braunii* reported in the previous studies (Table 6).

4.6.2. Nitrate uptake kinetics and specific nitrate uptake rates under different light intensities

Sodium nitrate consumption kinetics under different irradiance level was calculated by using Eq. (17). The experimental data was fitted in Eq. (18) and the estimated parameter values of S_0, $Y_{X/S}$ and m are listed in Table 2. A good correlation with the model equation indicated that nitrate consumption in FPBR by *B. braunii* could be

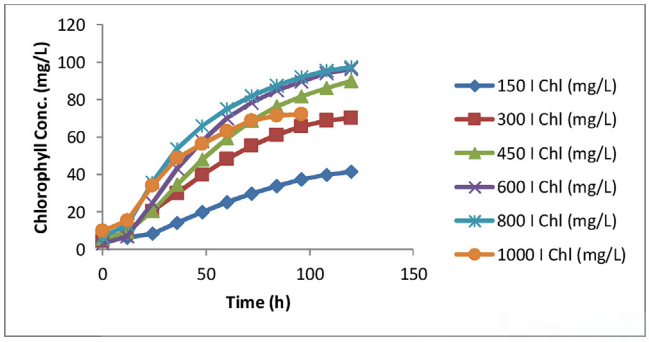

Fig. 6. Chlorophyll concentration of *B. braunii* in flat panel photobioreactor at different light intensity.

Table 6
Comparison of specific growth rate of *B. braunii* with the literature reported values.

Light Intensity ($\mu mol\ m^{-2}\ s^{-1}$)	$\%CO_2$	Specific growth rate (d^{-1})	Reference
850	1	0.50	[59]
250	0.3	0.42	[65]
1.2 klux	2	0.07[a]	[66]
150	20	0.13[a]	[45]
200	0	0.10[a]	[57]
800	1	1.344	Present Study

[a] Calculated values from the given data in literatures.

well described using Eq. (18). In addition, the values of $Y_{X/S}$ at 150, 300 and 450 $\mu mol\ m^{-2}\ s^{-1}$ light intensities were similar, but lower than those observed at 600, 800 and 1000 $\mu mol\ m^{-2}\ s^{-1}$ (Table 2). This suggested that intermediate light intensity was more suitable compared to high or low light intensity. The values of maintenance coefficient (m) in all cultures were either very low or negative, which potentially indicated that a small amount of light in culture was required to maintain the metabolic activity of microalgal cell. The values of $Y_{X/S}$ as shown in Table 2, continuously increased with an increase in light intensity upto the 600 $\mu mol\ m^{-2}\ s^{-1}$, however, further increase in light intensity reduced the values of $Y_{X/S}$, this indicates that high light intensity negatively affect the nitrate consumption rate and biomass yield on nitrate under the influence on high irradiance.

To quantitatively analyze the effect of light intensities on nitrate removal, the specific nitrate uptake rate (q_s^{max}) of *B. braunii* was calculated based on Eq. (22). Under low light conditions (150 $\mu mol\ m^{-2}\ s^{-1}$), it was observed that specific nitrate uptake rate 0.0313 $g\ g_b^{-1}\ h^{-1}$ was the highest. As the light intensity increased, corresponding q_s^{max} decreased and the lowest value of q_s^{max} was 0.0140 $g\ g_b^{-1}\ h^{-1}$ observed at 1000 $\mu mol\ m^{-2}\ s^{-1}$ (Table 4). The nitrate uptake mechanism in phytoplanktons is not completely understood, although it is assumed that active transport of nitrate across the cell membrane is an energy intensive process [61]. At the moment, the fact that algae had a higher value of $Y_{X/S}$ and lower values of q_s^{max} under the higher light intensities, cannot be explained and needs to be investigated further. These results are in accordance to Gonçalves et al. [62] who reported similar trend of nitrogen removal under the influence of high light intensity, and shown that increase in light intensity from 105 to 180 $\mu mol\ m^{-2}\ s^{-1}$ the two species of microalgae, *Chlorella vulgaris* and *Synechocystis salina* reduced nitrogen removal rate from 2.78 to 2.43 $mg\ L^{-1}\ d^{-1}$ and 2.54 to 1.97 $mg\ L^{-1}\ d^{-1}$ respectively. The results reported in present study has also shown similar trend of nitrate consumption under different level of irradiance.

4.6.3. Lipid formation kinetics under different light intensities

Lipid formation kinetics was analyzed using Luedeking-Piret Eq. (23). The experimental data was fitted in Eq. (24) and the parameters values were listed in Table 2. Based on observation of Fig. 5, and correlation coefficient in Table 2, the experimental data was fitting well to the model equation, indicating the lipid production in *B. braunii* culture in FPBR can be best described by Luedeking-Piret equation. As depicted in Table 2, the growth associated coefficient (α) increased with increase in the biomass concentration upto the 450 $\mu mol\ m^{-2}\ s^{-1}$ light intensity, suggesting that lipid accumulation is growth associated in this range (150–450 $\mu mol\ m^{-2}\ s^{-1}$), further increase in light intensity from (600–1000 $\mu mol\ m^{-2}\ s^{-1}$) value of α decreased, indicating that high light intensity negatively affect the lipid accumulation in *B. braunii*. The results are consistent with Ho et al. [55] as their study indicated that higher light intensity (>420 $\mu mol\ m^{-2}\ s^{-1}$) reduced the lipid content and lipid yield in *S. obliquus* CNW-N. The non-growth associated coefficient (β) was found negative for 300 and 450 $\mu mol\ m^{-2}\ s^{-1}$ light intensity, but under low light (150 $\mu mol\ m^{-2}\ s^{-1}$) and high light intensities (600–1000 $\mu mol\ m^{-2}\ s^{-1}$) the value of β varied from (1.2 to $7.3 \times 10^{-4}\ g\ g^{-1}$), suggesting that lipid formation under this range of light intensity is partially growth associated (Class 3). Although the kinetic parameters obtained in this study suggested that optimal range of light intensity for maximum lipid production lied between 300 to 450 $\mu mol\ m^{-2}\ s^{-1}$. This could be explained further by the lipid yield on light energy.

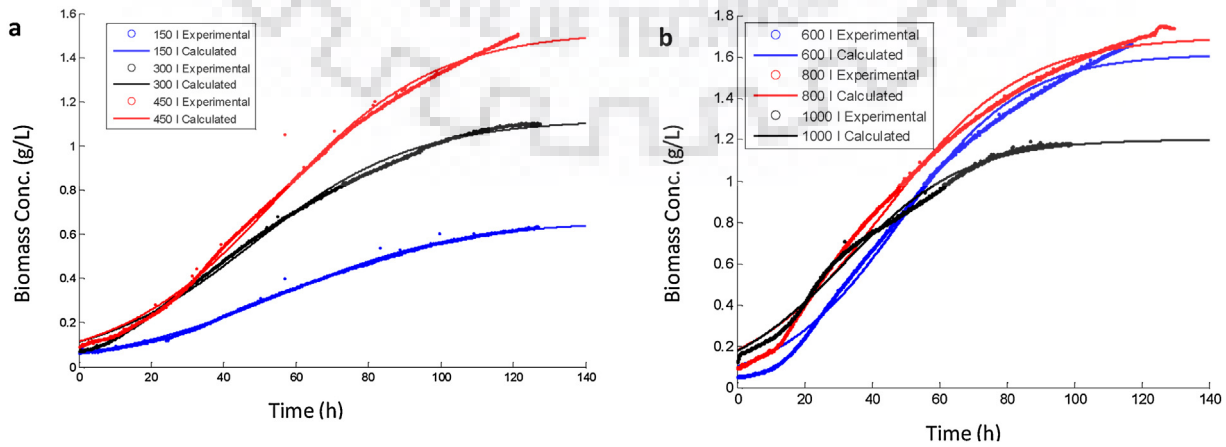

Fig. 7. (a) and (b) Simulated cell growth profile of *B. braunii* in flat panel photobioreactor at different light intensities. Experimental data (approximate 1500 data points) is fitted with logistic equation. X_{max} and K_c obtained from simulated logistic model in MATLAB.

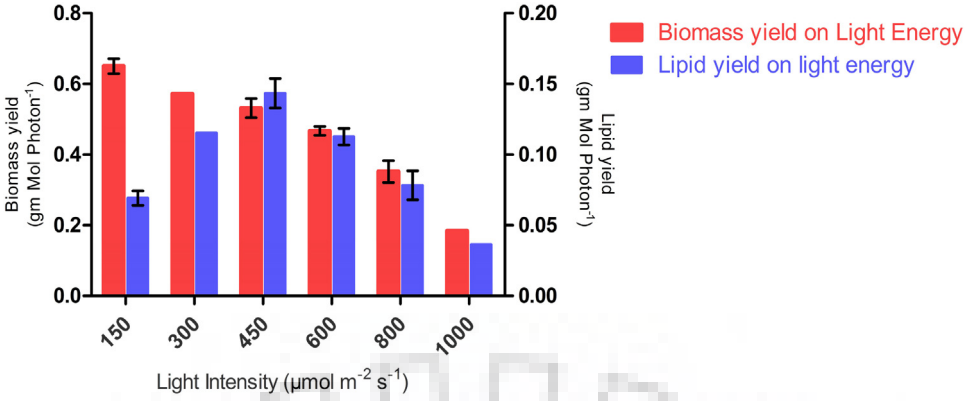

Fig. 8. Showing the effect of light intensities on biomass and lipid yield.

4.7. *Effect of light intensities on biomass and lipid yield*

The effect of light intensity on biomass yield and lipid yield of *B. braunii* were summarized in Fig. 8. Biomass yield on light energy was decreased from 0.65 to 0.23 g mol photons^{-1} in a linear mode. This suggests that higher algal growth at high light intensities reduced the effective light penetration inside the photobioreactor and results in lower biomass yield. The similar results were also reported by Zijffers et al. [63] who explained that increase in biomass concentration at high light intensity may decreased the light utilization efficiency of microalgae. The results of the present studies were compared with the other photobioreactor systems in which *B. braunii* were cultivated, such as Cheng et al. [64] reported biomass yield on light energy had value of 0.75 g mol photons^{-1} at 100 μmol m^{-2} s^{-1}. In addition, the lipid yields on light energy (Fig. 8) increased from 0.069 to 0.146 g mol photons^{-1} for the light intensity range of 150–450 μmol m^{-2} s^{-1}, further increase in light intensity, a steeper decrease in lipid yield was observed at 600 μmol m^{-2} s^{-1} and follows the similar trend when the light intensity beyond the 450 μmol m^{-2} s^{-1}. These results indicate that mid level light intensities up to the 450 μmol m^{-2} s^{-1} in flat panel photobioreactor is optimum for higher lipid productivities.

5. Conclusions

In the present study, the effect of varying light regimes on light dynamics, biomass growth and lipid kinetics in flat panel photobioreactor has been evaluated. Simulation of light energy flux balance across the panel width showed the light distribution pattern inside the photobioreactor. Self shading of the microalgae cell reduced the effective light penetration beyond the 3 cm width of the photobioreactor irrespective of the incident light intensity at high biomass concentration. The lowest value of biomass and lipid yield on light energy was 0.23 and 0.045 g mol photons^{-1} achieved at 1000 μmol m^{-2} s^{-1}. The maximum lipid yield and lipid content of 0.146 g mol photons^{-1} and 27.37% w/w was achieved at 450 μmol m^{-2} s^{-1} light intensity. Growth kinetics and lipid kinetics models were found to give reasonably good fit with experimental data. It is concluded that *B. braunii* shows optimum biomass and lipid productivities with mid level light intensities region (300–600 μmol m^{-2} s^{-1}) and higher light intensities produced the photooxidative damage to the microalgae cell. Suitable light distribution pattern facilitate its application in improved design of photobioreactor productivity system in flat panel photobioreactor.

Acknowledgements

We gratefully acknowledge the financial support for Department of Biotechnology (DBT), Government of India for providing JRF fellowship to SSK (Fellowship Grant No.: 8798-35-044) for completion of the project (Contingency Grant No.: 8798-35-061).

Appendix A. Supplementary data

Supplementary data associated with this article can be found, in the online version, at https://doi.org/10.1016/j.bej.2018.03.001.

References

[1] R. Huerlimann, R. de Nys, K. Heimann, Growth lipid content, productivity, and fatty acid composition of tropical microalgae for scale-up production, Biotechnol. Bioeng. 107 (2010) 245–257.
[2] B.S.B. Bamba, P. Lozano, F. Adjé, A. Ouattara, M.A. Vian, C. Tranchant, Y. Lozano, Effects of temperature and other operational parameters on *Chlorella vulgaris* mass cultivation in a simple and low-cost column photobioreactor, Appl. Biochem. Biotechnol. 177 (2015) 389–406.
[3] J. Cabello, A.T. Cervantes, L. Sánchez, S. Revah, M. Morales, Effect of the temperature, ph and irradiance on the photosynthetic activity by *Scenedesmus obtusiusculus* under nitrogen replete and deplete conditions, Bioresour. Technol. 181 (2015) 128–135.
[4] G. Breuer, P.P. Lamers, D.E. Martens, R.B. Draaisma, R.H. Wijffels, Effect of light intensity ph, and temperature on triacylglycerol (tag) accumulation induced by nitrogen starvation in *Scenedesmus obliquus*, Bioresour. Technol. 143 (2013) 1–9.
[5] Y. Zhao, J. Wang, H. Zhang, C. Yan, Y. Zhang, Effects of various LED light wavelengths and intensities on microalgae-based simultaneous biogas upgrading and digestate nutrient reduction process, Bioresour. Technol. 136 (2013) 461–468.
[6] J. Wang, J. Liu, T. Liu, The difference in effective light penetration may explain the superiority in photosynthetic efficiency of attached cultivation over the conventional open pond for microalgae, Biotechnol. Biofuels 8 (2015) 49–61.
[7] B.D. Fernandes, G.M. Dragone, J.A. Teixeira, A.A. Vicente, Light regime characterization in an airlift photobioreactor for production of microalgae with high starch content, Appl. Biochem. Biotechnol. 161 (2010) 218–226.
[8] I. Gajda, J. Greenman, C. Melhuish, I. Ieropoulos, Self-sustainable electricity production from algae grown in a microbial fuel cell system, Biomass Bioenergy 82 (2015) 87–93.
[9] L. Brennan, P. Owende, Biofuels from microalgae—a review of technologies for production processing, and extractions of biofuels and co-products, Renew. Sustain. Energy Rev. 14 (2010) 557–577.
[10] J. Dauchet, S. Blanco, J.F. Cornet, R. Fournier, Calculation of the radiative properties of photosynthetic microorganisms, J. Quant. Spectrosc. Radiat. Transf. 161 (2015) 60–84.
[11] R. Kandilian, T.C. Tsao, L. Pilon, Control of incident irradiance on a batch operated flat-plate photobioreactor, Chem. Eng. Sci. 119 (2014) 99–108.
[12] A.P. Carvalho, S.O. Silva, J.M. Baptista, F.X. Malcata, Light requirements in microalgal photobioreactors: an overview of biophotonic aspects, Appl. Microbiol. Biotechnol. 89 (2010) 1275–1288.
[13] N. Murata, S. Takahashi, Y. Nishiyama, S.I. Allakhverdiev, Photoinhibition of photosystem II under environmental stress, Biochim. Biophys. Acta Bioenergy 1767 (2007) 414–421.

[14] J.F. Cornet, C.G. Dussap, J.B. Gros, A simplified monodimensional approach for modeling coupling between radiant light transfer and growth kinetics in photobioreactors, Chem. Eng. Sci. 50 (1995) 1489–1500.
[15] J.F. Cornet, C.G. Dussap, G.A. Dubertret, Structured model for simulation of cultures of the cyanobacterium *Spirulina platensis* in photobioreactors: I. Coupling between light transfer and growth kinetics, Biotechnol. Bioeng. 40 (1992) 817–825.
[16] H. Berberoglu, L. Pilon, Experimental measurements of the radiation characteristics of *Anabaena variabilis* ATCC 29413-U and *Rhodobacter sphaeroides* ATCC 49419, Int. J. Hydrogen Energy 32 (2007) 4772–4785.
[17] E. Lee, J. Pruvost, X. He, R. Munipalli, L. Pilon, Design tool and guidelines for outdoor photobioreactors, Chem. Eng. Sci. 106 (2014) 18–29.
[18] B. Kong, R.D. Vigil, Simulation of photosynthetically active radiation distribution in algal photobioreactors using a multidimensional spectral radiation model, Bioresour. Technol. 158 (2014) 141–148.
[19] L. Pottier, J. Pruvost, J. Deremetz, J.F. Cornet, J. Legrand, C.G. Dussap, A fully predictive model for one-dimensional light attenuation by *Chlamydomonas reinhardtii* in a torus photobioreactor, Biotechnol. Bioeng. 91 (2005) 569–582.
[20] Z. Csögör, M. Herrenbauer, K. Schmidt, C. Posten, Light distribution in a novel photobioreactor- modelling for optimization, J. Appl. Phycol. 13 (2001) 325–333.
[21] J. Pruvost, L. Pottier, J. Legrand, Numerical investigation of hydrodynamic and mixing conditions in a torus photobioreactor, Chem. Eng. Sci. 61 (2006) 4476–4489.
[22] Q. Huang, L. Yao, T. Liu, J. Yang, Simulation of the light evolution in an annular photobioreactor for the cultivation of *Porphyridium cruentum*, Chem. Eng. Sci. 84 (2012) 718–726.
[23] A. Limert, A. Kienle, Exact and efficient solution of the radiative transport equation for the semi-infinite medium, Sci. Rep. 3 (2013) 2018.
[24] T.E. Murphy, H. Berberoglu, Flux balancing of light and nutrients in a biofilm photobioreactor for maximizing photosynthetic productivity, Biotechnol. Prog. 30 (2014) 348–359.
[25] L. Pilon, H. Berberoğlu, R. Kandilian, Radiation transfer in photobiological carbon dioxide fixation and fuel production by microalgae, J. Quant. Spectrosc. Radiat. Transf. 112 (2011) 2639–2660.
[26] M.F. Modest, Radiative Heat Transfer, third ed., Elsevier, Oxford, UK, 2013.
[27] R. Kandilian, A. Soulies, B. Rousseau, J. Pruvost, J. Legrand, L. Pilon, Simple method to measure spectral absorption cross-section of microalgae, Chem. Eng. Sci. 146 (2016) 357–368.
[28] K. Issarapayup, S. Powtongsook, P. Pavasant, Flat panel airlift photobioreactors for cultivation of vegetative cells of microalga *Haematococcus pluvialis*, J. Biotechnol. 142 (2009) 227–232.
[29] J.J. Gilbert, S. Ray, D. Das, Hydrogen production using *Rhodobacter sphaeroides* (O.U. 001) in a flat panel rocking photobioreactor, Int. J. Hydrogen Energy 36 (2011) 3434–3441.
[30] K. Kumar, D. Das, Growth characteristics of *Chlorella sorokiniana* in airlift and bubble column photobioreactors, Bioresour. Technol. 116 (2012) 307–313.
[31] Y. He, L. Chen, Y. Zhou, H. Chen, X. Zhou, F. Cai, J. Huang, M. Wang, B. Chen, Z. Guo, Analysis and model delineation of marine microalgae growth and lipid accumulation in flat-plate photobioreactor, Biochem. Eng. J. 111 (2016) 108–116.
[32] APHA, Standard Methods for the Examination of Water and Wastewater, 14 ed., APHA American Public Health Association, 1976.
[33] S. Aslan, I.K. Kapdan, Batch kinetics of nitrogen and phosphorus removal from synthetic wastewater by algae, Ecol. Eng. 28 (2006) 64–70.
[34] Y.S. Yun, S.B. Lee, J.M. Park, C.I. Lee, J.W. Yang, Carbon dioxide fixation by algal cultivation using wastewater nutrients, J. Chem. Technol. Biotechnol. 69 (1997) 451–455.
[35] Y.S. Cheng, Y. Zheng, J.V. Gheynst, Rapid quantitative analysis of lipids using a colorimetric method in a microplate format, Lipids 46 (2011) 95–103.
[36] A.R. Byreddy, A. Gupta, C.J. Barrow, M. Puri, A quick colorimetric method for total lipid quantification in microalgae, J. Microbiol. Methods 125 (2016) 28–32.
[37] M. Leupold, S. Hindersin, M. Kerner, D. Hanelt, The effect of discontinuous airlift mixing in outdoor flat panel photobioreactors on growth of *Scenedesmus obliquus*, Bioprocess Biosyst. Eng. 36 (2013) 1653–1663.
[38] H. Berberoglu, P.S. Gomez, L. Pilon, Radiation characteristics of *Botryococcus braunii*, *Chlorococcum littorale*, and *Chlorella* sp. used for fixation and biofuel production, J. Quant. Spectrosc. Radiat. Transf. 110 (2009) 1879–1893.
[39] H. Berberoglu, L. Pilon, A. Melis, Radiation characteristics of *Chlamydomonas reinhardtii* CC125 and its truncated chlorophyll antenna transformants tla1, tlaX and tla1-CW+, Int. J. Hydrogen Energy 33 (2008) 6467–6483.
[40] E. Jacob-Lopes, S. Revah, S. Hernández, K. Shirai, T.T. Franco, Development of operational strategies to remove carbon dioxide in photobioreactors, Chem. Eng. J. 153 (2009) 120–126.
[41] I. Ketseoglou, G. Bouwer, Optimization of photobioreactor growth conditions for a cyanobacterium expressing mosquitocidal *Bacillus thuringiensis* Cry proteins, J. Biotechnol. 167 (2013) 64–71.
[42] A. Converti, A. Lodi, A.D. Borghi, C. Solisio, Cultivation of *Spirulina platensis* in a combined airlift-tubular reactor system, Biochem. Eng. J. 32 (2006) 13–18.
[43] K. Kumar, A. Sirasale, D. Das, Use of image analysis tool for the development of light distribution pattern inside the photobioreactor for the algal cultivation, Bioresour. Technol. 143 (2013) 88–95.
[44] C. Yeesang, B. Cheirsilp, Effect of nitrogen salt, and iron content in the growth medium and light intensity on lipid production by microalgae isolated from freshwater sources in Thailand, Bioresour. Technol. 102 (2011) 3034–3040.
[45] Y. Ge, J. Liu, G. Tian, Growth characteristics of *Botryococcus braunii* 765 under high CO_2 concentration in photobioreactor, Bioresour. Technol. 102 (2011) 130–134.
[46] C. Yoo, S.Y. Jun, J.Y. Lee, C.Y. Ahn, H.M. Oh, Selection of microalgae for lipid production under high levels carbon dioxide, Bioresour. Technol. 101 (2010) S71–S74.
[47] C. Yeesang, B. Cheirsilp, Low-cost production of green microalga *Botryococcus braunii* biomass with high lipid content through mixotrophic and photoautotrophic cultivation, Appl. Biochem. Biotechnol. 174 (2014) 116–129.
[48] E.B. Sydney, W. Sturm, J.C. de Carvalho, V.T. Soccol, C. Larroche, A. Pandey, C.R. Soccol, Potential carbon dioxide fixation by industrially important microalgae, Bioresour. Technol. 101 (2010) 5892–5896.
[49] L.S. Pérez-Mora, M.C. Matsudo, E.A.C. Gomes, J.C.M. Carvalho, An investigation into producing *Botryococcus braunii* in a tubular photobioreactor, J. Chem. Technol. Biotechnol. 91 (2016) 3053–3060.
[50] J.C. Ogbonna, H. Tanaka, Light requirement and photosynthetic cell cultivation – development of processes for efficient light utilization in photobioreactors, J. Appl. Phycol. 12 (2000) 207–218.
[51] G.H. Gim, R.J. Jaewon, M.J. Kim, P.I. Kim, S.W. Kim, Effects of carbon source and light intensity on the growth and total lipid production of three microalgae under different culture conditions, J. Ind. Microbiol. Biotechnol. 43 (2016) 605–616.
[52] H. Takache, J. Pruvost, J.F. Cornet, Kinetic modeling of the photosynthetic growth of *Chlamydomonas reinhardtii* in a photobioreactor, Biotechnol. Prog. 28 (2012) 681–692.
[53] B. Cheirsilp, S. Torpee, Enhanced growth and lipid production of microalgae under mixotrophic culture condition: effect of light intensity, glucose concentration and fed-batch cultivation, Bioresour. Technol. 110 (2012) 510–516.
[54] A.C. Guedes, L.A. Meireles, H.M. Amaro, F.X. Malcata, Changes in lipid class and fatty acid composition of cultures of *Pavlova lutheri*, in response to light intensity, J. Am. Oil Chem. Soc. 87 (2010) 791–801.
[55] S.H. Ho, C.Y. Chen, J.S. Chang, Effect of light intensity and nitrogen starvation on CO_2 fixation and lipid/carbohydrate production of an indigenous microalga *Scenedesmus obliquus* CNW-N, Bioresour. Technol. 113 (2012) 244–252.
[56] H. Zhang, W. Wang, Y. Li, W. Yang, G. Shen, Mixotrophic cultivation of *Botryococcus braunii*, Biomass Bioenergy 35 (2011) 1710–1715.
[57] S. Ruangsomboon, Effect of light, nutrient, cultivation time and salinity on lipid production of newly isolated strain of the green microalga, *Botryococcus braunii* KMITL 2, Bioresour. Technol. 109 (2012) 261–265.
[58] H.B. Chen, J.Y. Wu, C.F. Wang, C.C. Fu, C.J. Shieh, C.I. Chen, C.Y. Wang, Y.C. Liu, Modeling on chlorophyll a and phycocyanin production by *Spirulina platensis* under various light-emitting diodes, Biochem. Eng. J. 53 (2010) 52–56.
[59] T. Yoshimura, S. Okada, M. Honda, Culture of the hydrocarbon producing microalga *Botryococcus braunii* strain showa: optimal CO_2, salinity, temperature, and irradiance conditions, Bioresour. Technol. 133 (2013) 232–239.
[60] D. Sasi, P. Mitra, A. Vigueras, G.A. Hill, Growth kinetics and lipid production using *Chlorella vulgaris* in a circulating loop photobioreactor, J. Chem. Technol. Biotechnol. 86 (6) (2011) 875–880.
[61] Anderson, Effects of light intensity on nitrate and nitrite uptake and excretion by *Chaetoceros curvisetus*, Mar. Biol. 62 (1981) 257–261.
[62] A.L. Gonçalves, J.C.M. Pires, M. Simões, The effects of light and temperature on microalgal growth and nutrient removal: an experimental and mathematical approach, RSC Adv. 6 (2016) 22896–22907.
[63] J.W. Zijffers, K.J. Schippers, K. Zheng, M. Janssen, J. Tramper, R.H. Wijffels, Maximum photosynthetic yield of green microalgae in photobioreactors, Mar. Biotechnol. 12 (2010) 708–718.
[64] P. Cheng, B. Ji, L. Gao, W. Zhang, J. Wang, T. Liu, The growth, lipid and hydrocarbon production of *Botryococcus braunii* with attached cultivation, Bioresour. Technol. 138 (2013) 95–100.
[65] F.R. Wolf, A.M. Nonomura, J.A. Bassham, Growth and branched hydrocarbon production in a strain of *Botryococcus braunii* (Chlorophyta), J. Phycol. 21 (1985) 388–396.
[66] A.R. Rao, R. Sarada, G.A. Ravishankar, Influence of CO_2 on growth and hydrocarbon production in *Botryococcus braunii*, J. Microbiol. Biotechnol. 17 (2007) 414–419.
[67] A. Sukenik, Y. Carmeli, T. Berner, Regulation of fatty acid composition by irradiance level in the eustigmatophyte *Nannochloropsis* sp, J. Phycol. 25 (1989) 686–692.
[68] A. Sukenik, Ecophysiological considerations in the optimization of eicosapentaenoic acid production by *Nannochloropsis* sp. (Eustigmatophyceae), Bioresour. Technol. 35 (1991) 263–269.
[69] T. Chrismadha, M.A. Borowitzka, Effect of cell-density and irradiance on growth, proximate composition and eicosapentaenoic acid production of *Phaeodactylum tricornutum* grown in a tubular photobioreactor, J. Appl. Phycol. 6 (1994) 67–74.